AD

USAAMRDL TECHNICAL REPORT 72-21

ADVANCED-TECHNOLOGY HIGH-CAPACITY HOIST-DRIVE SYSTEM

By
D. Stein
R. F. Campbell
N. N. Rothman
J. Shefrin

April 1972

EUSTIS DIRECTORATE
U. S. ARMY AIR MOBILITY RESEARCH AND DEVELOPMENT LABORATORY
FORT EUSTIS, VIRGINIA

CONTRACT DAAJ02-70-C-0042
THE BOEING COMPANY
VERTOL DIVISION
PHILADELPHIA, PENNSYLVANIA

Disclaimers

The findings in this report are not to be construed as an official Department of the Army position unless so designated by other authorized documents.

When Government drawings, specifications, or other data are used for any purpose other than in connection with a definitely related Government procurement operation, the US Government thereby incurs no responsibility nor any obligation whatsoever; and the fact that the Government may have formulated, furnished, or in any way supplied the said drawings, specifications, or other data is not to be regarded by implication or otherwise as in any manner licensing the holder or any other person or corporation, or conveying any rights or permission, to manufacture, use, or sell any patented invention that may in any way be related thereto.

Trade names cited in this report do not constitute an official endorsement or approval of the use of such commercial hardware or software.

Disposition Instructions

Destroy this report when no longer needed. Do not return it to the originator.

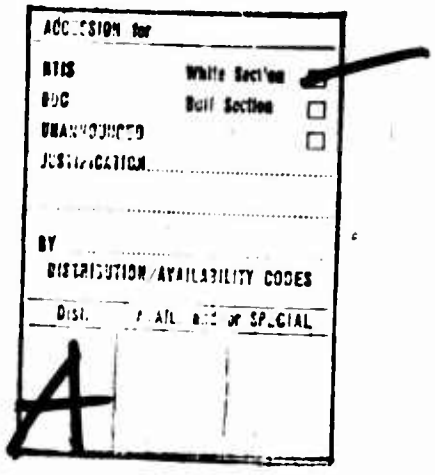

Project 1F162203A254
Contract DAAJ02-70-C-0042
USAAMRDL Technical Report 72-21
April 1972

ADVANCED-TECHNOLOGY HIGH-CAPACITY HOIST-DRIVE SYSTEM

Final Report

D210-10405-1

By

D. Stein
R. F. Campbell
N. N. Rothman
J. Shefrin

Prepared by

The Boeing Company
Vertol Division
Philadelphia, Pennsylvania

for

EUSTIS DIRECTORATE
U.S. ARMY AIR MOBILITY RESEARCH AND DEVELOPMENT LABORATORY
FORT EUSTIS, VIRGINIA

Unclassified
Security Classification

DOCUMENT CONTROL DATA - R & D

(Security classification of title, body of abstract and indexing annotation must be entered when the overall report is classified)

1. ORIGINATING ACTIVITY *(Corporate author)*
The Boeing Company, Vertol Division
Boeing Center, Philadelphia, Pennsylvania

2a. REPORT SECURITY CLASSIFICATION
Unclassified

2b. GROUP

3. REPORT TITLE
Advanced Technology High-Capacity Hoist Drive System

4. DESCRIPTIVE NOTES *(Type of report and inclusive dates)*
Final Technical Report

5. AUTHOR(S) *(First name, middle initial, last name)*
Dennis Stein
Richard F. Campbell
Newt N. Rothman
Joseph Shefrin

6. REPORT DATE	7a. TOTAL NO. OF PAGES	7b. NO. OF REFS
April 1972	209	

8a. CONTRACT OR GRANT NO.	9a. ORIGINATOR'S REPORT NUMBER(S)
DAAJ02-70-C-0042	
b. PROJECT NO. IF 162203A254	USAAMRDL Technical Report 72-21
c.	9b. OTHER REPORT NO(S) *(Any other numbers that may be assigned this report)*
d.	D210-10405-1

10. DISTRIBUTION STATEMENT
Approved for public release; distribution unlimited.

11. SUPPLEMENTARY NOTES	12. SPONSORING MILITARY ACTIVITY
	U.S. Army Air Mobility Research and Development Laboratory Fort Eustis, Virginia

13. ABSTRACT

Previous studies of current airborne hoist drive systems for handling external loads indicate that use of present technology to design hoist systems with larger capacities will result in excessive weights, incompatible configurations, complex controls, and other undesirable factors. A pneumatic air-turbine motor drive shows the best potential for powering high-capacity systems. For helicopter hoisting applications, there is no practical limit for system capacity.

This report documents a program of design and design analysis of an advanced technology hoist-drive subsystem applicable to a family of cargo hoists with capacities ranging from 12.5 to 50 tons.

DD FORM 1 NOV 68 1473 REPLACES DD FORM 1473, 1 JAN 64, WHICH IS OBSOLETE FOR ARMY USE.

Unclassified
Security Classification

14. KEY WORDS	LINK A		LINK B		LINK C	
	ROLE	WT	ROLE	WT	ROLE	WT
Air Compressor						
Air Turbine Motor (ATM)						
Dynamic Braking						
External Cargo Handling System						
Heavy Lift Helicopter (HLH)						
Hoist Weight Analysis						
Multipoint Suspension						
Pneumatic Drives						
Pneumatic System Requirements						
Reverse Rotating Turbines						
Variable Speed Hoists						
12.5- to 50-Ton-Capacity Hoist Systems						

DEPARTMENT OF THE ARMY
U. S. ARMY AIR MOBILITY RESEARCH & DEVELOPMENT LABORATOR
EUSTIS DIRECTORATE
FORT EUSTIS, VIRGINIA 23604

This report was prepared by the Boeing Company, Vertol Division under the terms of Contract DAAJ02-70-C-0042. It documents a program of design and design analysis of an advanced-technology hoist-drive subsystem applicable to a family of airborne cargo hoists with capacities ranging from 12.5 to 50 tons. Boeing concluded that a pneumatic drive system has the best potential for powering a high-capacity cargo ho ..

The pneumatic hoist-drive power system concept within : _ context of an integrated secondary power concept represents a feasible solution to cargo hoisting problems associated with a high-capacity external load handling system. The feasibility of the pneumatic concept has been further substantiated under the HLH component development program, and a pneumatic-powered hoist is specified for the HLH.

The conclusions contained herein are concurred in by this Directorate.

The technical monitor for this contract was Mr. Richard E. Lane of the Aircraft Subsystems and Equipment Division.

SUMMARY

Future-generation cargo helicopters will carry significantly larger payloads than present helicopters; therefore, the hoist systems of these helicopters must also handle larger loads. Future systems may be required to accommodate loads up to 50 tons or greater.

Previous studies of current airborne hoist systems handling external loads indicate that we cannot simply use present technology to design hoist systems with larger capacities. Such extrapolations of current technology will result in excessive weights, incompatible configurations, complex controls, and other undesirable factors.

This report documents a program of design and design analysis of an advanced-technology hoist-drive subsystem applicable to a family of airborne cargo hoists with capacities ranging from 12.5 to 50 tons. The work was performed in two phases: Phase I, preliminary design and analysis; and Phase II, final design.

It is concluded that a pneumatic drive system shows the best potential for powering these high-capacity hoist systems.

FOREWORD

The Boeing Company's Vertol Division conducted this program for the Eustis Directorate, U.S. Army Air Mobility Research and Development Laboratory, under contract DAAJ02-70-C-0042 (DA Project 1F162203A254).

USAAMRDL Technical direction for this study was provided by Mr. Richard E. Lane, Project Engineer, Air Cargo Systems Branch, Aircraft Subsystems and Equipment Division. Additional direction and guidance were obtained from Messrs J. E. Forehand and J. N. Daniels in their initiation of coordination meetings on concurrent complementary subcontracts under their sponsorship. As a result, such coordination meetings were held between Boeing-Vertol, Battelle, and Northrop to integrate requirements and criteria for the hoist drive, tension member, and load stabilization studies related to external cargo transport by helicopter.

Significant contributions were also made by industry in furnishing substantiating performance test data demonstrating the feasibility of the pneumatic hoist-drive concept. The authors gratefully acknowledge this assistance by the following:

AiResearch Manufacturing Division, The Garrett Corporation, Phoenix, Arizona, and Los Angeles, California

Battelle Columbus Laboratories, Long Beach, California

Bendix - Fluid Power Division, Utica, New York

Hamilton-Standard, Division of United Aircraft, Windsor Locks, Connecticut

Northrop - Nortronics, Hawthorne, California

Plessey Airborne Corporation, Hillside, New Jersey

Rolls-Royce, Inc., Small Engine Division, Leavesden, U.K.

Sundstrand, Aerospace Group, Rockford, Illinois

TABLE OF CONTENTS

	Page
SUMMARY	iii
FOREWORD	v
LIST OF ILLUSTRATIONS	x
LIST OF TABLES	xv
SIGNIFICANT FINDINGS	1
System Weight	2
Estimated Power Level Required	2
Safety, Maintainability, and Reliability Consideration	2
Heat Dissipation Requirements	2
Fuel Cost of Bleeding Main Engines for Hoisting	3
Reverse Rotation and Overspeed Capability	3
The Hoist-Drive System Design	4
Risk Assessment	5
SELECTION OF POWER DRIVES	6
Electrical	6
Mechanical	6
Hydraulic	6
Pneumatic	7
COMPARING PNEUMATIC AND HYDRAULIC SYSTEMS	15
Amount of Hardware	15
Efficiency, Power, Weight, and Heat Dissipation	15
Braking During Lowering Mode	15
Accommodating a 2G Load	20
Reliability	20
Maintainability	29
Safety	29
Vulnerability and Survivability	34
SYSTEM REQUIREMENTS	36
Design Day	36
Operating Ambients	36
Temperature Limitations	36
Hoisting Modes	36
Design Load	37
Pneumatic Power Source	37
Pneumatic Power Distribution System	37
Pneumatic and Hoist-Drive System Control Design	38
Pneumatic Power Redundancy	38
Variable Hoist Span	38
Dynamic Braking	38
Static/Emergency Brakes	38
System Performance	39

Page

Component Efficiencies and System Losses. 41
Pneumatic System Pressure 41
Conductor Sizing 41
Air-Turbine Motor 43
Air Compressor/Pneumatic Power Generating System . 48
Main Engine Bleed Pneumatic Power Generating System 50

PRELIMINARY DESIGN OF THE HOIST SYSTEM. 52
Integration of the Pneumatic Hoist-Drive Design . . 52
System Components 56
Dual Tension Member Hoist Design 56
Tension Member Design 62

THE AIR-TURBINE MOTOR (ATM) 67
Turbine Configurations Considered 68
Operational Characteristics 72
Radial Versus Axial Turbine Wheels 75
Turbine Nozzle Configuration 75
Analytical Data Substantiation 76
Turbine Overspeed Capability 89
Variable-G Accommodation With an Impulse-Type ATM . 89
Air-Turbine Nozzle Area Design. 91

THE AIR COMPRESSOR. 95
Compressor Performance and Power Level Requirements 95
Alternative Compressors 100
Summary on Compressors 101

THE CONTROL SYSTEM. 109

THE GEARING SYSTEM 114

WEIGHT ANALYSIS 121

PNEUMATIC POWER GENERATION COST 130
Pneumatic Power Generation Trade-off Studies . . . 132
Engine Bleed Fuel Cost 132
Trade-off Study Summary 132

SYSTEM CONCEPT DEMONSTRATION TESTING 143
Test Setup No. 1. 143
Test Setup No. 2. 151
STRESS ANALYSIS SUMMARY 159
Centrifugal Blade Stresses 159
Natural Frequency of Axial Blades by "Beam Theory" 159
Turbine Disc Analysis 159

Page

Hoist-Drum Triple-Planetary Reduction Gearbox . . . 160
Air Turbine High-Speed Gearbox 160

HOIST-DRIVE DESIGN FOR 20-TON-CAPACITY SYSTEM 165
Single-Cable Hoists 166
Single-Point Layout Vs. Level Wind 183
Maintainability and Reliability 186
Weight Development 186
Load Isolation Analysis 187

CONCEPT STUDY MODEL 192

DISTRIBUTION. 195

LIST OF ILLUSTRATIONS

Figure		Page
1	Servovalve Hoist Drive	9
2	Servopump Hoist Drive	10
3	Servovalve Complementary Circuitry	11
4	Servopump Complementary Circuitry	12
5	Pneumatic Hoist Drive	13
6	Alternative Secondary Pneumatic Power Generation	14
7	Performance of Hydraulic and Pneumatic Motors Above Design Load	21
8	Hydraulic Hoist-Drive Block Diagram, Identifying Symbols and Presenting Equations for Calculating Reliability	26
9	Hydraulic Hoist-Drive Complementary System Block Diagram, Identifying Symbols and Presenting Equations for Calculating Reliability	27
10	Pneumatic Hoist-Drive Block Diagram, Identifying Symbols and Presenting Equations for Calculating Reliability	28
11	Projected Improvement in Reliability of Pneumatic Hoist-Drive System	31
12	Hazards of a Cargo Handling System	32
13	Torque Versus Speed for Fixed- and Variable-Nozzle Turbines	42
14	Tandem-Rotor Helicopter - Boeing's HLH	53
15	An Integrated Pneumatic Hoist System	54
16	A Movable, Dual-Winch System Used for Both Multipoint and Single-Point Suspensions	55
17	Telescoping Pneumatic Power Conductors	57

Figure		Page
18	Dual-Drum Hoist	58
19	Effect of the Ratio of Load Length to Hoist Separation on the Capacity of a Single Hoist . .	60
20	Cable Diameter Versus Strength - MIL-C-5424 and Improved Cable Under Development	63
21	Fatigue Characteristics of Various Cables	65
22	Loss per Sheave for Two Diameters of Cables (d) and Various Diameters of Sheaves (D)	66
23	Velocity Diagram for Impulse Turbine	72
24	Frictionless Turbine Blading Conversion Efficiency Versus Velocity Ratio for Nozzle Angles of 15 and 20 Degrees	77
25	Maximum Shaft Horsepower per Unit Flow Versus Nozzle Exit Velocity for Nozzle Angles of 15 and 20 Degrees	77
26	Shaft Power Generation Versus Nozzle Exit Velocity at Variable-Velocity Ratios	78
27	Shaft Power Versus Nozzle Area (Applicable Only for Constant Tip Speed to Exit Velocity Ratios) .	78
28	Blade Force Versus Velocity Ratio	79
29	Rate of Descent for Constant Expansion Ratio, Variable Nozzle Turbine	79
30	Axial Versus Radial Wheel Characteristics	80
31	Fixed Nozzle	81
32	Variable Nozzle	82
33	Partial Admission Nozzle	83
34	Test Data for Bendix Air Turbine Starter	84
35	Driving and Braking Performance of the AiResearch Air Turbine Starter	85
36	Variation of Torque With Speed and Pressure (From NASA TN D-5090)	86

Figure		Page
37	Dynamic Braking Capability (Test Bed)	87
38	Forward and Reverse Rotation	87
39	Relative Turbine Velocity and Efficiency and Airflow Required Versus "G" Design Requirements .	92
40	Nozzle Area Required for a Constant Hoist of 23 Tons at 60 Feet per Minute Versus Ambient Temperature	94
41	Air Compressor - Allison Model 250	96
42	Performance Map of an Available Air Compressor .	97
43	Compressor Performance Versus Ambient Temperature	98
44	Load Compressor Characteristics for the Rolls-Royce RS 360-18	102
45	Estimated Performance at Aerodynamic Overspeed for the Rolls-Royce RS 360-18	103
46	Load Compressor Characteristics for the Rolls-Royce RS 360-18	104
47	Compressor Installation on the Rolls-Royce RS 360-18	105
48	Baseline Hoist Control System	111
49	Control System Element and Air Vehicle Interface . .	112
50	Estimated Performance of the Optimized Air Turbine Motor (AiResearch)	113
51	Fixed-Ring Differential System	115
52	Four-Planetary System	116
53	Fixed-Sun Differential System	117
54	Three-Spur, Two-Planetary System	118
55	Two-Spur, Two-Planetary System	119
56	Baseline Gearing System - Triple Planetary . . .	120
57	Component Weight Versus System Capacity	124

Figure		Page
58	Weight Versus Capacity for a Single Hoist	128
59	Weight Versus Capacity for a Total Hoist System	129
60	Single-Stage Axial Turbine Performance Showing Efficiencies	131
61	Pneumatic System - Concept A	135
62	Pneumatic System - Concept B	136
63	Pneumatic System - Concept C	137
64	Pneumatic System - Concept D	138
65	Engine Bleed Versus Fuel Consumption for Engines A, B, and C	140
66	Test Setup No. 1	144
67	Location of Test Probes	144
68	Temperature Rise Generated by Reverse Running of Turbine	146
69	Blade Windage Loss	148
70	Disc Windage Loss	149
71	Total Turbine and Component Windage Loss	150
72	Air Turbine Motor Modified to Combine Hoisting and Reversing Functions (Sundstrand)	154
73	Breadboard Unit on Test Stand	155
74	Effects of Windage-Control Devices (Sundstrand)	156
75	Composite Trace of Modified Air-Turbine-Drive Speed Characteristics	157
76	Summary of Hoisting and Reversing Wheel Performance	158
77	General Arrangement of System	167
78	Section Through Hoist	169
79	Side View of Hoist	171

Figure		Page
80	Arrangement of ATM, High-Speed Gearbox, and Brake	173
81	Arrangement of Compressor on APU	175
82	Level-Wind Hoist	177
83	Single-Point Payout Hoist	178
84	Twin-Drum In-Line Hoist	181
85	Single-Drum Twin-Cable Hoist	182
86	Level-Wind Twin-Drum Hoist	184
87	Single-Point Payout Twin-Drum Hoist	185
88	Cable Area Versus Cable Strength	188
89	Structural Interface Weight	189
90	Pneumatic Hoist-Drive Concept Study Model	193

LIST OF TABLES

Table		Page
I	Assumed Component Design Efficiency of Hydraulic and Pneumatic Systems	16
II	Power Parameters of Hydraulic and Pneumatic Systems	17
III	Weight Estimates of Hydraulic and Pneumatic Components - Single Power Source	18
IV	Weight Estimates of Hydraulic and Pneumatic Components - Redundant Power Source	19
V	Predicted Reliability of Hydraulic and Pneumatic Hoist-Drive Systems	22
VI	Hydraulic Hoist-Drive Components Reliability Data	24
VII	Pneumatic Hoist-Drive Components Reliability Data and Goals	25
VIII	Hydraulic and Pneumatic Hoist System Maintenance Requirements	30
IX	Potential Hazards of Hydraulic and Pneumatic Systems	33
X	Total Presented Area of Hydraulic Drive System .	35
XI	Load Asymmetry Accommodation With 2.5G Factor, 30-Degree Coning, and Fixed "Drag" Factor	61
XII	Load Asymmetry Accommodation With 2.0G Factor, 30-Degree Coning, and Fixed "Drag" Factor	61
XIII	Load Asymmetry Accommodation With 2.5G Factor, Fixed Drag Factor, and No Coning Angle	62
XIV	Axial and Radial Turbine Features	69
XV	G-Capability Vs. Relative Airflow, Velocity & Efficiency	91
XVI	Compressor Performance Versus Ambients	99

Table		Page
XVII	Discharge Temperature and Compressor Power Absorption Versus Variable Ambients	100
XVIII	Component Exponential Value	123
XIX	Hoist Systems Component Weight Breakdown . . .	126
XX	Hoist Systems Component Weight Breakdown - Backup Data	127
XXI	Individual System Power Requirements	133
XXII	Minimum Simultaneous Power to Meet Requirements	134
XXIII	Pneumatic Power Systems - Primary Differences in Characteristics	139
XXIV	Investigated Engine Bleed Air/Fuel Cost Characteristics	139
XXV	Component Weight Comparison	141
XXVI	System Concept Weight Comparison	141
XXVII	In-Flight Fuel Flow Requirement Comparison (Based on Minimum Simultaneous Power)	142
XXVIII	Clockwise Rotation Temperature Increase Versus Time - Chamber Blanked (Valve Closed). .	145
XXIX	Clockwise Rotation Temperature Increase Versus Time - Chamber Blank Removed (Valve Open) . . .	145
XXX	Windage Losses of Disc Without Blades (Gearing Included)	151
XXXI	Gear Data - Hoist-Drum Triple-Planetary Reduction Gear Box	161
XXXII	Gear Loads - Hoist-Drum Triple-Planetary Reduction Gearbox	162
XXXIII	Shaft Torque - Hoist-Drum Triple-Planetary Reduction Gearbox	162
XXXIV	Bearing Loads - Hoist-Drum Triple-Planetary Reduction Gearbox	163
XXXV	Gear Data - Air Turbine High-Speed Gearbox . .	163

Table		Page
XXXVI	Gear Loads - Air Turbine High-Speed Gearbox	163
XXXVII	Shaft Torque - Air Turbine High-Speed Gearbox	164
XXXVIII	Bearing Loads - Air Turbine High-Speed Gearbox	164
XXXIX	Summary of Hoist Parameters	190
XL	System Weight Summary	191

SIGNIFICANT FINDINGS

Technology to support transition from current-capacity hoist drives for system capacities to next- and future-generation cargo transport helicopters has been established as a result of this study. This technology is based on the pneumatic power system concept, which knows no practical limit on hoist system capacity predicated on the safe assumption that the airborne vehicle's main propulsion power is derived from modern large airflow capacity air-breathing power plants.

Representative current technology drives were based on USAAVLABS Technical Report 67-46* and Report 67-51**. Both studies are based on hydraulic drive concept designs.

The pneumatic hoist-drive power system concept represents advanced technology due to a variety of factors, the most outstanding of which are:

- The power medium is nontoxic and nonflammable.
- Fluid logistics are eliminated.
- System weight is low.
- Personnel and fire hazards are minimized due to low system pressure and temperature.
- Pneumatic system is inherently flexible, is compatible with other aircraft power systems, provides for growth capability including modifications, and permits ease of integration and air vehicle installation.
- Small leaks will not affect mission performance and are easily repairable.
- Bidirectional overspeed capability is nearly 200 percent of design speed with empty hook and proportionately higher speeds with partial loads.
- System reliability is good, and maintenance is at a minimum.

*USAAVLABS Technical Report 67-46, Design Study of Heavy Lift Helicopter External Load Handling System, November 1967, AD828283.

**USAAVLABS Technical Report 67-51, Heavy-Lift Helicopter External Cargo Handling System Design Study, October 1967, AD826531L.

- Performance efficiency is high, and the turbine motor characteristics are ideally suited for dynamic braking, thus eliminating mechanical friction brakes and their associated heat dissipation and wear problems.

- The air turbine characteristics are inherently well suited to compensate for transient acceleration loadings.

- Fuel cost to perform hoisting mission is very low.

Substantiations of the above are discussed in detail in the text of this report. Some of the highlights with reference to the appropriate text sections are as follows:

SYSTEM WEIGHT

Based on a 50-foot separation distance between the hoists and the power generation source, the comparative system weights of the pneumatic and hydraulic (current technology) drives with a capacity of 25 tons show marked differences. The hydraulic drive with a single power source would weigh 874 pounds; redundant power would weigh 414 pounds. This gives a system total of 1288 pounds. But the pneumatic drive weighs only 286 pounds — 265 pounds for single-power source and 21 pounds for the redundant power.

ESTIMATED POWER LEVEL REQUIRED

Power requirements for current versus advanced technology drives based on continuous full-capacity hoisting are 184 horsepower for the pneumatic concept and 186.3 horsepower for the hydraulic concept. No power consumption is required for the pneumatic approach during transport when main engine bleed power is utilized. The hydraulic concept requires continuous power estimated at 25 percent of total due to continuous pump rotation powered by the main transmission.

SAFETY, MAINTAINABILITY, AND RELIABILITY CONSIDERATION

Comparative evaluation of the above factors indicates superiority of the advanced-technology pneumatic concept in every respect, as substantiated in the text.

HEAT DISSIPATION REQUIREMENTS

Based on continuous hoisting, the heat generated for both systems is 2630 Btu's per minute for the hydraulic and 270 Btu's

per minute for the pneumatic concept. A nonregenerative braking of the hydraulic system requires 3940 Btu's per minute heat dissipation capacity.

FUEL COST OF BLEEDING MAIN ENGINES FOR HOISTING

Utilizing main engine bleed air as the power source for pneumatic hoisting proved to be the most economical of any practical hoist-drive concept when the hoist drive is designed on an integrated basis and when the main engine propulsion system is designed for one engine out (OEI) capability.

The fuel cost data presented in the text were corroborated with three independent engine manufacturers. Assuming engine A to be representative of the installed power plant (this engine was selected for the Boeing HLH design), the total fuel consumption for continuous 25-ton full-capacity hoisting is approximately 55 pounds per hour, based on simultaneous three-engine bleed.

As to practical aspects of hoisting power utilization, it is expected that full-capacity hoisting will not exceed 10 percent of flight time. On this basis, the total fuel cost for a one-hour mission is 5.5 pounds.

Bleeding the engine has an additional advantage in that no independent rotating components are required. The bleeding system is required for other aircraft functions such as main-engine starting.

REVERSE ROTATION AND OVERSPEED CAPABILITY

On the basis of actual tests, the empty cable payout is accomplished with a separate reversing wheel mounted directly to the hoisting wheel shaft. No clutch is required. The reversing wheel peak power output is designed for the 200-percent rotation of the hoisting wheel speed. The reversing wheel drag is estimated to reduce the empty cable hoisting speed between 190 and 195 percent of the hoisting design velocity of 60 feet per minute.

Efficiency reduction of the hoisting wheel is estimated to be 1 to 2 percent. This reduction, however, is offset by the elimination of the complexity of clutch installation; considering the low fuel consumption for main engine bleeding, it was decided to accept this penalty in performance.

THE HOIST-DRIVE SYSTEM DESIGN

The selected hoist system design was based on considerations of fuel consumption, producibility, and practicability. Demonstration tests of relative performance included: dynamic braking, acceleration of the system rotational speed, heat generation during hoisting and dynamic braking, capability of accommodating acceleration loading, and bidirectional overspeed capability.

The significant highlights of the design are:

- The selected turbine was axial due to higher acceleration (stall torque) accommodation capability and superior dynamic braking capability. The torque/speed linear characteristics in both positive and negative speed regions simplify further the control system design.

- To accommodate turbine reverse rotation, an independent reversing turbine was installed and is directly coupled to the hoisting wheel shaft.

- There is no mechanical disconnect or clutching between the hoisting wheel and the load

- Clutching between the reversing wheel and the hoisting wheel is eliminated due to complexity and maintainability requirements. The aerodynamic drag torque of the reversing wheel, based on tests conducted, is relatively low due to smaller reversing wheel size.

- The design is capable of 200-percent reverse speed rotation and nearly 200-percent over design speeds in hoisting mode with no load.

- Fixed-nozzle configuration was selected, with upstream flow control valves. The variable nozzle approach was discarded due to complexity of installation. The potential minor improvement in performance at the same partial load/speed capacities is offset by better acceleration accommodation of the fixed nozzle coupled with the low cost of fuel due to minor increase in the airflow when derived from bleeding the main engines.

- The static/emergency brake is installed downstream of the high-speed gearing reduction within the ATM housing. This approach permits low-weight and low-torque brake design.

- Forced lubrication was assumed for the turbine shaft bearing and for the high-speed gear reduction. The pump was assumed to be a G-rotor attached to the shafting and capable of pumping in any rotation.

- A cooling system was not designed for this application. Based on similar power-drive applications, it was found that natural convection and conduction will be adequate, particularly due to intermittent hoisting application with rather long duration nonhoisting periods while transporting the acquired load with the helicopter.

- The control-actuation power was assumed to be pneumatic primarily due to the availability of this type of power. The control functions, including response, can be accomplished satisfactorily with the pneumatic concept.

RISK ASSESSMENT

Other than problems normally associated with turbomachinery development, there are no risks of consequence. Some compromise regarding an optimum turbine efficiency goal of 85 percent may have to be made, not because of available technology to achieve this objective but on the basis of cost effectiveness of efficiency versus dollars when the system is analyzed on a full aircraft integration basis. No problems to achieve 80-percent compressor adiabatic efficiency are evident. Size and weight penalty are inconsequential for the turbine, the compressor, and the power conductors.

The selected fixed-nozzle geometry design is considered adequate. The complexity of variable-geometry turbine nozzle designs is, for this application, not warranted. The limited-potential airflow savings at some partial load or speed is not considered adequate to utilize the complexities of the variable-nozzle approach.

The control design primarily for the synchronization speed capability of both hoists must be resolved through testing. The problem complexity is, however, identical to any type of power drive system.

SELECTION OF POWER DRIVES

The types of drives that Boeing considered for use for high-capacity airborne hoists are voltage electrical, mechanical, hydraulic, and pneumatic.

ELECTRICAL

The low-voltage electric-drive concept was rejected because of excessive weight of its components — particularly the conductors, the motor, and the AC-to-DC conversion equipment — and because of its excessive current requirements, which could amount to 3000 amperes when based on 24-volt DC supply for a 20-ton system.

The high-voltage electric-drive concept was rejected because of its weight, its poor low-speed control characteristics for descending loads, and its still-unproven reverse-rotation control concept, which requires the dissipation of potentially high heat from the armature in the load-reversing modes.

MECHANICAL

The mechanical drive system was rejected because of the impracticable complexities of providing variable hoisting speeds and routing long shafts within the aircraft.

HYDRAULIC

A hydraulic-drive system is well suited for the hoist-drive application and is used widely in airborne and industrial hoist systems. The hydraulic system is in fact currently used on limited high-capacity airborne hoists.

Several hydraulic hoist-drive systems were investigated, but the most promising were the servovalve and the servopump concepts. The schematic representations of both concepts are shown in Figures 1 and 2. Both illustrations show two hoists per aircraft. The complementary circuitries for both concepts are shown in Figures 3 and 4.

The servovalve concept is based on constant-speed, variable-flow pump operation at constant pressure delivery. The servovalve regulates the flow to the hydraulic motor, thereby providing variable control of hoist speed and motor-reversing

speed. The motor pressure is a function of the load capacity hoisted. The servovalve system uses the concept of regenerative braking, wherein the energy of the load being lowered is transmitted to the rotor system via the pump, which becomes a motor during the lowering mode.

The servopump concept is based on a constant-speed, variable-flow, variable-pressure operation. The pressure is a function of the load hoisted. The hoisting speed is controlled by the "overcenter" swashplate displacement. Flow reversal is accomplished by displacing the swashplate over the center to obtain the flow (speed) required. Power regeneration for this concept is not feasible.

The servopump is considered to be better than the servovalve for the following reasons:

- High-pressure drop through the servovalve (1/3 of total delivered by pump), dictating larger motors and pumps.
- Excessive-heat-dissipation system required by servovalve, particularly during the lowering mode.
- High power requirements for the servovalve concept, regardless of the loads hoisted.
- Limited availability of high-capacity servovalves.

The hydraulic system represents the best of current technology, and this servopump concept thus represents the most advanced hydraulic system.

PNEUMATIC

A pneumatic hoist-drive system represents advanced technology. Schematic representation of the pneumatic system is shown in Figure 5. The drivers considered are air turbines, due to their relatively high efficiencies, as compared with positive-displacement devices. The primary source of power is the APU shaft-driven compressor, while the redundant power source is engine bleed.

In the unlikely event that the engines could not be bled because of extremely large performance penalties, an alternative for the secondary power source generation is shown in Figure 6. Here, the main rotor transmission drives the compressor, as in the hydraulic systems of Figures 1 and 2, where the pumps are driven by the transmission.

This pneumatic hoist-drive system uses a regenerative turbine with a variable-area nozzle to limit the high fuel losses

caused by the constant power demand by the compressor. The turbine, regardless of the power setting of the hoist-drive system, maintains a constant pressure in the system and thereby eliminates control problems in other systems. The turbine can also regenerate 40 to 70 percent (depending on ambient temperature) of the power which the compressor absorbs, and at the same time provide heat to the aircraft compartments.

The constant power demand of the compressor could be overcome by installing an on-off clutch between the transmission and the compressor; also the power absorbed by the load compressor could be minimized by installing variable inlet guide vanes. But previous experience with poor clutching performance and the complexities of variable inlet guide vanes discounted these approaches.

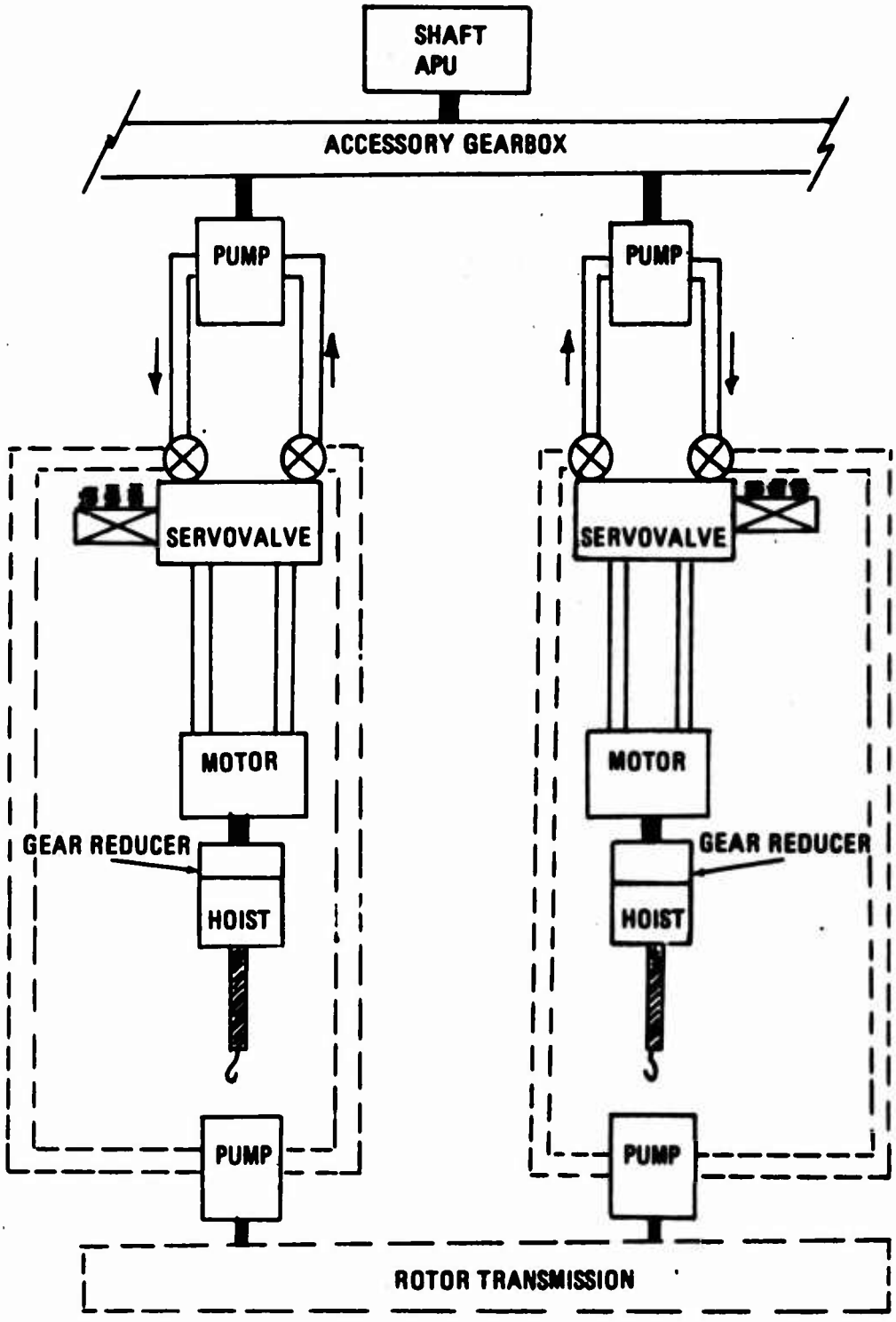

Figure 1. Servovalve Hoist Drive.

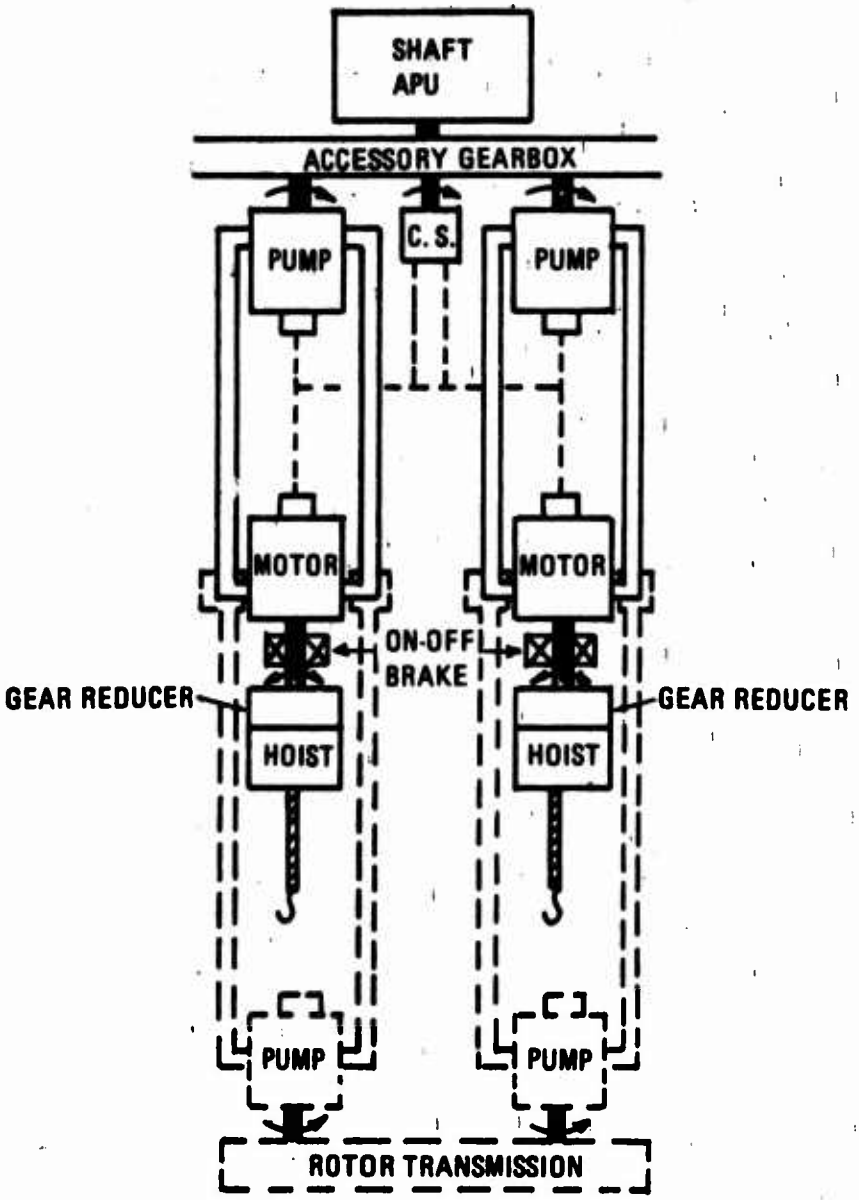

Figure 2. Servopump Hoist Drive.

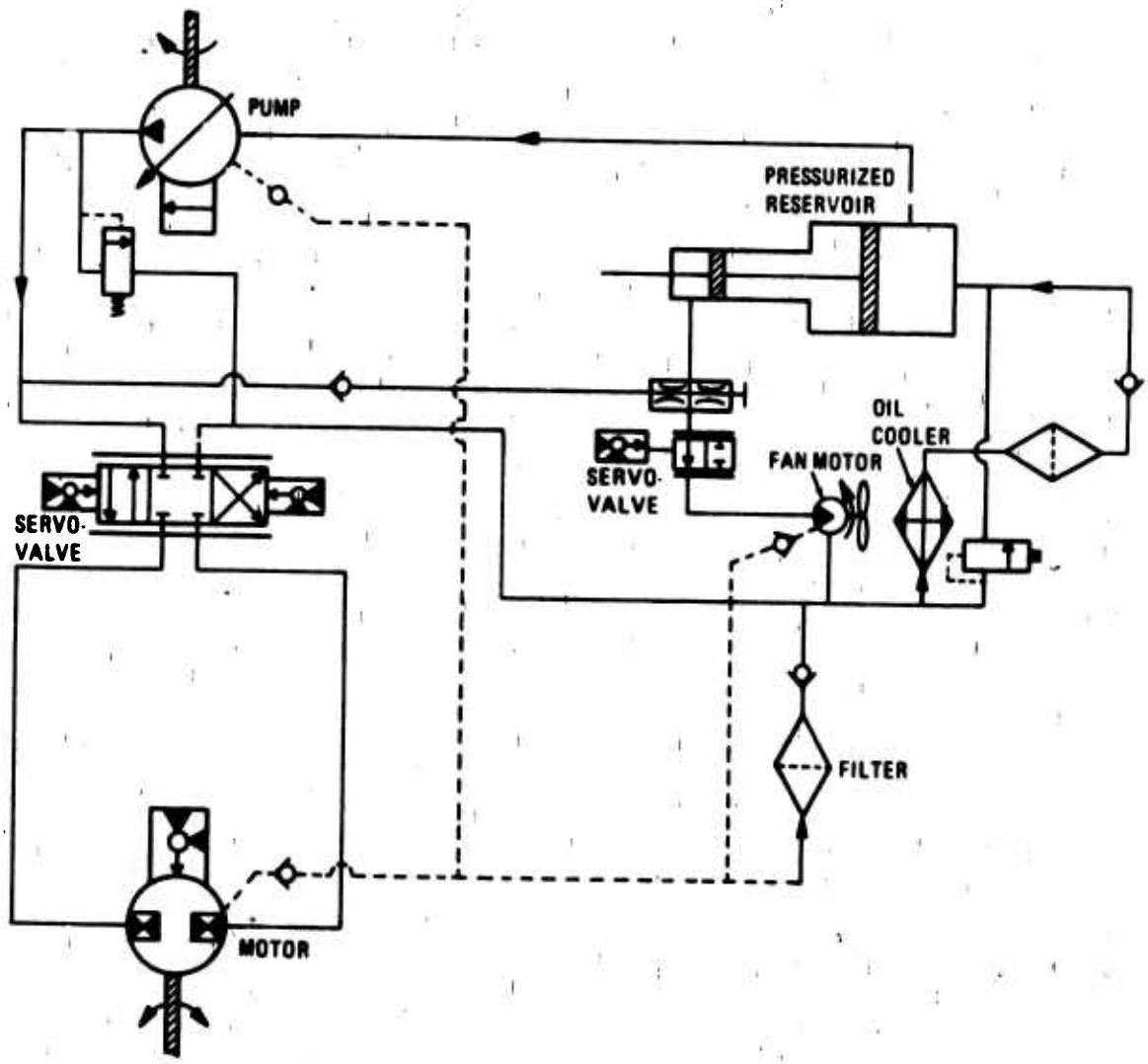

Figure 3. Servovalve Complementary Circuitry.

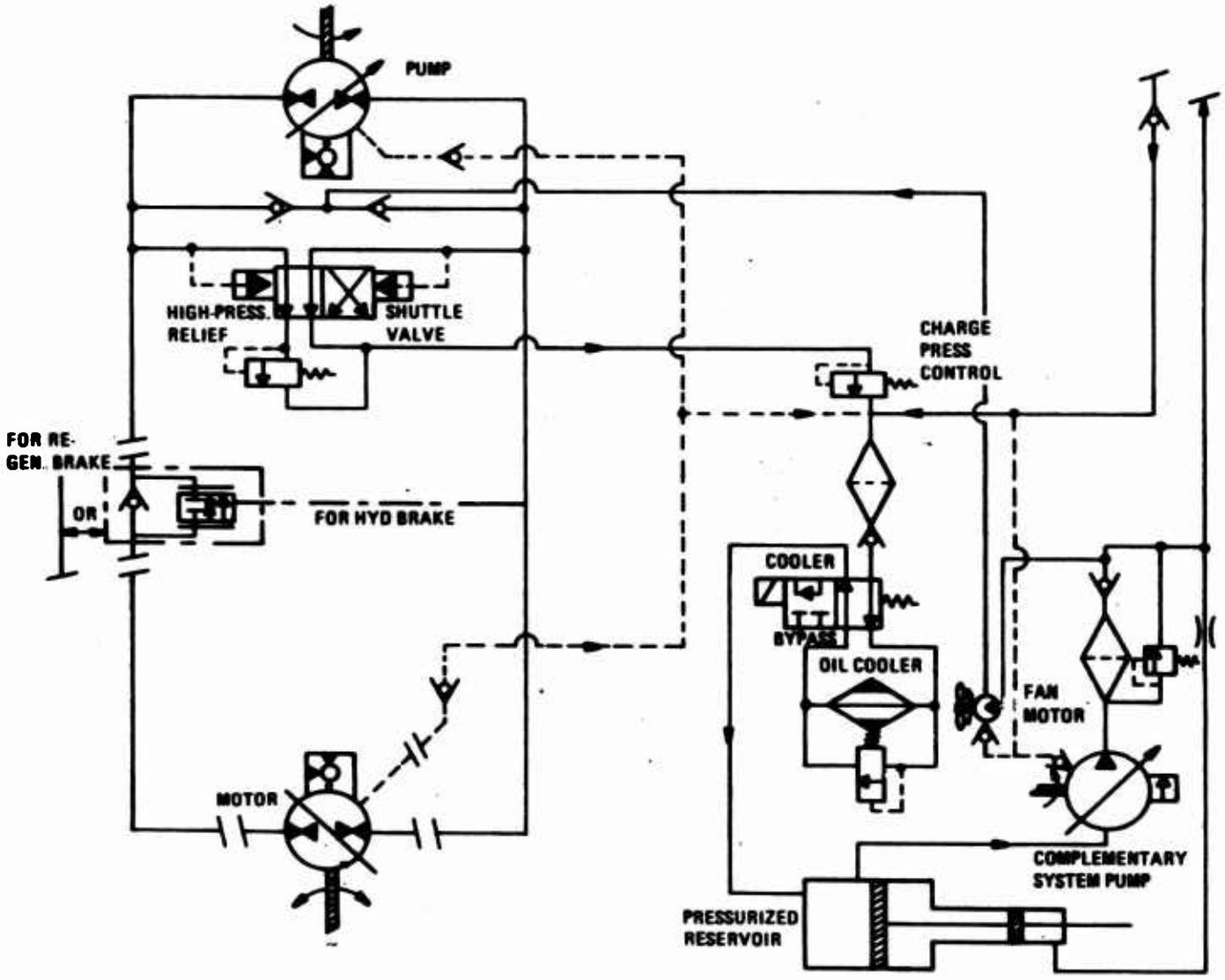

Figure 4. Servopump Complementary Circuitry.

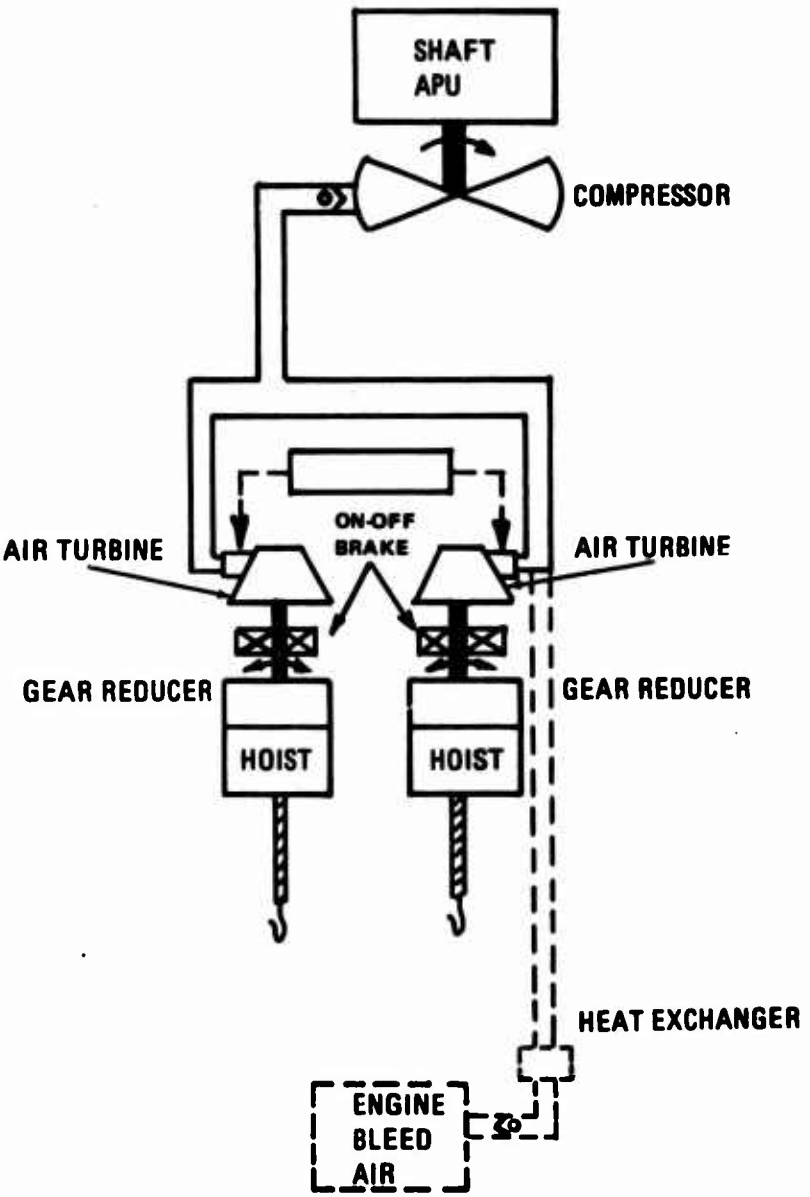

Figure 5. Pneumatic Hoist Drive.

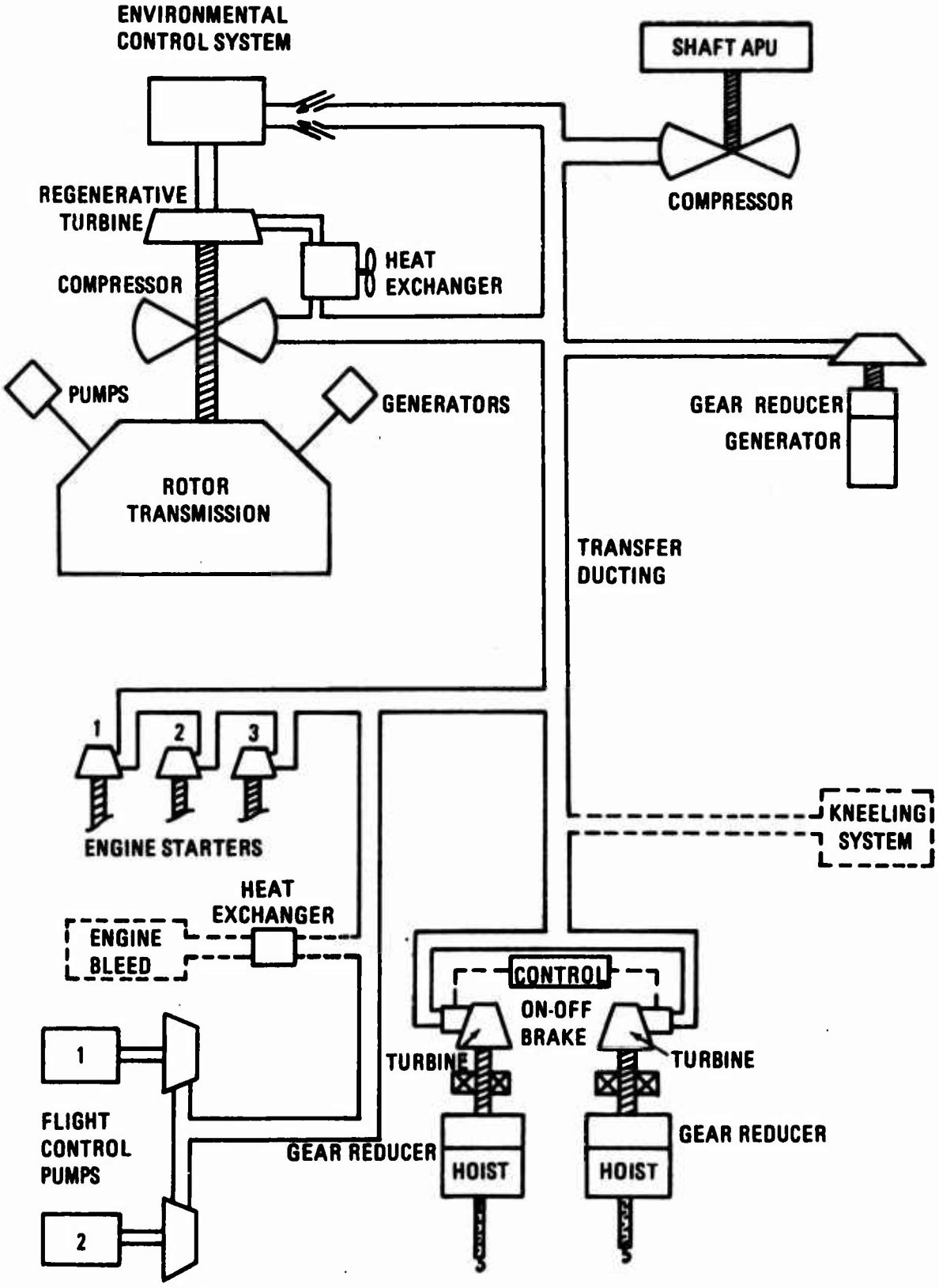

Figure 6. Alternative Secondary Pneumatic Power Generation.

COMPARING PNEUMATIC AND HYDRAULIC SYSTEMS

Boeing-Vertol selected the pneumatic system for the final design; it offers numerous advantages and overcomes some of the drawbacks of a hydraulic servopump system. This section outlines some of the areas in which the two systems were compared.

AMOUNT OF HARDWARE

If we assume that the pumps of the hydraulic system and the compressor of the pneumatic system are driven by shaft APU as the prime power source, the servopump system requires four conductors, one supply and one return to each motor, each one about 50 feet long; the pneumatic system requires only one conductor, approximately 65 feet long. The hydraulic system requires four additional conductors to transfer the redundant power, but the pneumatic system requires no additional conductor to transfer the redundant power. Further, the hydraulic system requires four hydraulic pumps -- two redundant and two prime -- while the pneumatic system requires only one compressor.

EFFICIENCY, POWER, WEIGHT, AND HEAT DISSIPATION

Tables I, II, III, and IV compare the hydraulic and the pneumatic hoist-drive systems within an overall integrated secondary power system. The comparison is based on a two-point suspension system with a capacity of 25 tons and a hoisting velocity of 60 feet per minute.

The hydraulic system would display a minimum heat-dissipation requirement of 2630 Btu/min, while the pneumatic system displayed only 270. Pneumatic system cooling is required for the high-speed gear reducer and for minor turbine cooling. Cooling for the main gear reducer and hoist mechanism is not considered for either drive. (A nonregenerative-type braking for hydraulics will require 3940 Btu/min heat dissipation capacity.)

BRAKING DURING LOWERING MODE

We decided not to use mechanical friction brakes during the lowering mode of a fully loaded hoist. Friction brakes generate excessive heat and exhibit poor reliability. Lowering the

load, therefore, is accomplished with the available working fluid and the motors themselves.

The braking energy in the hydraulic system is absorbed by the drive through the pump, which in this mode becomes a motor. The lowering speed is controlled by the pump swashplate position.

TABLE I. ASSUMED COMPONENT DESIGN EFFICIENCY OF HYDRAULIC AND PNEUMATIC SYSTEMS

Component	Efficiency (%)	
	Hydraulic	Pneumatic
Pump	85	-
Motor	85*	-
Compressor	-	80
Turbine	-	85
High-Speed Gear Reducer	-	95
Gearing and Hoist** (Mechanical Efficiency)	75	75

*A hydraulic-motor efficiency of 85% is not possible unless the motor is at maximum displacement, which is dictated for g loading considerations; estimated efficiencies are closer to 65%. This condition may be improved by future development; otherwise, a 30% increase in the power input shown in Table II is required.

**Efficiency on the basis of this study is approximately 85%. This change is reflected in the definition of system losses.

TABLE II. POWER PARAMETERS OF HYDRAULIC AND PNEUMATIC SYSTEMS

Description	Power (hp)	
	Hydraulic	Pneumatic
Total Power Absorbed by Load	91.0	91.0
Motor Output Power Required	121.0	127.5
Motor Losses	18.2	19.1
Pump/Compressor Losses	26.4	17.4
Transport Losses	10.4	20.0
Power Input to Pumps or Compressor	176.0	184.0
Complementary System Power	10.3*	-
Total System Power Input	186.3	184.0

*Complementary system for hydraulics consists of power for heat dissipation, servo-flow control, and leakage compensation within loops. Pneumatic power is negligible.

TABLE III. WEIGHT ESTIMATES OF HYDRAULIC AND PNEUMATIC COMPONENTS—SINGLE POWER SOURCE

Component	Hydraulic		Pneumatic	
	Number	Weight (lb)	Number	Weight (lb)
Pumps	2	90	-	-
Compressors	-	-	1	23
Motors	2	120	2	30
Complementary Pumps	2	20	-	-
Fluid Reservoirs	2	48	-	-
Heat Exchangers, Including Motor and Fan	2	36	-	-
High-Speed Gear Reducers With Integral Lube Pump, Heat Exchanger, and Fan	-	-	2	36*
Power-Transfer Lines (Fittings, Fluid and Supports)	4	480**	1	96
Filters, Controls, Servos, Relief Valves, and Misc.	2	80	2	80
Total***		874		265

*An independent high-speed gear reducer is assumed. Integral turbine cooling and lubrication system is included.

**Weight for the hydraulic lines is based on 2.4 pounds per linear foot (including fittings, support and fluid; steel weight for the pneumatic lines is based on stainless tubing 0.025 inch thick, plus a factor of 2 for supports, etc.

***The total does not include an on-off brake or a high-ratio gear reducer with an integral brake for either system. Gear reducer weight is a function of hoist-drum diameter and is dependent on tension-member configuration (single cable or reeved).

TABLE IV. WEIGHT ESTIMATES OF HYDRAULIC AND PNEUMATIC COMPONENTS—REDUNDANT POWER SOURCE*

Description	Hydraulic		Pneumatic	
	Number	Weight (lb)	Number	Weight (lb)
Redundant Power Pumps	2	90	1	-
Redundant Complementary Pumps	2	90	-	-
"Delta" Fluid Reservoirs	2	24	-	-***
"Delta" Power Transfer Lines	4	240**	-	3
Crossover Valving Sets	8	40	1	6
Engine-Bleed Air Pressure Regulator	-	-	1	5
Engine-Bleed Air Height Exchanger with Aspirator	-	-	1	10
REDUNDANT SYSTEM TOTAL		414		21

*The redundant hydraulic system represents the most austere approach. No redundant complementary system is provided. The interface between the prime and redundant power is accomplished with crossover valving sets (four to the power loops; four to the complementary systems).

**A separation of 25 feet between the redundant power source and the hoist-drive power-loop connection is assumed.

***Redundant pneumatic power transfer lines are integral with the engine starting system. There is no charge, therefore, to the hoist-drive system.

Pneumatic dynamic braking is accomplished in a similar manner, except that the braking energy is absorbed by the turbine and reflected in increased air temperature, which is diverted outboard. Rate-of-descent control in this mode is accomplished by varying the air supply to the turbine through the forward rotation nozzles, where the lowering speed is inversely proportional to the airflow.

ACCOMMODATING A 2G LOAD

The motor for hoisting application supplies the torque to drive the hoist. This torque is a function of the load, the drum diameter, and the gear reduction. The torque-generating capability of the hydraulic motor is a function of its displacement and the maximum supply pressure, so the motor must be designed for twice its normal displacement to accommodate a 2.0g loading. This results in larger size and increased weight. The hoist speed is controlled by the pump swashplate. But the air-turbine motor, when based on an impulse turbine design, is not penalized in the same manner. Its characteristics inherently accommodate a 2.0g loading. The hoisting speed will decrease to zero at 2.0g, but the system will be fully capable of holding the load during short acceleration transients. (Accelerations higher than 2.0g for the pneumatic system are discussed under the Air Turbine Motor.)

Performance characteristics for hydraulic and pneumatic motors operating above design load are shown in Figure 7. The hydraulic motor in this illustration, for purpose of control simplicity, is assumed to be of a two-position swashplate design.

RELIABILITY

The reliability analysis of the hydraulic and pneumatic systems was based on current technology. The mission reliability of the hoist drive was interpreted as the probability of the system performing successfully for a required mission duration. The mission time for a flight vehicle was considered as two hours, with two sorties minimum. Since the hoist drive is not required to operate during the entire flight, the hoist time was assumed to be .5 hour per flight hour. This time is felt to be conservative to account for hoist-drive system failure which may occur in flight when the system is inoperative. Table V presents the results of this analysis.

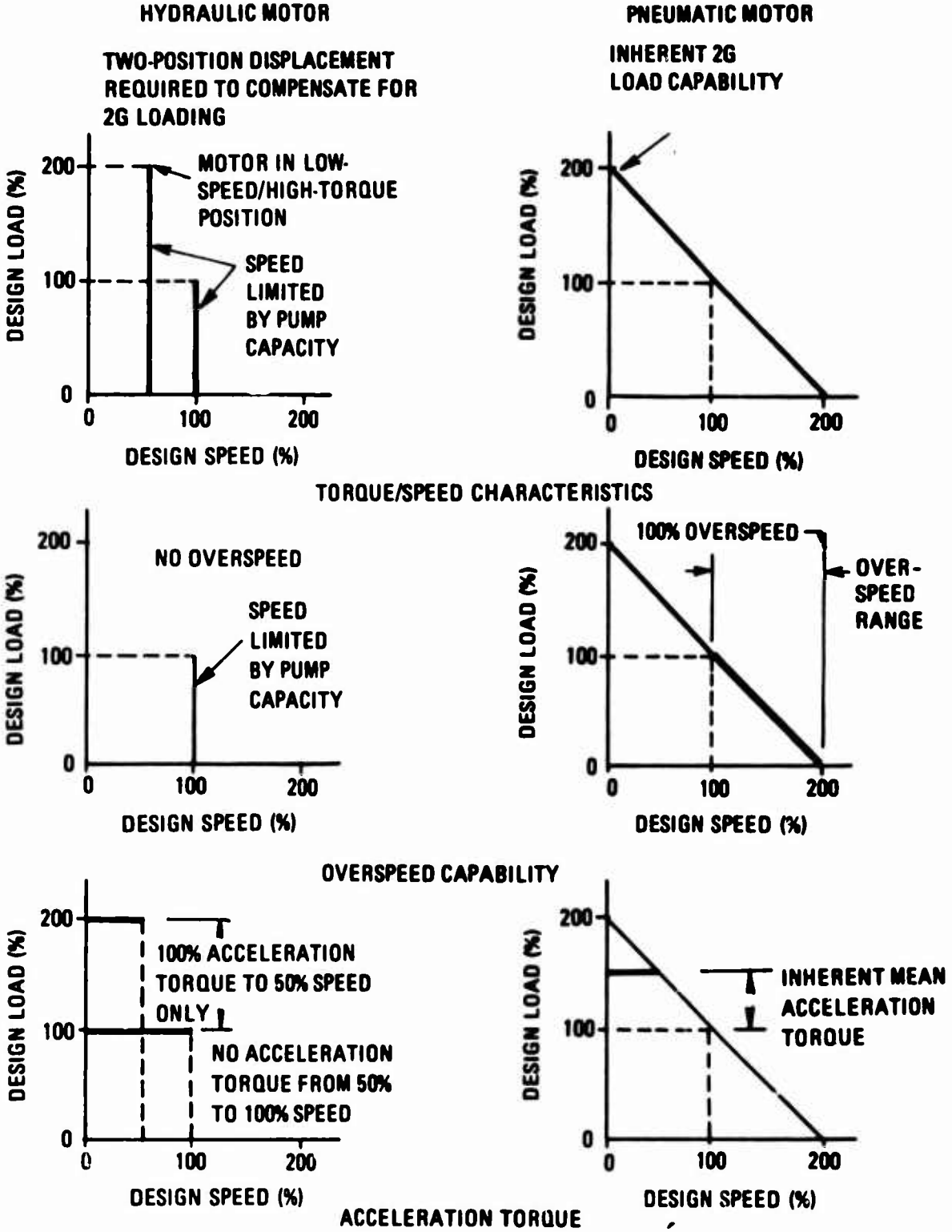

Figure 7. Performance of Hydraulic and Pneumatic Motors Above Design Load.

TABLE V. PREDICTED RELIABILITY OF HYDRAULIC AND PNEUMATIC HOIST-DRIVE SYSTEMS			
System	Total Malfunction Rate	Mission Failures Per Flt Hr	Mission Reliability
Hydraulic Hoist Drive	.035890	.000416	.999169
Pneumatic Hoist Drive	.006065	.000160	.999680
Goal—Hoist Drive	.002426	.000064	.999873
Total Aircraft System	1.050300	.009557	98.100000

Malfunctions Defined

Total Malfunctions — All reported events which, upon troubleshooting, result in isolation and correction of a malfunction.

Primary Malfunctions — Malfunctions not caused by faulty maintenance, improper handling, improper operator technique, FOD, or failure of related components.

Nonprimary Malfunctions — Malfunctions caused by faulty maintenance, improper handling, etc.

Functional Failure — Malfunctions resulting in complete loss or extensive degradation of an item's function.

Mission-Oriented Failure — Malfunctions which affect the capability of the aircraft to perform its function to the extent that a flight is aborted, cancelled or delayed.

Malfunction-Induced Removal — Events which, upon troubleshooting, result in malfunctions being correctable by removal and replacement of the item or component.

On-Board Fixes — Events which, upon troubleshooting, are correctable by maintenance without removal.

Data Base

The reliability analyses were based on data contained in the following documents:

- D8-2477 - CH-47C, BOEING CH-47C RELIABILITY AND MAINTAINABILITY FIELD EXPERIENCE, U.S. ARMY AVIATION TEST BOAPD, FORT RUCKER, ALABAMA

  Operatiónal and maintenance data recorded by personnel maintaining aircraft at the Test Board facility were forwarded to Boeing for further analysis. Data covers a 15-month period from April 1968 to June 1969.

- D6-53584 - Boeing, AIRCRAFT FIELD EXPERIENCE COMPONENT ANALYSIS

  This document contains an analysis of military maintenance data on a representative list of commonly used aircraft components, statistically extracted from military records by the Boeing Military Aircraft Data Central. Aircraft covered in this report are B-52, B-58, C-123, C-130, KC-135, C-141, F-4C, F-104C, F-105D, and T-38A.

- D6-10095 - Boeing, SST PREDICTION STANDARD RATES

  This document summarizes Boeing's experience on the 707, 720, and 727 commercial aircraft fleet. Operational and maintenance data were analyzed and tabulated as standard rates for use in SST predictions.

- SP63-470, USN, FAILURE RATE DATA HANDBOOK (FARADA)

  Tri-service and NASA program of data collection and analysis of data from industry and the Armed Forces.

- D6-57166C - 130E-2 - AIRCRAFT FIELD EXPERIENCE - C-130

  Operational and maintenance data as recorded in the USAF 66-1 data system are analyzed and documented.

Data from these sources were used to supplement CH-47C data in instances where comparable components were not available in the CH-47C or where data were considered inadequate. An adjustment factor (K) of 2 was used to correlate fixed-wing aircraft data to the helicopter environment. Tables VI and VII present the data base. Figures 8, 9, and 10 show models used for calculating reliability.

TABLE VI. HYDRAULIC HOIST-DRIVE COMPONENTS RELIABILITY DATA

Component	Number Per Aircraft	Total Malfunction Aircraft	Functional Failure Rate
Pumps			
Pump	4	.001500	.000750
Control Valve	4	.000320	.000160
Check Valve	12	.000120	.000068
Hose	28	.000290	.000029
Tube	8	.000170	.000017
Shutoff Valve	8	.000260	.000130
APU Accessory Gear-box	1	.000188	.000041
Motors			
Motor	2	.000570	.000142
Transfer Valve	2	.000260	.000130
Check Valve	4	.000120	.000068
Hose	4	.000290	.000029
Tube	4	.000170	.000017
Complementary System			
Pressure Reg. Valve	4	.000420	.000139
Filter	4	.000340	.000068
Check Valve	10	.000120	.000068
Thermal Bypass Valve	2	.000220	.000073
Pressure Bypass Valve	2	.000220	.000073
Cooler	2	.000400	.000048
Reservoir	2	.000100	.000020
Pump	2	.000750	.000375
Shutoff Valve	2	.000260	.000086
Bleed Valve	8	.000130	.000065
Hose	10	.000290	.000029
Tube	6	.000170	.000017

TABLE VII. PNEUMATIC HOIST-DRIVE COMPONENTS RELIABILITY DATA AND GOALS

Component	Number Per Aircraft	Data		Goals	
		Component Total Malf. Rate	Funct. Fail. Rate (Mission)	Component Total Malf. Rate	Funct. Fail. Rate (Mission)
Hoist-Drive Components					
Air Turbine Motor	2	.000835	.000085	.000334	.000034
Muffler/Exhaust	2	.000400	.000000	.000160	.000000
Air Duct	1	.000800	.000008	.000320	.000003
Shutoff Valve	1	.000180	.000090	.000072	.000036
Electr. Motor/Lube Contr Pump	2	.000100	.000025	.000040	.000010
Components Affecting Mission Reliability*					
Check Valves	5	.000120	.000040	.000048	.000016
Bleed Air Shutoff Valves	3	.000180	.000090	.000072	.000036
Press. Reg. Valve	1	.000670	.000190	.000268	.000076
Temp. Reg. Valve	1	.000670	.000190	.000268	.000078
Heat Exchanger	1	.000430	.000043	.000172	.000017
Heat Exch. Atm.	1	.000480	.000048	.000192	.000019
Compressor	1	.000300	.000030	.000120	.000012
Main Duct	1	.000250	.000001	.000100	.000000
Equipment Added to Other Systems By Selection of Pneumatic Hoist Concept**					
Generator Pump Atm.	1	.000835	.000000	.000334	.000000
Atm. Exhaust Ass'y	1	.000400	.000000	.000160	.000000
Atm. Shutoff Valve	1	.000180	.000000	.000072	.000000
Atm. Supply Duct	1	.000200	.000000	.000080	.000000
Generator/Pump Gearbox	1	.000800	.000000	-	.000000

* Not considered in total malfunction calculations for the hoist-drive system since failures would occur regardless of drive medium selection. These components would normally affect mission reliability only through the pneumatic hoist drive.

**Components added to the aircraft total malfunction rate due to selection of pneumatic hoist-drive system.

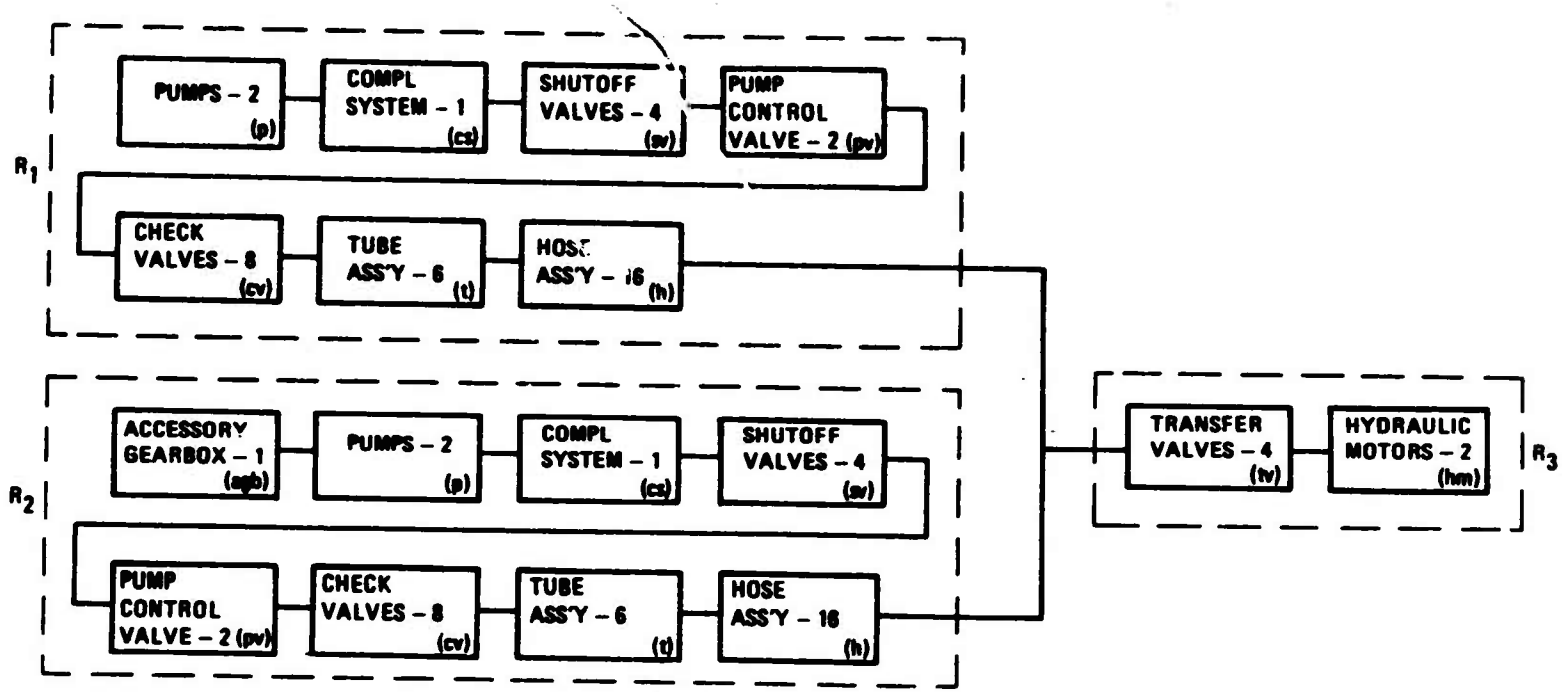

$$R_{HYD\ HOIST\ DRIVE} = [\,1-(1-R_1)(1-R_2)\,]\ R_{tv}^{4}\ R_{hm}^{2}\ R_3$$

WHERE:

$R_1 = e^{-t\lambda_1};\ \lambda_1 = 2\lambda_p + \lambda_{cs} + 4\lambda_{sv} + 2\lambda_{pv} + 8\lambda_{cv} + 6\lambda_t + 16\lambda_h$

$R_2 = e^{-t\lambda_2};\ \lambda_2 = \lambda_1 + \lambda_{agb}$

$R_3 = e^{-t\lambda_3};\ \lambda_3 = 4\lambda_{tv} + 2\lambda_{hm}$

$R_{hhd} = [\,1-(1-e^{-\lambda_1})(1-e^{-\lambda_2 t})\,]\ e^{-\lambda_3 t}$

Figure 8. Hydraulic Hoist-Drive Block Diagram, Identifying Symbols and Presenting Equations for Calculating Reliability.

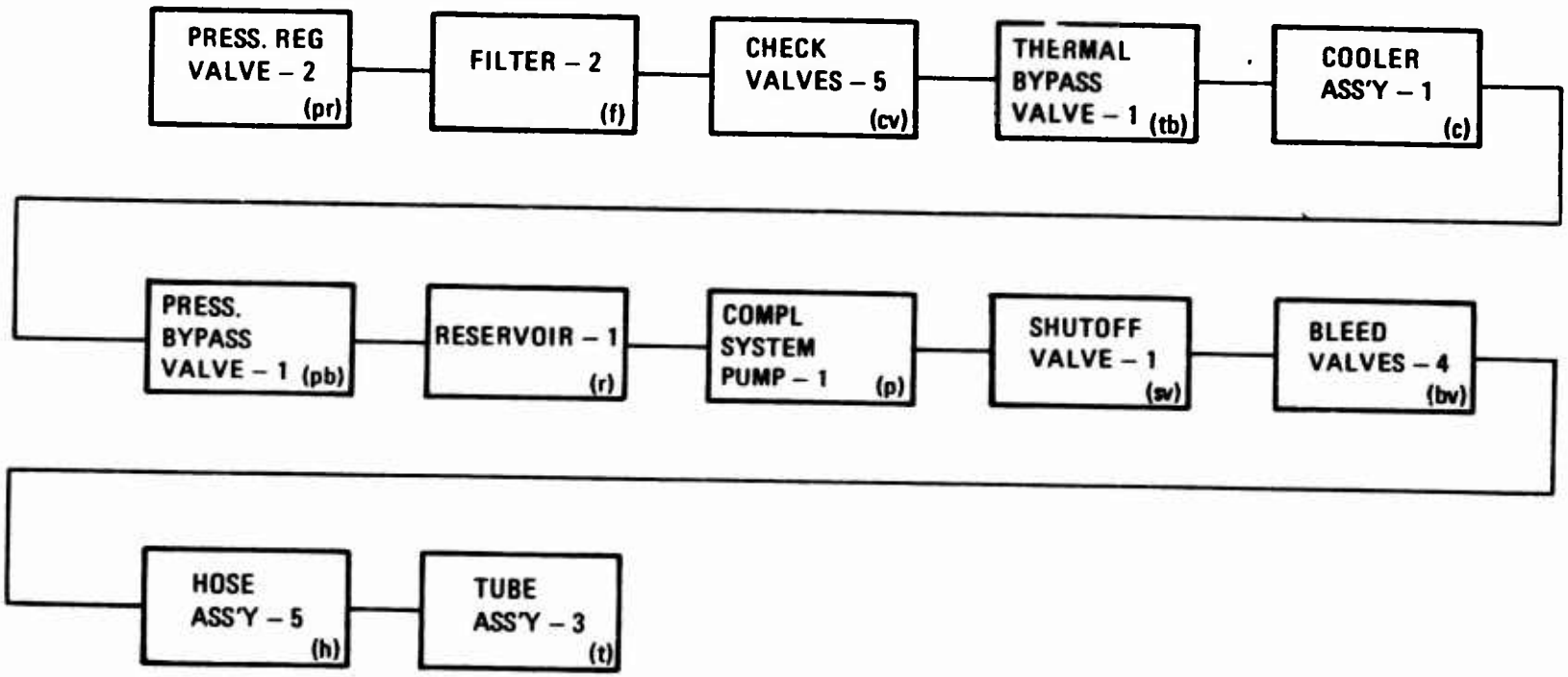

RELIABILITY

COMPLEMENTARY SYSTEM (cs)

$$= R_{pr}^2 \; R_f^2 \; R_{cv}^5 \; R_{tb} \; R_c \; R_{pb} \; R_r \; R_p \; R_{sv} \; R_{bv}^4 \; R_h^5 \; R_t^3$$

$$= e^{-t} \Sigma (2\lambda_{pr} + 2\lambda_f + 5\lambda_{cv} + \lambda_{tb} + \lambda_c + \lambda_{pb} + \lambda_r + \lambda_p + \lambda_{sv} + 4\lambda_{bv} + 5\lambda_h + 3\lambda_t)$$

FAILURE

$$= e^{-t} \lambda_{cs}$$

RATE (cs)

$$= 2\lambda_{pr} + 2\lambda_f + 5\lambda_{cv} + \lambda_{tb} + \lambda_c + \lambda_{pb} + \lambda_r + \lambda_p + \lambda_{sv} + \lambda_{bv} + 5\lambda_h + 3\lambda_t$$

Figure 9. Hydraulic Hoist-Drive Complementary System Block Diagram, Identifying Symbols and Presenting Equations for Calculating Reliability.

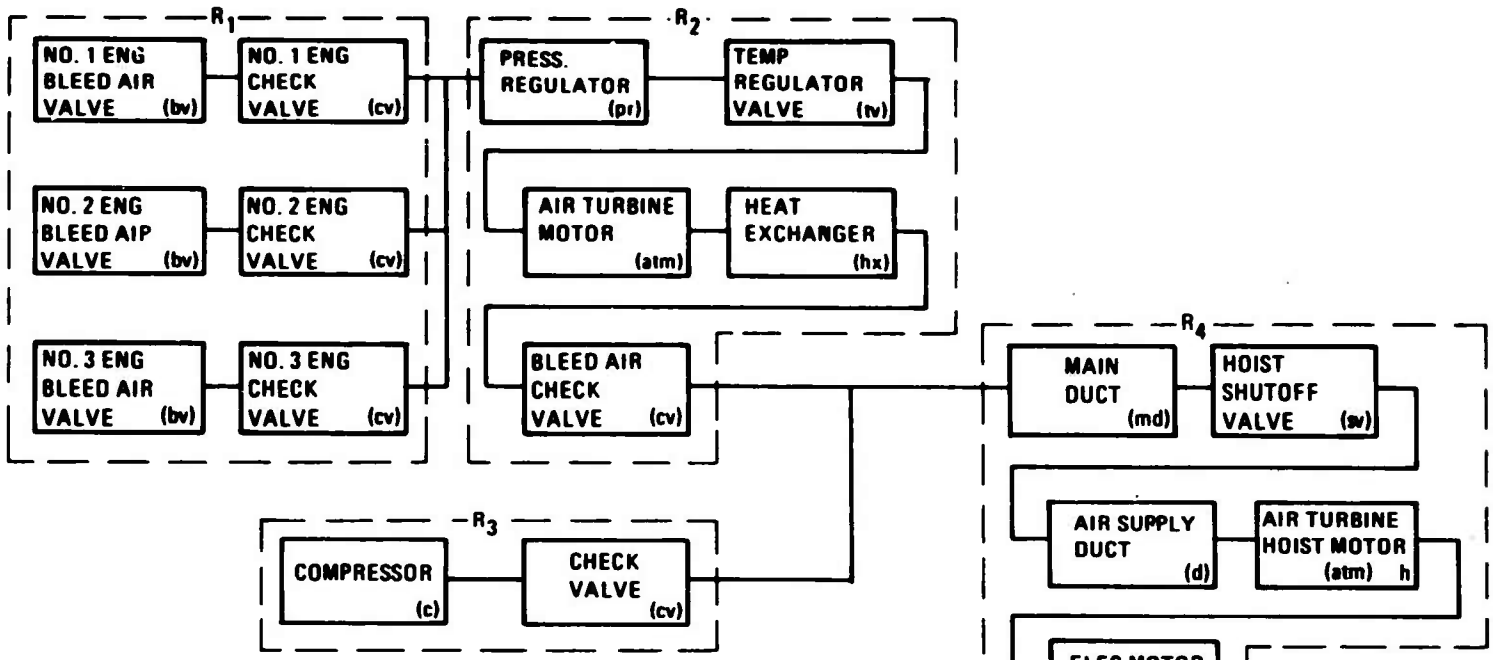

$$R_{\text{PNEUMATIC HOIST DRIVE}} = |1-(1-R_1R_2)(1-R_3)|\ R_4$$

WHERE:

$$R_1 = 1-(1-R_{bv}\cdot R_{cv})^3 = 1-[1-e^{-t(\lambda_{cu}+\lambda_{cv})}]^3$$

$$R_2 = R_{pr}\ R_{tv}\ R_{atm}\ R_{hx}\ R_{cv} = e^{-t\lambda 2};\ \lambda_2 = \lambda_{pr}+\lambda_{tv}+\lambda_{atm}+\lambda_{hx}+\lambda_{cv}$$

$$R_3 = R_c\ R_{cv} = e^{-t\lambda 3};\ \lambda_3 = \lambda_c+\lambda_{cv}$$

$$R_4 = R_{md}\ R_{sv}\ R_d\ R^2_{atm\,h}\ R^2_{mp} = e^{-t\lambda 4};\ \lambda_4 = \lambda_{md}+\lambda_{sv}+\lambda_0+2\lambda_{atm,h}+2\lambda_{mp}$$

Figure 10. Pneumatic Hoist-Drive Block Diagram, Identifying Symbols and Presenting Equations for Calculating Reliability.

Reliability Goals

Reliability goals were developed for components of the pneumatic system from the reliability analyses of the pneumatic hoist-drive system. Table VII shows these goals. System goals shown in Table V were calculated based on the component goals. Since the data used in the analysis is representative of mature 1965 design technology, it was necessary to extend this to a technology base expected in the 1972 era. Figure 11 shows a trend curve for air turbine motors developed from data obtained from a survey of industry conducted as part of Eustis Directorate, Army Air Mobility Research and Development Laboratory Contract DAAJ02-70-C-0046, USAAMRDL Technical Report 71-52. SECONDARY POWER SYSTEM STUDY FOR ADVANCED ROTARY-WING AIRCRAFT. The reliability objective developed was based on a 40% reduction in failure rate.

MAINTAINABILITY

Based on the reliability calculations, the comparative "world-wide" maintenance man-hours per flight hour (MMH/FH) for the hydraulic and pneumatic hoist systems are shown in Table VIII.

SAFETY

Objective

The safety objective in the design of the hoist-drive system is to ensure that the operation of the proposed system in the projected environment would not endanger the safety of personnel or cause damage to aircraft equipment in the event of a failure in the hoist-drive system. Specific attention was applied to the avoidance of potential critical (Class III) or catastrophic (Class IV) hazards as defined in MIL-STD-822, paragraph 3.14. Figure 12 summarizes the hazards which must be controlled for the total cargo handling system.

Potential Hazards of Power Drive

Sources of potential hazards and appropriate countermeasures associated for both the hydraulic and the pneumatic hoist-drive systems are shown in Table IX. Both pneumatic and hydraulic systems have been used in aircraft designs with acceptable levels of safety. The combustible nature of hydraulic fluid, however, has historically been a concern of both designers and users of aircraft. Even though designs for the most part have been successful in preventing in-flight

TABLE VIII. HYDRAULIC AND PNEUMATIC HOIST SYSTEM MAINTENANCE REQUIREMENTS

Subsystem	Hydraulic					Pneumatic					MTTR[e]	
	Unscheduled MMH/FH[a]			Sched. MMH/FH	Total MMH/FH	Unscheduled MMH/FH			Sched. MMH/FH	Total MMH/FH		
	Org.[b]	D.S.[c]	G.S.[d]	Org.		Org.	D.S.	G.S.	Org.		Hyd.	Pneu.
Controls Controls, Feedback Logic Sensors	.0139	.0085				.0138	.0084					
Power Drive (Hyd. Pumps. Motors, Tubing, Hoses, etc.)	.1254	.0124	.0468	.126	.461	.0057	.0061	.040	.038	.240	.62	.43
Suspension Cables, Hooks Release	.1001	.0061				.1000	.0061					
Winch Gearing, Brake, Drum, Strut, etc.	.0181	.0036				.0182	.0036					
Totals	.257	.031	.047	.126	.461	.138	.024	.040	.038	.240		

a MMH/FH - Maintenance Man-hours Per Flight Hour
b Org. - Organization Maintenance Level
c D.S. - Direct Support Maintenance Level
d G.S. - General Support Maintenance Level
e MTTR - Mean Time To Repair

ignition of hydraulic fluids, the protective devices and isolation features are often defeated as a secondary effect or they become destroyed in a crash. The air in the pneumatic system, in contrast, is noncombustible and is of such low pressure and temperature as to present no hazard to the aircraft. Note that most of the components employed in a pneumatic hoist-drive concept would be present in the aircraft even if another system of hoist power were selected. Hence, a pneumatic hoist-drive system will add little to the aircraft's hazardous energy sources.

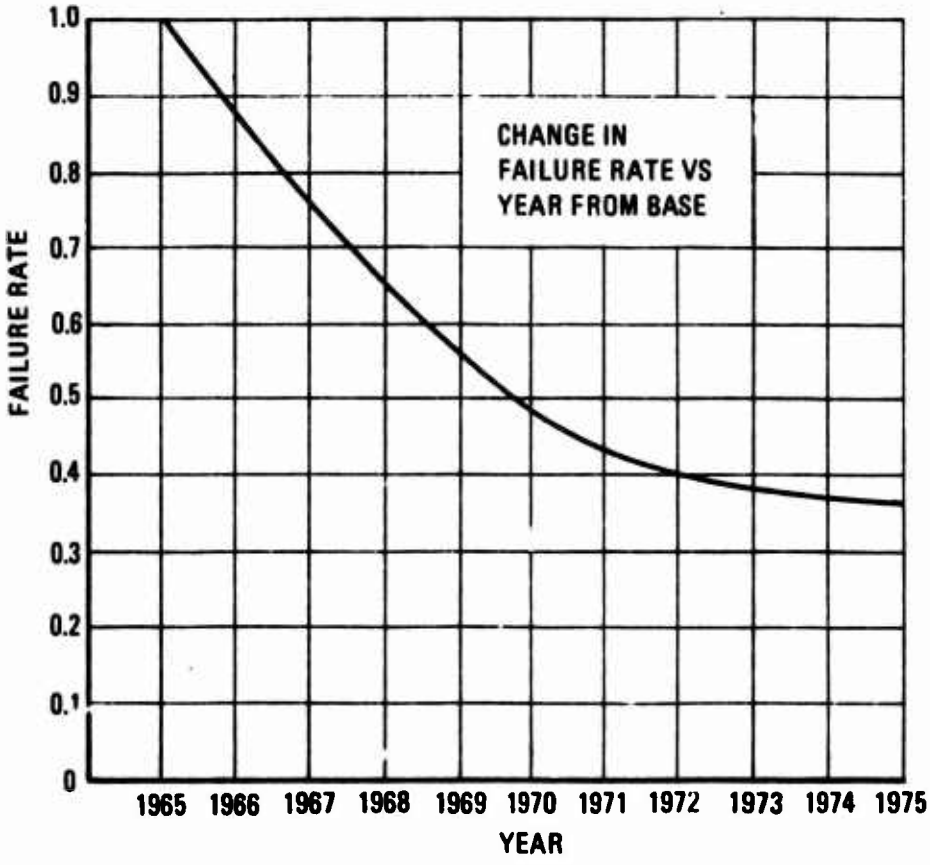

Figure 11. Projected Improvement in Reliability of Pneumatic Hoist-Drive System.

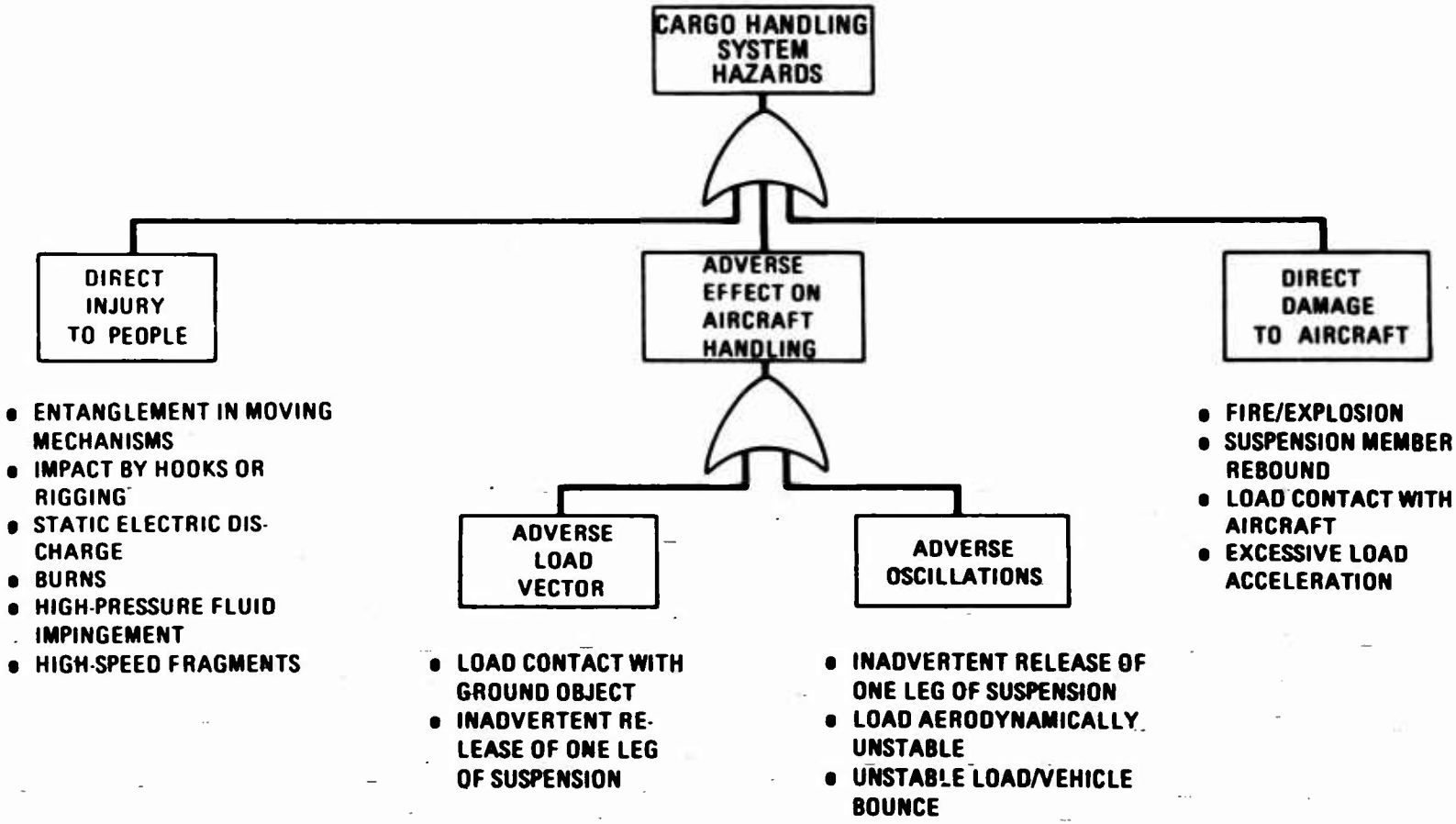

Figure 12. Hazards of a Cargo Handling System.

TABLE IX. POTENTIAL HAZARDS OF HYDRAULIC AND PNEUMATIC SYSTEMS

Failure Mode	Effect on Operation	Class Hazard	Design Considerations	
			Hydraulic	Pneumatic
1. Fire	• Direct damage to aircraft or personnel • Potential loss of a/c control due to structural damage, injury to pilot, or damage to flight controls.	III	• Controls required to isolate hydraulic lines from ignition sources. Provisions must also prevent leaked fluid from migrating to ignition source.	• No flammable fluid source in the system.
2. Impinges High-Pressure Fluid on Personnel	• Direct injury to personnel.	III	• Provisions required to isolate hydr. lines & components from crew space. 3000 psi hydr. fluid is hazardous.	• No high pressure source.
3. Hot Fluid Impinges on Personnel	• Direct injury to personnel.	III	• Provisions required to isolate hydr. lines & personnel from crew space. 3000°F hydr. fluid has rel. high heat capacity. Danger of dripping or flowing into inhabited areas.	• Air has low heat capacity. Continued exposure to direct blast of air would be required to cause injury. Hot air rapidly disperses into ambient air.
4. Fragmentation From High-Speed Components	• Possible injury to personnel or aircraft.	III	• No high-speed components.	• ATMs' case will contain hub burst.
5. Loss of Power Medium to A Hoist-Drive Motor	• Winch system stops; brakes engage with loss of pressure. Other winch in some configurations can be worked independently.	III	• Redundant hydr. supplies are provided up to the winch motor transfer valve.	• Redundant air supplies are provided to the main pneumatic duct ass'y. Failure of the duct to the extent required to cause loss of air supply is considered remote. Gross loss of air in the present configuration would result in loss of air to both hoists.
6. Fluid Conductor Rupture	• Possible occurrence failure modes 1-3 or 5	IV	• Same as shown for individual failure modes.	• Same as shown for individual failure modes.
	• Possible fragmentation from conductor may cause direct injury to personnel.	III	• Hydraulic fluid does not possess much compressive energy and would not be expected to produce fragments in the event of a rupture.	• Low-pressure air does not possess enough compressive energy to cause a fragmentation hazard.

VULNERABILITY AND SURVIVABILITY

Survivability criteria were established for the probability of a "B" kill for a 90-10 mix ratio between 7.62rm and 12.7rm projectiles.

Using the CH-47 combat experience in the Vietnam environment, the hit density based on 1,000,000 flight hours is 1.4 hits/sq. ft. of surface area. Additionally, the CH-46/CH-47 experience indicates that of the 200 hits in the hydraulic system, 6 have caused in-flight fires. Therefore, the probability of a fire given a hit in the hydraulic hoist system is:

$$P_{fkh} = 6/200 = .03$$

The vulnerable area of the hydraulic hoist system scaled to the high-capacity requirement is:

$$A_r = (A_p)\ (P_{fkh})$$

$$A_r = (140.4)\ (.03) = 4.21 \text{ sq ft}$$

where A_p is total presented area.

If the hydraulic hoist system were to be employed in an RVN-type of environment, the expected number of "B" kills in an equivalent 1,000,000 flight hours is:

$$K_b = (1.4)\ (4.21) = 5.87$$

or approximately 6 aircraft.

Component values used in the analysis are shown in Table X.

The probability of a "B" kill for the pneumatic hoist system concept is eliminated; no fire hazard is present in the system.

Safety of the pneumatic hoist-drive system is felt to be superior to the hydraulic system. Although successful hydraulic systems have been employed in aircraft, the problem of a flammable fluid source has always been present in these systems. The size and capacity requirements of a hydraulic hoist system for such aircraft as the heavy-lift aircraft will only add to this problem. In a combat situation, the larger vulnerable area associated with this hydraulic system will present a much larger target than the hydraulic systems employed in current helicopters.

TABLE X. TOTAL PRESENTED AREA OF HYDRAULIC DRIVE SYSTEM

Component	Quantity	Estimated Size	Total Presented Area (sq ft)
Pumps, hydraulic, supply	4	5 in. dia. x 5 in. length	2.64
Motor, hydraulic	2	1.25 x pump area	1.64
Coolers	2	10 in. x 10 in. x 5 in.	4.80
Pumps, Complementary	2	.25 x supply pump	.33
Lines (tubes, hoses, valves etc.)	10	1 in. dia x 50 ft length	131.00
		Total	140.40

SYSTEM REQUIREMENTS

After selecting the type of power drive — the advanced-technology pneumatic concept — specific system requirements were developed to guide the final design. Based on studies conducted which also include actual flight test data analysis and further reflecting the current Army thinking, the hoist design performance for both single- and multipoint hoisting modes shall meet the following criteria:

DESIGN DAY

To accommodate anticipated growth at sea level, 95°F ambient operations, the system performance is based on 4000-ft static 95°F ambient design-day conditions.

OPERATING AMBIENTS

The operating ambient conditions are from -65°F to +125°F at pressure altitudes from 0 to 10,000 feet.

TEMPERATURE LIMITATIONS

The maximum air-supply temperature within the fuselage shall be limited to 450°F.

HOISTING MODES

The system shall provide for two hoisting modes:

- Two-point (multipoint) suspension mode utilizing two hoists and hoist drives, each capable of independent speed and reversing control and synchronous, bi-directional variable-speed operation for variable load capacities.
- Single-point suspension mode accomplished by coupling the suspension system of both hoists into a single-point adapter and hook assembly. Infinitely variable bidirectional speed-control capability for variable external load capacities is required.

DESIGN LOAD

The system shall accommodate in both hoisting modes and external load design capacities with conditions as follows:

- Without application of the brake, the hoist-drive system shall be capable of positively holding the design load when subjected to 2.5g acceleration.
- Under 1.0g conditions, the system shall accommodate design load at a minimum hoisting velocity of up to 60 feet per minute.
- Load asymmetry accommodation based on 60/40 percent load distribution with the greater load on either hoist.
- The system, including the hoist and hoist-drive, shall further accommodate an increased demand from a 30-degree coning angle, aerodynamic drag, and the hook and tension-member weight.

PNEUMATIC POWER SOURCE

The two sources of pneumatic power are:

- Simultaneous bleed from three main propulsion engines. The bleed passes through a pressure regulator and a precooler, wherein the air supply is conditioned to the hoist-drive system pressure requirements and compatible with temperature limitations.
- Compressor-generated power designed to supply air characteristics that result in an optimum hoist-drive system design within the appropriate pressure levels and temperature limitations.

PNEUMATIC POWER DISTRIBUTION SYSTEM

The additional nonhoist-related aircraft systems powered pneumatically are the main engine starting, the environmental controls system, the two hydraulic pump air turbine drives, and the air-turbine-driven electrical alternator. Maximum capacities and simultaneous air capacity requirement, when full-capacity hoisting is required, are estimated at 30 percent above the full-hoisting airflow requirement.

PNEUMATIC AND HOIST-DRIVE SYSTEM CONTROL DESIGN

All facets of the total aircraft pneumatic system control, distribution, priority, and operation must be compatible for the control of the hoist system. The hoist system shall be operated by the pilot, copilot, load-control crewman, and ground-stationed operator. Control priority is reserved for the pilot.

PNEUMATIC POWER REDUNDANCY

The primary in-flight pneumatic power source shall be main engine bleed. In the event that one engine bleeding system fails, yet all three engines are operative, the remaining two bleeding systems shall supply adequate bleed to power all power systems, including full hoisting power.

In the event one engine fails, the APU shall be started. Full-capacity hoisting power, including the other pneumatic power systems requirements, is supplied by the APU-driven compressor. For ground operation and for system checkout, the APU-generated pneumatic is utilized. Provisions for ground cart connections and/or "buddy system" operation shall be provided.

VARIABLE HOIST SPAN

The distance between the two hoists shall be variable to accommodate variable-length external loads. Hoist positioning shall be accomplished without disconnecting/reconnecting the pneumatic power distribution system ducting.

DYNAMIC BRAKING

The concept of dynamic braking shall be employed for load lowering and in-flight load attitude control, and shall be accomplished with the air turbine motors of the hoist-drive system. Infinitely variable rate-of-descent control is required.

STATIC/EMERGENCY BRAKES

The static brakes are designed for holding and for emergency dynamic braking in the event that the ATM dynamic braking malfunctions. One full-load dynamic braking cycle at design capacity is required before replacement and/or repair.

SYSTEM PERFORMANCE

The system capacity is based on a two-point suspension mode capable of accommodating the design load under the following conditions:

- The load is coupled through the suspension system of two independent hoists capable of synchronous and independent bidirectional velocity and direction control. Each hoist is powered by separate hoist-drive systems consisting of air turbine drivers.

- Each hoist is capable of accommodating 60 percent of the external load resulting in a permissible load longitudinal cg shift that is based on a 60/40 load distribution on either hoist.

- In addition to the external load weight, each hoist shall accommodate the suspension system weight, consisting of the coupling and the tension member plus the accommodation of the negative lift factor of estimated equivalent to be 1,512 pounds. (This is based on a frontal area of 100 square feet at 130 knots.)

- The minimum vertical hoisting velocity under these conditions is 60 fpm with the design load.

- A capacity increase of 15 percent in the tension-member pull and hence in the torque on the hoist drum is required due to a 30-degree coning angle (tension member angle with the vertical).

- Minimum torque-generating capability of the hoist driver is based on the above conditions. These torque requirements are in conjunction with the design velocity hoisting.

- The minimum stall torque developed by the hoist driver(s) is based on the design external load subjected to a 2.5g acceleration under all conditions defined. Application of the brake for this capability is not acceptable.

- Vertical hoisting velocity requirement with zero load is 120 fpm. (Proportionate speed reduction due to tension member and coupling weight is acceptable).

- Hoisting velocities with external load capacities less than the specified design load capacity shall be

increased proportionately consistent with the air turbine torque/speed characteristics and capability.

- The empty-hook payout speed objective at design-day condition is 120 fpm. This capability is based on zero weight assisting the reversing rotation. Disconnect or clutching between the hoisting driver and the drum is not acceptable.

- The minimum specified hoisting velocity of 60 fpm under design load conditions shall be exceeded to the fullest extent of the air-turbine driver capability, limited only by the availability of the pneumatic power supply.

- For design-day ambients under 95°F, the system capacity shall equal or exceed design-day system capacity.

- Reduced system capacity at ambient temperatures above 95°F and/or higher altitudes than 4000 feet will be acceptable. However, the percentage change in capacity shall not be greater than the percentage change in helicopter lift capability consistent with the "average" engine lapse rate at normal power settings.

- Empty-hook hoisting and payout velocity reduction is acceptable provided the reduction does not exceed the nozzle spouting velocity reduction as a result of colder air supply temperature.

- The hoist system will be designed for a minimum life of 10,800 cycles. Each cycle consists of: (1) deploy cable unloaded, (2) pick up and hoist load (3) deploy load, and (4) release load and hoist unloaded tension member.

- The minimum fatigue load spectrum for each of the suspension modes shall be as follows:

  — 10% of cycles at 125% of design load

  — 75% of cycles at 100% of design load

  — 10% of cycles at 50% of design load

  — 5% of cycles at 25% of design load

Dynamic Braking

Lowering the load at infinitely variable speed from zero to a minimum of 60 fpm shall be accomplished with the

air-turbine motors. The wheel design reversing rotation torque/speed characteristics shall be consistent with the referenced characteristics of Figure 13. Application of the friction brake for this function is not acceptable except for emergency conditions.

COMPONENT EFFICIENCIES AND SYSTEM LOSSES

The major component efficiencies and system losses are as follows:

- Low-speed gearing integral with the hoist drum based on approximately 400:1 gear reduction is 90 percent efficient at design speed and load.
- High-speed gearing integral with the air-turbine motor driver based on 10-12:1 gearing reduction is 95 percent efficient at design speed and load.
- Cable bending and miscellaneous losses are 5 percent.
- Pneumatic power transfer pressure losses between the generating sources and the air turbine motor driver are 5 percent of the source pressure absolute.
- Temperature loss between the source(s) and the drivers is 10 percent of the actual compressor ΔT based on 80 percent adiabatic compressor efficiency at design-day conditions.
- Adiabatic turbine efficiency based on design-day conditions at optimum operating point is 85 percent.
- The constant-speed, shaft-driven, adiabatic compressor efficiency shall be 80 percent minimum at design-day conditions.

PNEUMATIC SYSTEM PRESSURE

The pressure limitations are based on the compressor efficiency and limiting temperature of 450°F maximum. On the basis of 80 percent minimum compressor adiabatic efficiency, the system supply pressure shall be 4.3 atmospheres.

CONDUCTOR SIZING

The conductors are designed on the basis of maximum simultaneous airflow requirements as defined above and based on

VARIABLE-NOZZLE TURBINE

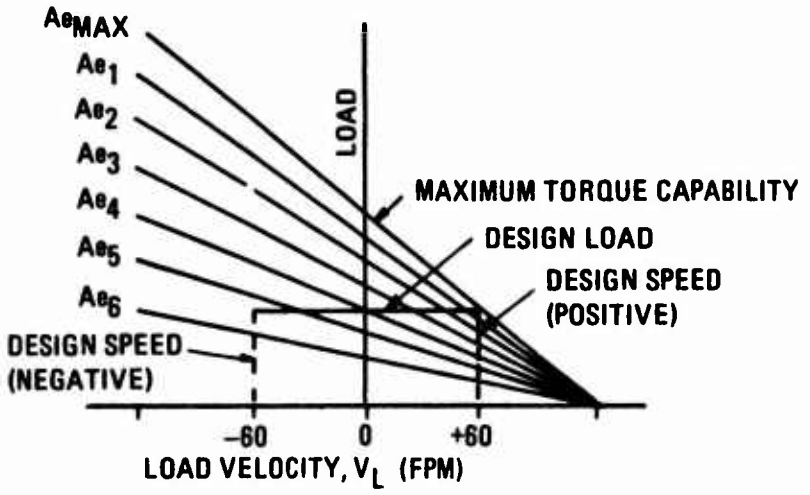

FIXED-NOZZLE TURBINE

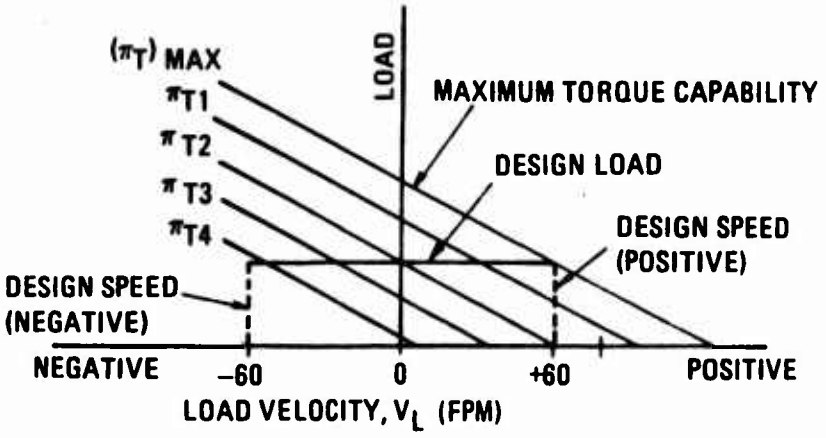

Figure 13. Torque Versus Speed for Fixed- and Variable-Nozzle Turbines.

pressure drop limitation for defined airflow. Single conductors (no redundancy) are assumed.

AIR-TURBINE MOTOR

Two independent motors of identical capacity and performance characteristics are required for the hoist-drive system. The air-turbine motor shall meet the following requirements (quantitative values shown are based on a 20-ton system design):

- Each shall be independently controllable or both may operate in synchronization.
- Each motor housing shall be designed on an integrated basis and shall consist of the following components:
  - — Hoisting wheel (forward rotation)
  - — Nozzle assembly for hoisting
  - — Reversing wheel (where applicable)
  - — Reversing nozzle(s)
  - — Forced-lubrication system
  - — Disconnect or clutching between reversing wheel and hoisting
  - — Heat-dissipation system
  - — Airflow controller for forward and reverse rotation
  - — Control actuator
  - — Control-power generator
  - — High-speed gear reducer
  - — Output shaft
  - — Mounting interface with static/emergency brake
  - — Control interface with static/emergency brake
  - — Signal-conductor interface
  - — Static brake (need not be integral with the ATM housing)

- The output speed from the high-speed gear reducer at zero load (free-running turbine speed) shall be 8,000 rpm. (The gear-reduction ratio is a function of the selected hoisting wheel mean diameter.)

- Predicated on impulse turbine wheel design, the high-speed gearing output optimum operating point is 4000 rpm, which corresponds to a minimum hoisting velocity of 60 fpm.

- The stall torque generating capacity of the wheel is based on its capability to react a 62,137-pound vertical load pull multiplied by the coning angle factor of 1.15 at a lever arm of .677 feet divided by the low-speed gear reduction of 298:1 divided by the high-speed reduction of 12:1 for the 20-ton system as dictated by the wheel design.

- Each turbine wheel operating at the optimum point, and when designed for the requirements above, is capable of generating 56.2 horsepower based on 60 fpm hoisting speed. The high-speed gearing output power is 53.3 horsepower, which is based on 95 percent high-speed gearing efficiency.

- For ATM designs utilizing nonclutched reversing wheels, the hoisting wheel design capacity must be increased by an amount equivalent to the reversing wheel drag torque. Higher airflow penalties are acceptable only when definite improvements are demonstrated.

- The effective nozzle area shall be designed for the power requirement and for the design-day conditions defined.

- Design-day pneumatic airflow requirements are based on 4.08 pressure ratio and 414^{o}F temperature available at the turbine. Maximum airflow per turbine at its maximum power generating capacity is 41.1 pounds per minute and is predicated on 85 percent total to static turbine efficiency. (Minor modification due to optimum point shift as a result of nondesign-day, larger-nozzle-area requirements is acceptable).

- Total design-day airflow requirements for both air-turbine drivers are based on 60/40 percent load distribution on either hoist. On this basis, the objective for maximum airflow requirements for full-capacity hoisting is 68.5 pounds per minute. (Minor modification due to optimum efficiency shift is acceptable.)

- For nondesign-day conditions, the airflow requirements shall be determined by analysis based on the APU-driven constant-speed load compressor, applicable transfer losses, and the efficiency deterioration of the air turbine. The minimum analyses shall be conducted for -65°F, 4000-foot conditions; 125°F, sea level conditions; and 95°F, 10,000-foot altitude conditions. The valves, the nozzle-area design, and the control system shall be designed for the total operating ambient spectrum.

- Special provisions to meet the 120-fpm empty-hook hoisting under nondesign-day conditions are not required. The speed reduction will, however, not exceed the theoretical nozzle spouting velocity reduction based on design-day conditions.

- Total airflow for powered reversing rotation shall not exceed the maximum requirements for design-day and nondesign-day analyses.

- Acceptable hoisting nozzle assembly designs are: (1) fixed geometry, (2) variable geometry, and (3) partial admission. Substantiation of any concept is required by analysis, which shall define response characteristics, size impact, controllability of the hoist-drive system, and turbine efficiencies.

- For the purpose of 120-fpm empty-hook payout, installation of a reversing wheel is acceptable. The reversing wheel shall have adequate capacity to overcome the hoisting wheel's aerodynamic drag, which is directly coupled (no mechanical disconnect) through the static brake to the hoist drum. The reversing wheel shall be a module within the ATM housing. Reversing wheel clutching is acceptable. The clutch shall be a module within the ATM housing.

- The hoisting wheel torque/speed characteristics in the negative region shall be compatible with the characteristics of Figure 13. These characteristics enable the wheel to perform the dynamic braking function and to identify discrete reverse rotation torque/speed characteristics for a specific airflow for effective rate-of-descent control with load.

- Significant temperature rise across the turbine has been demonstrated during dynamic braking. The temperature rise for 120-fpm reverse-hoist rotation is significantly higher. For purposes of determining material for the hoisting wheel, motor housing, and associated components, design support

tests in addition to analysis will be required. To minimize the temperature rise during reversing rotations, installation of additional reversing nozzles to the hoisting wheel is acceptable. A special device to limit the hoisting wheel drag is encouraged.

- A lubrication system shall be provided. Unless substantiated otherwise, forced lubrication will be assumed.

- The heat-dissipation requirements are based on the efficiency of high-speed gearing, bearing losses, and conduction from the air supply temperature. Additional heat is generated during dynamic braking and reverse rotation. Heat dissipation analysis shall be conducted on the basis of three hoisting cycles per hour, each cycle consisting of two full-speed reversing payouts and empty reel-in, followed immediately by full-capacity hoisting and then approximately 10 minutes of no activity. The heat sink is ambient air.

- The type of airflow controller is predicated on the design of the nozzle assembly. The controller response characteristics to enable variable-speed/load accommodations and to provide synchronous speed capability of both hoists are the prime requirements. For fixed-geometry nozzle designs, the sliding-valve-control approach (due to linearity) is preferred over the butterfly valve control. There are, however, no specific valve design requirements.

- Acceptable types of control power are electrical, hydraulic, and/or pneumatic. In the event hydraulic actuating power is used, the motor powering the lubricating pump shall be utilized for this function.

- The high-speed gear reducer shall be designed for 4,000 rpm shaft output dictated by the hoist interface requirement. The gearing efficiency shall be 95 percent minimum at design operating conditions. Design capacities and speed requirements for the high-speed gearing are consistent with the requirements defined.

- The high-speed gearing output shaft is mounted through the static/emergency brake and is directly coupled to the low-speed gearing, which is integral with the hoist drum. Static brake design concepts that are mounted on the high-speed turbine wheel shaft and are integral within the ATM housing may be considered.

- The static brake design and its operation require the highest order of attention due to its safety function and emergency features. The following characteristics are therefore required:

  — The brake is normally "on".

  — During hoisting operation, the brake-release mechanism does not function until the motor-generated torque is adequate to react the load. Mere substantiation of pneumatic power availability to the motor is inadequate.

  — Brake-actuating power is generated within the motor housing.

  — Application of the brake-actuating power shall be gradual and shall not induce accelerations exceeding the levels for which the hoist-drive system components (including airframe structure) are designed.

  — Irrespective of the hoist operator speed selection (airflow), the control system shall be designed in series with the brake-release mechanism with an automatic "dwell" (zero speed) period when the brake is being released.

  — The brake mechanism is engaged whenever zero turbine speed commands.

  — The minimum static holding capability of the brake is equivalent to 48,300 foot-pounds divided by the appropriate gearing reduction.

  — The brake "normal mode of operation" is designed for on-off condition.

  — One full-capacity dynamic braking operation under maximum loading and velocity conditions is required before brake corrective maintenance, repair, or replacement is initiated.

  — Frequent brake operation checkout capability shall be provided in the control system and component design. Loss-of-brake-actuating power automatic signal is required.

— The intelligence and sensor data requiring the ATM control interface shall consist of, but not be limited to, the following:

Load sensing

Tension-member angle

Hoisting-speed, including closed-loop speed control

Operator-to-ATM hoisting command signals

Position-sensing, including proximity switches

Temperature/pressure sensors

Ambient-condition sensors

Pneumatic-power generator status

For synchronous speed control, the concept of slave and master control shall be employed, wherein the master control represents the hoist carrying the larger load.

AIR COMPRESSOR/PNEUMATIC POWER GENERATING SYSTEM

The air compressor provides hoisting power during ground operation and checkout and serves as pneumatic power source backup for secondary power in the event that one of the three main engines fails. The compressor-generated pneumatics shall also serve as the power source for the integrated tests.

The compressor performance and operational requirements are as follows:

- The compressor is shaft driven at a constant speed from the aircraft-installed auxiliary power unit (APU). The APU is assumed to be a free turbine power unit with an integrally controlled, constant-speed, powered shaft output.

- At design-day conditions, the compressor discharge temperature shall be 450°F maximum, based on 4.3:1 pressure ratio.

- The compressor capacity is based on full-capacity hoisting airflow requirement, and simultaneous air requirement for nonhoist-related aircraft systems. At

design-day conditions, the total airflow required is 89 pounds per minute of air.

- The compressor adiabatic efficiency shall be 80 percent minimum.

- The compressor discharge pressure control is accomplished through a series of variable orifices in the various power drive systems, including dump valves controlled by appropriate pressure regulators. The environmental control system (ECS) is predicated on a variable-geometry nozzle design. Utilization of the ECS nozzle for the purpose of compressor discharge pressure control is encouraged and is based on maximum through-flow of 89 pounds per minute at 4.3:1 pressure ratio.

- A surge control/dump valve is required. Its dumping capacity shall range from 0 to a maximum of 89 pounds per minute at design-day conditions. The dumping capacity shall further be capable of significantly increased airflow dumping when operated at SL -65°F conditions.

- Inlet particle separator shall be an integral part of the compressor. Utilization of the particle separator for both the load compressor and the APU inlets shall be considered.

- Compressor input shaft speed is predicated on the compressor rotating speed required that will provide the necessary design-day requirement for the quantity and air quality as defined above. The two applicable solutions are:

  — Integrate the load compressor and the gearing required within the APU. The ideal solution consists of a perfect speed match between the APU power turbine speed and the compressor speed required.

  — Design a step-up gearbox which shall be directly coupled to the APU output shaft assumed to operate at 6,000 rpm. The gearing ratio is based on the compressor rotational speed required.

- Compressor discharge temperatures at higher than design-day ambient conditions are expected to exceed the 450°F design limitations. The applicable criteria and potential solutions to meet these temperature limitations are:

— Reduce the pneumatic system discharge pressure to the extent that, based on the compressor performance characteristics, the discharge temperature shall not exceed 450°F. The requirement for 120 feet per minute no-load hoisting velocity may be reduced accordingly, but not to exceed the delta pressure reduction. The hoisting-capacity (load-weight) reduction shall not exceed the reduction of helicopter lift capability due to elevated temperature operations.

— Utilization of the engine bleed precooler for the purpose of limiting the compressor discharge temperature is acceptable providing the precooler and associated pneumatic conductors are isolated from the fuselage (APU compartment, etc.).

- The compressor-performance characteristics shall be such that during all hoisting operating ambients and conditions, the surge limit will not be reached.

- No limitations exist on the type of compressor design. These include multistage axial, single- and multistage centrifugal, and a combination of both as required.

- Compressor physical size requirements are critical only in that they facilitate the interface primarily with the APU. Compressor weight is, however, a major factor and shall be at a minimum. The weight objective is 26 pounds.

- New compressor design and development is not encouraged for reasons of excessive cost and development time required. Utilization of existing units and modifications thereof are recommended.

- Of significant importance in the compressor selection is the capacity and performance at nondesign-day conditions, particularly at colder ambients. Compressor capacities must equal or exceed full-capacity hoisting at all design-day ambients below 95°F.

MAIN ENGINE BLEED PNEUMATIC POWER GENERATING SYSTEM

The prime source of pneumatic power for airborne hoisting is main engine bleed.

Toward the objective of establishing these requirements, the operational concept and performance definitions are as follows:

- Three engines are bled simultaneously. Three independent bleed valve systems are required.

- Each bleed valve capacity is designed on the basis of 50 percent flow capacity of the total pneumatic system, including full-capacity hoisting required, and is equal to 58 pounds per minute at design day. (Increased flow capacity is required at colder ambients.) This approach provides redundancy in the event one bleeding system fails.

- The bleed pressure is dependent on the engine power setting, but shall never drop below 4.3 atmospheres.

- The engine-bleed air is conditioned to 4.3 atmospheres and 450°F maximum temperature. Unless proven impractical, a single cooler and one pressure regulator is assumed for the air quality conditioning.

- The precooler design shall be based on 116 pounds per minute flow at appropriate engine-bleed temperature. The heat sink is 125°F maximum temperature ambient air. (The values are based on design-day conditions.)

- Variable-delivery forced ambient-air cooling system is required. The bleed air shall not be cooled below 450°F.

- The cooling system power is pneumatically available from the main engine bleeding.

- The bleeding system shall be designed on the basis of the hoist system operation response characteristics required and shall include the power-transfer system (pneumatic conducted) considerations.

- The bleed-system design shall ensure that all engines are simultaneously supplying equally balanced mass airflows.

PRELIMINARY DESIGN OF THE HOIST SYSTEM

INTEGRATION OF THE PNEUMATIC HOIST-DRIVE DESIGN

The hoist-drive study was conducted on an integrated basis within the total air vehicle, indicating the various aircraft subsystem interface with that of the hoist-drive system. The vehicle selected was a tandem-rotor configuration and is as shown in Figure 14. The hoist-drive system, however, is applicable to any helicopter configuration and is equally adaptable for other than two-point hoisting.

One such concept of pneumatic hoist-drive system integrated with the other vehicle subsystems is shown in Figure 16. (In this concept the power conductors directly chargeable to the hoist drive run only from point A to the hoists at their selected positions.) Telescopic conductors permit the hoist to move to various positions. Note further that independent of hoisting, the pneumatic conductors are necessary for the ECS and the hydraulic pump, whose locations cannot be changed on the basis of established requirements. The plumbing complexities in the rear pylon are necessary regardless of the hoists. The slight increase in conductor diameter due to hoisting is relatively insignificant.

In this configuration, the source of power is the APU-driven compressor or the engine bleed properly conditioned in order not to exceed the 450°F temperature limit. The desired pressure is controlled by the regulator shown. All three engines are bled. In the event of valving malfunction of one engine, adequate bleed air is available from the remaining two engines. The APU may also be operated in flight. More than single power redundancy for hoisting is therefore available for all conditions.

The study was based on a movable dual-winch configuration to incorporate both multipoint suspension systems. For multipoint operations, the winches are located in the aircraft in a manner that exhibits capability of supporting the forward and aft ends of the typical cargo (such as 8-x 20-foot containers) that can be flown at high speeds. For single-point operations, the same two winches are moved toward the center, the two cables are coupled, and a larger-capacity hook is attached. Figure 16 shows this single-point suspension.

The design of the hoist-drive system components was also based on an integrated design with the hoist in a manner similar to

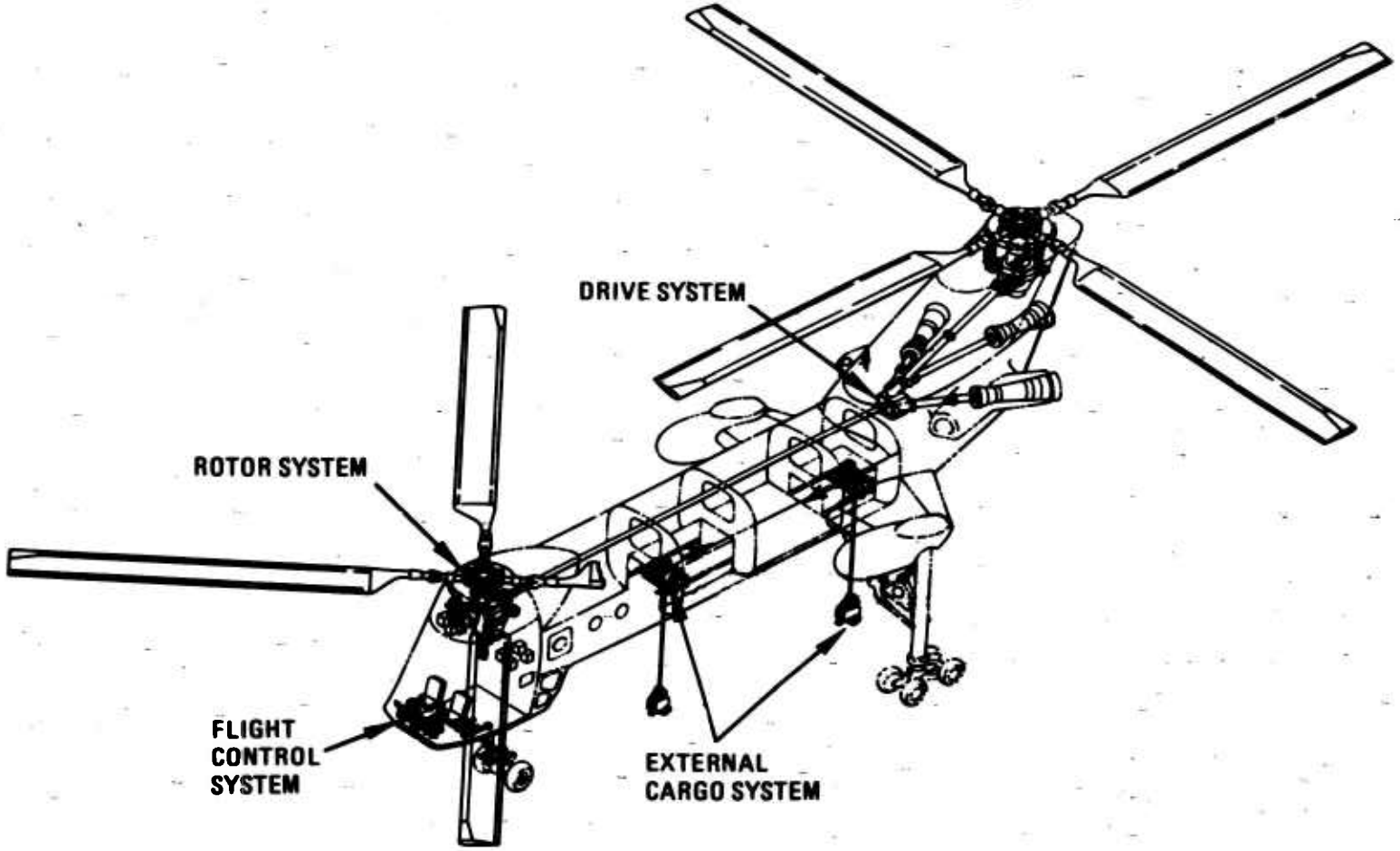

Figure 14. Tandem-Rotor Helicopter - Boeing's HLH.

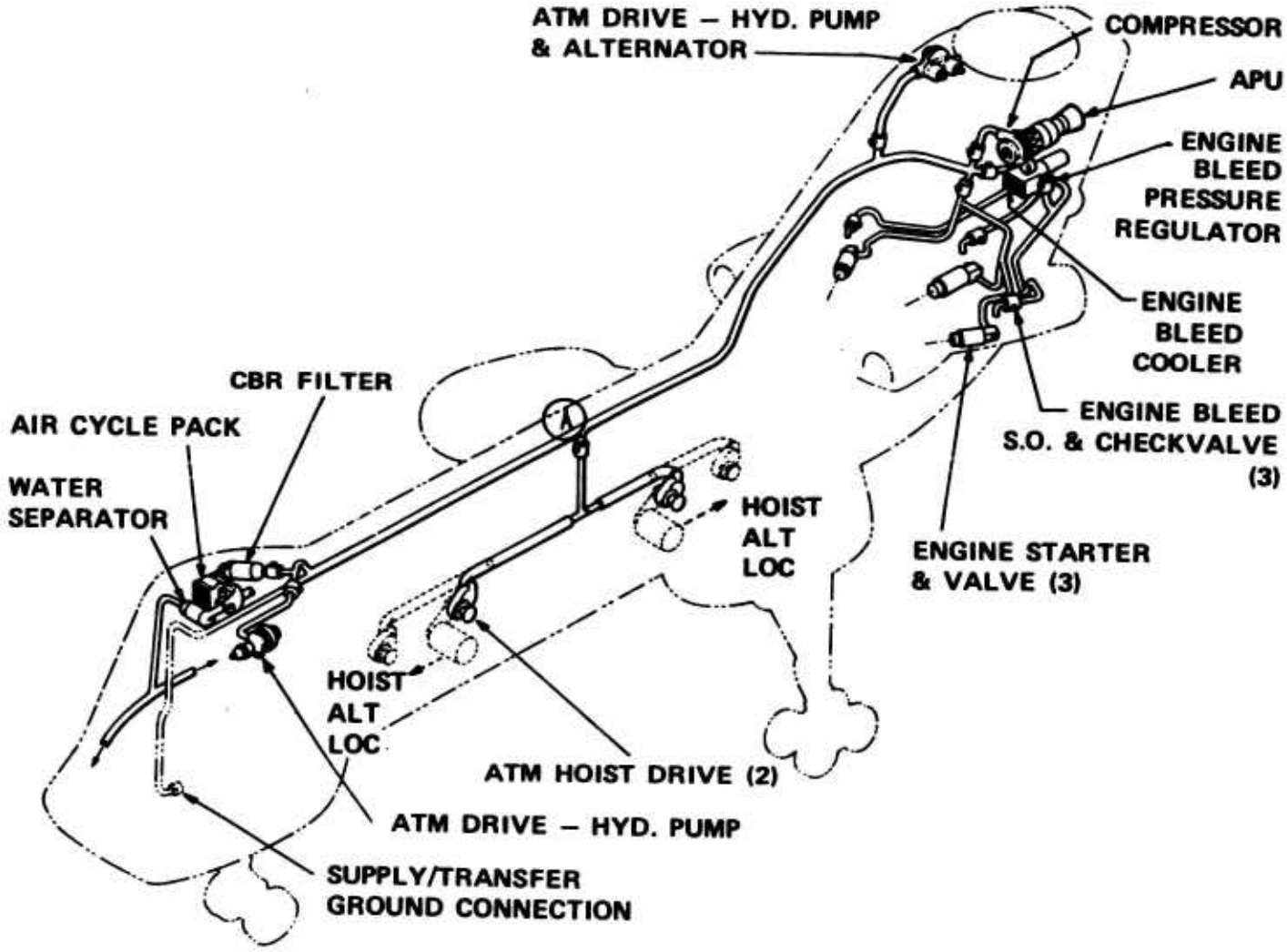

Figure 15. An Integrated Pneumatic Hoist System.

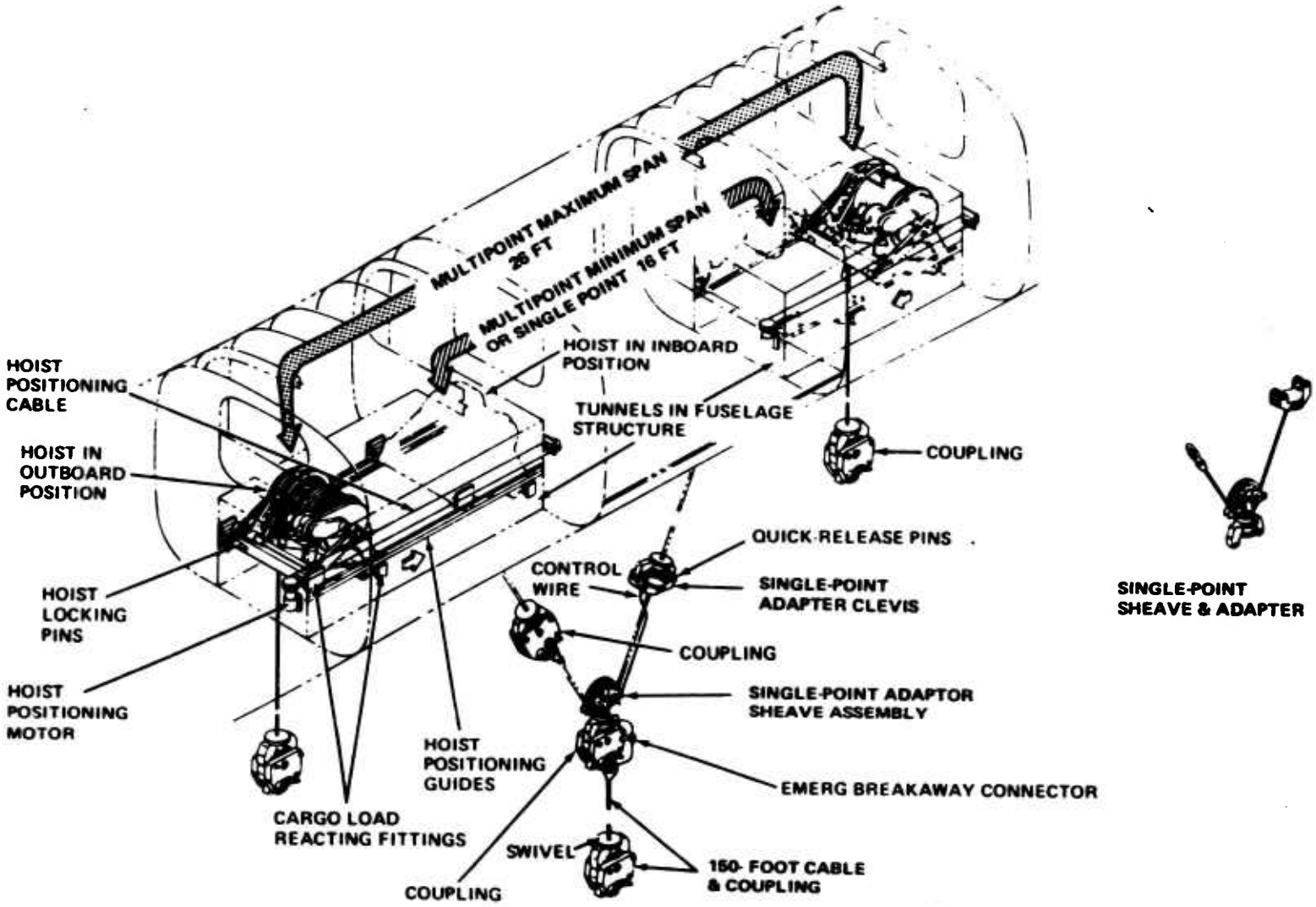

Figure 16. A Movable, Dual-Winch System Used for Both Multipoint and Single-Point Suspensions.

the requirement of designing an external cargo system that must be integrated with the air vehicle design.

For the purpose of this study, two movable hoists sliding on trolleys to the various desired positions were considered, as shown in Figure 16. Pneumatic power was provided at various hoist positions through a telescopic conductor, as shown in Figure 17.

SYSTEM COMPONENTS

Before the initiation of the hoist-drive design, a definite relation between the drum and the hoist driver must be established. To go further, the drum design is normally based on an appropriate drum-to-cable diameter ratio; the necessary conclusion therefore is that the tension member design and definition are essential before the hoist-drive design can be initiated.

DUAL TENSION MEMBER HOIST DESIGN

The dual-drum concept of the hoist assembly of Figure 18 has been selected primarily for the purpose of utilizing smaller diameter dual cables for excessive loads. The additional advantage of this approach lies in the fact that if each load member is instrumented for load measurements and a significant load-carrying imbalance between the two members is indicated, deterioration of one member is automatically indicated. Weight analyses conducted further indicate that the dual-drum approach is not heavier than a single-drum approach for identical capacities.

A further distinct advantage of the dual-drum approach is that regular-lay rotating cables can be used -- one left- and one right-lay cable are required. Since both cables are attached to a fixed connector producing a fixed-end pull, rather than a swivel connector, both cables are automatically torque balanced. The end result is higher strength for the same diameter cables or diameter cables for the same capacity.

When related to the hoist-drive gearing, the torque is in fact decreased due to higher drum speed and smaller drum sizes. Estimated gearing torque reduction is 30 percent when compared to the single-drum design.

This system approach will be utilized for total hoist capacities exceeding 15 tons.

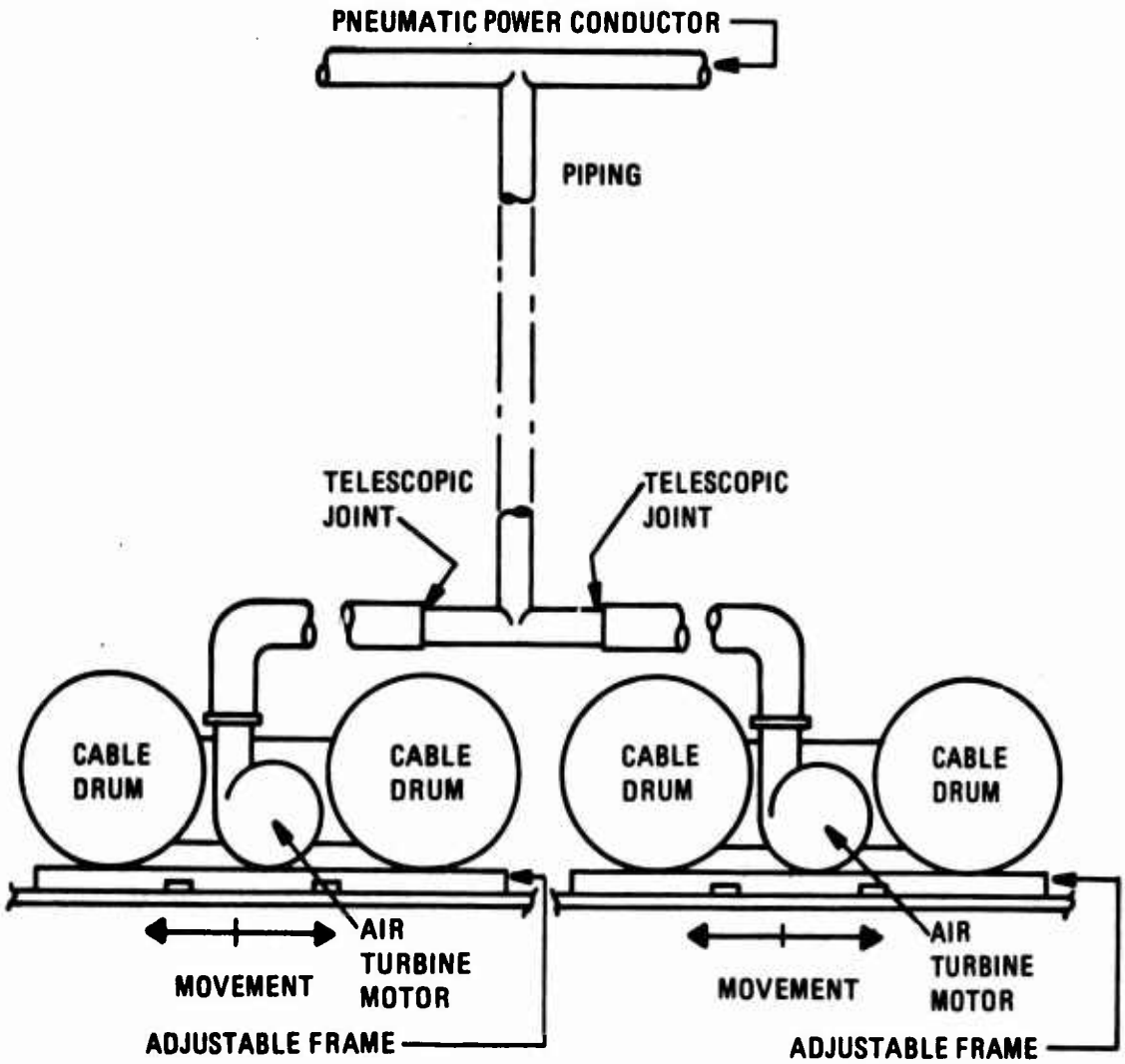

Figure 17. Telescoping Pneumatic Power Conductors.

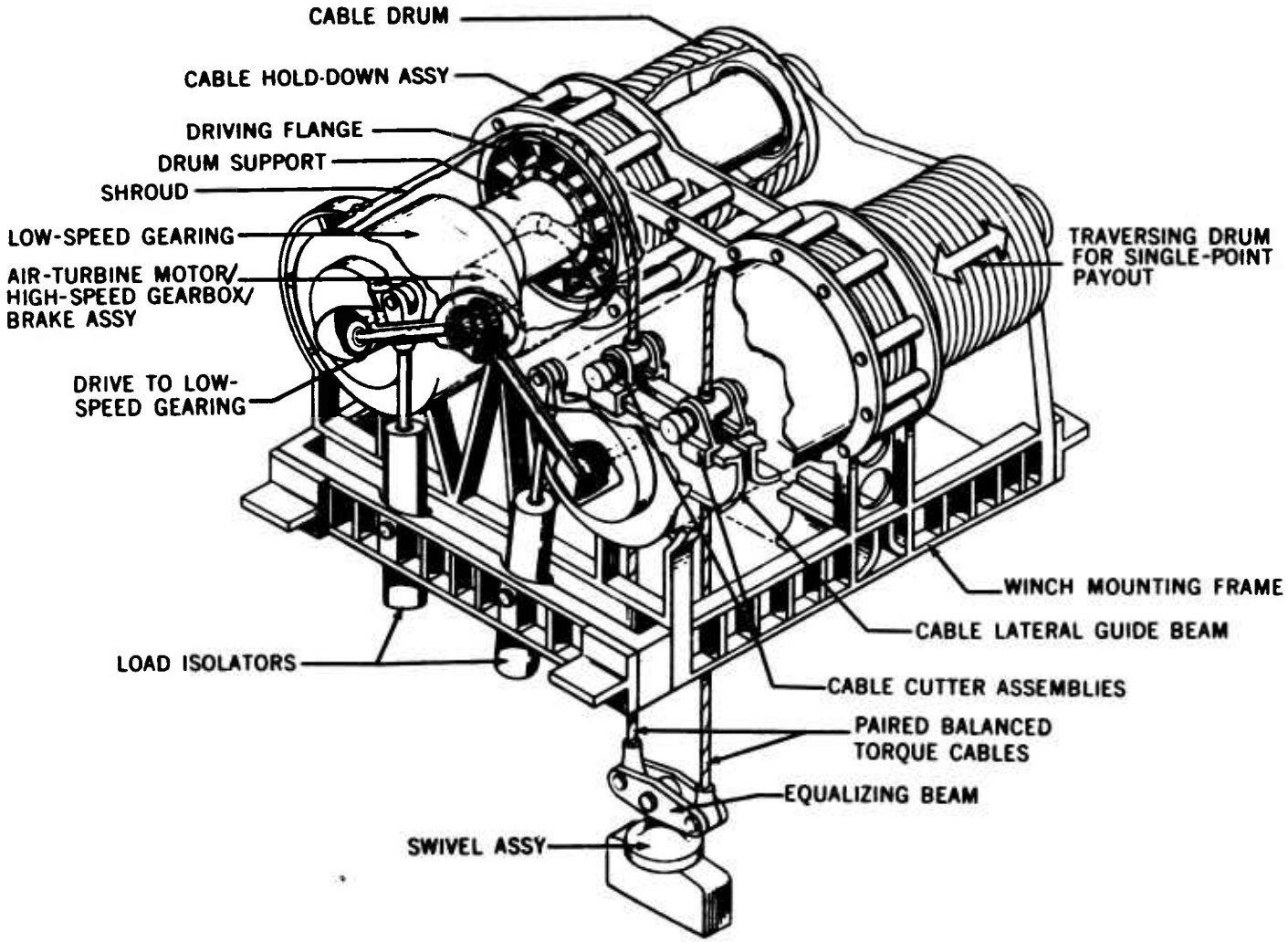

Figure 18. Dual-Drum Hoist.

CG Offset and Impact on Hoist Separation

Compensation for the load cg offset may be accomplished by hoist separation. The resultant effect is smaller capacity hoists for analogous capability. An arbitrarily selected load split on each hoist, independent of the relative length of the load to the hoist separator, is not realistic; therefore, this interdependence is essential to be considered. This relationship is illustrated in Figure 19. Realistic criteria for the hoist-drive capacity were based on the following analysis. The total system capacity for the analysis was based on 28 tons.

Load Asymmetry Determination

The objective here was to determine individual hoist-drive capacity for the purpose of accommodating asymmetrical loads in the multipoint suspension modes.

Referenced Backup Data

- ASRD for HLH/ATC Program, Page 19, Paragraph 2a

  "The center of gravity of loaded MIL-VANS shall be assumed to vary longitudinally plus and minus 10% of the internal length measured from the geometric center of the enclosed space."

- SAE Container Standard

  "The center of gravity for the SAE standard varies no more than plus or minus 5% of internal length measured from geometric center of enclosed space. The SAE standard for c.g. does not consider helicopter operations."

- CDC Definition of Maximum Gross Weight of 40-Ft Containers

  "The maximum gross weight of 40 ft. container shall not exceed 25 tons."

Design and Rationale. The applicable baseline criterion for an individual hoist design was predicated on the following:

- The separation distance between the two hoists varies from 16 to 26 feet.

LEGEND

L = LOAD LENGTH (FEET)
S = WINCH SEPARATION (FEET)
X = CG DISPLACEMENT (FEET)

$Y = \frac{X}{L/S}$ 100 (PERCENT CG SHIFT)

$K = \frac{L}{S}$ LOAD/SPAN RATIO

T = HOIST CAPACITY (TONS)
W = TOTAL HOIST CAPACITY (TONS)

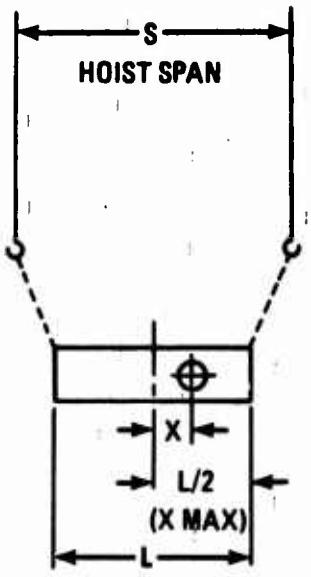

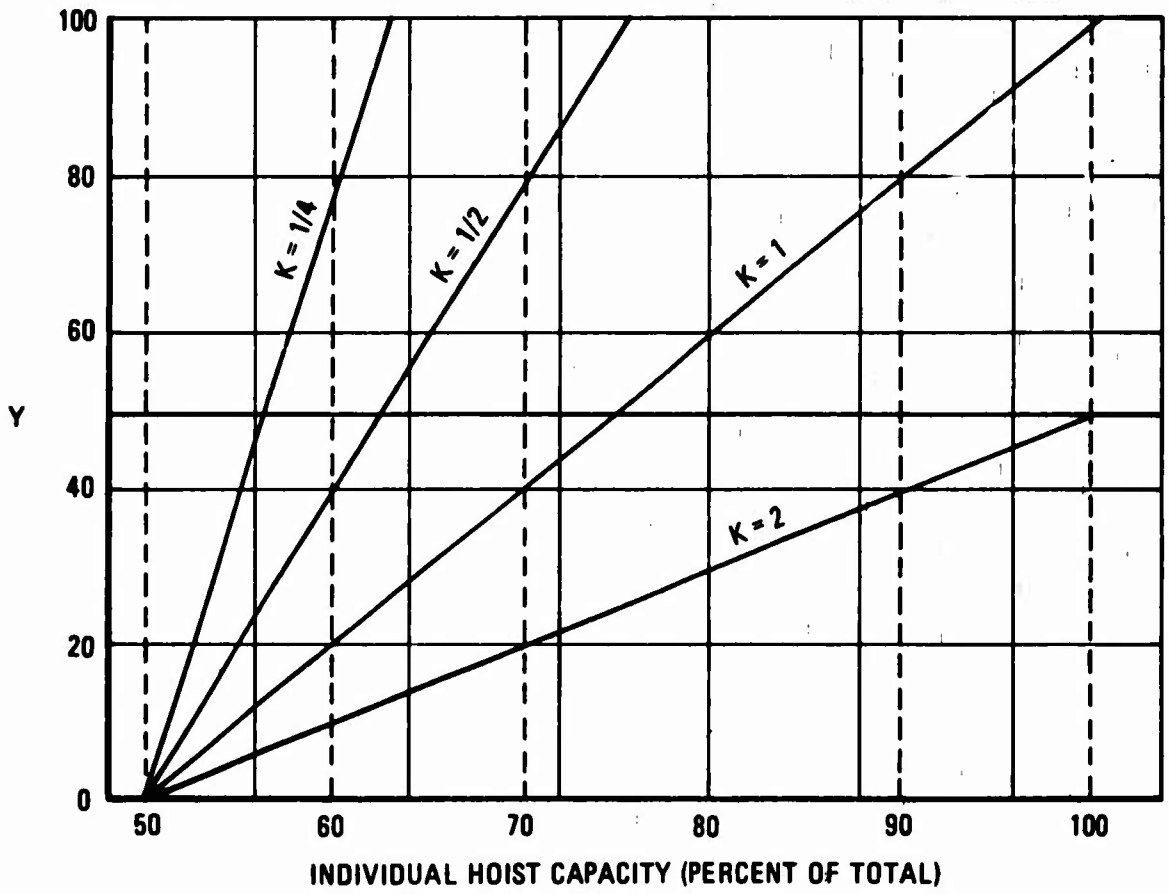

Figure 19. Effect of the Ratio of Load Length to Hoist Separation on the Capacity of a Single Hoist.

Predicated on the criteria defined above, the load asymmetry accommodation capabilities for the following three conditions are shown in Tables XI to XIII.

- G factor of 2.5, 30-degree coning angle, and appropriate drag factor.
- G factor of 2.0, plus 30-degree coning angle, and appropriate drag factor.
- G factor of 2.5, appropriate drag factor, and no coning angle.

TABLE XI. LOAD ASYMMETRY ACCOMMODATION WITH 2.5G FACTOR, 30-DEGREE CONING, AND FIXED DRAG FACTOR

Load Length (feet)	Hoist Separation (feet)	Load Weight (tons)	Permissible Longitudinal CG Shift (feet)	CG Shift (% of length)
20	26	28	2.6	13.0
20	20	28	2.0	10.0
20	16	28	1.6	8.0
40	26	23	6	15.0
40	26	24	4.5	11.25
40	26	28	2.6	6.5

TABLE XII. LOAD ASYMMETRY ACCOMMODATION WITH 2.0G FACTOR, 30-DEGREE CONING, AND FIXED DRAG FACTOR

Load Length (feet)	Hoist Separation (feet)	Load Weight (tons)	Permissible Longitudinal CG Shift (feet)	CG Shift (% of length)
20	26	28	6.5	32.5
20	20	28	5.0	25.0
20	16	28	4.0	20.0
40	26	23	10.8	27.0
40	26	25	8.8	22.0
40	26	28	6.5	16.25

TABLE XIII. LOAD ASYMMETRY ACCOMMODATION WITH 2.5G FACTOR, FIXED DRAG FACTOR, AND NO CONING ANGLE				
Load Length (feet)	Hoist Separation (feet)	Load Weight (tons)	Permissible Longitudinal CG Shift (feet)	CG Shift (% of length)
20	26	28	5	25.0
20	20	28	3.85	19.2
20	16	28	3.1	15.5
40	26	23	8.9	22.2
40	26	25	8.2	18.0
40	26	28	5	12.5

Based on the facts known to date, it is concluded that 60/40 percent load asymmetry accommodation is adequate. Each hoist tension member shall be designed for 38,800 pounds total pull. Superimposed on the above will be a 2.5g factor, appropriate drag, and ultimate factor.

TENSION MEMBER DESIGN

For the purpose of defining realistic hoist-drive systems, the requirements for the tension members, their characteristics, and projected improvements are essential. For this study, the tension members are assumed to be steel cables. Current-technology cable strength is based on MIL-C-5424; minimum breaking strength versus cable diameter is shown in Figure 20, which also shows projected improvements in cables.

The applicable criteria for cable-strength selection are based on a two-hoist system, each hoist capable of carrying 60 percent of the total design load. Each cable therefore shall be based on the following:

$$P_B = (.6)\ (2.5)\ (1.5)\ (1.15)P_{DESIGN}$$

where P_B = cable breaking strength

P_{DESIGN} = hoist system capacity

(.6) = 60% of total design hoist load - each

2.5 = acceleration load factor

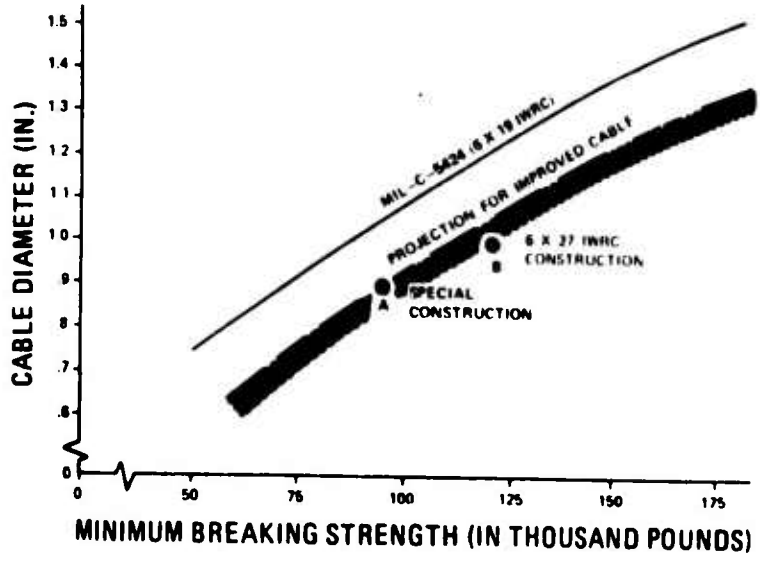

Figure 20. Cable Diameter Versus Strength - MIL-C-5424 and Improved Cable Under Development.

1.5 = ultimate design factor

1.15 = 30° coning angle factor (see coning angle requirements)

To meet the specified fatigue load spectrum of 10,800 cycles, the ratio of drum diameter to cable diameter (D/d) is 24. This requirement is based on an actual test conducted by NAEC Philadelphia. The results are shown in Figure 21.

Maximum Cable Diameter

The maximum cable diameter should be limited to 1-1/8 inches. Cables exceeding this diameter are extremely stiff and do not lend themselves to practical airborne application because they require very large drum diameters and produce excessive weight penalties.

Power Transmission Losses of Tension Members

Previous inputs and discussions with various hoist manufacturers indicated considerable transmission losses, which are defined as that force applied along the rope axis which is just sufficient to cause the rope to move over the sheave (or drum). These losses were previously estimated to be as high as 15 to 20 percent of the cable load.

Actual tests conducted with various rope configurations utilizing various diameter ratio sheaves negate these previously assumed high transmission losses, as indicated in Figure 22. These values indicate the net transmission losses and do not reflect bearing losses. It was also found that there was no significant variation in the transmission loss per sheave with angles of embrace of 90° and 180°. By deduction, it is therefore assumed that the effect on larger angle of embrace will not materially influence the data presented. As expected, the lower the ratio D/d, the higher the losses.

If the drum were considered as a series of sheaves, the losses could erroneously be considered proportional to the number of winds. Instead, however, the total transmission losses approximate those of a single sheave. This interesting reduction of the transmission losses from the ones assumed previously now permits some relaxation on the high gearing efficiencies previously imposed, with possibly significant hoist-system weight reductions.

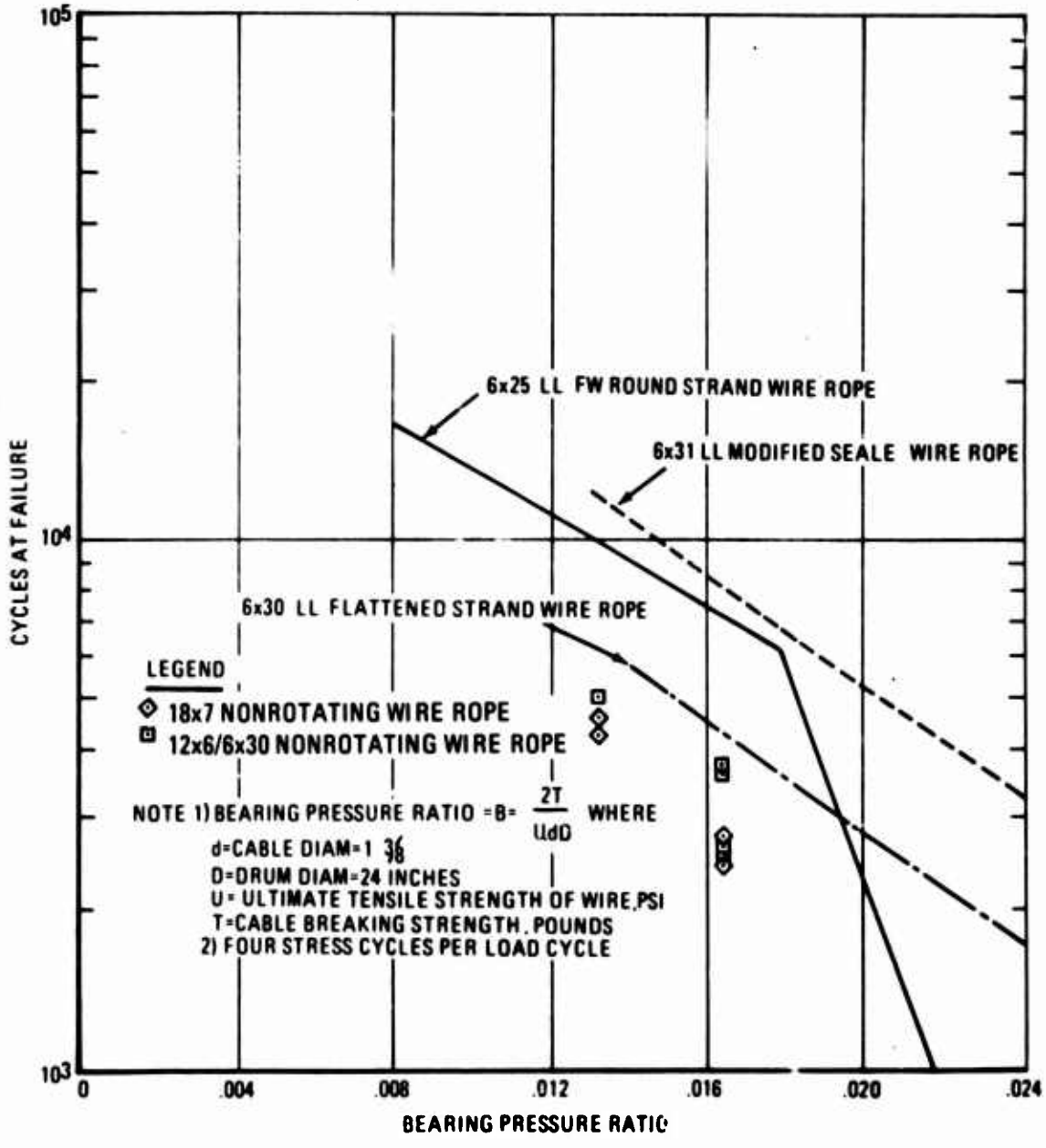

Figure 21. Fatigue Characteristics of Various Cables.

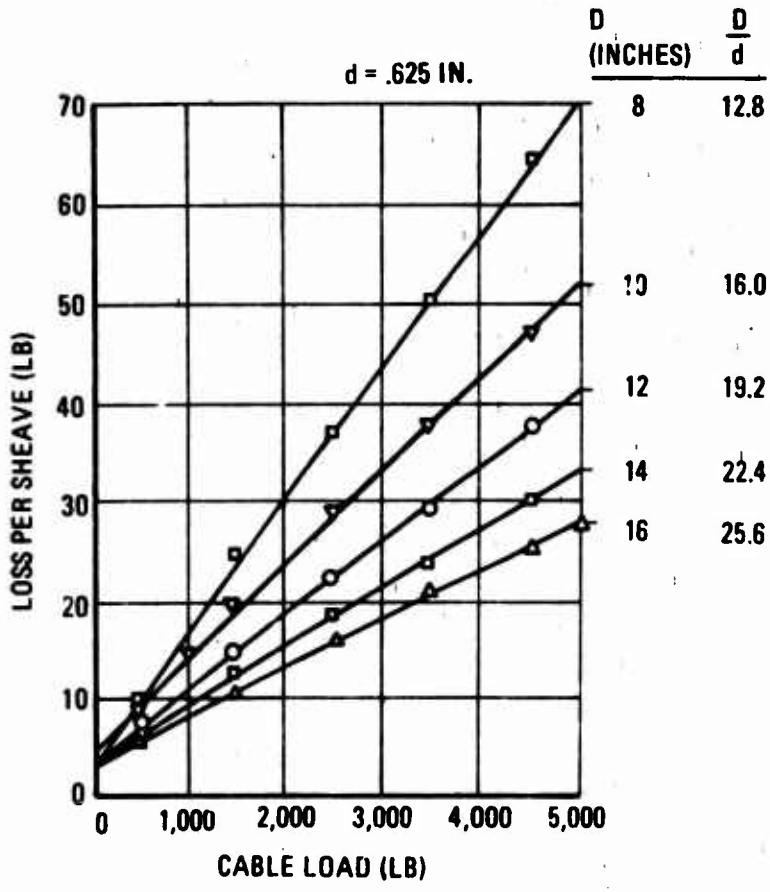

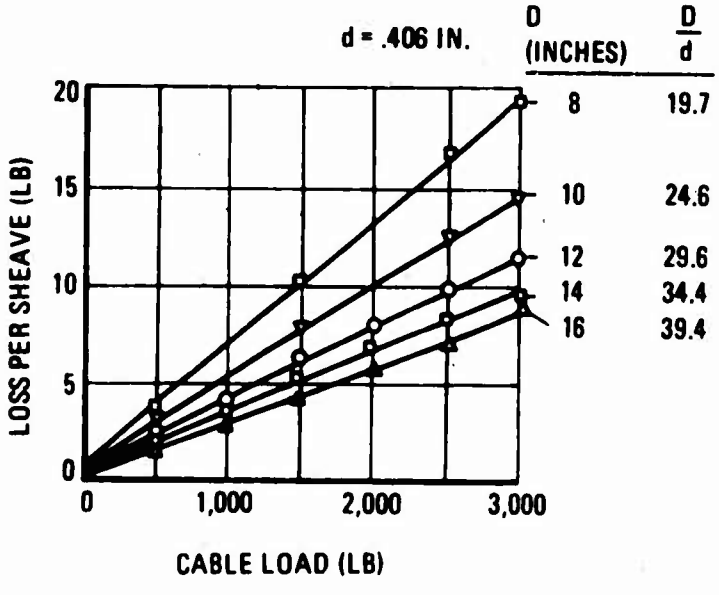

Figure 22. Loss per Sheave for Two Diameters of Cables (d) and Various Diameters of Sheaves (D).

THE AIR-TURBINE MOTOR (ATM)

The key to the pneumatic hoist-drive system design is the air-turbine motor. Its performance characteristics are ideally suited for this application, as demonstrated below. Application of air-turbine drive, particularly for airborne uses, is extensive and varied. Available equipment is designed and used effectively for applications such as:

- Jet-engine starters, consisting of an air-turbine motor and associated gear reducer.
- ATM-driven constant-speed hydraulic pumps.
- Environmental-control system (ECS), consisting of an ATM driving a compressor.
- ATM-driven constant-speed electrical generators.
- Controlled variable-speed ATM drives for wing-flap actuators and landing gear kneeling and retraction systems.
- ATM-driven compressors for pressurization systems and bleed-air generation for ECS.
- Turbine engines for shaft power and thrust generation. (This application stretches the point; nevertheless, it is an air-turbine drive.)

The various ATM drives operate either intermittently (starters, actuators) or continuously (ECS-, ATM-driven generators, etc.)

The analysis of the hoist power requirements carried out by Boeing clearly shows that an air turbine is the most suitable motor. An air turbine automatically gives an increase of output torque as speed is reduced by the load. Also, the unloaded speed increases to about twice the design speed.

Depending on the efficiency of the reduction gears and the torque/speed characteristics of the motor, maximum air consumption may be dictated either by the stall and maximum speed requirement or by the maximum hoisting power requirement. An ideal combination of gearbox efficiency and torque/speed characteristic would give the same airflow requirement for both these boundary conditions.

Air-supply conditions for the design case are 51 psia (4000 ft altitude) at 450°F at the turbine nozzles, and 12.7 psia at the exhaust. A number of turbine configurations have been examined and are briefly described below.

The configuration which appears to offer the best possibility of achieving the target performance for a 20-ton hoist capacity has an axial hoisting turbine wheel of approximately 4 inches in diameter and is combined with an axial reversing wheel over 2 inches in diameter. (Radial wheel for the reversing stage is equally acceptable.)

TURBINE CONFIGURATIONS CONSIDERED

It was not evident that an axial turbine provided the best overall characteristics for this application. Although the axial turbine has better torque/speed characteristics, a radial turbine can be more readily designed with reversible variable vanes, eliminating the control throttle and its associated losses.

The main criterion for selecting the ATM is to achieve the required minimum performance with the lowest maximum airflow. Hence, high efficiency is required at maximum hoisting power. Control of power by throttling is wasteful of power; if used, the throttle must be designed to give a very low pressure loss at full power.

Table XIV shows some of the features of axial and radial turbines.

Axial Impulse Turbine With Partial Admission

This design would have a nozzle ring with some nozzles angled in the reverse-rotation direction. Two air-supply ports connect the nozzle to the air control valve. This would be designed to progressively throttle the air supply to either set of nozzles, with a central zero position.

If full reverse speed could be achieved with not more than 30 percent reverse admission, the maximum achievable efficiency in the forward direction should be about 70 percent. The arrangement is simple, but it will not achieve the performance target.

TABLE XIV. AXIAL AND RADIAL TURBINE FEATURES		
Feature	Radial	Axial
Maximum efficiency, normal rotation	Good	Good
Maximum efficiency, reversed rotation	Good	Poor
Reversing nozzle design	Complicated, but reasonably effective	More complicated and not very effective in reverse
Fixed nozzle, partial admission design	Reasonably efficient in both directions	Poor in reverse
Torque speed characteristic	Good	Better
Air-consumption characteristic	Increases with speed reduction	Relatively independent of rpm
Most likely design point for torque and airflow	Stall	Maximum HP

Axial Turbine With Inner Reversing Blades

This would be a full-admission axial-impulse turbine having a pair of axial nozzle rings. The outer nozzle is designed for forward rotation, and the inner one is designed for reverse rotation. Power control would be by throttling.

The rotor has normal blades cut on the periphery, and an additional set of blades cut through the rotor to provide reversing blades. These "blades" may be virtually straight-sided slots, since the gas-approach angle will be nearly 90 degrees at maximum speed.

Since the reversing nozzles and blades are at a smaller diameter than the main blades, the maximum reverse speed could in principle be higher than maximum forward speed, with the same nozzle exit velocity.

This arrangement results in the neatest and most compact ATM design with a sufficient degree of design flexibility. However, there could be serious problems in the design and manufacture of the turbine wheel, which would be more highly

stressed than a conventional wheel. Given sufficient development time, it is believed that this approach would give the best design for the ATM, but the element of risk is too high for the short development program required.

Variable Nozzle Reversible Radial Turbine

This is a simple radial turbine with a nozzle ring having an even number of pivoting nozzle vanes.

With variable angle nozzles, reverse may be approached either through maximum nozzle area or through minimum nozzle area. The former can be done with well-shaped nozzles, but it is very bad from a control point of view. Such a nozzle would probably have to be used in conjunction with an inlet control throttle.

Reversing through zero area results in a limitation in nozzle shape, but the nozzle area can be used to control power. At maximum forward and reverse, the provisional design seems to give a very reasonable nozzle shape; in moving from maximum forward to maximum reverse, half the nozzles rotate through an angle of about 40 degrees, while the interleaving blades move in an opposite direction through an angle of about 14 degrees. From an efficiency point of view, this should be better than throttling, even if compromising nozzle geometry reduces maximum turbine efficiency, since there will be no additional throttling losses. However, the basic characteristics of a radial turbine give a high airflow requirement at stall, and this is sufficient to eliminate this approach.

Variable Nozzle Reversible Axial Turbine

Had tests shown that an axial-impulse wheel could be driven in reverse at the required speed, the pivoting nozzle design could be used with an axial wheel. However, the nozzle mechanism is more difficult to design for axial directed vanes; also, the performance of axial turbine nozzles is more critically dependent on nozzle shape than is the case with radial turbines. Therefore, the high element of risk eliminates this approach.

Twin-Wheel Axial Turbine

Although the use of a separate wheel solely for paying out an unloaded hook seems at first sight to be extravagant, there is much to be said for it.

Since it is required to operate at twice the maximum power, a wheel can be used and can be designed to give its maximum efficiency at a speed where the main wheel efficiency is zero. Also, since windage losses are proportional to the cube of rpm and the fifth power of diameter, the additional losses due to the reversing wheel should be low enough to make declutching unnecessary.

The main wheel design will be a simple conventional profile designed for maximum fatigue life and maximum bursting speed. If this is made from titanium, the bursting speed will be at least 50 percent higher than maximum unloaded runaway speed. The design of the reversing wheel will be carefully matched to the drag characteristic of the main wheel, to make excessive reverse speed impossible to achieve. This drag characteristic can only be approximately calculated, and will need to be established by testing. The only difficulty appears to be in the design of the turbine bearings and their lubrication.

This arrangement seems to offer the best possibility of achieving the required hoist performance with the minimum of design risk; it is therefore the one selected for this study.

Single-Axial Wheel With Combined Radial Reversing Stage

This is essentially similar to the proposal for a wheel with an inner row of reversing blades, but it avoids weakening the wheel, at the expense of complicating the exhaust ducting.

The shape of the wheel provides a good stress distribution, giving a high bursting speed. The diameter of the radial stage, complete with nozzle ring and a side volute, has to fit inside the nozzle ring of the axial stage. This should be possible since its design speed is twice that of the main stage.

The parasitic drag of the radial stage during normal operation at design speed will not be too high. A 3-inch radial wheel used on a Lucas diesel supercharger takes 5.5 hp at 100,000 rpm when the delivery is shut off. At 50,000 rpm, this would reduce the main stage output power by approximately 2 percent.

The rotor design is such that it can be mounted on a single bearing. The air ducting is complicated by the need to cater for the radial turbine exhaust, but this does not appear to be serious. The only performance shortcoming appears to be the low turbine brake torque available when hoisting an unloaded hook, and this can be catered for in the control system.

OPERATIONAL CHARACTERISTICS

The turbine operational characteristics were briefly reviewed to establish operational criteria. The turbine performance analysis considered was for pure impulse wheels. The comparative performance of radial versus axial design was obtained primarily from test results.

The turbine is a device that converts kinetic energy of the working fluid (bleed air) into mechanical energy in the form of shaft power. The working fluid energy level is a direct function of its pressure and temperature, and the effectiveness of the mechanical conversion is represented by the ratio of mechanical power generated over maximum power recoverable due to adiabatic expansion. The turbine efficiency is thus represented by:

$$\eta_T = \frac{\Delta T_T}{T_{Ti}\left[1 - \frac{1}{(\pi_T)^{\frac{n-1}{n}}}\right]}$$

where η_T = turbine adiabatic efficiency

ΔT_T = actual temperature drop across turbine (measured), °R

T_{Ti} = turbine inlet temperature, °R

$\frac{n-1}{n}$ = .283 (for air)

π_T = turbine expansion ratio

An expression for the kinetic energy of a moving stream of air transformed into a shaft can be obtained by means of the velocity diagram shown in Figure 23.

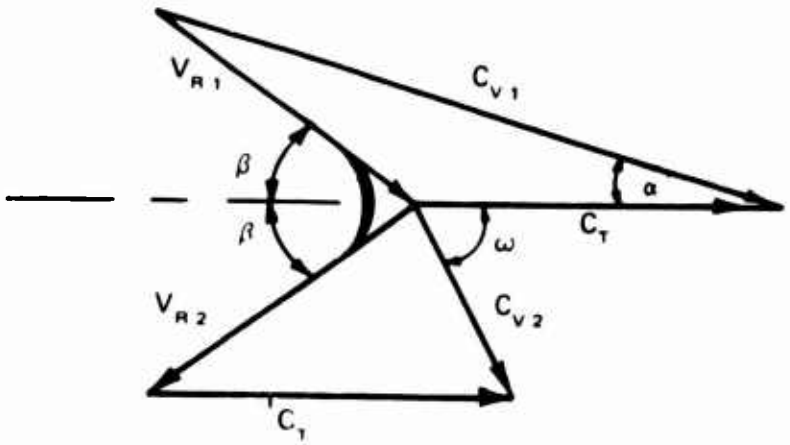

Figure 23. Velocity Diagram for Impulse Turbine.

The jet of air from the nozzle is directed at an angle (called the nozzle angle) with the direction of motion of the blades; the air is moving with an absolute velocity C_{V1}. The blade is rotating at a tangential speed (C_T) in the direction shown. The relative velocity of the air at the entrance (V_{Ri}) is the difference between vectors C_T and C_{Vi}. Impulse blading is symmetrical, or nearly so; and since there is no friction, the relative exit velocity V_{R2} equals V_{R1}. The absolute exit velocity of the air, C_{V2}, is the vector sum of the relative exit velocity V_{R2} and the tangential speed of the rotating blade. The enthalpy of the air entering and leaving the blades is the same since no expansion occurs and no loss in turbulence is assumed. Therefore, the only change in the energy of the air is the kinetic energy, measured by the absolute velocities C_{V1} and C_{V2}. This change of energy is delivered to the shaft as work. Thus, the shaft power (SP) for these ideal blades is the product of the mass flow (W) and the change in square of the air velocity through the turbine. The following equation represents this relationship:

$$SP = w \frac{C_{V1}^2 - C_{V2}^2}{2g} \text{ ft-lb/sec}$$
$$= C_{V1}^2$$

For the purpose of conserving space, the derivation of the subsequent equation is eliminated. The various interrelationships necessary for the design are defined graphically and mathematically and are as follows:

- <u>The theoretical nozzle exit velocity of the air</u>

$$C_V = \sqrt{2g\, J(H_1-H_2)} = 109.5\sqrt{T_{Ti}\left(1-\frac{1}{(\pi_T)^{\frac{n-1}{n}}}\right)}$$

where C_{V1} = exit velocity, feet per second

H = enthalpy, Btu's per pound

J = conversion factor, 278 foot-pounds per Btu

(The exit nozzle velocity is dependent on the turbine inlet temperature and the expansion ratio only, and is completely independent of the nozzle area.)

- Bleed air quantity flowing through the turbine is limited by the nozzle area and the maximum attainable bleed flow, W_{BL} is

$$W_{BL} = 1.015 \sqrt{\frac{1}{(\pi_T)^{1.434}} - \frac{1}{(\pi_T)^{1.717}}} \left(\frac{A_e \; P_{Ti}}{\sqrt{T_{Ti}}}\right)$$

which, for our specific application (sonic flow continuously), can be reduced to

$$W_{BL} = 15.6 \frac{A_e \; P_{Ti}}{\sqrt{T_{Ti}}}$$

where W_{BL} = bleed airflow, pounds per minute

A_e = effective nozzle are, square inches

P_{Ti} = turbine inlet pressure, absolute inches of mercury

- The torque-generating capability of the turbine is expressed as

$$T = \frac{W}{g} (C_{V1} \cos \alpha - C_{V2} \cos W$$

$$= \frac{2W}{g} C_{V1} \left(\cos\alpha - \frac{C_T}{C_{V1}}\right)$$

NOTE: angle ω is shown in Figure 23.

COS of angle α larger than 90° is a negative value.

When C_T is in reverse rotation, the torque generated $T = \frac{2W}{g} \left(C_{V1} \cos \alpha + \frac{C_T}{C_V}\right)$

- Maximum turbine efficiency occurs when the tip speed C_T to spouting velocity C_{V1} ratio is

$$\frac{C_T}{C_{V1}} = \frac{\cos \alpha}{2}$$

and the maximum efficiency attainable is

$$\eta \text{ MAX} = \cos^2 \alpha$$

Frictionless turbine efficiency versus tip speed to spouting velocity ratio for nozzle angles of 15 and 20 degrees is shown in Figure 24.

- Maximum shaft power generation capability per one pound per second of airflow versus nozzle spouting velocity is shown in Figure 25.

- Shaft power generation versus nozzle exit velocity at variable velocity ratios is shown in Figure 26.

- Shaft power versus nozzle area relationship is shown in Figure 27.

- Torque generating capability versus velocity ratio relationship for various nozzle areas is shown in Figure 28.

- Rate of descent control (torque generation in reverse) versus velocity ratio is shown in Figure 29.

RADIAL VERSUS AXIAL TURBINE WHEELS

Subsequent pages define the rationale for turbine wheel configuration. This selection process between the radial and the axial turbine wheel designs was based on the respective performance characteristics of each design (identified in Figure 30).

TURBINE NOZZLE CONFIGURATION

The selection process of the turbine nozzle configuration for the purpose of hoist-drive control was based on the following configurations:

- Fixed nozzle design with upstream butterfly valve control -- Figure 31.

- Variable nozzle design -- Figure 32.

- Partial admission nozzle design -- Figure 33.

The bidirectional variable-speed control with fixed- and variable-geometry nozzle air-turbine motor designs is accomplished by modulating the airflow into the turbine.

The torque speed characteristics for both nozzle configurations are shown in Figure 13.

ANALYTICAL DATA SUBSTANTIATION

Substantiation of analytical data has been considered the prime order of importance in this study effort. Toward this objective, test data were collected and actual tests were conducted. The following represent the test results:

- Fixed-geometry-nozzle axial-wheel air-turbine motor designs were tested to define torque/speed characteristics both in positive and negative speed ranges at various inlet pressures. The motors tested were coupled to a dynamometer, which served as a load and as a driver for reverse rotation. The test data are shown in Figures 34 and 35.

- A fixed-geometry nozzle radial wheel was tested on the same basis as the axial wheel. Figure 36 shows the results of this test.

- For the purpose of determining whether the dynamic braking concept with a radial wheel is feasible, a test was conducted by NASA personnel for a specific radial wheel motor, and the test results including comparison with the axial wheel are shown in Figure 37.

- The next series of tests consisted of reversing the ATM rotation to accomplish empty (unloaded) hook payout. Both an axial and a radial wheel were tested. To accomplish reversing capability, a reversing nozzle was required for both configurations. This enabled the airflow jet to be directed approximately 180° from the forward flow direction and into the back end of the blades. The test results for both wheels are shown in Figure 38.

- Turbine multistaging has not been considered due to complexity and number of nozzle sets required. It has been established that with the pressure ratios under consideration, an efficiency goal can be achieved with a single stage. No advantage with multistaging was evident for this application.

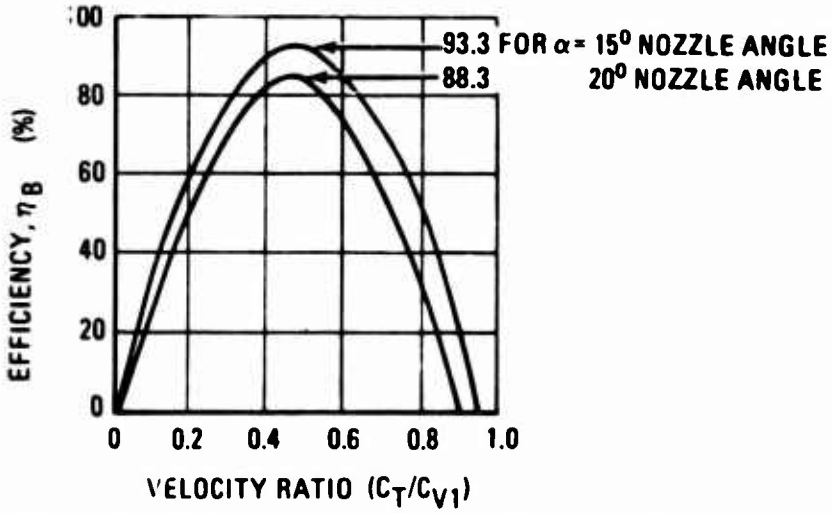

Figure 24. Frictionless Turbine Blading Conversion Efficiency Versus Velocity Ratio for Nozzle Angles of 15 and 20 Degrees.

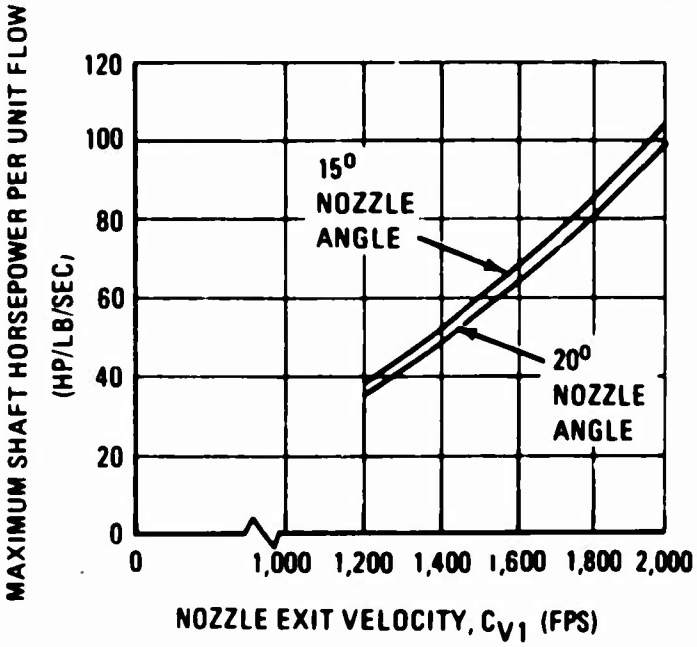

Figure 25. Maximum Shaft Horsepower per Unit Flow Versus Nozzle Exit Velocity for Nozzle Angles of 15 and 20 Degrees.

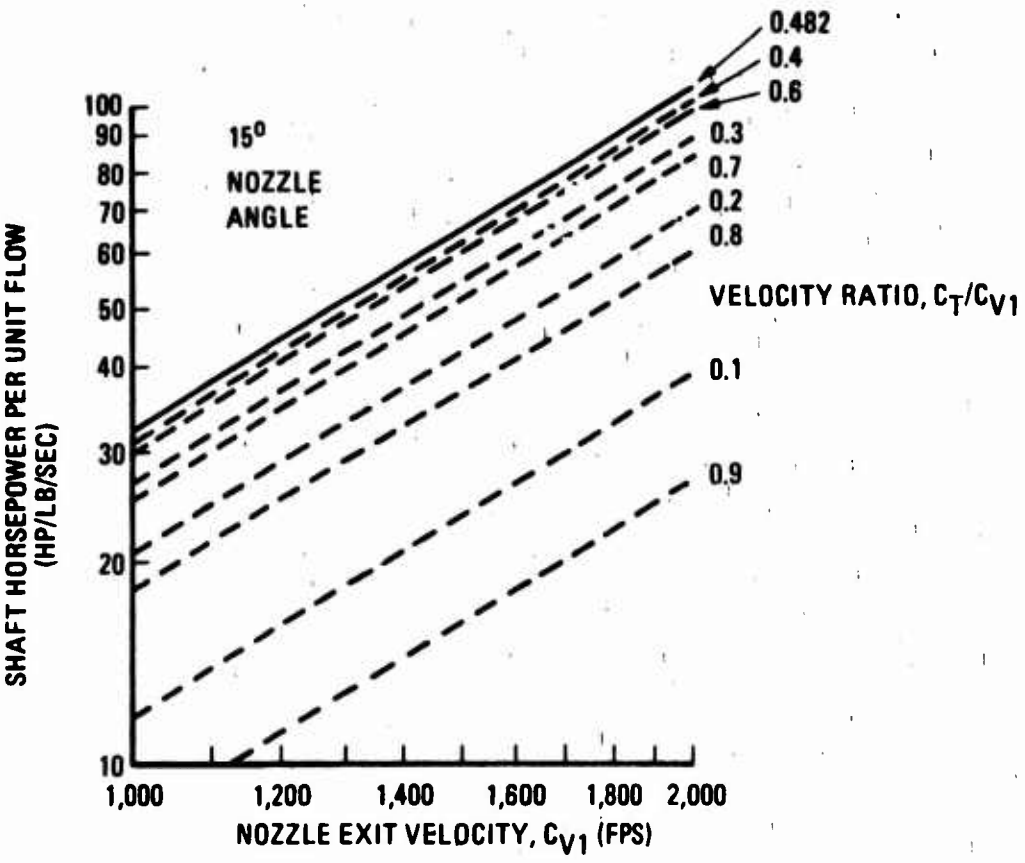

Figure 26. Shaft Power Generation Versus Nozzle Exit Velocity at Variable-Velocity Ratios.

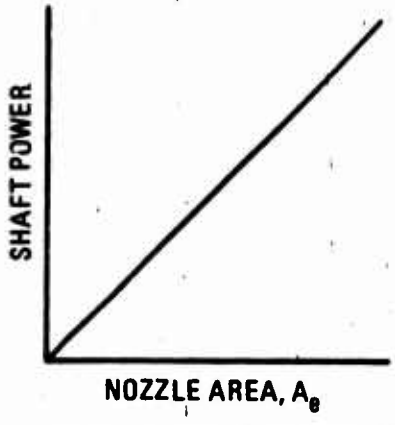

Figure 27. Shaft Power Versus Nozzle Area (Applicable Only for Constant Tip Speed to Exit Velocity Ratios).

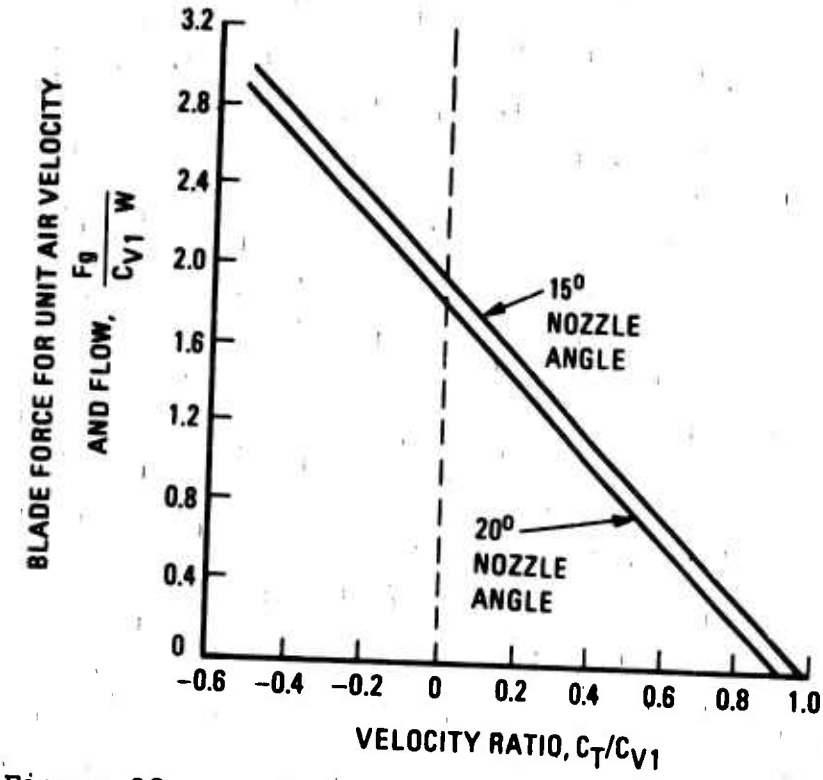

Figure 28. Blade Force Versus Velocity Ratio.

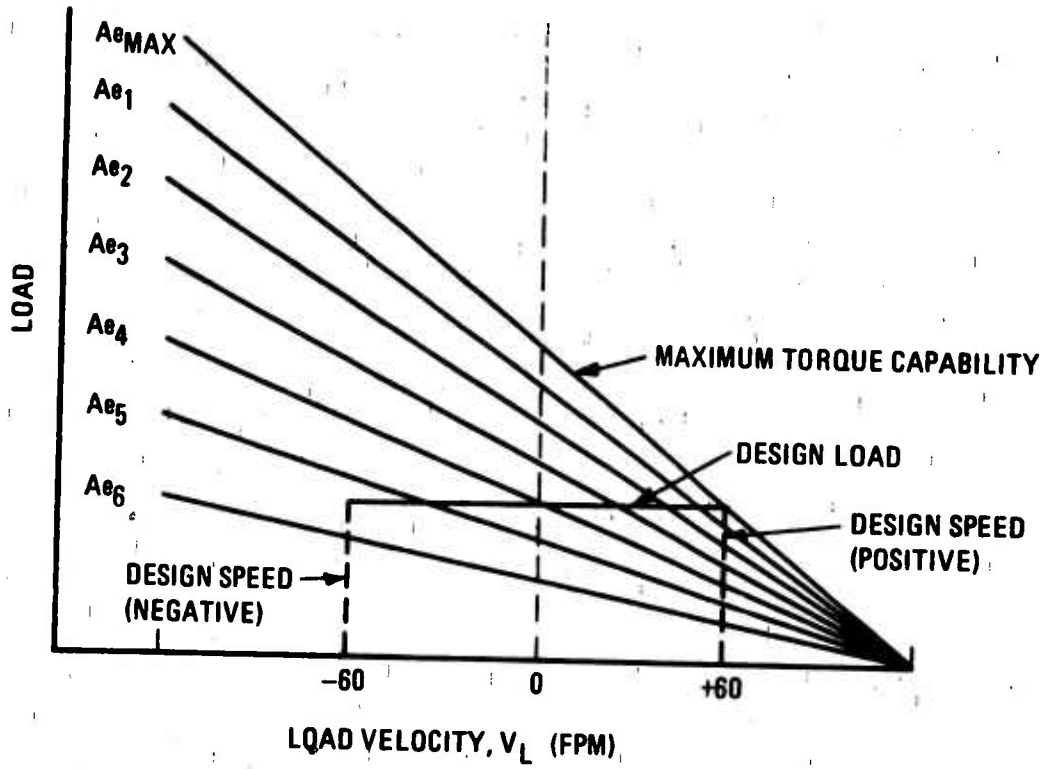

Figure 29. Rate of Descent for Constant Expansion Ratio, Variable Nozzle Turbine.

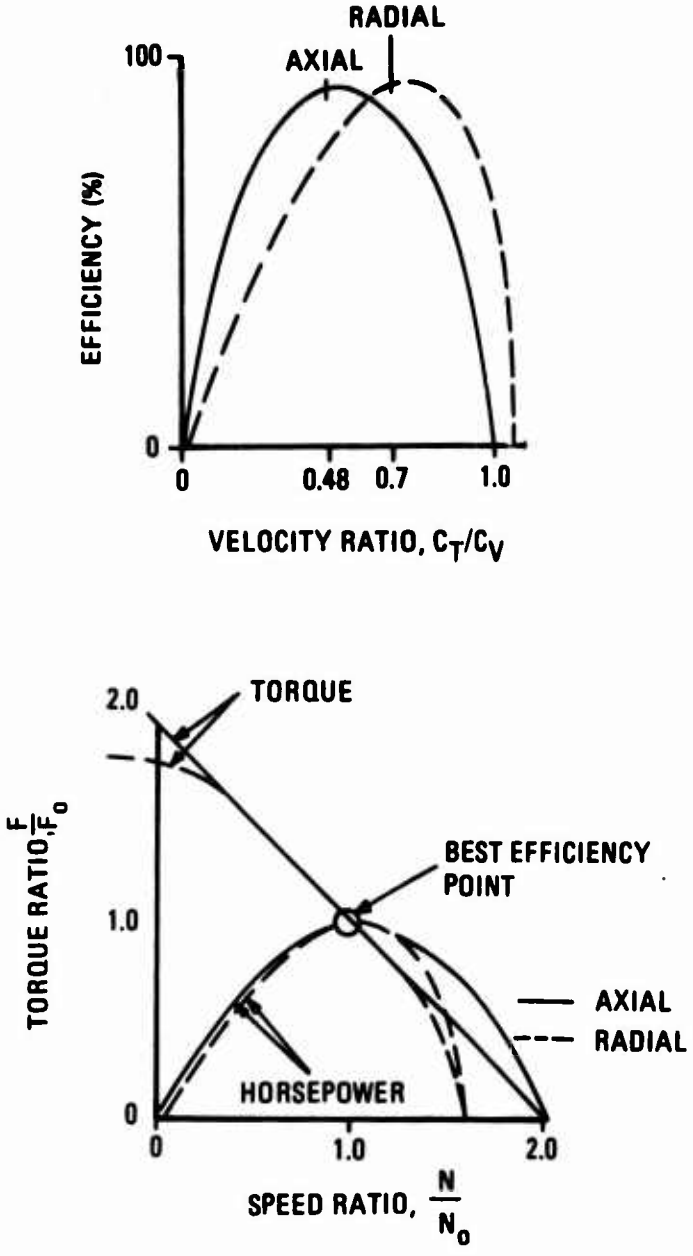

Figure 30. Axial Versus Radial Wheel Characteristics.

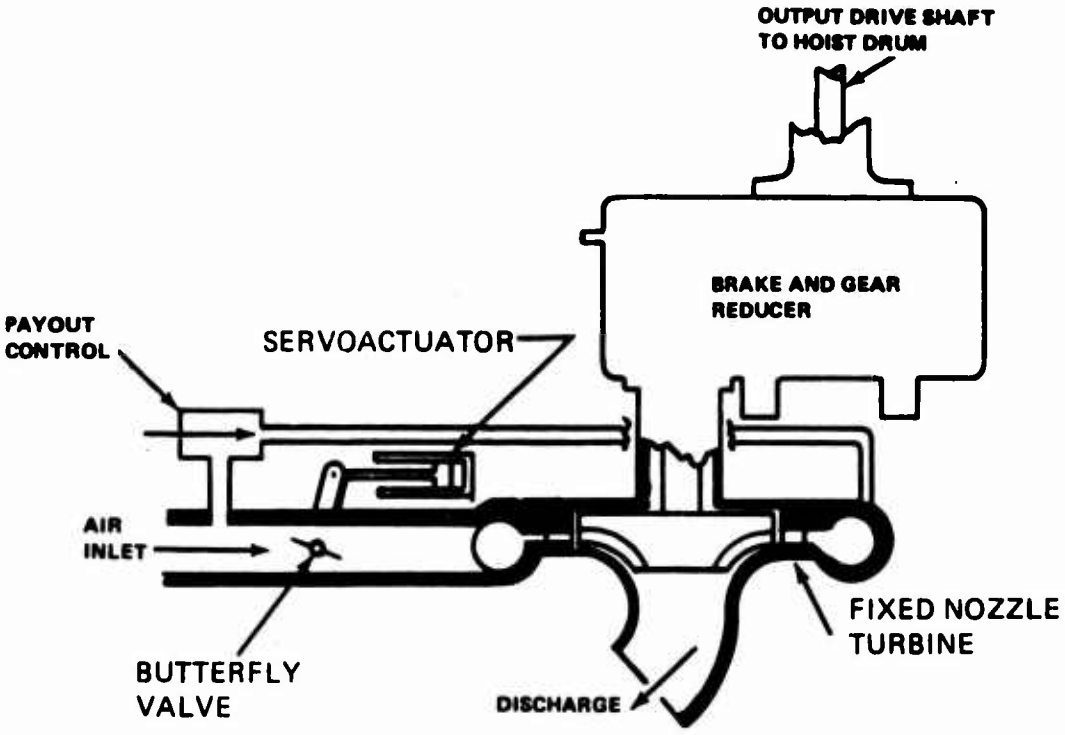

Figure 31. Fixed Nozzle.

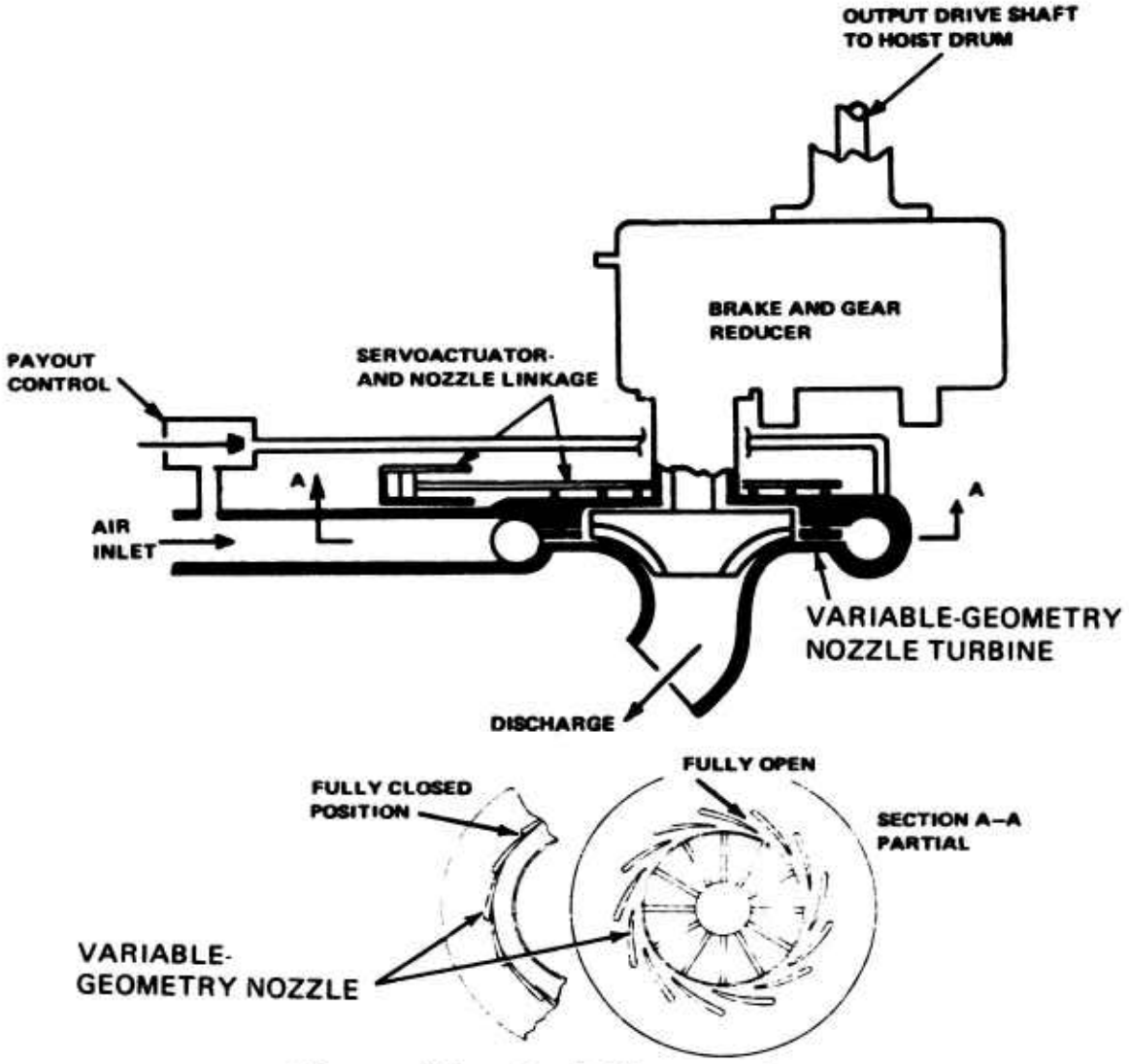

Figure 32. Variable Nozzle.

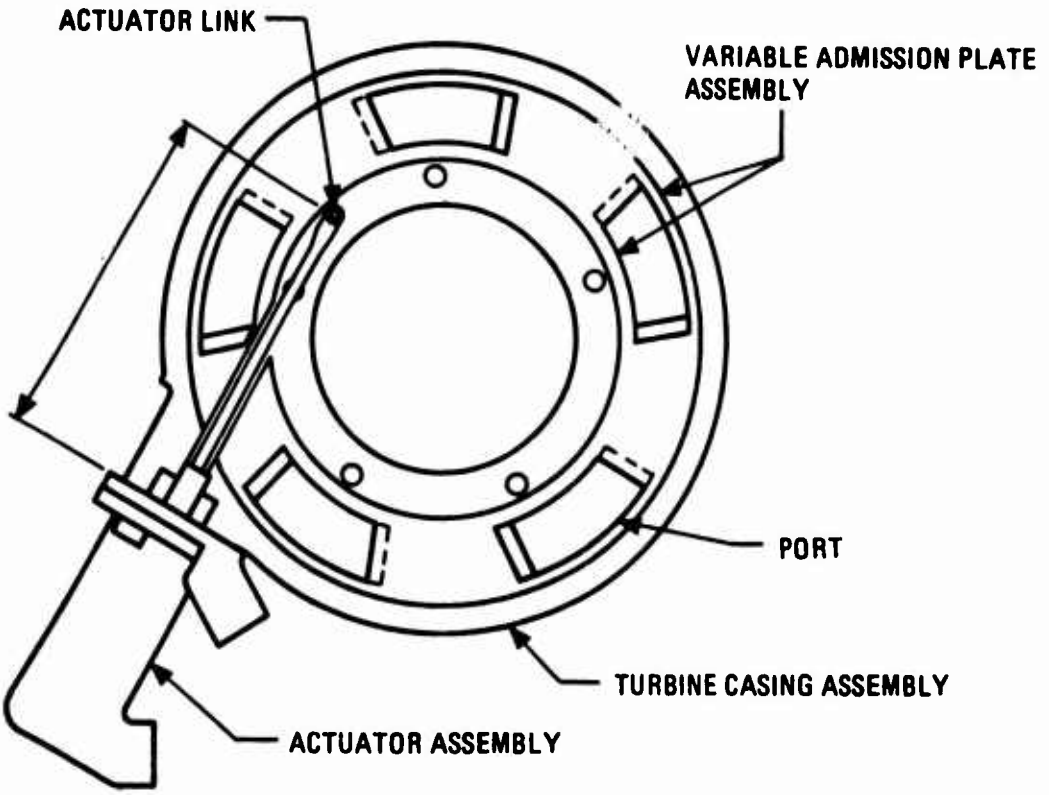

Figure 33. Partial Admission Nozzle.

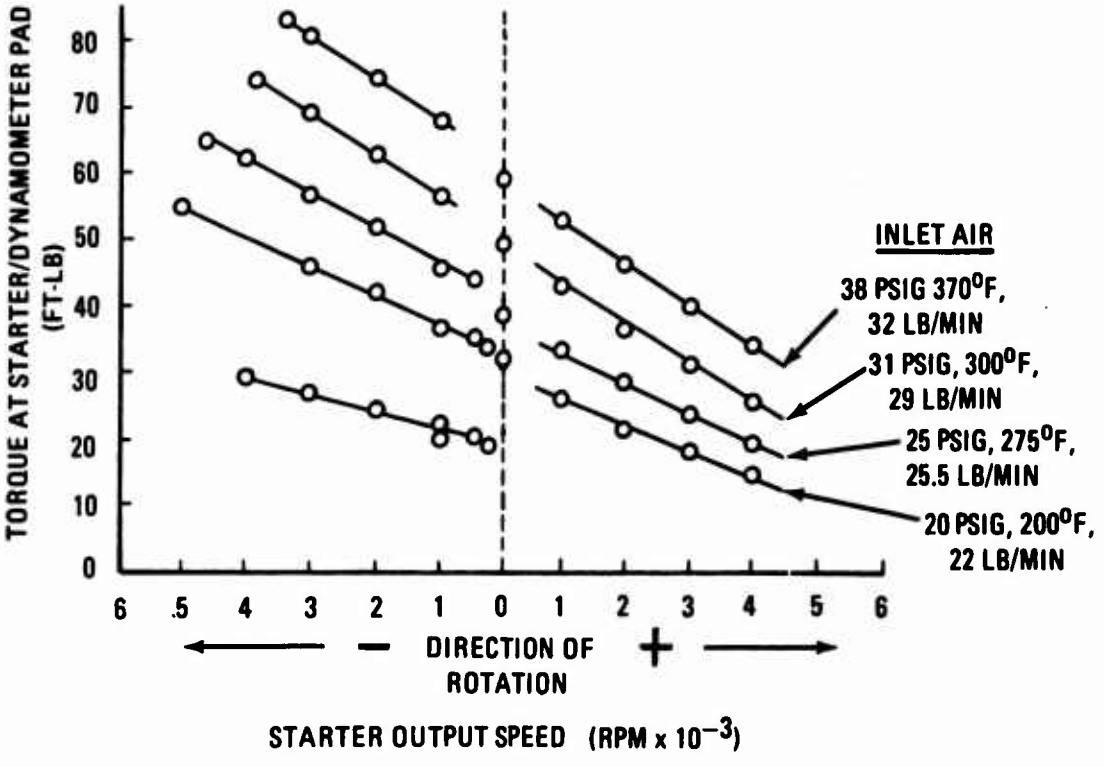

Figure 34. Test Data for Bendix Air Turbine Starter.

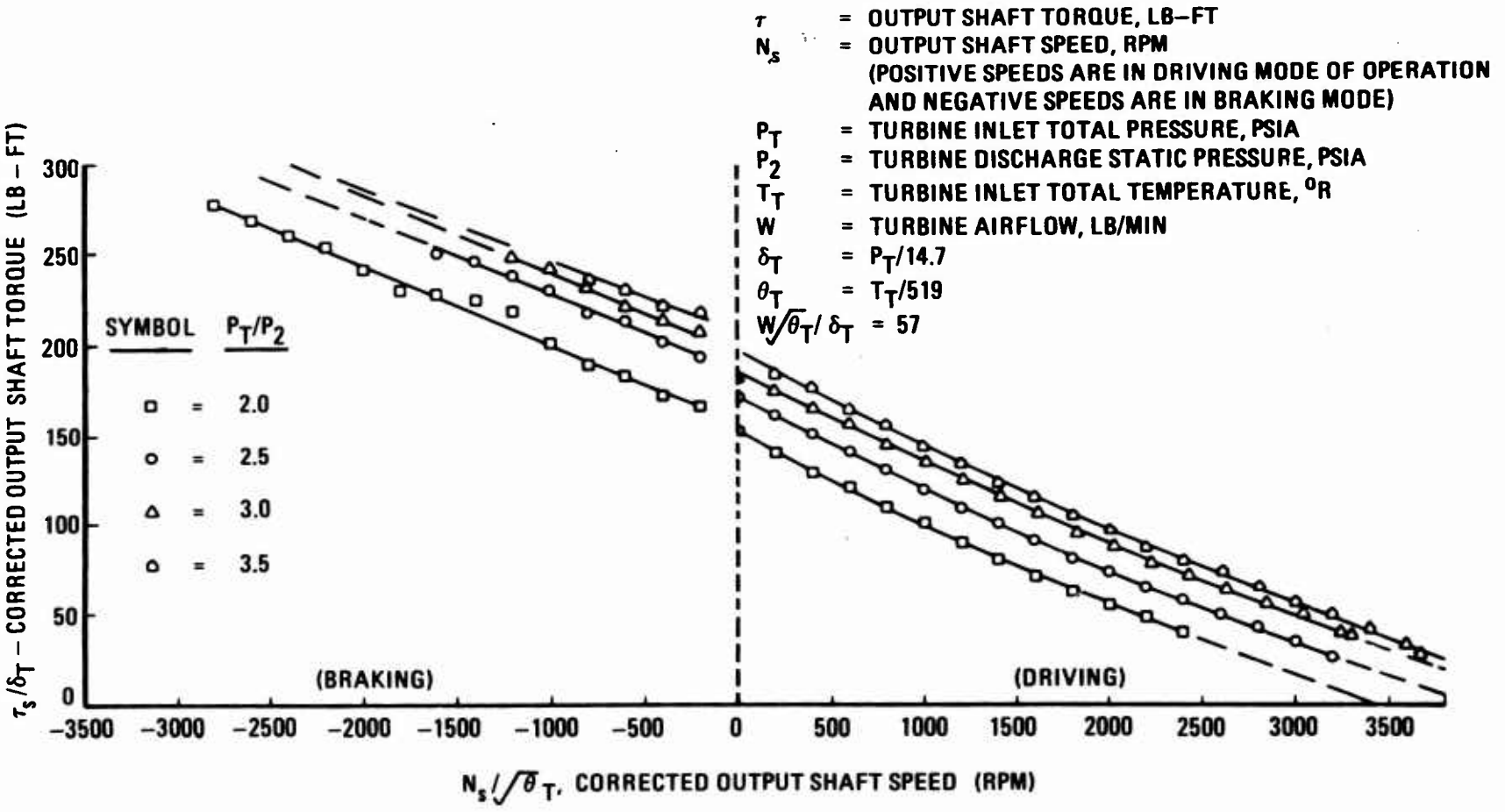

Figure 35. Driving and Braking Performance of the AiResearch Air Turbine Starter.

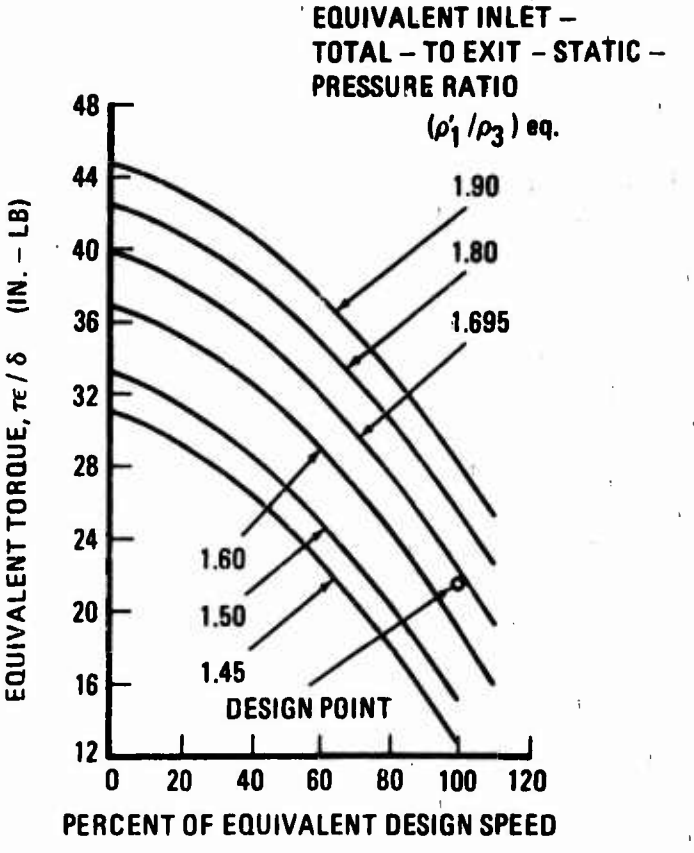

Figure 36. Variation of Torque With Speed and Pressure (From NASA TN D-5090).

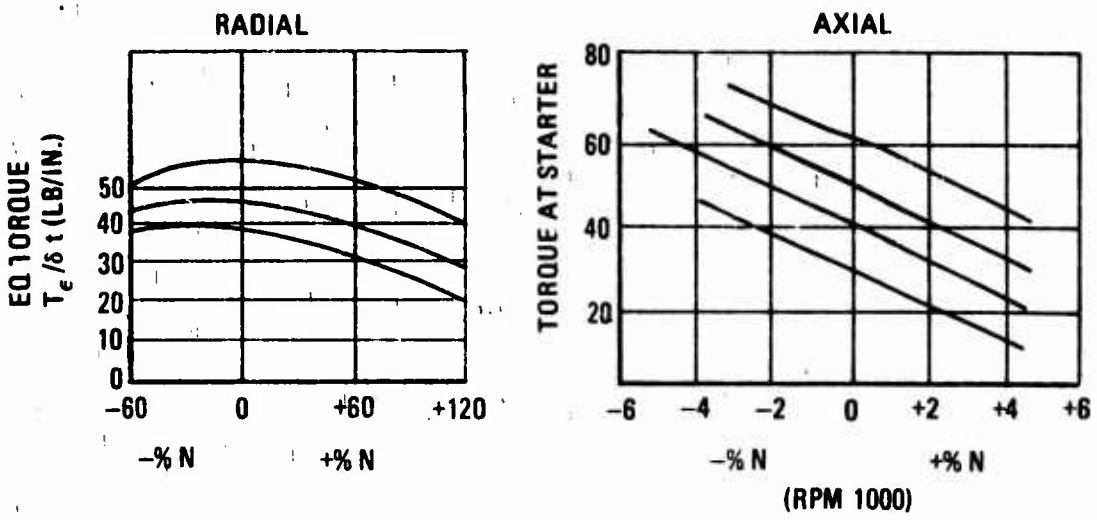

Figure 37. Dynamic Braking Capability (Test Bed).

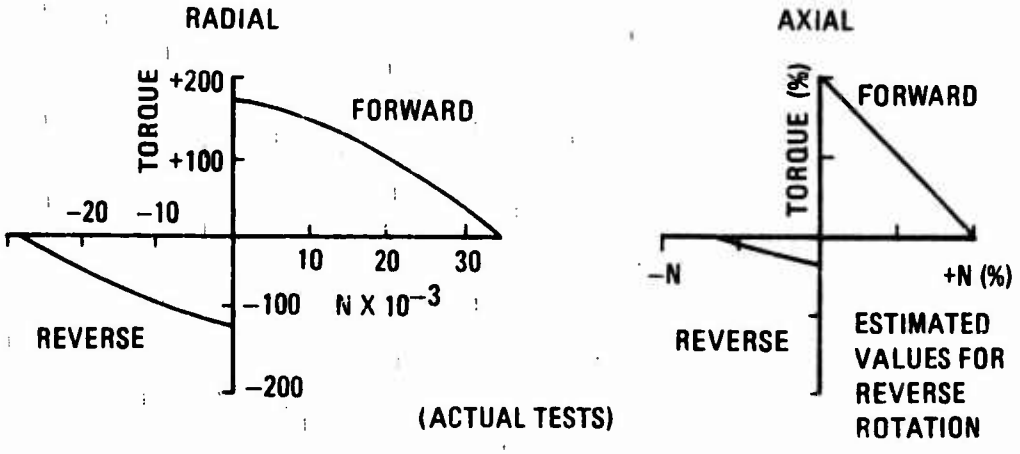

Figure 38. Forward and Reverse Rotation.

RADIAL VERSUS IMPULSE TURBINE DESIGNS

The performance characteristics of radial and impulse turbines were investigated; and the significant parameters affecting system design were compared. These parameters were: overspeed capability, impact on performance under variable ambient operation, turbine wheel diameter, gear reduction requirements, and acquisition and design. A comparison of radial and impulse turbine wheels is particularly significant in the investigation of the dynamic braking. The impulse turbine characteristics appear superior to the radial turbine. This was substantiated by actual tests conducted with both axial and radial wheels.

TURBINE DESIGN CONSIDERATIONS

The primary consideration in turbine design is the axial versus the radial configuration; applicable to both types is the determination of nozzle design -- fixed-geometry versus variable-geometry. Discussions with vendors indicated availability of either combinations with no major manufacturing problems of any system selected. The breakthrough with the axial turbine came about with "Anocut", which is a process of electronic machining of cutting blades from a single forging. In a recent program funded by the Air Force for an advanced technology small engine, one radial and one axial turbine within the same engine were used as a result of optimization studies conducted. To repeat, manufacturing problems or availability of any turbine configuration is no problem.

TURBINE WHEEL SELECTION SUMMARY

Based on analytical performance data of the respective wheels, and on the basis of the test data, the following conclusions are drawn:

- The axial wheels are more suited for variable-speed/load hoist control, due to their linear torque speed characteristics.
- The radial wheel must be approximately 1.4 times larger in diameter than the axial wheel. The ATM housing is therefore larger.
- The radial wheel in reverse rotation does not provide the discrete torque intelligence necessary for the rate-of-descent control for hoisting applications.

- The radial wheel's ratio of free running speed to optimum operating speed does not permit unloaded hook hoisting speeds to be equal to those of the axial wheel.

- The stall torque of the axial wheel is higher than that of the radial wheel.

- The variable-geometry nozzle design for the radial wheel is less complex than that for the axial wheel.

- Neither the axial nor the radial turbine provides high-speed (200%) empty-hook payout capability.

- The efficiency of both wheels is nearly the same.

- No significant difference in fabrication of either wheel exists, nor is there a substantial cost difference.

Based on the above, the axial wheel has been selected as the most appropriate for this application.

TURBINE OVERSPEED CAPABILITY

Considerations to date on the hoist-drive system analyses conducted were limited mainly to the design and lower-than-design speeds. Since hoisting is conducted when the helicopter hovers, in which mode the power setting for the main engine is at a maximum, it was considered important to provide higher-than-design hoist speeds in both directions with an empty hook. The fuel saving that could be realized with the higher speed is considerable indeed; the mission time could be reduced also.

The analysis and tests indicated that higher-than-design forward speeds are feasible. Twice the design speed with an axial wheel is possible, while approximately 40 percent above design speed may be possible with radial wheels (assuming design point operation is at maximum turbine efficiency). The reverse speed (paying out empty hook) of twice the design speed required a two-wheel ATM configuration, wherein one wheel is used for hoisting and dynamic braking while the other is used for reversing.

VARIABLE-G ACCOMMODATION WITH AN IMPULSE-TYPE ATM

When designed for maximum operating power efficiency, the impulse-type air-turbine motor will inherently accommodate a 2.0g acceleration of the load. At this acceleration level, the ATM will stall but hold the load steadily. The airflow through the ATM will be identical as for the optimum design velocity at 1g design load.

The torque generating capability of the ATM is

$$F = \frac{\overset{o}{W}}{g} C_{V1} \left(\cos \alpha - \frac{C_T}{C_V} \right)$$

where F = force on the blades, pounds (synonymous with torque)

$\overset{o}{W}$ = airflow, pounds per second

C_{V1} = jet velocity, fps

α = nozzle angle, degrees

g = acceleration due to gravity = 32.2 ft/sec^2

C_T = turbine wheel tip speed, fps

The stall torque generation capability occurs when g is zero; and for a fixed-nozzle spouting velocity, the stall torque is directly proportional to the airflow and is based on the assumption that there are no limits on an effective turbine nozzle area. Conversely, there is no theoretical limit on g-loading accommodation if adequate air supply is available.

For this study, however, the problem was to demonstrate the impact on power, speed, and efficiency when the turbine is required to accommodate higher than 2.0g acceleration loading. The following generalized mathematical relationships apply.

- The optimum efficiency is obtained when the tip speed of the rotating wheel is one-half of the product of the nozzle spouting velocity and the cosine of the nozzle angle $C_T = \frac{C_{V1} \cos \alpha}{2}$

- The overspeed capability of the turbine expressed in percent is $n = \frac{G^2}{G-1}$

- The airflow required is expressed as

$$\overset{o}{W} = \frac{(HP)opt}{\cos \alpha} \left(\frac{G^2}{G-1} \right)$$

- The relative turbine efficiency (based on optimum of 100 percent) $\eta_{rel} = \frac{1}{W_o}$

Based on the calculation derived above, the performance parameters of relative turbine efficiency, relative turbine velocity, and airflow requirements, W, are plotted vs "G" design requirements and are as shown in Figure 39. The data are tabulated in Table XV.

TABLE XV. G-CAPABILITY VS RELATIVE AIRFLOW, VELOCITY AND EFFICIENCY

"G" Capability	G^2	$\frac{G^2}{G-1}$	Airflow Required W_o	Rel. Max. Turbine Vel f(X) $(G-1)/G$	Rel. Effic. $\eta_{Rel} = \frac{1}{W_o} \times 100$
1.0	1	α	α	-	0
1.25	1.5	0.24	1.56	.2	64.2
1.4	1.96	4.9	1.22	.286	82
1.5	2.25	4.5	1.125	.333	89
1.6	2.56	4.27	1.06	.375	94.5
1.75	3.06	4.08	1.02	.428	98
1.88	3.54	4.02	1.004	.468	99.5
2	4	4	1.0	.5	100
2.2	4.84	4.03	1.008	.545	99
2.5	6.25	4.17	1.043	.6	96
3	9	4.5	1.125	.66	89
3.28	10.75	4.72	1.18	.696	84.7
3.5	12.2	4.9	1.225	.715	81.5

AIR-TURBINE NOZZLE AREA DESIGN

The effective nozzle area design, when based on a hot-day condition, will not permit adequate flow passage to accommodate at least equal hoisting capacity for cold ambients. This is attributable to the fact that the temperature of the air is much colder with the resulting lessening of the supplied air specific energy. The nozzle area design must therefore be based on some colder design-day conditions. (The above is based on a constant pressure ratio operation.) To compensate for the lower specific energy level, more airflow is required, which is available from the increased capability of air delivery from the compressor at the low temperature.

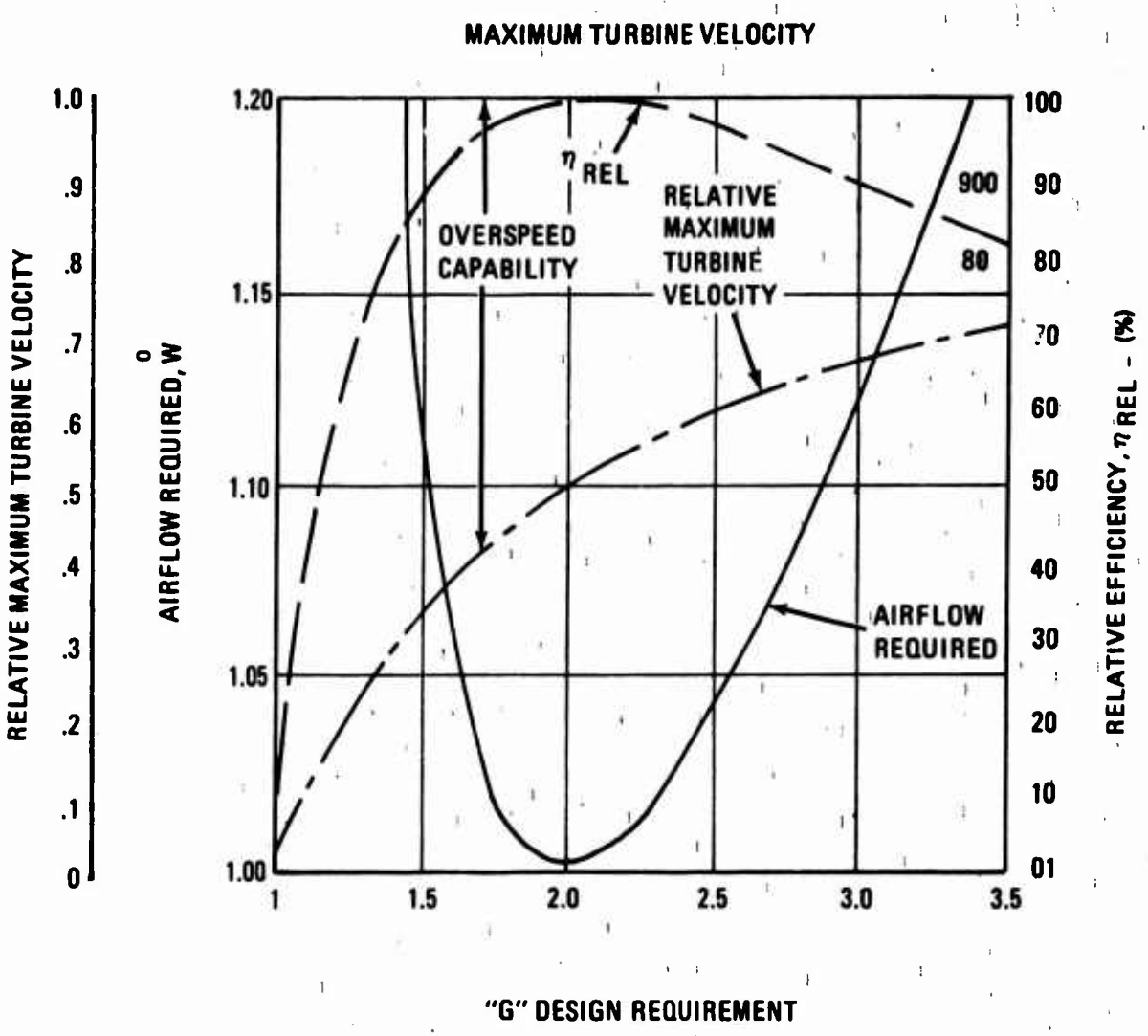

Figure 39. Relative Turbine Velocity and Efficiency and Airflow Required Versus "G" Design Requirements.

The analyses conducted herein were based on a particular compressor design yielding a 4:1 pressure ratio, which is maintained throughout the entire spectrum of operating ambients from -65°F to +95°F and includes both 4,000 feet and sea level operating conditions. Based on the performance characteristics of the above compressor, the turbine inlet temperature and the respective losses between the compressor and the turbine were calculated. On the basis of degrading turbine performance from the optimum design-day condition of 4,000 ft, 95°F, the nozzle area required for various ambients is as shown in Figure 40.

In order to provide the same hoisting capacity at 4,000 ft, -65°F conditions, the nozzle area required is approximately 11 percent higher than for the equivalent capacity at 4,000 ft, 95°F condition. The corresponding airflow requirement is 36 percent higher at the -65°F ambient condition.

The effective nozzle area must therefore be designed for the -65°F condition in order that no degradation of capacity at this temperature occurs. The adequacy of the increased air delivery from the compressor has been established.

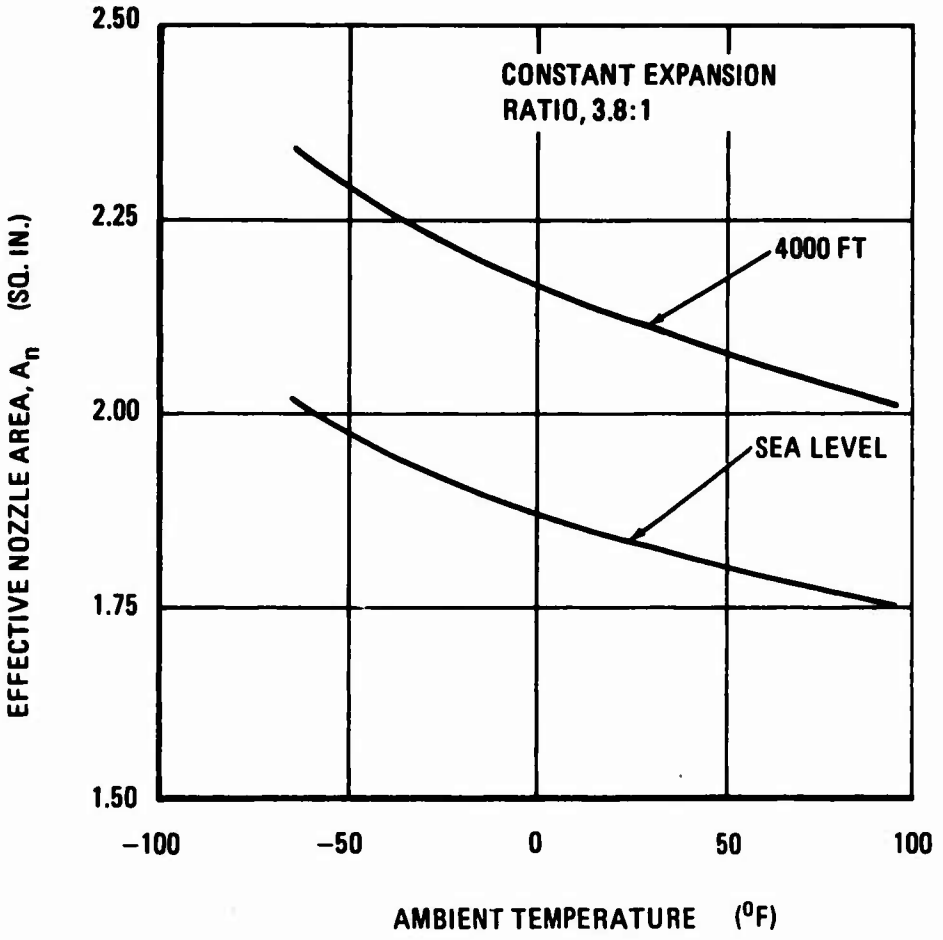

Figure 40. Nozzle Area Required for a Constant Hoist of 23 Tons at 60 Feet per Minute Versus Ambient Temperature.

THE AIR COMPRESSOR

The compressor for the pneumatic hoist-drive system is analogous to a pump for a hydraulic drive and to a generator for an electrical drive.

There were no limitations on type of compressor designs during this study. Either centrifugal, multistage axial, or a combination of centrifugal and axial was acceptable.

The imposed limitations were a minimum of 80% adiabatic compression efficiency, minimum weight, and high reliability.

Investigation of "off-the-shelf" units available, shown in Figure 41, that will meet these requirements resulted in the selection of a unit whose tested performance characteristics are shown in Figure 42.

This unit weighs approximately 26 pounds. It consists of six axial stages and one centrifugal stage and is ideally suited for hoisting capacities of up to 50 tons at sea-level standard conditions. This unit has been used in a small prime propulsion helicopter engine operating at pressure ratios in excess of 6:1 at corrected speeds of approximately 50,000 rpm.

COMPRESSOR PERFORMANCE AND POWER LEVEL REQUIREMENTS

Performance of the compressor design of Figure 41 has been calculated for the total spectrum of operating ambients and is shown in Figure 43. Table XVI shows the data used.

The purpose of this effort was to provide visibility regarding the power level requirements, air delivery, and compressor discharge temperature at various ambients for both sea level and 4,000-foot altitudes.

The above data are based on a constant-speed operation and a constant 4:1 pressure ratio. These calculations indicate power level requirements of 213 HP at 4,000 ft, 95°F design conditions and approximately 338 HP at sea level -65°F design day. The relative power magnitudes are identified for comparison purposes only. The compressor air delivery for the conditions specified is 112 pounds/minute and 210 pounds/minute, respectively. Both conditions are based on a constant pressure ratio.

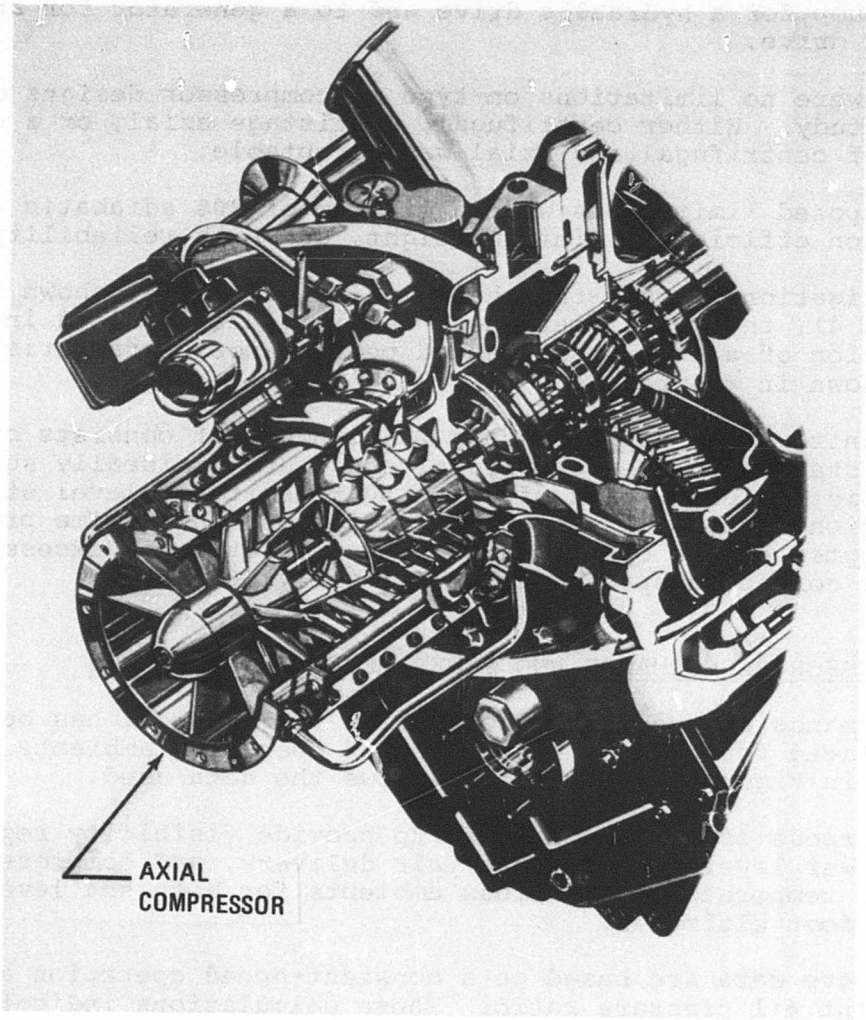

Figure 41. Air Compressor - Allison Model 250.

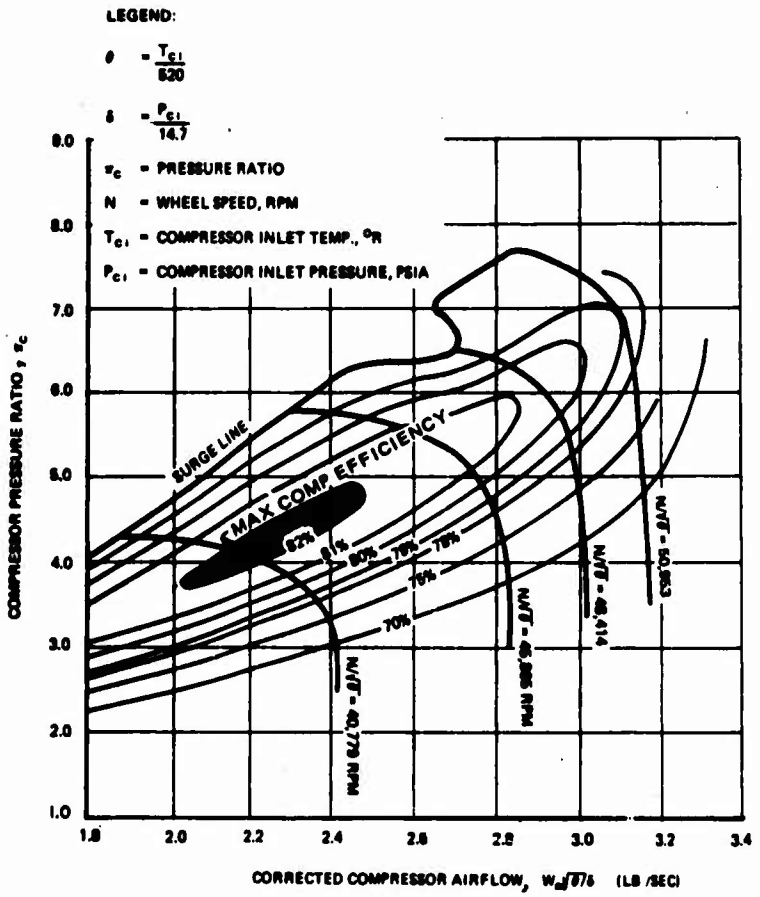

Figure 42. Performance Map of an Available Air Compressor.

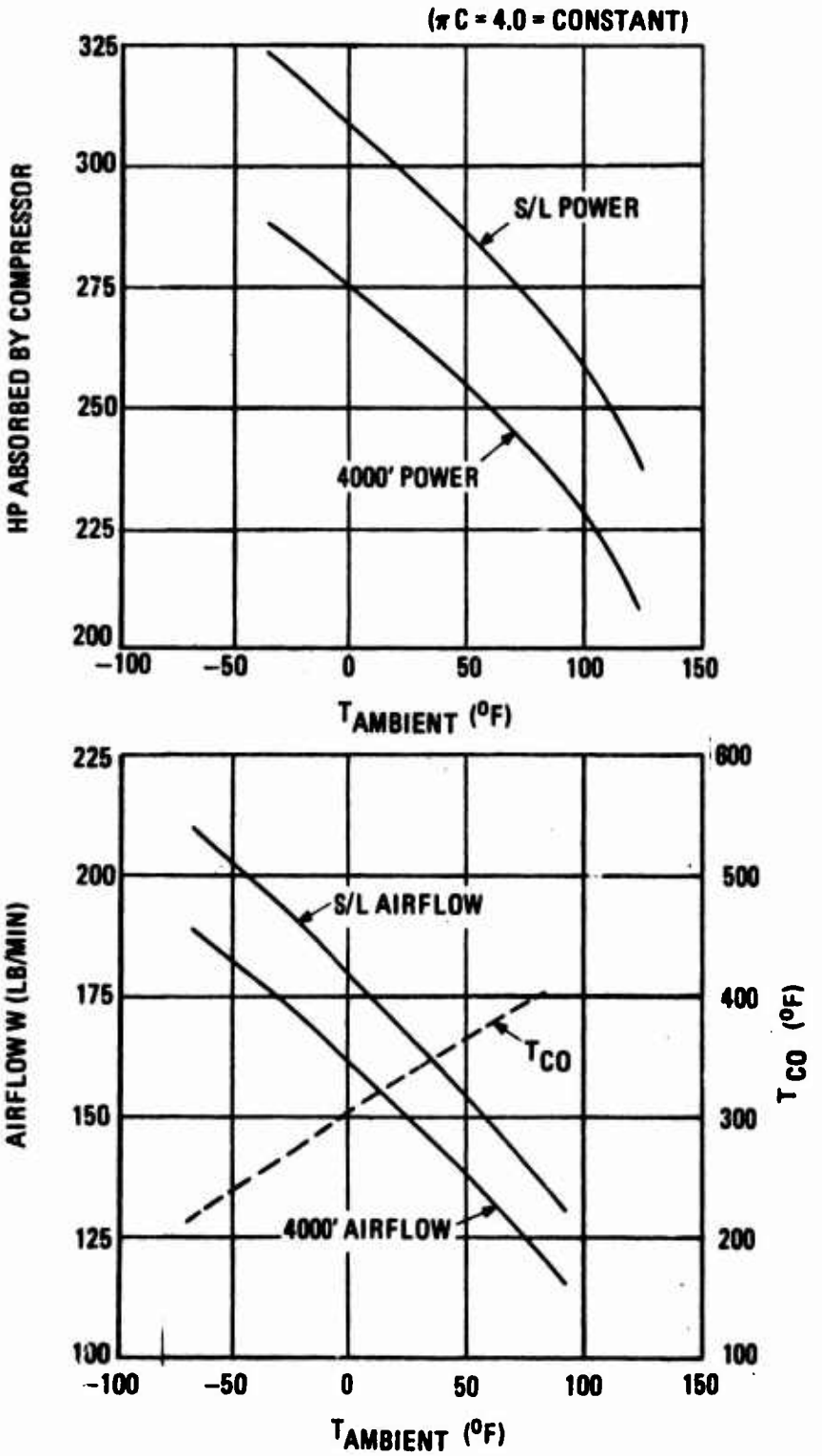

Figure 43. Compressor Performance Versus Ambient Temperature.

Predicated on a constant rotational input speed of 42,300 rpm and based on a constant pressure ratio of 4:1, the unit efficiency, the airflow, and the corrected speed are as tabulated in Table XVI.

TABLE XVI. COMPRESSOR PERFORMANCE VERSUS AMBIENTS

STATE-POINTS	T_{amb} (°R)	θ	$\sqrt{\theta}$	δ	$\frac{\sqrt{\theta}}{\delta}$	$\frac{\sqrt{\theta}}{\delta}$	$\dot{\omega}$	$\frac{N}{\sqrt{\theta}}$	N	H_c	$\frac{\dot{\omega}}{\omega_o}$
4000/95	555	1.070	1.035	.88808	1.165	2.25	1.93	40,779	42,300	82	1.0
S.L./95	555	1.065	1.035	1.00000	1.035	2.25	2.17	40,779	42,300	82	1.13
4000/60	520	1.000	1.000	.88808	1.125	2.50	2.22	42,300	42,300	79.5	1.15
S.L/60	520	1.000	1.000	1.00000	1.000	2.50	2.50	42,300	42,300	79.5	1.30
4000/0	460	.885	.942	.88808	1.060	2.75	2.60	44,800	42,300	74	1.35
S.L/0	460	.885 .760	.942	1.00000	.942	2.75	2.92	44,800	42,300	74	1.52
4000/-65	395	.760	.875	.88808	.985	3.10	3.15	48,300	42,300	67	1.63
S.L/-65	395	.760	.875	1.0000	.875	3.10	3.54	48,300	42,300	67	1.83

$$\theta = \frac{T_{amb}}{520} \ (^{o}R)$$

$$\delta = \frac{P}{29.92} \ (Hg) \quad (absol.)$$

N = rpm

ω_o = 4000' - 95°F airflow, lb/sec

$\dot{\omega}$ = lb/sec

η_c = compressor efficiency

Based on the compressor characteristics of Table XVI, the discharge temperature and the power absorbed by the compressor versus ambient conditions are tabulated in Table XVII as shown.

For the hoist-drive application, the corrected speed requirements are estimated to be under 40,000 rpm, with the resulting pressure ratio of approximately 43:1. This reduction in speed and lower pressure ratio are expected to result in better reliability and lower maintenance than in the original application.

TABLE XVII. DISCHARGE TEMPERATURE AND COMPRESSOR POWER ABSORPTION VERSUS VARIABLE AMBIENTS			
Altitude	T_{amb} (°F)	Compressor Discharge Temperature (°F)	Power Absorbed by Compressor (hp)
S.L.	95	421	242
S.L.	60	375	268
S.L.	0	299	298
S.L.	-65	218	301
4000	95	421	214
4000	60	375	238
4000	0	299	265
4000	-65	218	338

ALTERNATIVE COMPRESSORS

A suitable alternative single-stage centrifugal compressor is available in the form of the high-pressure compressor of the RS360-18 engine. The test characteristics of this compressor are shown in Figure 44.

The required pressure ratio of 4.3:1 and maximum air delivery termperature of 450°F can be achieved by aerodynamically overspeeding the compressor, estimated characteristics of which are shown on Figure 45. The rotational speed indicated is not a mechanical overspeed, being below the design speed of the impeller when run supercharged in an engine.

The load compressor will comprise an impeller and diffuser whose aerodynamic design is identical with the high-pressure compressor section of the RS360 gas generator. It will be aerodynamically oversped, compared to that of the gas generator, to achieve the required delivery pressure ratio of 4.3:1, and will be mounted in a volute casing of new design. This unit is located forward of the "core" compressor inlet.

The allowable flows which can be provided lie between 132 pounds/minute and 165 pounds/minute. Figure 46 shows a range comparable to these values. Estimated efficiency is approaching 80 percent.

This unit's estimated weight is 67 pounds, which includes the compressor rotor, the diffuser, and the volute casing. Operating speed for this application is estimated at 39,826 rpm.

The compressor size including the complete installation when coupled to the RS 360-18 engine is shown in Figure 47.

An alternate compressor design applicable for hoisting is expected from the F-15 APU engine. This unit is also centrifugal and is expected to weigh less than the selected design of 26 pounds. The peak efficiency, however, is estimated at 79%. Further performance and physical characteristics are, as of this writing, not available.

SUMMARY ON COMPRESSORS

Based on the above, compressor availability should constitute no problem. As hoisting capacities increase, compressors should be more plentiful. Efficiency increase with higher capacity unit is expected.

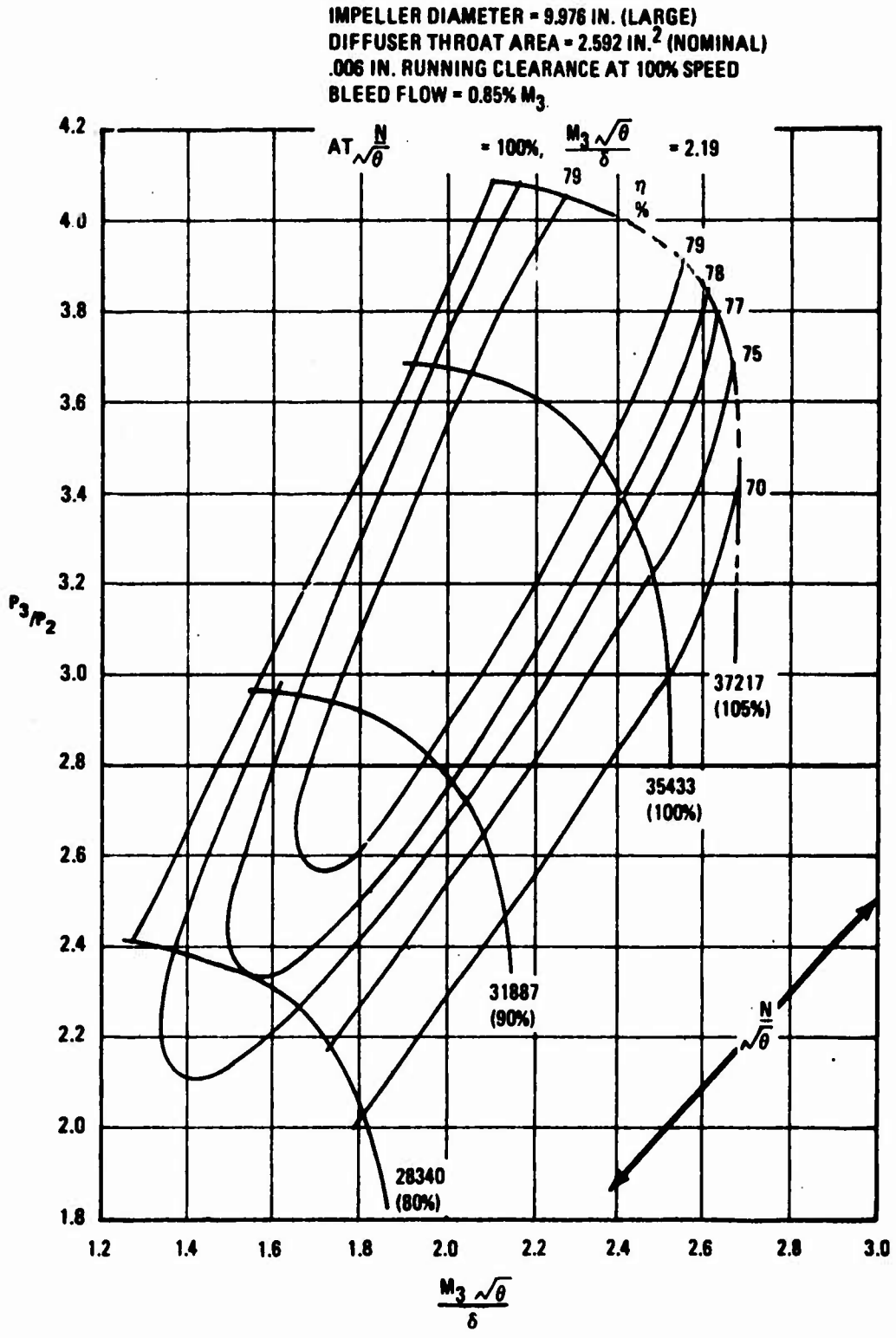

Figure 44. Load Compressor Characteristics for the Rolls-Royce RS 360-18.

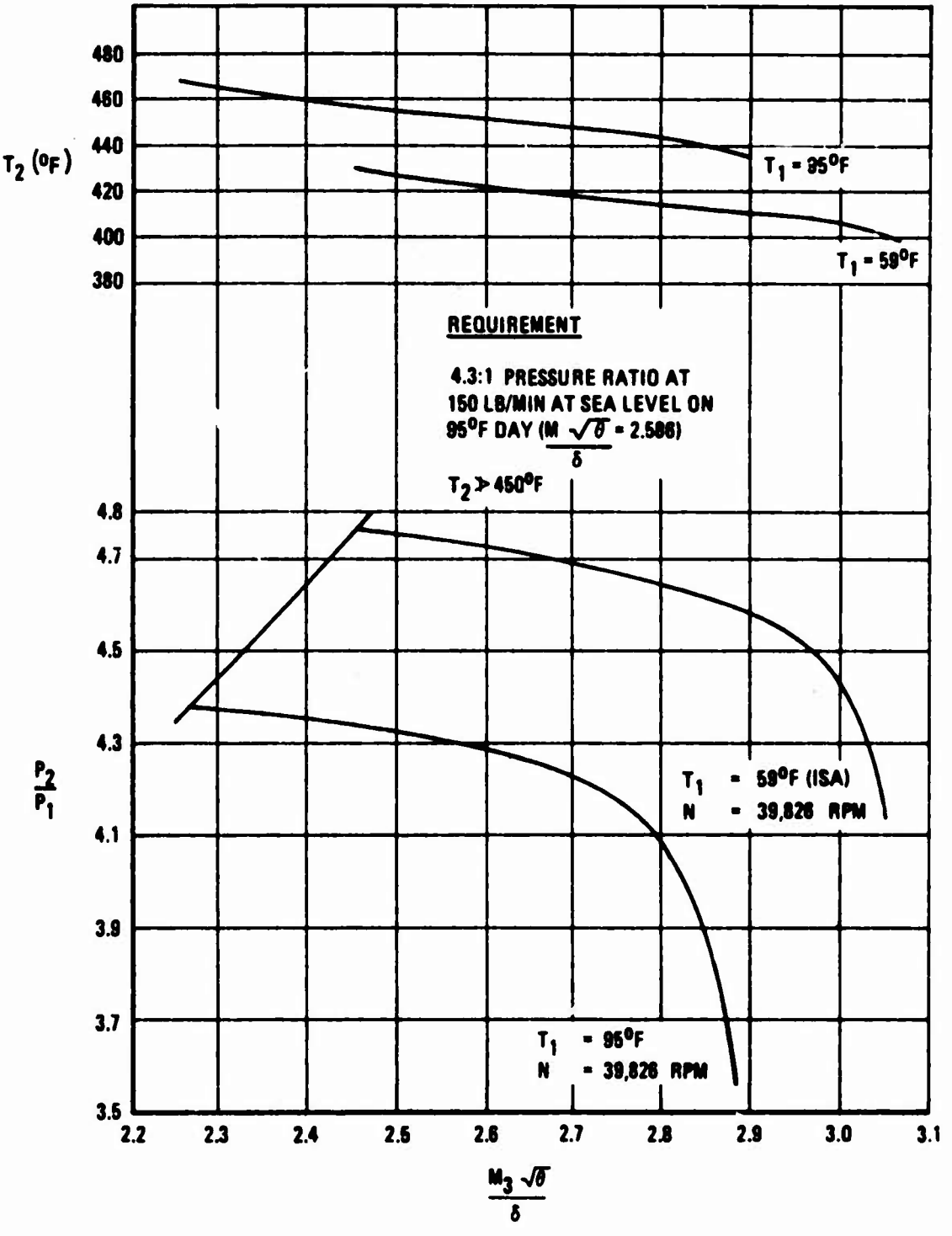

Figure 45. Estimated Performance at Aerodynamic Overspeed for the Rolls-Royce RS 360-18.

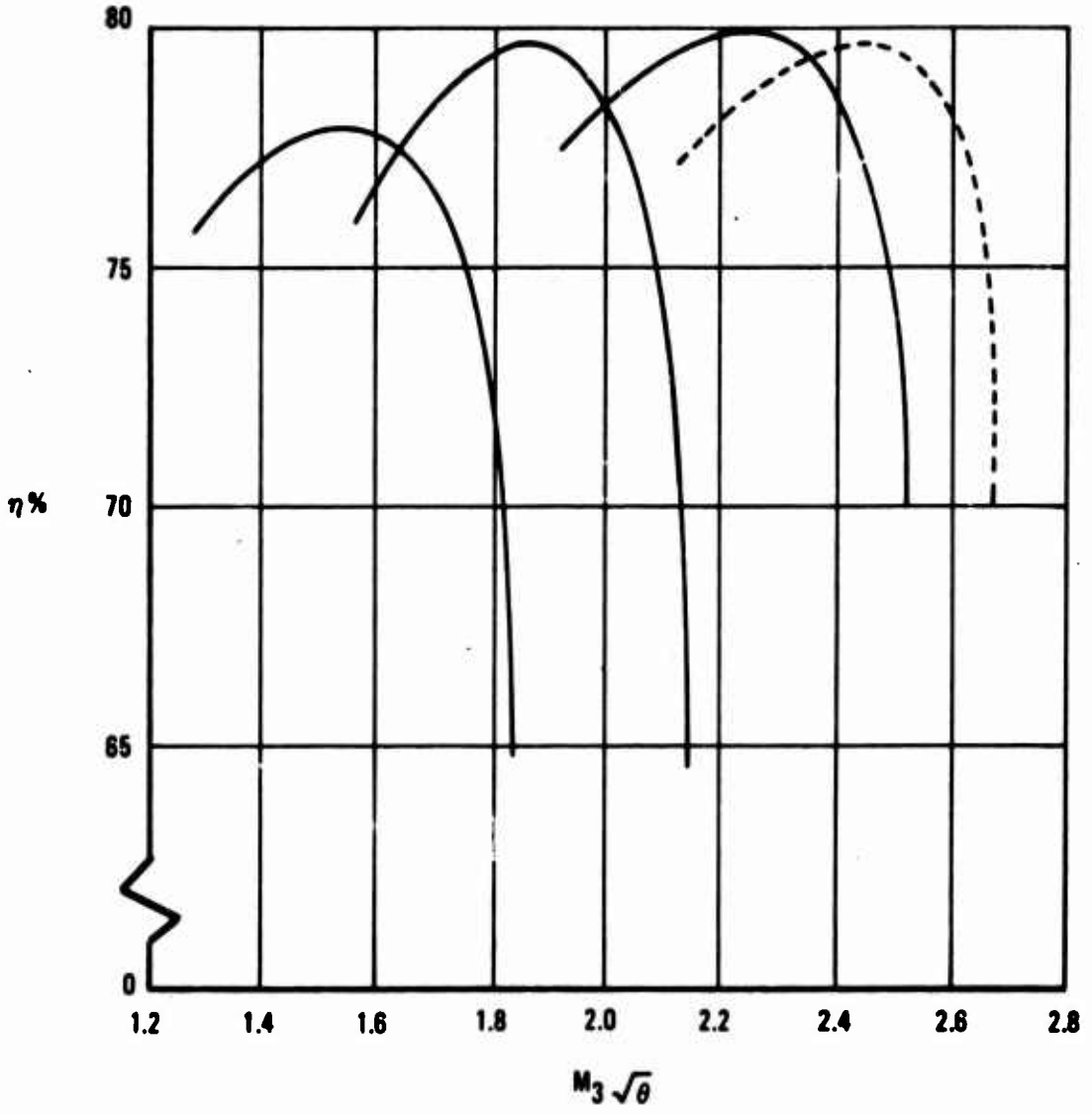

Figure 46. Load Compressor Characteristics for the Rolls-Royce RS 360-18.

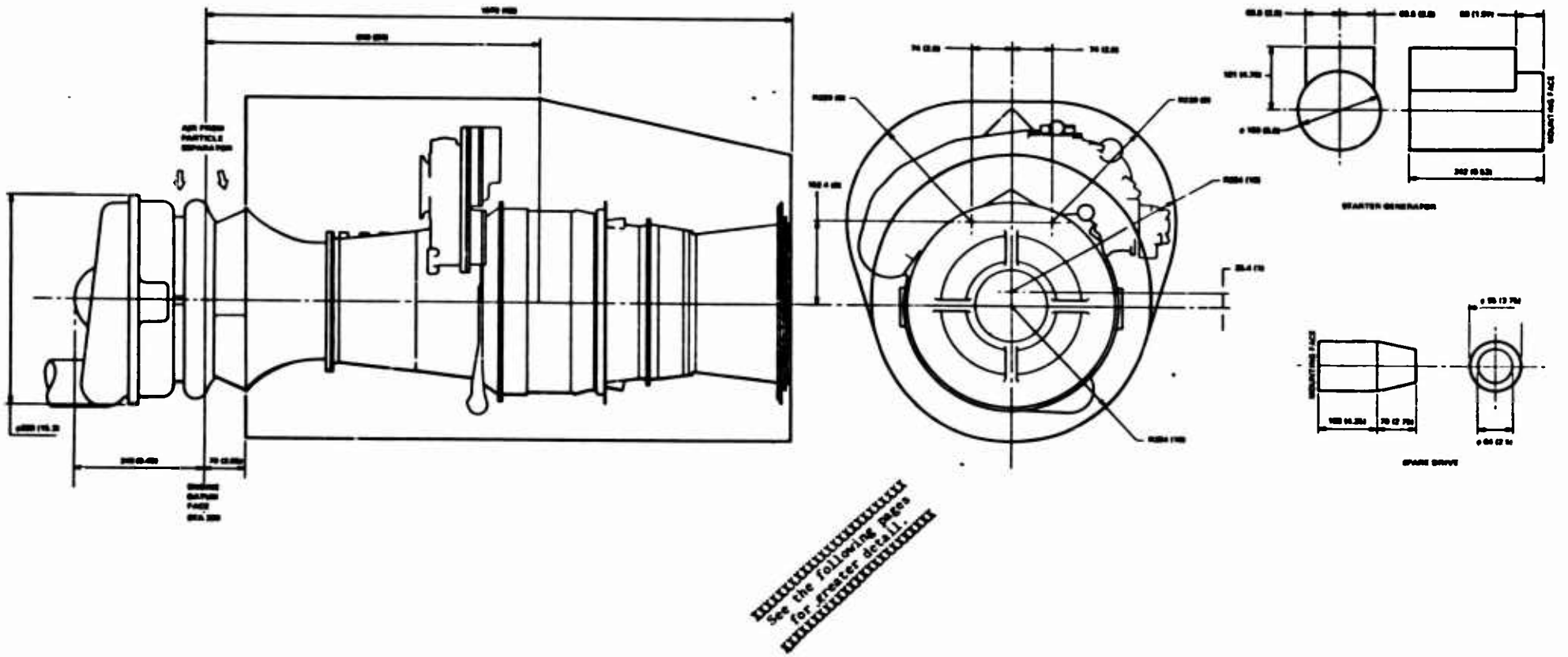

Figure 47. Compressor Installation on the Rolls-Royce RS 360-18 (Sheet 1 of 2).

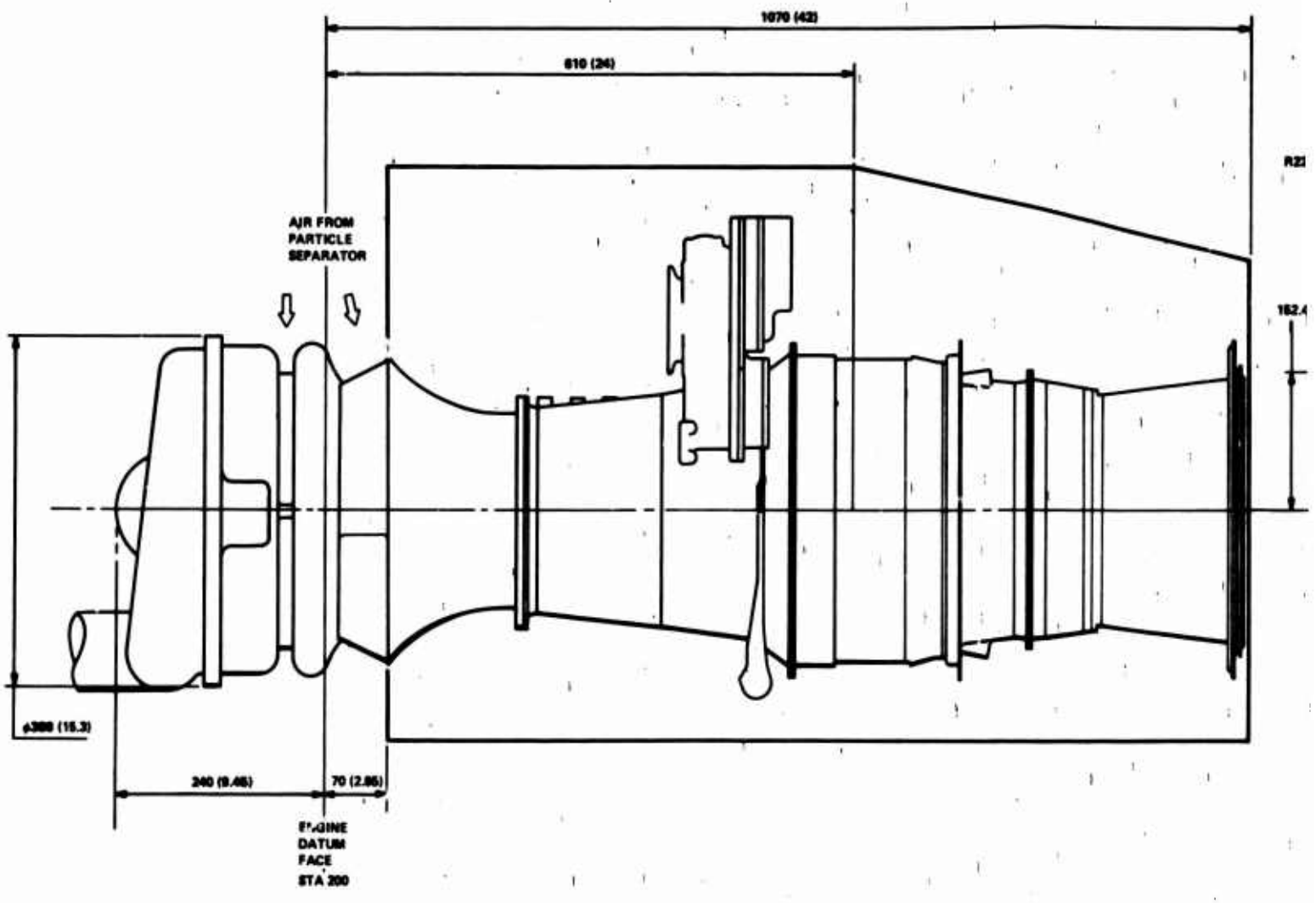

Figure 47. Compressor Installation on the Rolls-Royce RS 360-18 (Sheet 1 of 2).

105.2

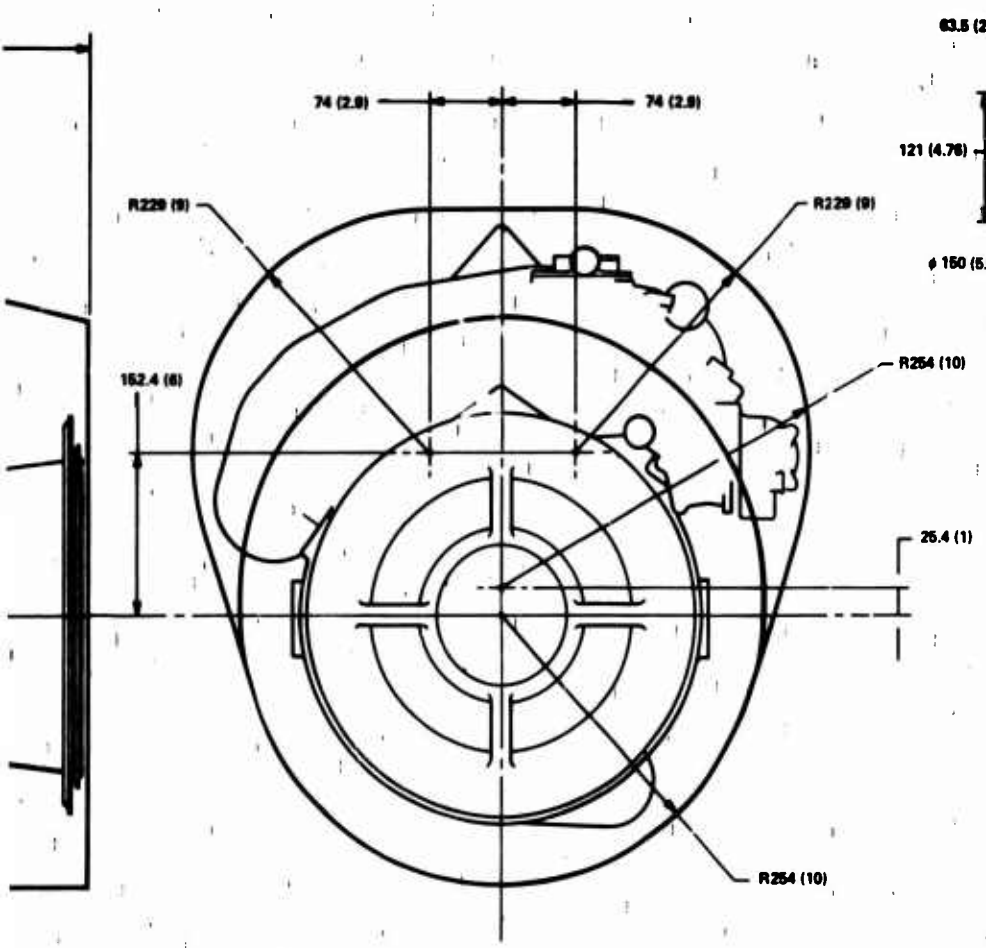

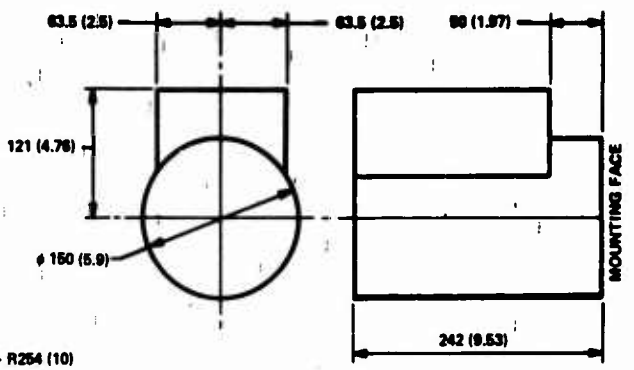

STARTER GENERATOR

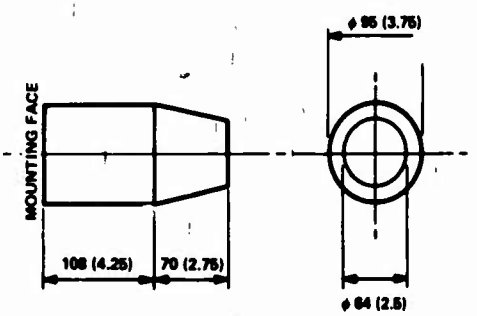

SPARE DRIVE

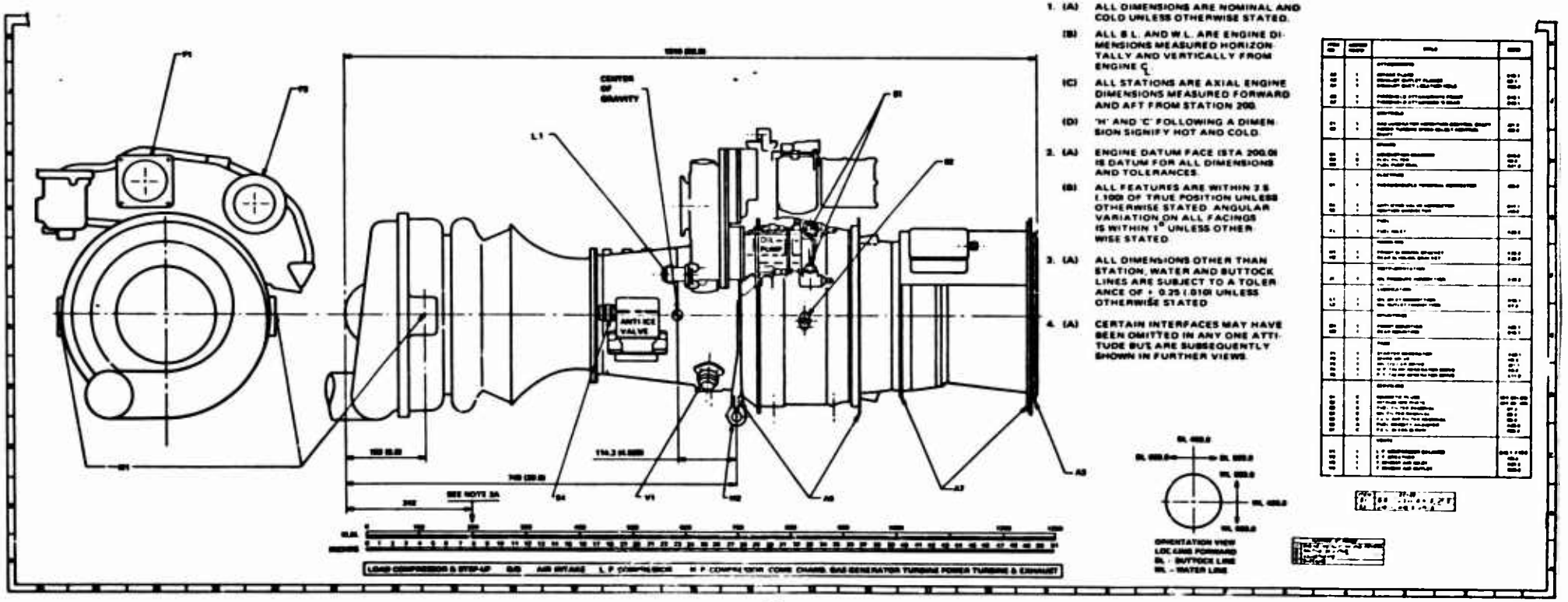

Figure 47. Continued (Sheet 2 of 2).

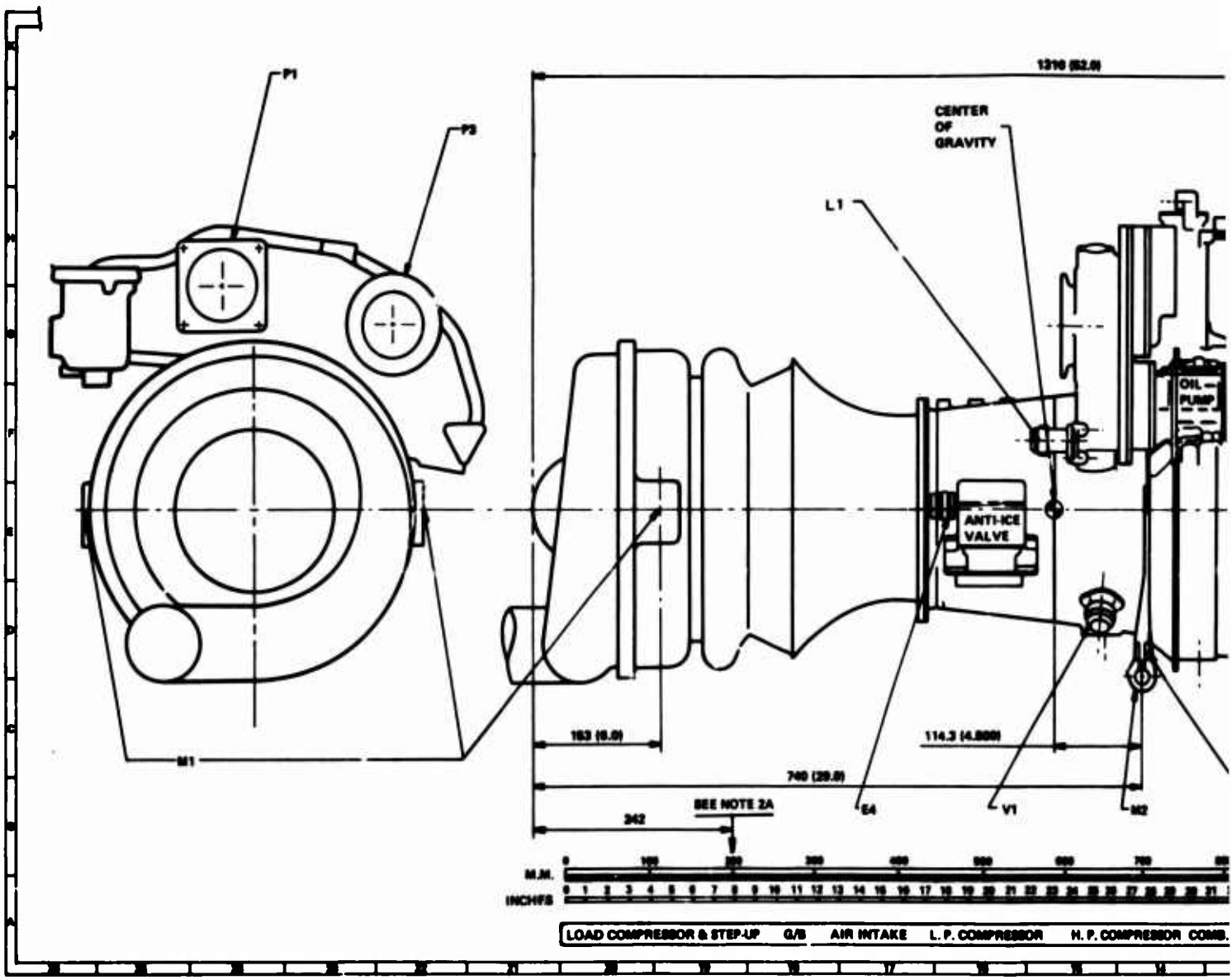

Figure 47. Continued (Sheet 2 of 2).

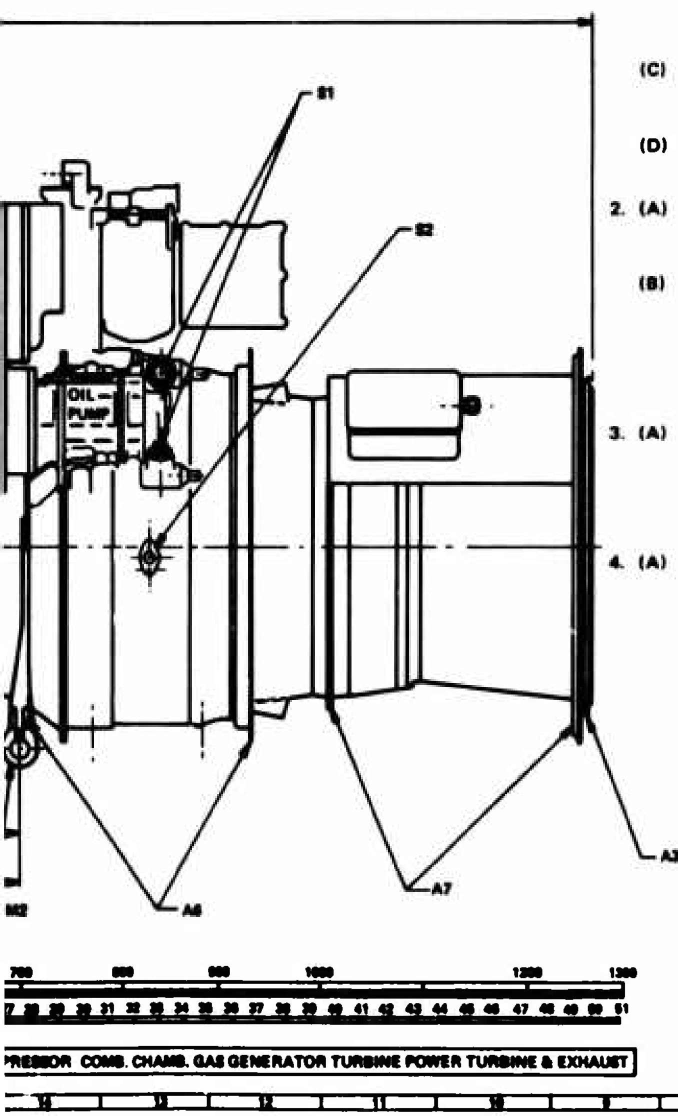

1. (A) ALL DIMENSIONS ARE NOMINAL AND COLD UNLESS OTHERWISE STATED.
   (B) ALL B.L. AND W.L. ARE ENGINE DIMENSIONS MEASURED HORIZONTALLY AND VERTICALLY FROM ENGINE ℄.
   (C) ALL STATIONS ARE AXIAL ENGINE DIMENSIONS MEASURED FORWARD AND AFT FROM STATION 200.
   (D) 'H' AND 'C' FOLLOWING A DIMENSION SIGNIFY HOT AND COLD.
2. (A) ENGINE DATUM FACE (STA 200.0) IS DATUM FOR ALL DIMENSIONS AND TOLERANCES.
   (B) ALL FEATURES ARE WITHIN 2.5 (.100) OF TRUE POSITION UNLESS OTHERWISE STATED. ANGULAR VARIATION ON ALL FACINGS IS WITHIN 1° UNLESS OTHERWISE STATED.
3. (A) ALL DIMENSIONS OTHER THAN STATION, WATER AND BUTTOCK LINES ARE SUBJECT TO A TOLERANCE OF ± 0.25 (.010) UNLESS OTHERWISE STATED.
4. (A) CERTAIN INTERFACES MAY HAVE BEEN OMITTED IN ANY ONE ATTITUDE BUT ARE SUBSEQUENTLY SHOWN IN FURTHER VIEWS.

ITEM NO.	[illegible]	TITLE	ZONE
		ATTACHMENTS	
A2	1	INTAKE FLANGE	[illegible]
A3	1	EXHAUST OUTLET FLANGE	[illegible]
A4	1	EXHAUST DUCT LOCATION HOLE	[illegible]
A6	1	FIREWALL ATTACHMENTS FRONT	[illegible]
A7	1	FIREWALL ATTACHMENTS REAR	[illegible]
		CONTROLS	
C1	1	GAS GENERATOR CONDITION CONTROL SHAFT	[illegible]
C2	1	POWER TURBINE SPEED SELECT CONTROL SHAFT	[illegible]
		DRAINS	
D1	1	COMBUSTION CHAMBER	[illegible]
D2	[illegible]	FUEL FILTER	[illegible]
D3	1	FUEL PUMP SEAL	[illegible]
		ELECTRICAL	
E1	1	THERMOCOUPLE TERMINAL CONNECTOR	[illegible]
E4	1	ANTI-ICING VALVE CONNECTOR	[illegible]
E5	1	IGNITION CONNECTOR	[illegible]
		FUEL	
F1	1	FUEL INLET	[illegible]
		HANDLING	
H1	1	FRONT SLINGING BRACKET	[illegible]
H2	1	REAR SLINGING BRACKET	[illegible]
		INSTRUMENTATION	
J1	1	OIL PRESSURE CONNECTION	[illegible]
		LUBRICATION	
L1	1	OIL INLET CONNECTION	[illegible]
L2	1	OIL OUTLET CONNECTION	[illegible]
		MOUNTINGS	
M1	1	FRONT MOUNTING	[illegible]
M2	1	REAR MOUNTING	[illegible]
		PADS	
P1	1	STARTER GENERATOR	[illegible]
P2	1	SPARE DRIVE	[illegible]
P3	1	OIL COOLER DRIVE	[illegible]
P4	1	[illegible] TACHO GENERATOR DRIVE	[illegible]
P5	1	P.T. TACHO GENERATOR DRIVE	[illegible]
		SERVICING	
S1	[illegible]	MAGNETIC PLUGS	[illegible]
S2	[illegible]	BORESCOPE PORTS	[illegible]
S3	[illegible]	FUEL FILTER REMOVAL	[illegible]
S4	[illegible]	OIL FILTER REMOVAL	[illegible]
S5	[illegible]	F.C.U. AIR FILTER REMOVAL	[illegible]
S6	[illegible]	FUEL DENSITY ADJUSTER	[illegible]
S7	[illegible]	F.C.U. BLEED SCREEN	[illegible]
		VENTS	
V1	1	L.P. COMPRESSOR BALANCE	[illegible]
V2	1	[illegible] BREATHER	[illegible]
V3	1	T_1 SENSOR AIR INLET	[illegible]
V4	1	T_1 SENSOR AIR OUTLET	[illegible]

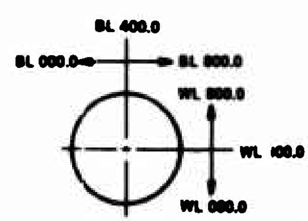

ORIENTATION VIEW
LOOKING FORWARD
BL – BUTTOCK LINE
WL – WATER LINE

THE CONTROL SYSTEM

The control schematic representing the baseline multipoint hoist system is shown in Figure 48. The control system design is based on a fully integrated hoist with the air vehicle controls. The elements considered for this control system are shown in Figure 49.

This schematic is based on the following:

- All sensors for feedback as well as open-loop control shall be electronic, where feasible, for rapid response.
- To minimize actuator size, the power for actuation shall be hydraulic.
- The lube pump in addition to lubrication shall provide the control power as well. Presently, a small constant-speed electric motor is considered the most effective. All components are located within the ATM housing.
- The control system will not be limited to the hoist drive only. It will be integrated with the air vehicle and control power system generator outputs such as pressure, temperature, speed, and safety protection.

Some rationale for the above approach is based on the following:

- For fast response characteristics and control power, hydraulics seem to be favored with electronic sensing and intelligence. Response time of 20 MS with good stability is used today for gas turbine engine control applications.
- The pneumatic system response without rate correction anticipator is estimated at 200 MS. The response with an anticipator is 100 MS.
- In the control system design, the stability, rather than the response characteristics, is the important consideration.
- Estimated maximum frequency limit with large pneumatic valves is 2 cps.

- The hydraulic system must be maintained at reasonable temperatures; otherwise, the viscosity effect may deteriorate the response time by a factor of 10. There are no problems in this area with the pneumatic hoist.

Controversial opinions exist relative to response characteristics for fixed- versus variable-geometry nozzle design. The concensus, however, is that for this application, there are no significant differences with either nozzle design.

Some apprehension has been expressed regarding response and compensation for the very high inertia of a 12-ton load (750 slug ft^2). These fears are groundless — the equivalent projected load inertia at the turbine shaft is only 4.7×10^{-5} slug-ft^2. (This compares to a 60-HP hydraulic pump drive for the "747", whose inertia is 1.315×10^{-3}. Typical main engine starters applicable to the HLH see inertia from 1.73 to 7.85 slug-ft^2.)

Average theoretical angular acceleration based on the average accelerating torque of the pneumatic drive (does not consider turbine, wheel, and gearing inertia) is 16 rad/sec^2, which corresponds to a linear load acceleration of .495G (much too rapid an acceleration for helicopters).

Estimated time from 0 to design rpm is theoretically 65 milliseconds. An estimated acceleration time for a similar application where turbine wheel and gearing inertias are included is shown in Figure 50. Higher response rates are feasible.

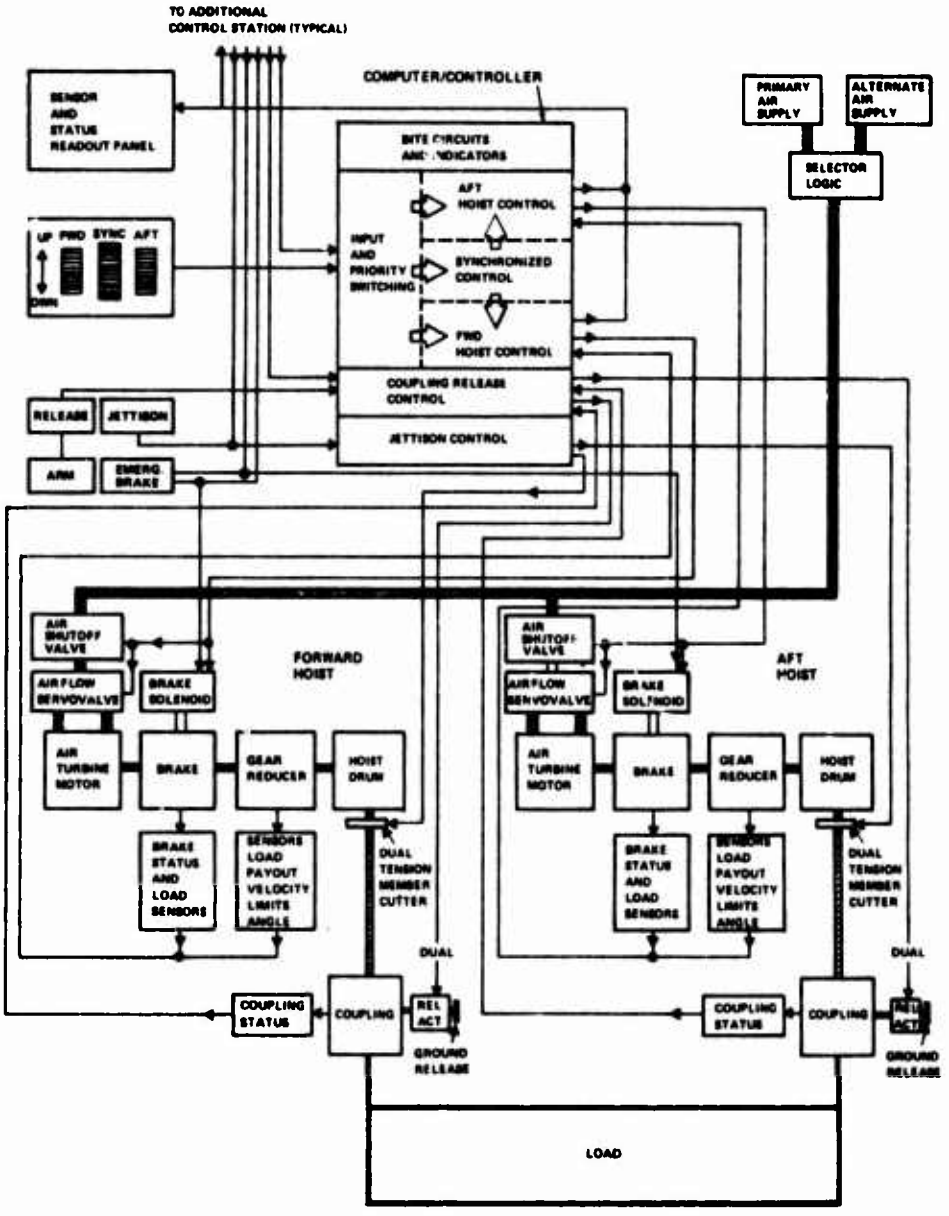

Figure 48. Baseline Hoist Control System.

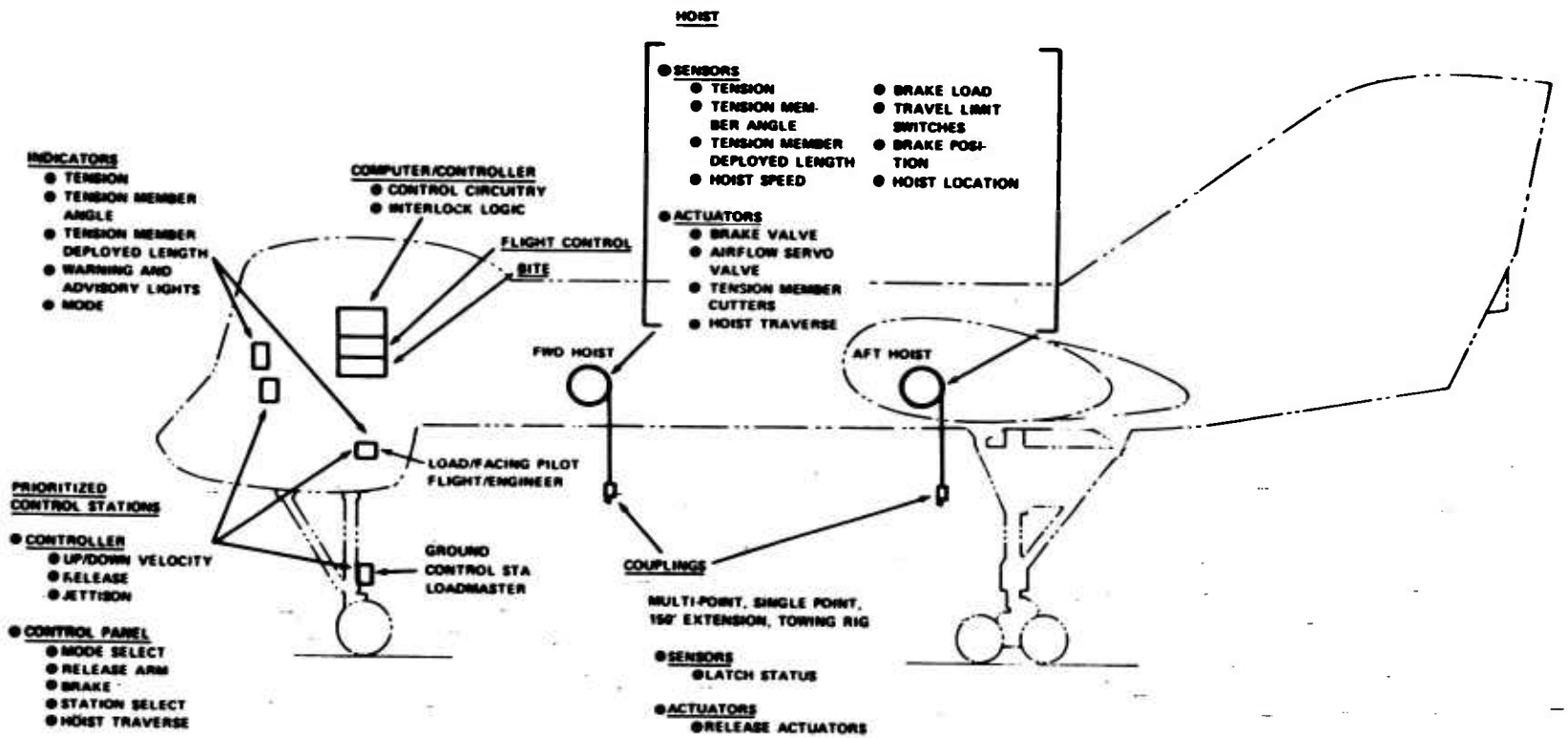

Figure 49. Control System Element and Air Vehicle Interface.

NOTES:

1. OPERATION SHOWN IS FOR SEA LEVEL WITH ATM DISCHARGE PRESSURE EQUAL TO 14.7 PSIA
2. PERFORMANCE SHOWN FOR ATM INLET PRESSURE EQUAL TO 29.2 PSIG, WHICH IS MINIMUM PRESSURE REQUIRED TO MEET AN 0.24 SECOND ACCELERATION TIME AFTER ATM INLET VALVE INITIATION
3. PERFORMANCE CALCULATED FOR MINIMUM BLEED-AIR TEMPERATURE OF 340°F
4. DRIVE INERTIA, I_p = 0.003934 SLUG–FT^2

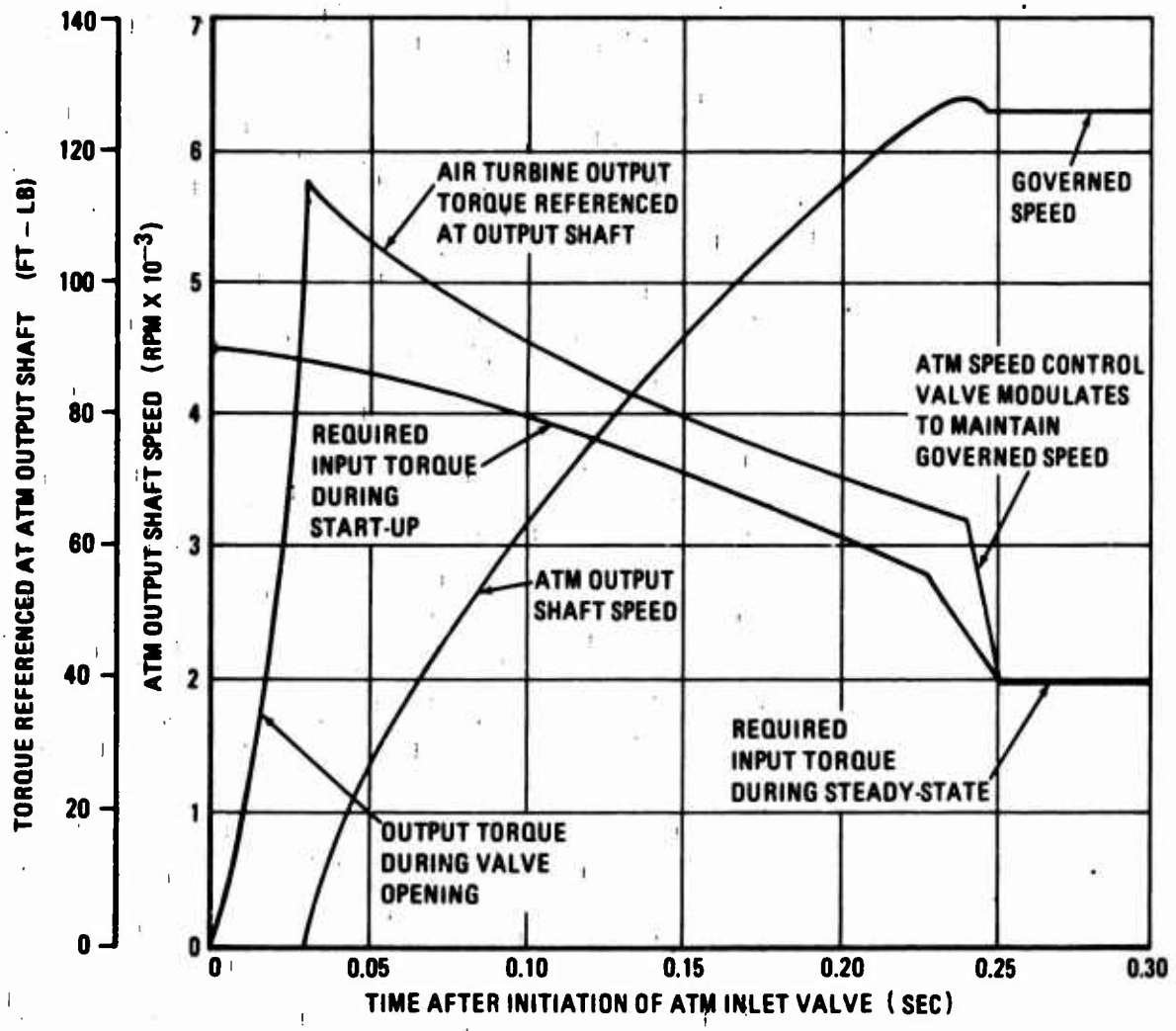

Figure 50. Estimated Performance of the Optimized Air Turbine Motor (AiResearch).

THE GEARING SYSTEM

Considerable effort was directed toward gearing design, primarily because of conflicting vendor inputs relative to the projected gearing system weights, which varied from 150 pounds to as high as 800 pounds per hoist.

Faced with this confusing situation, Boeing/Vertol has conducted independent in-house evaluations of various configuration gearing designs, which included, among others:

- Fixed-Ring Differential System — Figure 51
- Four-Planetary System — Figure 52
- Fixed-Sun Differential System — Figure 53
- Three-Spur, Two-Planetary System — Figure 54
- Two-Spur, Two-Planetary System — Figure 55

The various configurations were weight and stress analyzed; on the basis of the Boeing/Vertol computer analysis program, the most effective gearing system selected for the baseline hoist design is as shown in Figure 56.

Studies conducted subsequent to the above gearing analyses indicate that the ATM, with its integral high-speed gearing, can provide a shaft output which is concentric with the axis of the drum.

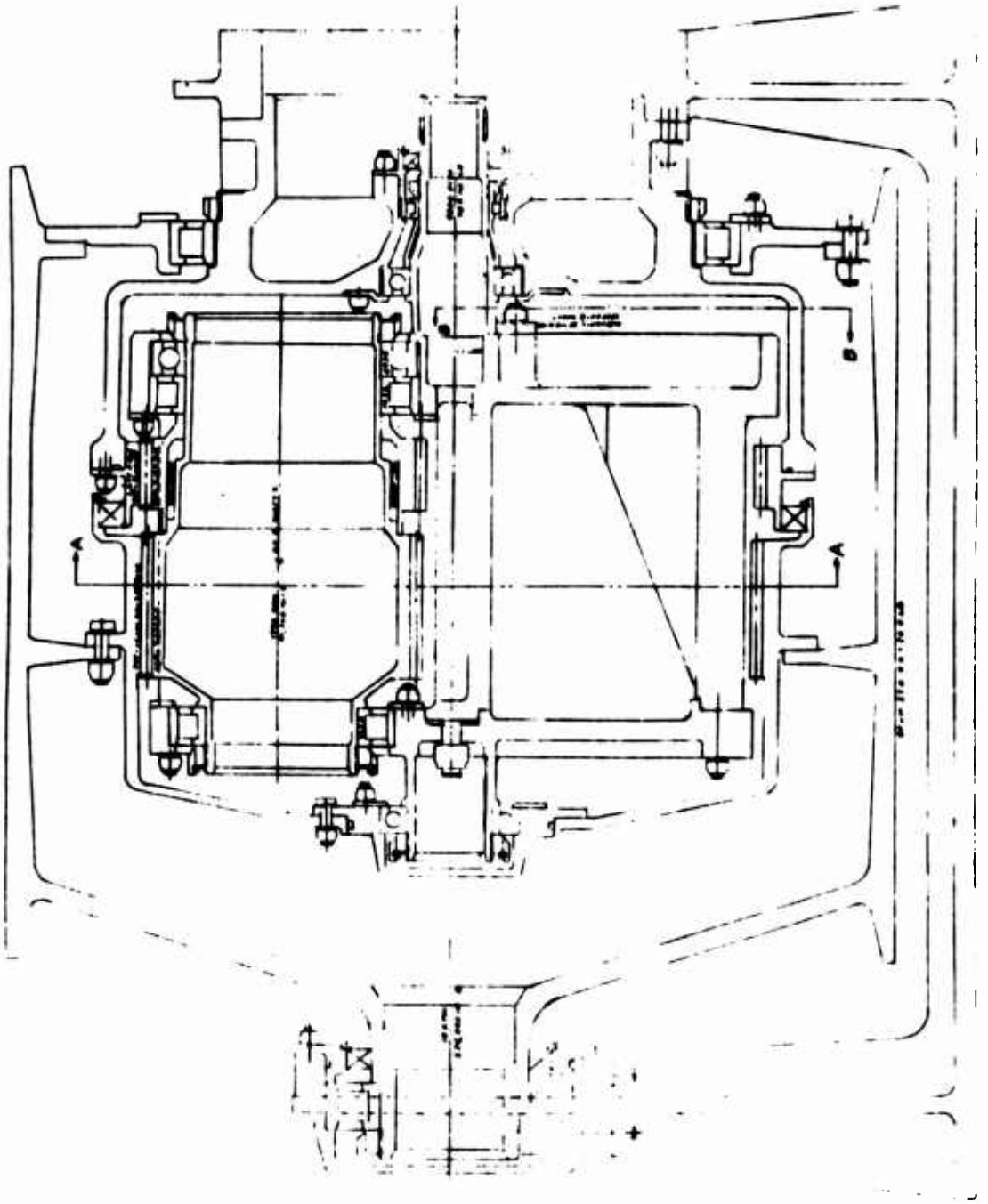

Figure 51. Fixed-Ring Differential System.

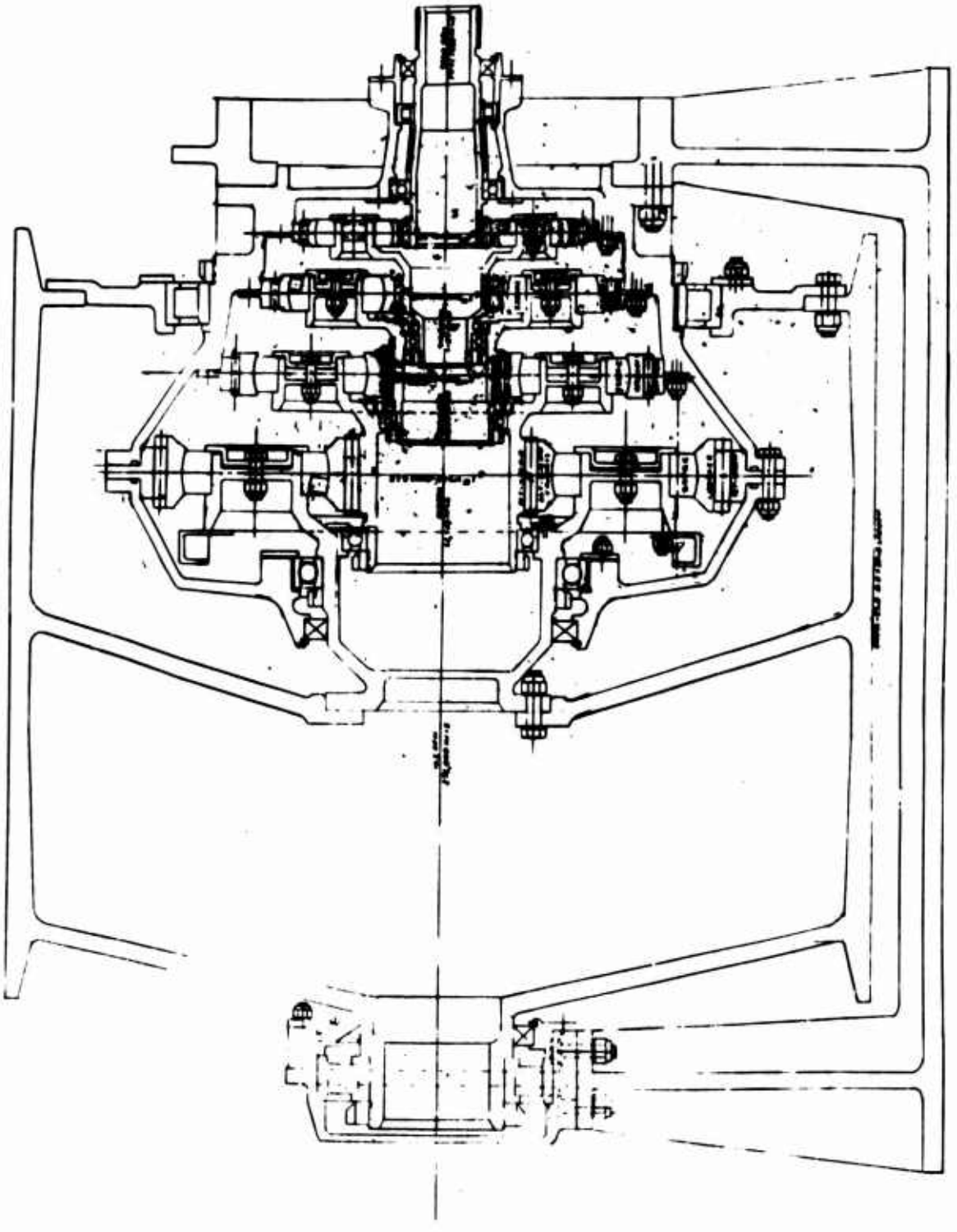

Figure 52. Four-Planetary System.

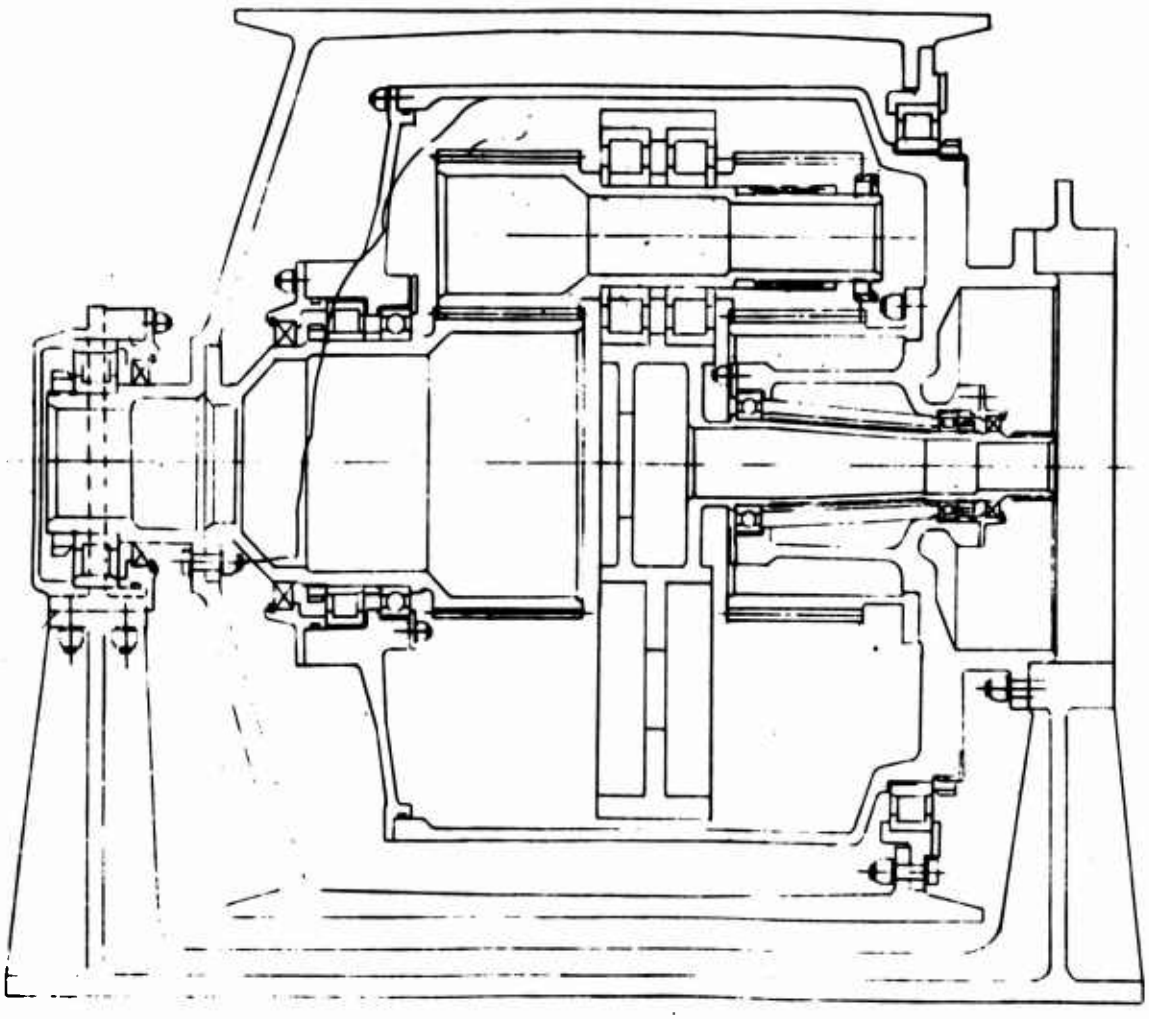

Figure 53. Fixed-Sun Differential System.

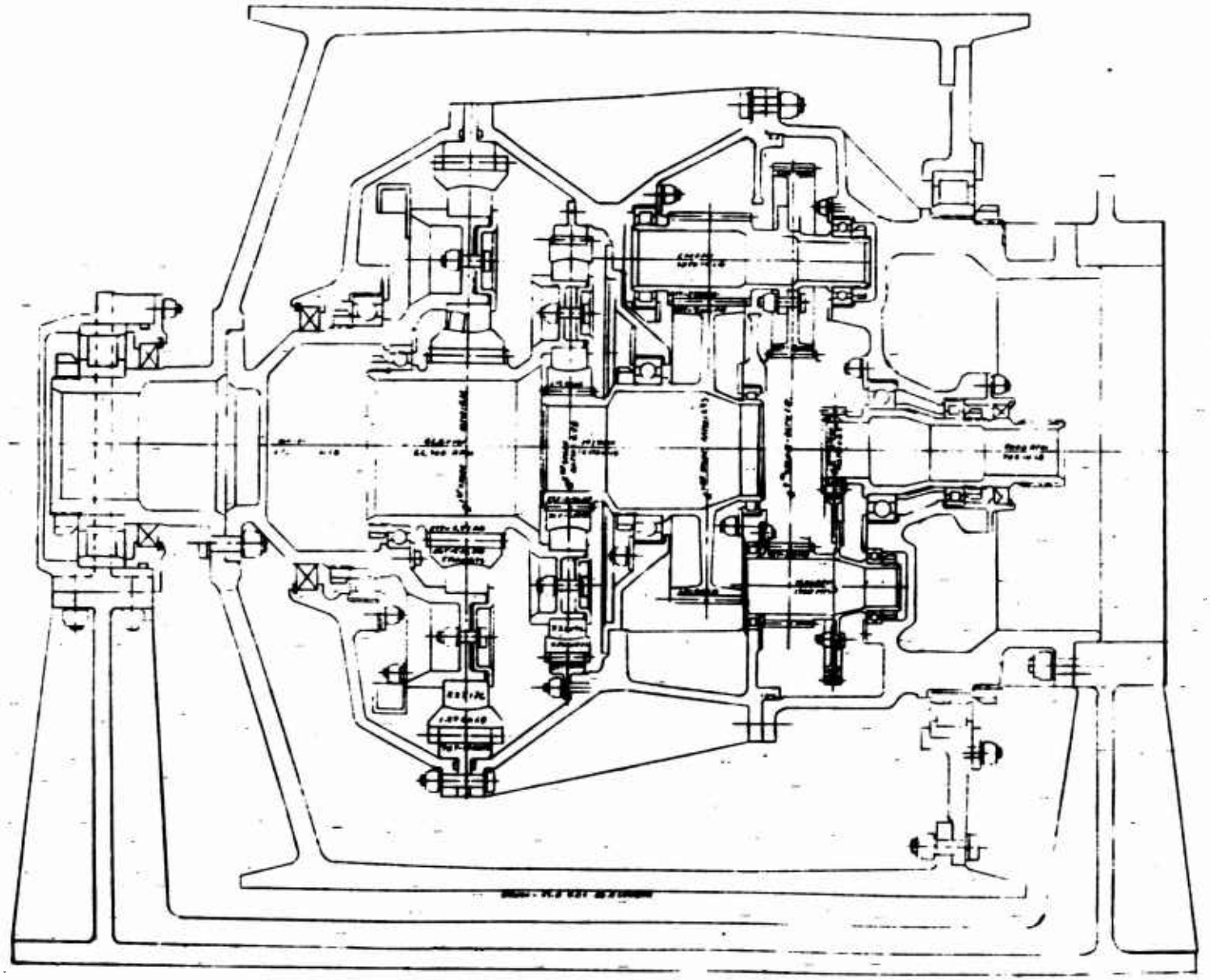

Figure 54. Three-Spur, Two-Planetary System.

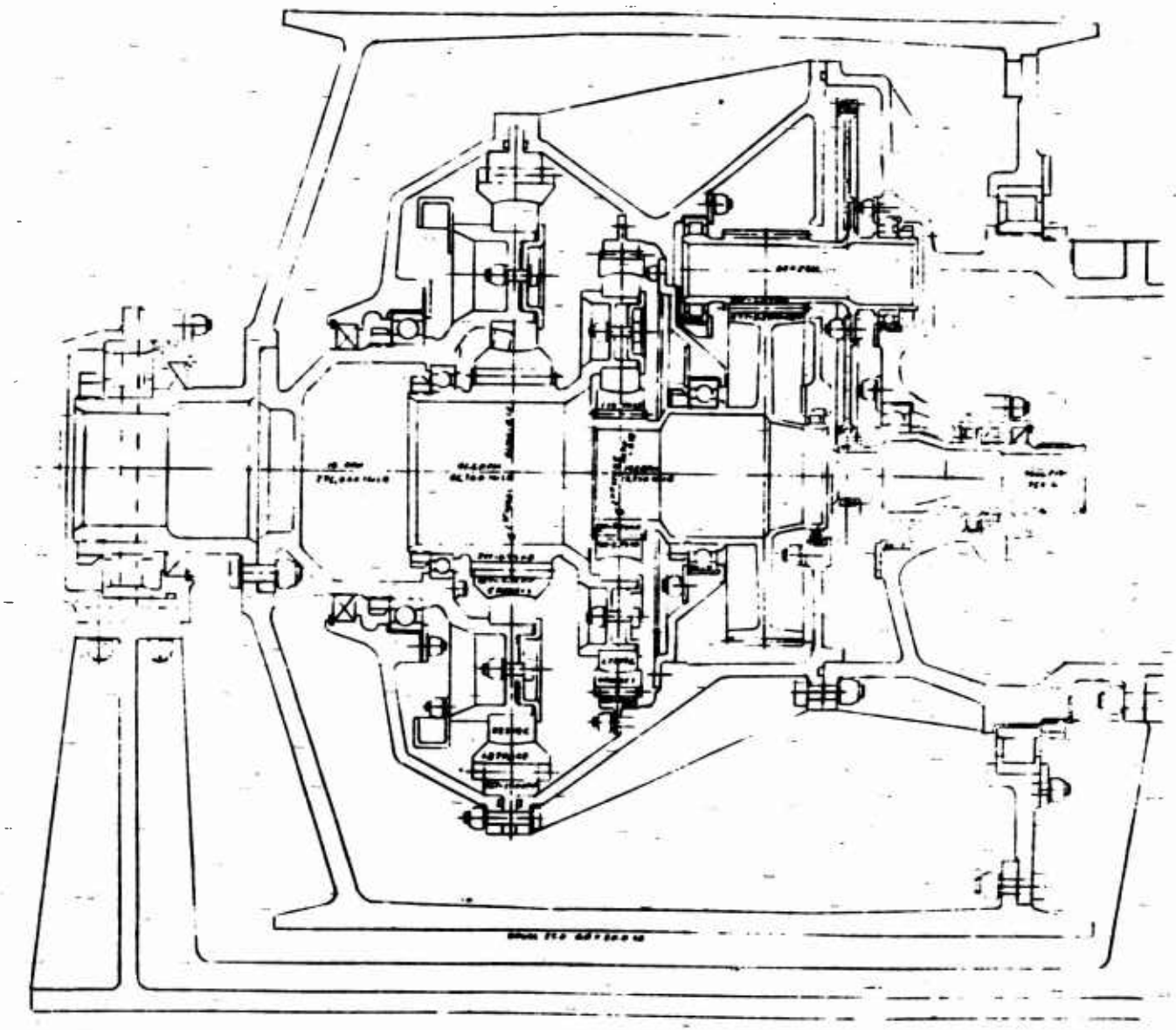

Figure 55. Two-Spur, Two-Planetary System.

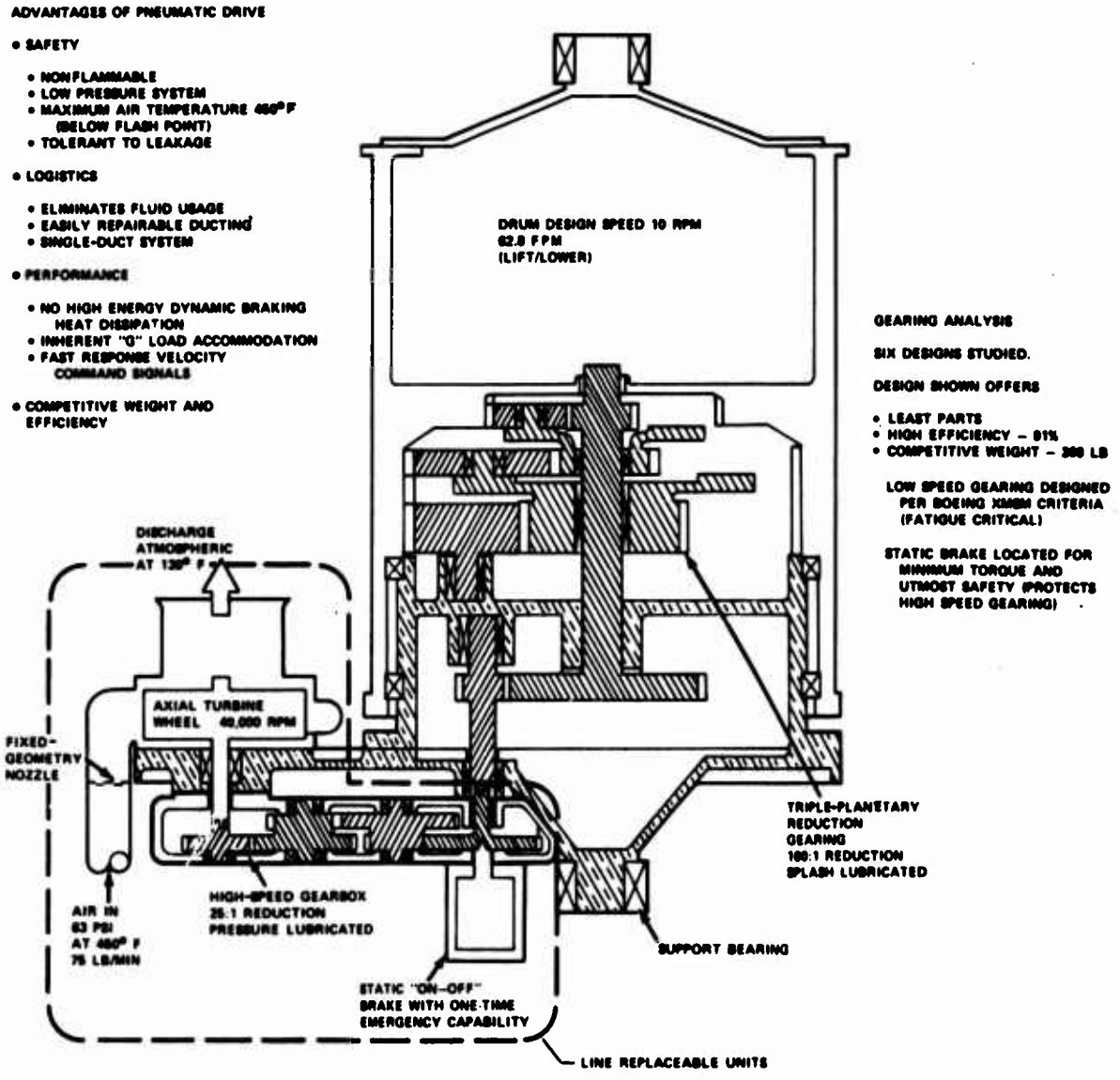

Figure 56. Baseline Gearing System - Triple Planetary.

WEIGHT ANALYSIS

Very encouraging results for realistic weight-trend projections for various hoisting capacities are indicated from the analysis to date. These projections not only apply to the hoist drive, but encompass the total hoist system complete to the hook.

The basic approach used consists of individual component analysis as related to the variable hoisting capacities under consideration. Most components are interdependent and, in fact, pyramid with each other, while some components are dependent on the load capacity only. The key to the solution lies in the mathematical expression of the various interdependencies, with the focal point dictated by the load capacity.

This approach is applicable to present-day cables and improved tension member technology, and is also applicable to any hoist configurations such as capstan or drum-type hoist designs.

The necessary steps required for realistic parametric weight projection for the various capacity hoist systems are as follows:

- A baseline hoist system (say, 20 tons) is designed. Individual components are designed on the basis of best technology available.

- The basic drum diameter to cable diameter ratio selected is maintained constant for all capacities considered. Cable construction is assumed constant for all hoists. Stress values, as well as unit loading, are also maintained constant.

  The cable load-carrying capacity and its gradual deterioration with increased cable diameter are assumed to maintain the same relative degradation as the present technology cables exhibit, and are based on properties defined in MIL-C-5424.

- The baseline hoist weight is the sum of individual components expressed as

$$W_H = W_1 + W_2 + W_3 + W_4 + - - - - - -$$

  where subscripts 1, 2, - - - - - denote individual components considered, such as cables, drum, gearing, and structure.

- Each component represents a certain percentage of the total system weight; and for the purpose of projecting relative total hoist system weight increase ratio, based on the increased capacity ratio compared to the baseline hoist design, the applicable relations are

$$\frac{W}{W_{\cdot H}}^{n_H} = A \left(\frac{P}{P}_{\cdot 1}\right)^{n_1} + B \left(\frac{P}{P}_{\cdot 2}\right)^{n_2} + C \left(\frac{P}{P}_{\cdot 3}\right)^{n_3} + D \left(\frac{P}{P}_{\cdot 4}\right)^{n_4} + - - -$$

where W_o = total weight of the baseline hoist

$\frac{W}{W_o}$ = ratio of hoist weight for higher capacity designs

P_o = baseline hoist capacity

$\frac{P}{P_o}$ = relative ratio of higher capacity hoists compared to the baseline capacity

n_H = Exponential value for the total hoist

$n_1, n_2, n_3, - - -$ = Exponential value for individual components

A, B, C, -------- = Component percentage weight of the total baseline hoist system

- A mathematical expression in terms of the exponential values is derived next, and is based on physical characteristics and degradation factors (where applicable) for each respective component. Note that a mathematical solution of exponential value is the key to the problem. In some instances, it is simple; in others, various nonlinearities exist; frequently, empirical relationships are employed.

- The expo ntial value n_H for the total hoist system is calculated from the relationship developed in (4) above.

- The hoist weight ratio (compared to the baseline capacity design) is calculated for any capacity hoist ratios.

- The various exponent values are then analyzed and reexamined. High exponential values are those contributing most significantly to the total hoist weight increase. The components with high exponential value are therefore the areas requiring additional investigation; they also identify the areas of most useful effort in weight reduction analysis.

The applicable major component exponential value developed analytically, based on component percentage of a baseline 20-ton hoist system design, is shown in Table XVIII. Figure 57 shows that an increase in system capacity causes an increase in component weight.

TABLE XVIII. COMPONENT EXPONENTIAL VALUE

Major Component	Exponential Value	Percent of System Total
Drum		
Deadwrap portion	1.68	3.34
Livewrap portion	1.10	12.50
Total		15.84
Gearing		
Total	1.23	19.47
Tension Member (Cable)		
Deadwrap Portion	1.80	3.47
Livewrap portion	1.10	12.90
Total		16.37
Support Structure		
Structure Members	1.01	17.40
Bearings	1.25	5.80
Total		23.19
Level Wind	1.01	10.18
Load Isolate	1.00	4.34
Coupling	1.00	6.73
ATM Drive	1.00	3.89

Tables XIX and XX give weight data for systems of various capacities. Figure 58 shows weight versus capacity for a single hoist, and Figure 59 shows weight versus capacity for a total system.

The weight of a hoist system for tandem helicopters with payloads up to 50 tons should be a constant 2.3 percent of design gross weight.

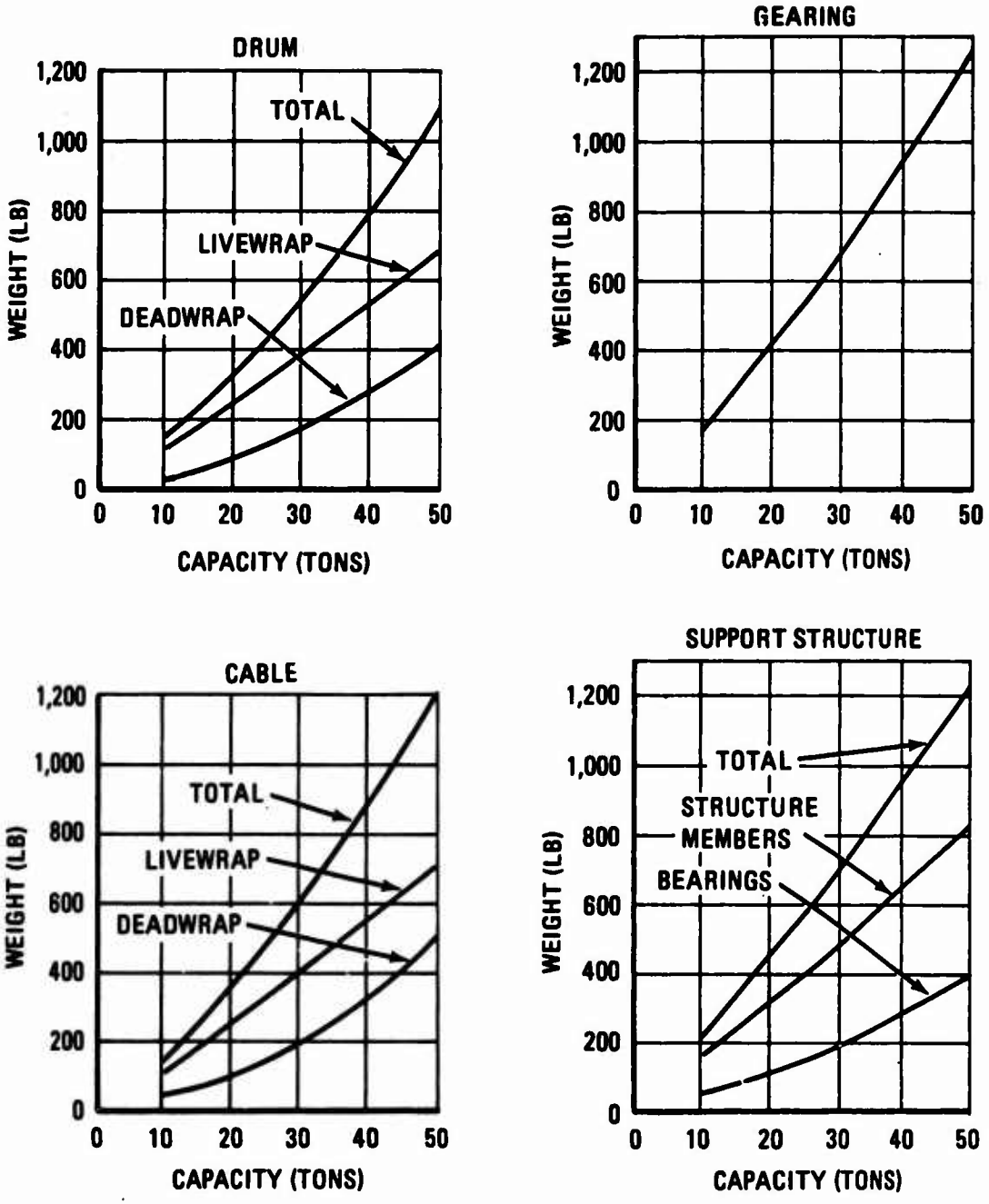

Figure 57. Component Weight Versus System Capacity (Sheet 1 of 2).

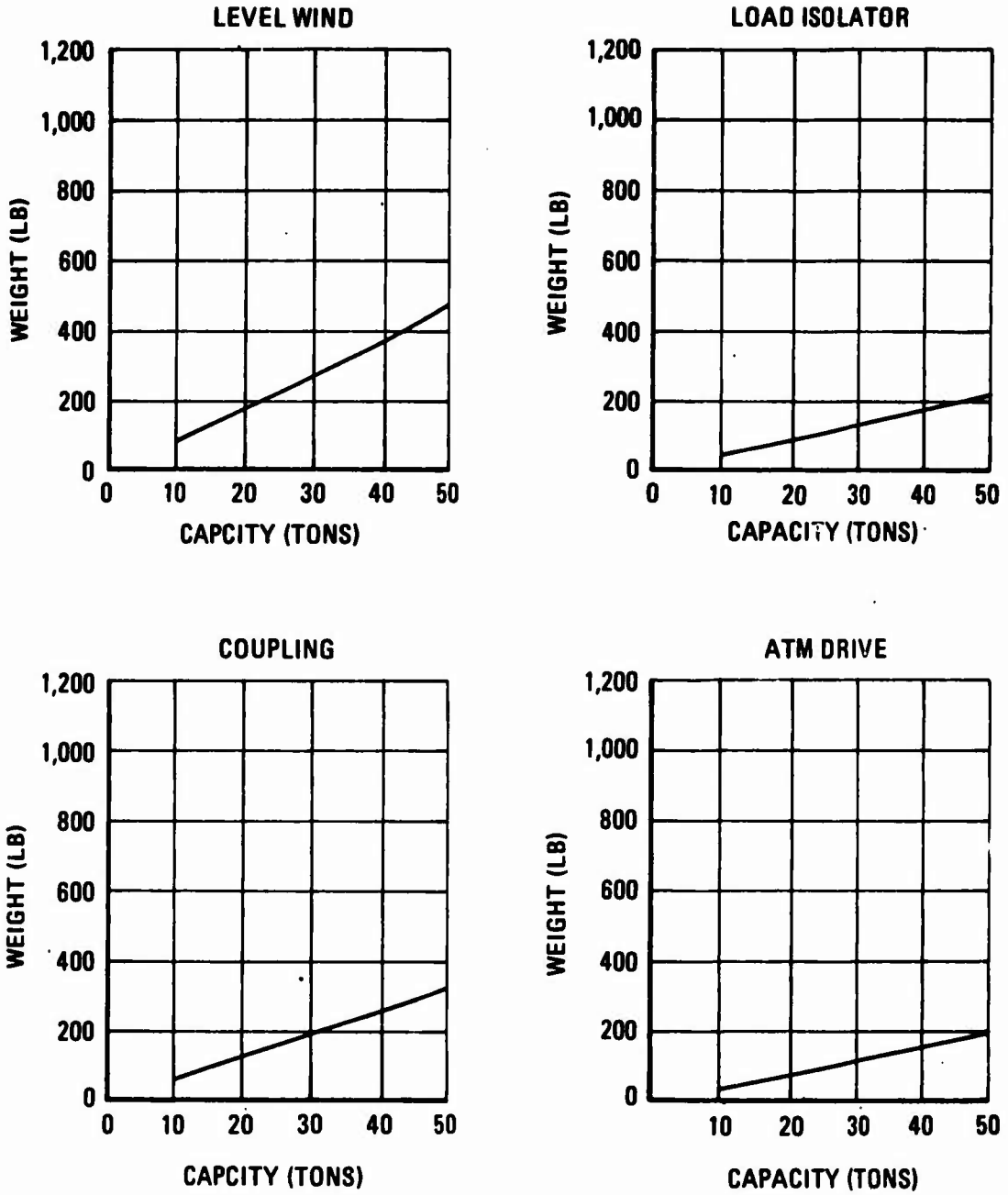

Figure 57. Continued (Sheet 2 of 2).

TABLE XIX. HOIST SYSTEMS COMPONENT WEIGHT BREAKDOWN

Major Component	Baseline 12-Ton		10-Ton		20-Ton		30-Ton		40-Ton		50-Ton	
	% of system	pounds	% of system	pounds	% of system	pounds	% of system	pounds	% of system	pounds	% of system	pounds
Drum												
Deadwrap Portion	3.34	37.70	3.02	277.60	4.37	88.40	5.40	175.90	6.21	283.40	6.93	414.70
Livewrap Portion	12.50	141.00	12.57	115.50	12.20	246.60	11.85	386.80	11.59	428.80	11.33	678.50
Total	15.89	178.00	15.60	143.26	16.57	335.00	17.26	562.70	17.80	812.20	18.26	1093.20
Gearing	19.47	220.00	19.13	175.70	20.30	410.30	20.83	678.90	21.10	962.50	21.24	1272.00
Tension Member Cable												
Deadwrap Portion	3.47	39.20	3.07	28.20	4.83	97.60	6.26	204.00	7.45	340.00	8.54	511.30
Livewrap Portion	12.90	145.80	12.98	119.20	12.59	245.50	12.25	399.30	11.96	545.70	11.70	700.30
Total	16.37	185.00	16.05	147.40	17.42	352.10	18.51	603.30	19.41	885.70	20.24	1211.60
Support Structure												
Structure Members	17.40	196.20	17.79	163.40	16.23	328.00	15.22	496.00	14.48	660.60	13.87	830.70
Bearings	5.80	66.60	5.68	52.20	6.11	123.50	6.32	206.00	6.44	293.80	6.51	390.00
Total	23.90	262.80	23.47	215.50	22.33	451.50	21.54	702.00	20.92	954.50	20.39	1220.70
Level Wind	10.18	115.00	10.41	95.60	9.49	191.90	8.90	290.20	8.47	386.50	8.12	486.00
Load Isolator	4.34	49.00	4.44	4.09	4.03	81.40	3.76	122.60	3.57	162.80	3.44	204.30
Coupling	6.73	76.00	6.90	63.30	6.25	126.20	5.83	190.10	5.53	252.50	5.29	316.70
ATM Drive	3.89	44.00	3.99	36.60	3.61	73.00	3.37	109.90	3.20	145.90	3.06	183.10
Totals	100.00	1130.50	100.00	918.30	100.00	2021.40	100.00	3259.70	100.00	4561.90	100.00	5987.60

TABLE XX. HOIST SYSTEMS COMPONENT WEIGHT BREAKDOWN--BACKUP DATA

Major Component	Capacity Tons P/P	12 1.0	10 .833	20 1.66	30 2.5	40 2.32	50 4.165
Drum							
Deadwrap Portion	(1.68)	1.0	.7356	2.343	4.662	7.508	10.988
Livewrap Portion	(1.10)	1.0	.8179	1.746	2.739	3.744	4.804
Total		2.0	1.5535	4.089	7.401	11.252	15.592
Gearing	(1.23)						
Total		1.0	.7987	1.865	3.086	4.375	5.783
Tension Member Cable							
Deadwrap Portion	(1.80)	1.0	.7197	2.489	5.203	8.671	13.040
Livewrap Portion	(1.10)	1.0	.8179	1.746	2.739	3.744	4.804
Total		2.0	1.5376	4.234	7.942	12.415	17.844
Support Structure							
Structure Members	(1.01)	1.0	.8310	1.668	2.523	3.360	4.225
Bearings	(1.25)	1.0	.7958	1.884	3.143	4.482	5.950
Total		2.0	1.6268	3.552	5.666	7.842	10.175
Level Wind	(1.01)						
Total		1.0	.8310	1.668	2.523	3.360	4.225
Load Isolator	(1.00)						
Total		1.0	.8330	1.660	2.500	3.320	4.165
Coupling	(1.00)						
Total		1.0	.8330	1.660	2.500	3.320	4.165
ATM Drive	(1.00)						
Total		1.0	.8330	1.660	2.500	3.320	4.165

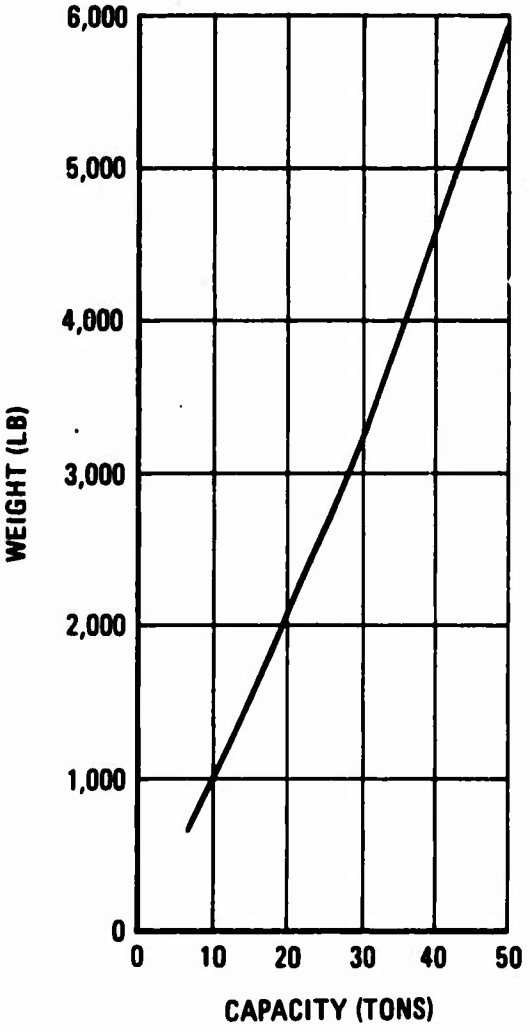

Figure 58. Weight Versus Capacity for a Single Hoist.

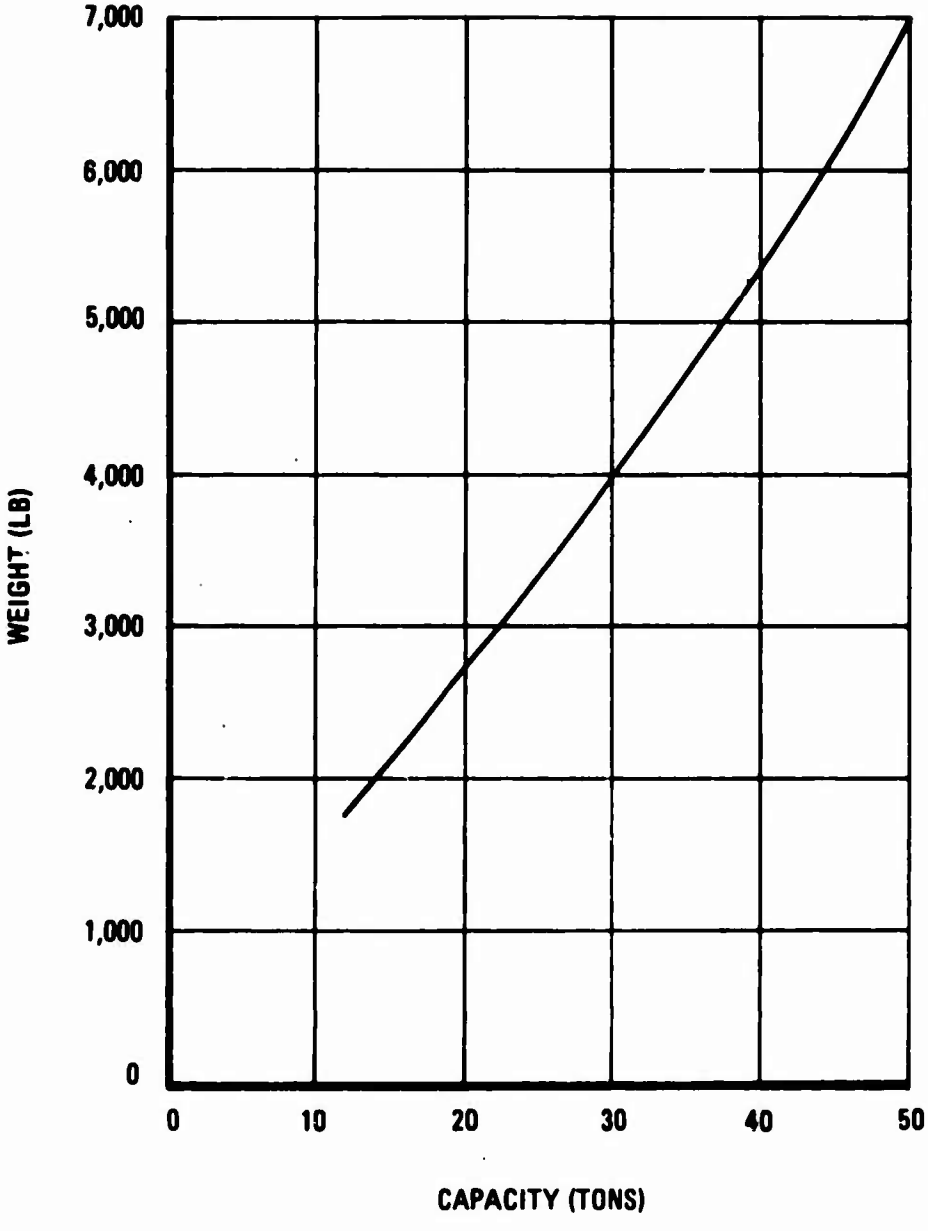

Figure 59. Weight Versus Capacity for a Total Hoist System.

PNEUMATIC POWER GENERATION COST

Frequent comments about pneumatic system inefficiency often lead to elimination of the pneumatic concepts on this basis alone. If one accepts adiabatic compressor efficiencies of 80% and corresponding turbine efficiency of up to 85% (Figures 42 and 60 show a performance sample), the combined efficiency of the system (losses neglected) will be 74%, not 0.85 x 0.80, which is due to partial regeneration of the compressor inefficiency reflected in higher turbine inlet termperature, which corresponds roughly to a hydraulic pump/motor combination overall efficiency of 86% each.

What must be suspected is that the operating speed of the air turbine is often not matched properly with optimum design speed of the turbine. The effect of the proper speed matching of hydraulic components is considerably less sensitive than is the ATM. Mismatched speed with air turbines will result in drastic performance loss as indicated in Figure 30.

Similar to the generally held belief about the inefficiency of pneumatic power system generation, another almost universal belief exists regarding the exorbitant cost of bleeding main engines for pneumatic power systems. There is an element of truth in this assumption, except that in this specific hoist-drive analysis based on the integrated HLH design approach, it does not apply. On the basis of the conducted trade-off studies below, it was substantiated that bleeding the main engine for power to the hoists is the safest and the most economical method, regardless of any power drive system selected.

The following are the prime factors that make this possible:

- The design conditions for the air vehicle require the engines to operate at 60 to 80 percent of normal rating, except during an emergency engine-out situation.

- The bleed air requirement for full-capacity hoisting represents less than 3 percent of the total engine air through-flow.

- In the event that one engine fails and hoisting is still required, the on-board APU will be started to provide hoist power.

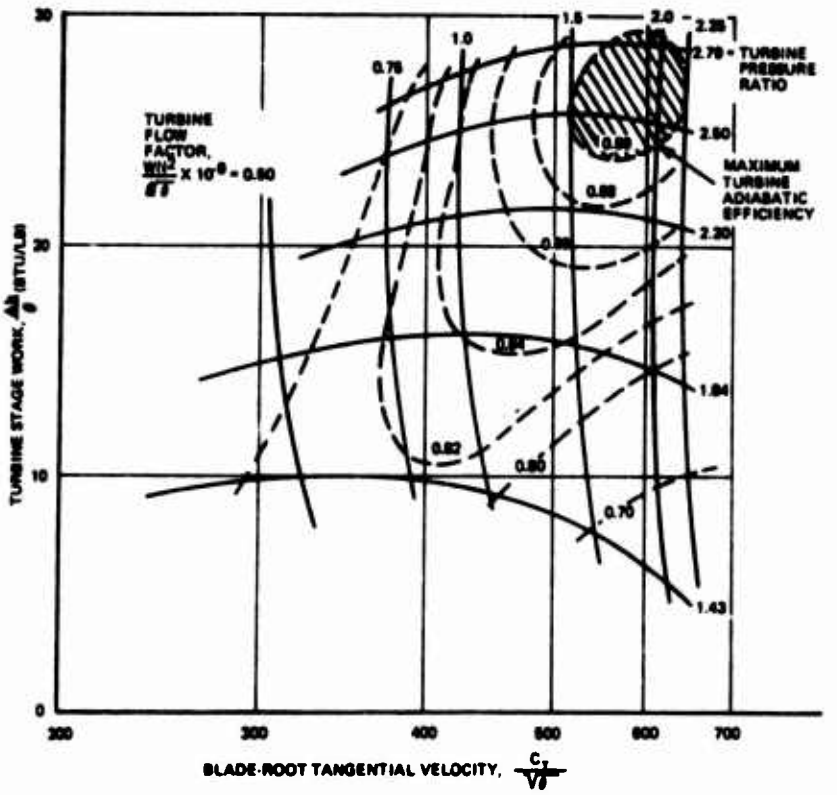

Figure 60. Single-Stage Axial Turbine Performance Showing Efficiencies.

- Bleed ports are available at the lower compression stages, resulting in not much higher than design pressure required for the ATM, and only minimal cooling is required to the limiting temperature of 450°F.

PNEUMATIC POWER GENERATION TRADE-OFF STUDIES

The power generation study was conducted on an integrated basis combining the hoist-drive system with other aircraft power systems. This integrated power system was based on an aircraft design capable of carrying a 28-ton external load. The load hoisting velocity was based on 60 feet per minute.

The estimated individual system power requirements are shown in Table XXI.

The estimated minimum simultaneous power requirements are shown in Table XXII.

Four different concepts of pneumatic power generation were investigated. These concepts are shown in Figures 61, 62, 63 and 64. The primary differences and operating characteristics are summarized in Table XXIII.

The analysis for in-flight fuel requirements was based on a 1.5-hour aircraft mission.

ENGINE BLEED FUEL COST

In order to establish meaningful data upon which the final system of pneumatic power generation was selected, three applicable engines for this 28-ton-payload aircraft were investigated. The overall pressure ratio of the three engines varied from 12:1 up to 22:1. All engines were analyzed for interstage bleeding. The fuel penalty, the percentage of bleed air with respect to total air through-flow, and the bleed pressure ratio at various power settings are shown in Table XXIV.

A simplified version of the above table indicating delta fuel flow versus bleed air mass flow as well as the appropriate percentage based on 53 lb/min bleed is shown in Figure 65.

TRADE-OFF STUDY SUMMARY

The subsequent tables summarize (1) the component weight comparison of the four concepts (Table XXV) investigated, (2) the total fuel and component weight differential between the

TABLE XXI. INDIVIDUAL SYSTEM POWER REQUIREMENTS

Subsystem		Estimated Requirements	
		Min.	Max.
Hoists			
Power absorbed by load, total	(hp)	102.5	
Total motor output (η_{mech} = .80)	(hp)	128	
Input power to compressor (η_C η_T = .65-.69)	(hp)	186	197
Losses due to asymmetry	(hp)	3.7	3.9
Shaft power for hoisting, total	(hp)	190	201
Airflow required, W_{BL}	(lb/min)	94.5	100
Flight Control Pumps			
Est. pump capacity, total	(gpm)	30	
Max. power to pumps (η_{pump} = .85)	(hp)	61.7	
Additional power to compressor	(hp)	89.5	95
Airflow required	(lb/min)	44.5	47.2
Generators			
Design capacity assumed at 20 KVA	(hp)	26.8	
Turbine output (η_{gen} = .85)	(hp)	31.2	
Airflow required	(lb/min)	22.6	24.0
Compressor power in	(hp)	45	48
ECS			
Design flow	(lb/min)	60	
Min. flow (with max. hoisting)	(lb/min)	20	
Compressor power	(hp)	40.2	

TABLE XXII. MINIMUM SIMULTANEOUS POWER TO MEET REQUIREMENTS				
Subsystem	HP		Airflow (lb/min)	
	Min.	Max.	Min.	Max.
Hoist	190	201	94.5	100
Generators (based on 5KVA)	11.25	12	5.65	6
Flight Control Pumps (based on 2/3 capacity)	59.5	63.4	29.7	31.5
Min. ECS	40.2	40.2	20	20
Total	301	317	150	158
Average	308		153	

various concepts (Table XXVI), and (3) in-flight fuel flow requirement comparison for the selected four concepts (Table XXVII).

It is concluded that:

- Concept B shows the best fuel economy.
- Concept B shows the best weight economy.
- Concept B can provide full ECS during periods of maximum hoisting, if desired.

This study further shows that bleeding the engine for this specific application is superior by far. Observe that full-capacity hoisting for 10 percent of the aircraft mission time of 1.5 hours (.15) is only 10 pounds total. A more realistic figure for full-capacity hoisting is probably 5 percent mission time, with the net result of total fuel consumption of 5 pounds directly chargeable to the hoist-drive system.

In addition to providing fuel economy, bleeding the engine has an additional advantage in that no independent rotating components are required.

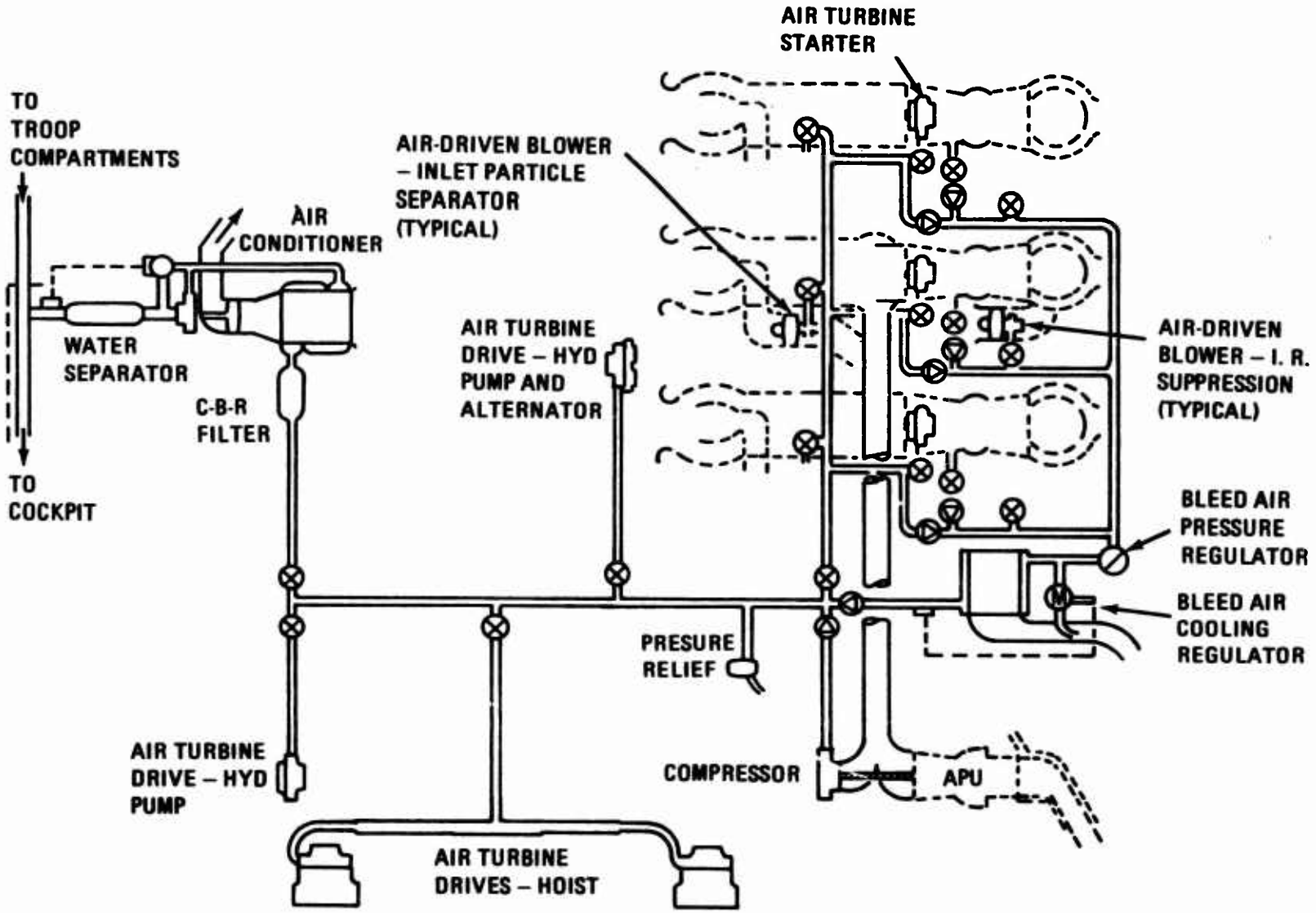

Figure 61. Pneumatic System - Concept A.

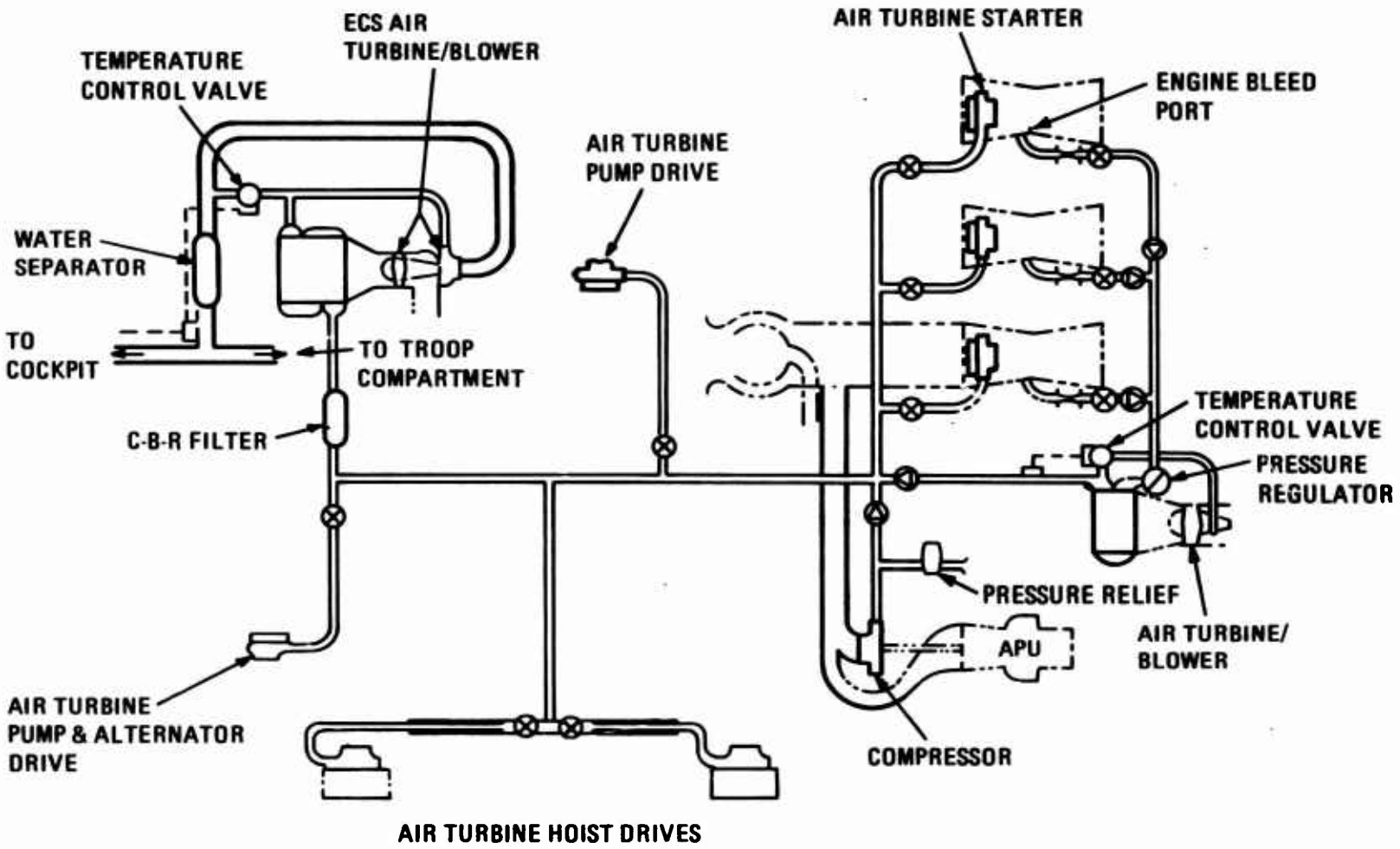

Figure 62. Pneumatic System - Concept B.

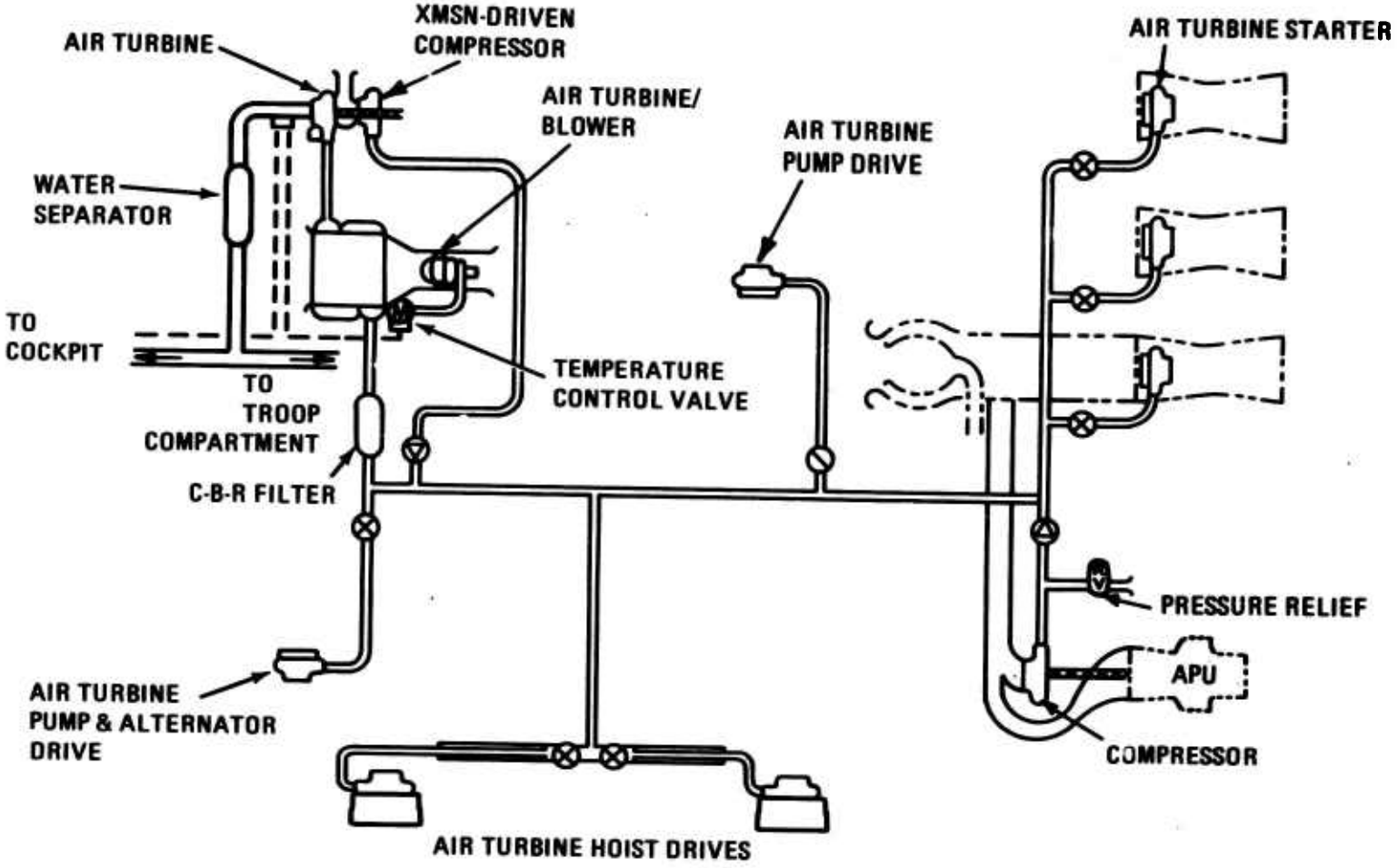

Figure 63. Pneumatic System - Concept C.

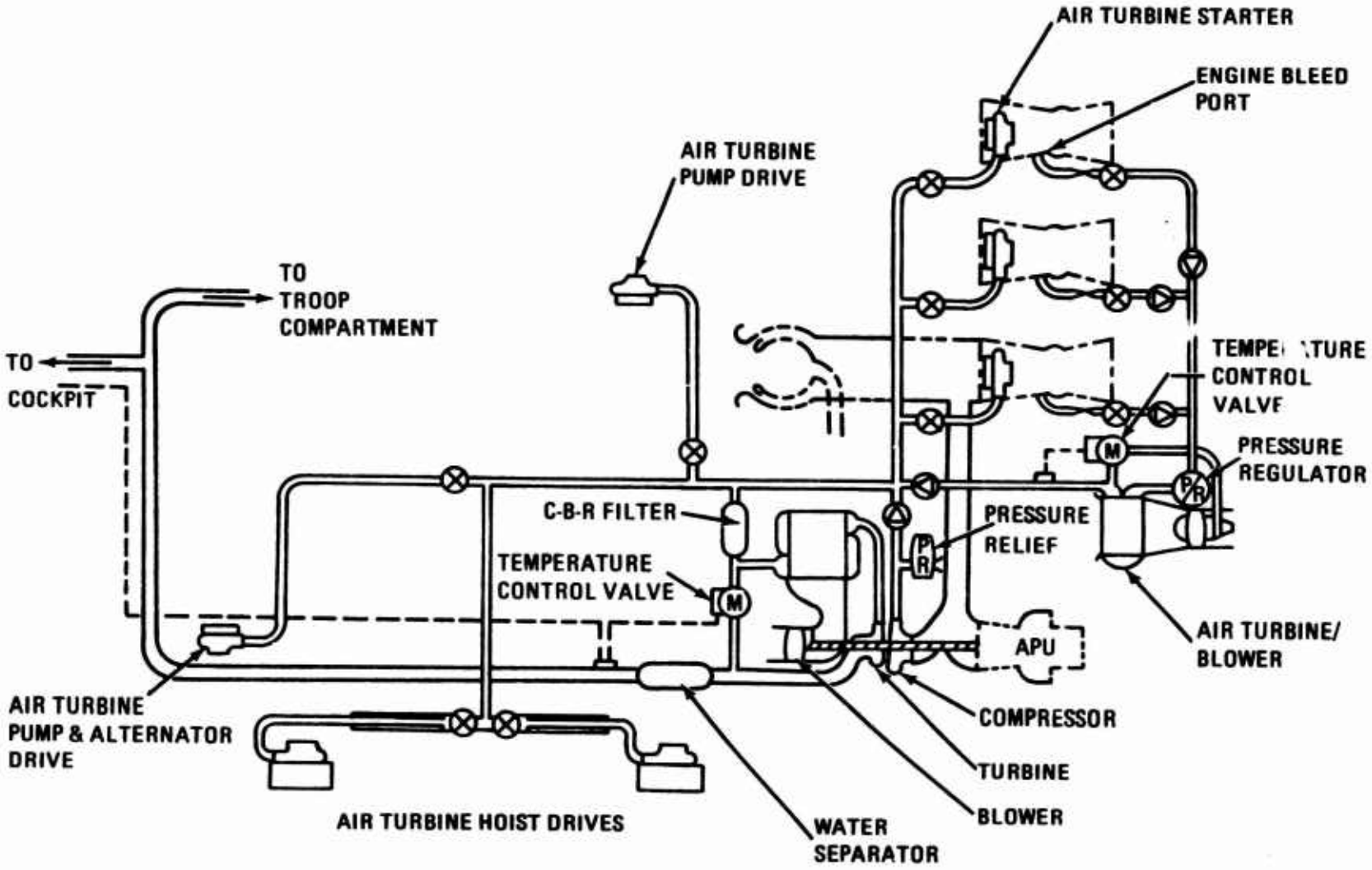

Figure 64. Pneumatic System - Concept D.

TABLE XXIII. PNEUMATIC POWER SYSTEMS-PRIMARY DIFFERENCES IN CHARACTERISTICS

Configuration	Air Source		Environmental Control System		
				Flight Operation	
	Primary	Backup	Ground Operation	On Primary Air	On Backup Air
A	APU Driven Compressor With Xmsn. Mtd. ECS Turbine	Engine Bleed	Heating Only	Heating and Cooling	Heating and Cooling
B	Engine Bleed	APU Driven Comp.	Heating and Cooling	Heating and Cooling	Heating and Cooling
C	Xmsn-Driven Comp. With Xmsn. Mtd. ECS Turbine	APU Driven Comp.	Heating Only	Heating and Cooling	Heating (Perhaps Cooling)
D	APU Driven Compressor With APU Mtd. ECS Turbine	Engine Bleed	Heating and Cooling	Heating and Cooling	Heating Only

TABLE XXIV. INVESTIGATED ENGINE BLEED AIR/FUEL COST CHARACTERISTICS

Engine	Power Setting (%)	Bleed Air		ΔFuel Flow		Pressure Ratio (π)	Bleed Air Temp (dF)
		(lb/hr)	(%)	(lb/hr)	(%)		
C	30	53.3	3.14	61	4.78	π_{10}=6.0	450°F
	70	53.3	2.53	73	3.69	π_{10}=6.8	600°F
B	72	50	3.0	40	2.22	π =4.2	430°F
A	71.4	50	2.28	30.4	1.24	π_9=4.8	--
		150	6.85	101.5	4.12		
	85.5	50	2.14	36.5	1.30	π_9=5.15	--
		150	6.41	109.6	3.90		
	100	50	2.03	42.6	1.35	π_9=5.30	--
		150	6.10	120.8	3.81		

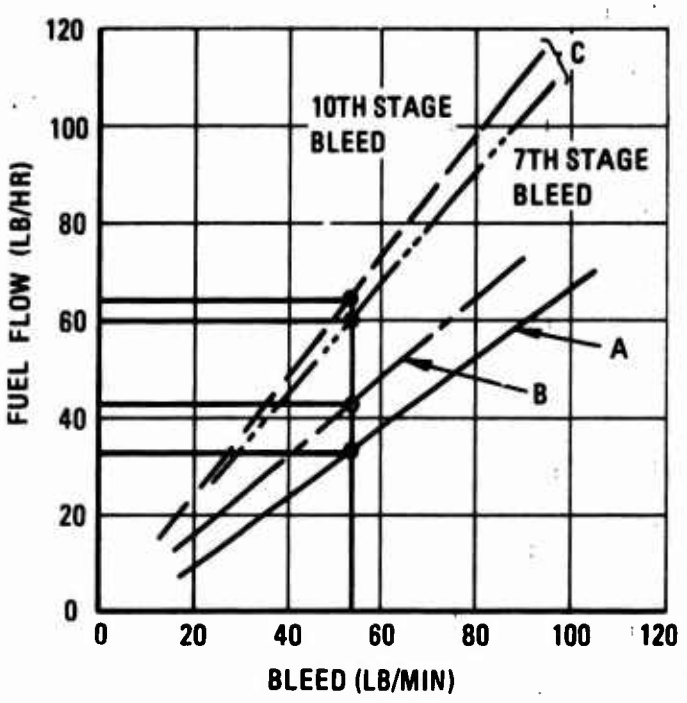

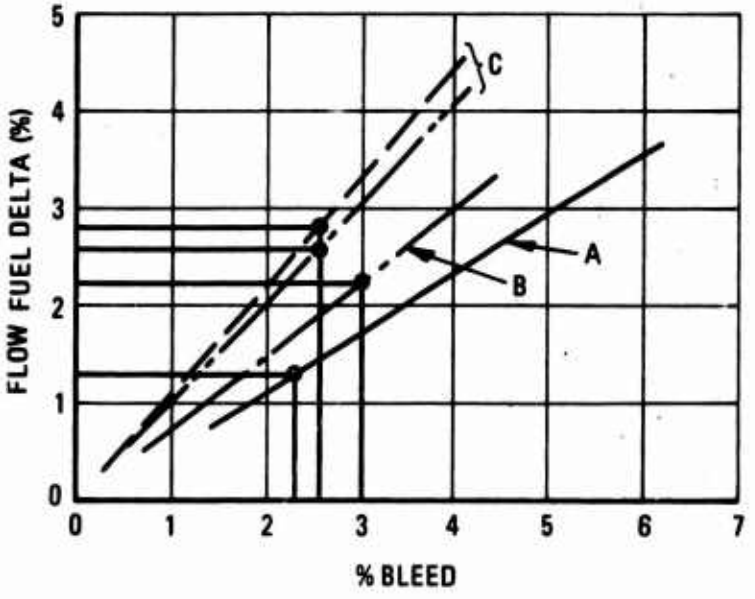

Figure 65. Engine Bleed Versus Fuel Consumption for Engines A, B, and C.

TABLE XXV. COMPONENT WEIGHT COMPARISON

Item Description	Concept Weights (lb) "A"	"B"	"C"	"D"
APU				
Baseline at 6000 rpm	184	146	184	184
Less internal gearing (estimate)	-30	-10	-30	-30
Net Weight	154	136	154	154
APU Compressor	26	20	26	26
Regenerative Turbine	45	-	45	45
Air Cycle Machine	-	30	-	-
XMSN Driven Compressor	-	-	26	-
XMSN Drive for Compressor	22	-	25	-
ECS Heat Exchanger	25	10	25	25
Moisture Separator	10	5	10	10
ECS Fan/Exducer	10	5	10	10
ECS Distribution Delta	15	-	15	100
CBR Filtration Unit	120	60	120	120
Main Engine Bleed Air Manifolding & Control	30	30	-	30
Main Engine Bleed Air Valves (3)	15	15	-	15
Precooler and Fan	25	25	-	25
Pressure Regulator and Flow Control	5	5	-	5
TOTALS	502	341	456	565

Note: Only components that vary are considered.

TABLE XXVI. SYSTEM CONCEPT WEIGHT COMPARISON

Concept	Net Weight Differences for 1.5-Hour Mission Fuel	Components	Total
A	+120.5 (58.8)	+161	+281.5 (219.8)
B	0	0	0
C	+ 33.5 (-28.2)	+115	+148.5 (86.8)
D	+ 64.5 (2.8)	+224	+288.5 (226.8)

TABLE XXVII. IN-FLIGHT FUEL FLOW REQUIREMENT COMPARISON (BASED ON MIN. SIMULTANEOUS POWER)

Description		"A"	"B"	"C"	"D"
Min. Simultaneous Power	(lb/min)	20	60*	20	20
ECS Airflow, Minimum	(lb/min)	30	30	30	30
Flight Control Pump Airflow (W_{max} = 46 lb./min.)					
Simultaneous Electrical Airflow	(lb/min)	6	6	6	6
Hoisting Airflow	(lb/min)	97	97	97	97
Total	(lb/min)	153	193	153	153
Equivalent Shaft Power Required	(hp)	308	N/A	308	308
Estimated SFC		.65	N/A	.462	-130
Fuel to Drive Compressor for 1.5 hr.	(lb)	300	N/A	213	300
Regenerative Capability	(hp)	-130	N/A	-130	-130
Period of Regeneration	(hr)	1.35	N/A	1.35	1.35
Fuel Saving from Regeneration	(lb)	-79	N/A	-79	-135
Engine Bleed Required When Not Hoisting	(lb/min)	-	96	-	-
Fuel Cost, No Hoisting	(lb)	-	90.5(146)	-	-
Fuel Cost, Full Hoisting (.15 hr.)	(lb)	19	10(16.2)	13.5	19
Total Fuel - 1-1/2 hr. mission	(lb)	221	100.5 (162.2)		165

*Concept "B" permits full ECS operation during hoisting.

SYSTEM CONCEPT DEMONSTRATION TESTING

A series of tests was conducted for the purpose of determining the various unknowns that do not lend themselves to analysis and for the purpose of demonstrating the system concept operation.

No attempt for optimization was made nor was there a specific capacity system design intended. The data presented therefore are primarily qualitative, with the quantitative values obtained used for backup only.

TEST SETUP NO. 1

The objective of this test was to determine the following:

- Heat generation and maximum temperature encountered within the ATM housing as a result of forced driving of the turbine wheel by an external source such as a dynamometer (analogous to the hoisted load driving the turbine).
- Windage losses of a driven turbine wheel in forward and reverse direction. The objective is to determine what size reversing wheel is required for empty-hook reversing speed payout.

The unit test consisted of a pure impulse wheel of 6.25 inches OD and 5.0 inches ID. The original motor consisted of partial admission nozzles.

Schematic representation of the test setup is shown in Figure 66.

Heat Generation

Temperature and pressure probes within the unit were located as shown in Figure 67, where:

T_1 = Turbine exit areas

T_2 = Area immediately adjacent to the turbine wheel

T_3 = Nozzle inlet area indicating gas temperature as a consequence of ventilation and recirculation

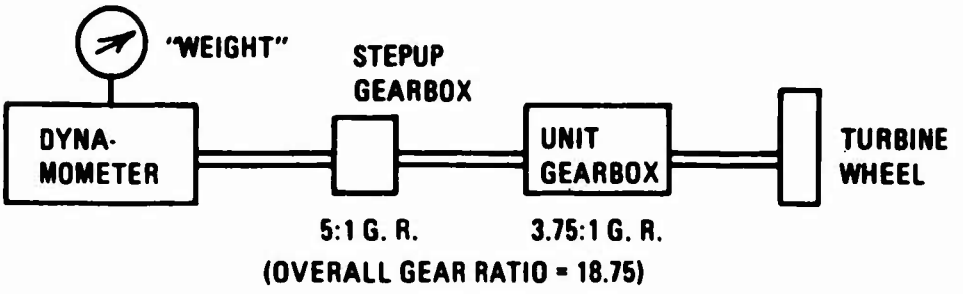

Figure 66. Test Setup No. 1.

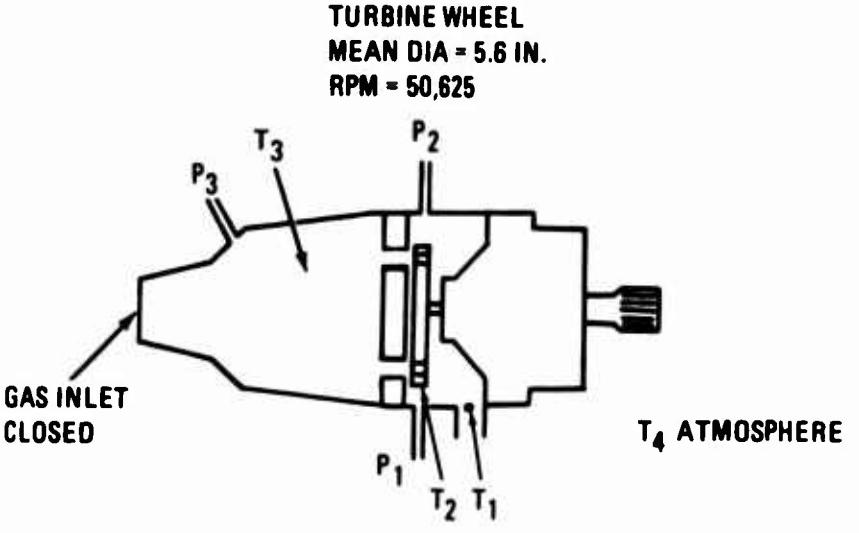

Figure 67. Location of Test Probes.

T_4 = Gearbox oil temperature

The pressures were recorded in inches of water gage.

The dynamometer speed was adjusted to a constant rotation of 2700 rpm, resulting in the turbine wheel speed of 50,625 rpm.

The turbine was rotated clockwise (reverse) and counterclockwise (forward) with the turbine inlet and open to the atmosphere.

The results of this test are shown in Tables XXVIII and XXIX, and Figure 68.

TABLE XXVIII. CLOCKWISE ROTATION TEMPERATURE INCREASE VERSUS TIME - CHAMBER BLANKED (VALVE CLOSED)

Time (sec)	T_1 (°F)	T_2 (°F)	T_3 (°F)	T_4 (°F)	P_1 ("H_2O")	P_2 ("H_2O")	P_3 ("H_2O")	Turbine Speed (rpm)
Acceleration time 30 - 60 sec from zero to 50,600 RPM								
0	352	627	176	-	3.8	1.6	4.4	50,625
60	430	738	212		3.5	1.8	3.9	50,625
120	446	823	248	-	3.4	1.7	3.8	50,625
180	472	878	292	-	3.5	1.7	3.8	50,625
240	490	913	338	132	-	-	-	50,625
300	509	932	374	137	-	-	-	50,625

TABLE XXIX. CLOCKWISE ROTATION TEMPERATURE INCREASE VERSUS TIME - CHAMBER BLANK REMOVED (VALVE OPEN)

Time (sec)	T_1 (°F)	T_2 (°F)	T_3 (°F)	T_4 (°F)	P_1 ("H_2O")	P_2 ("H_2O")	P_3 ("H_2O")	Turbine Speed (rpm)
0	212	563	292	91	6.5	12.1	1.6	50,625
60	273	643	374	102	5.7	11.0	1.5	50,625
120	302	698	446	110	5.6	10.8	1.5	50,625
180	320	734	500	112	5.3	10.5	1.5	50,625
240	338	752	545	-	5.2	10.1	1.5	50,625

From the tabulated data and from Figure 68, it is apparent that the highest generated temperature, T_2, is immediately adjacent to the turbine wheel as would normally be expected. The maximum temperature after 300 seconds of operation was 932°F, indicating that a special high-temperature alloy for the blades is not required.

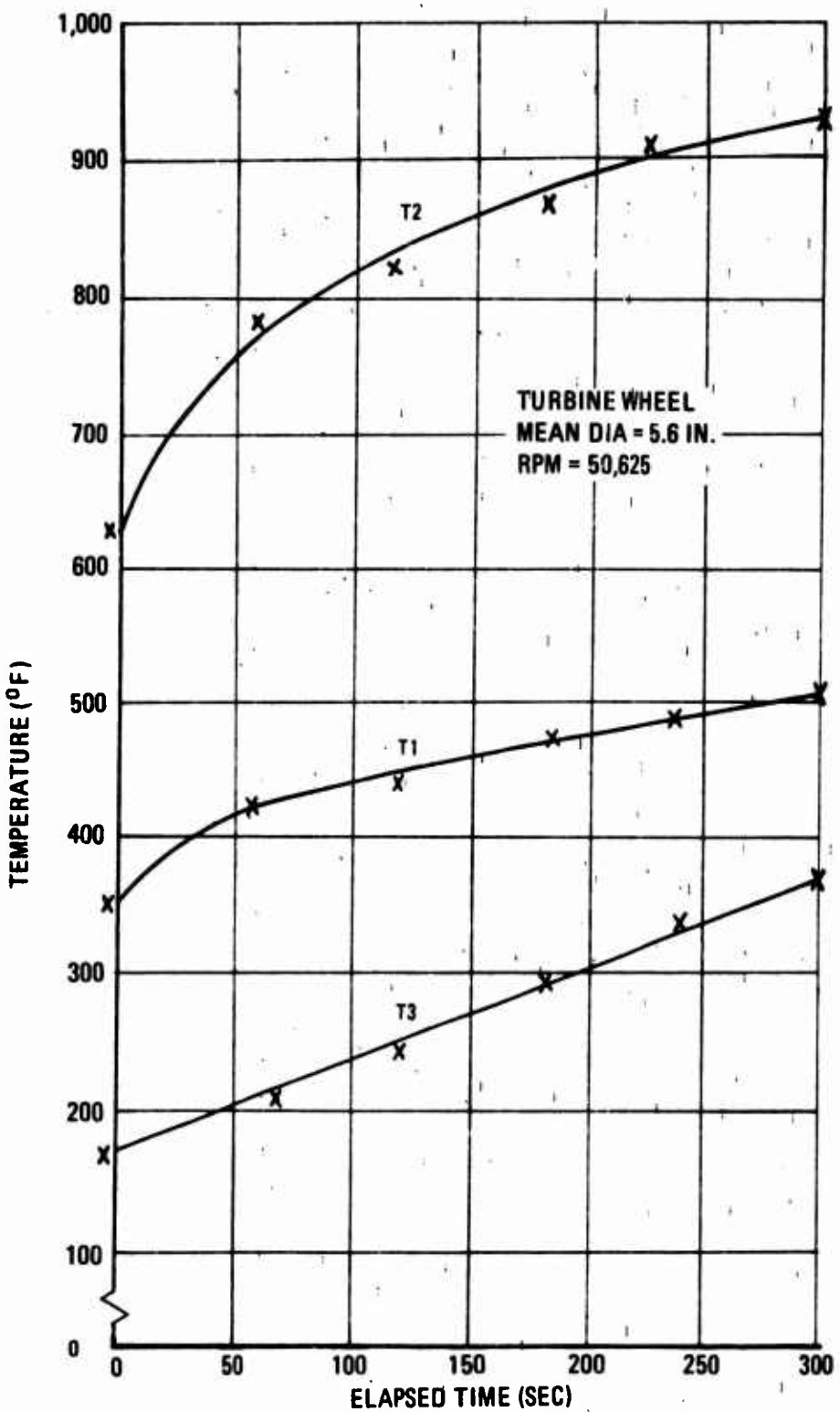

Figure 68. Temperature Rise Generated by Reverse Running of Turbine.

It is further indicated that the slope of the curve is continually decreasing and is attributed to rapid rate of heat conduction. In practical hoisting application, the high speed reversing time duration is not expected to exceed 100 seconds, and the resulting temperatures expected will therefore be significantly lower.

For dynamic braking, the temperature rise is expected to be significantly less due to lower rate of descent and due to the air supply (that provides energy for the braking) cooling effect.

Power Requirement Due to Windage Losses

With the test setup described above, quantitative determination of windage losses was attempted. Tests were conducted with a 6.25-inch-diameter wheel.

The first series of tests was conducted with bladed and unbladed discs over a range of speeds. Figure 69 is based on power difference between bladed and unbladed discs and therefore reflects the blade losses only. This approach was necessary since both gearing losses were not readily determinable.

Subsequent tests were run with the turbine wheel without blades and the results are tabulated in Table XXX. A graph of these data is shown in Figure 70.

On the basis of Figures 69 and 70, the maximum total windage losses of the blades and the discs, as well as some gear transmission losses, are shown in Figure 71.

An analysis of the blade windage losses of Figure 71 confirms that:

- With the control valve shut (blanked), windage losses--particularly at higher speed--can be reduced significantly.
- Blade windage losses are relatively constant for forward and reverse rotation.
- An empirical relationship between windage power and speed of rotation can be expressed as

$$\frac{P_2}{P_1} = \left(\frac{N_2}{N_1}\right)^2 \quad \text{(control valve closed)}$$

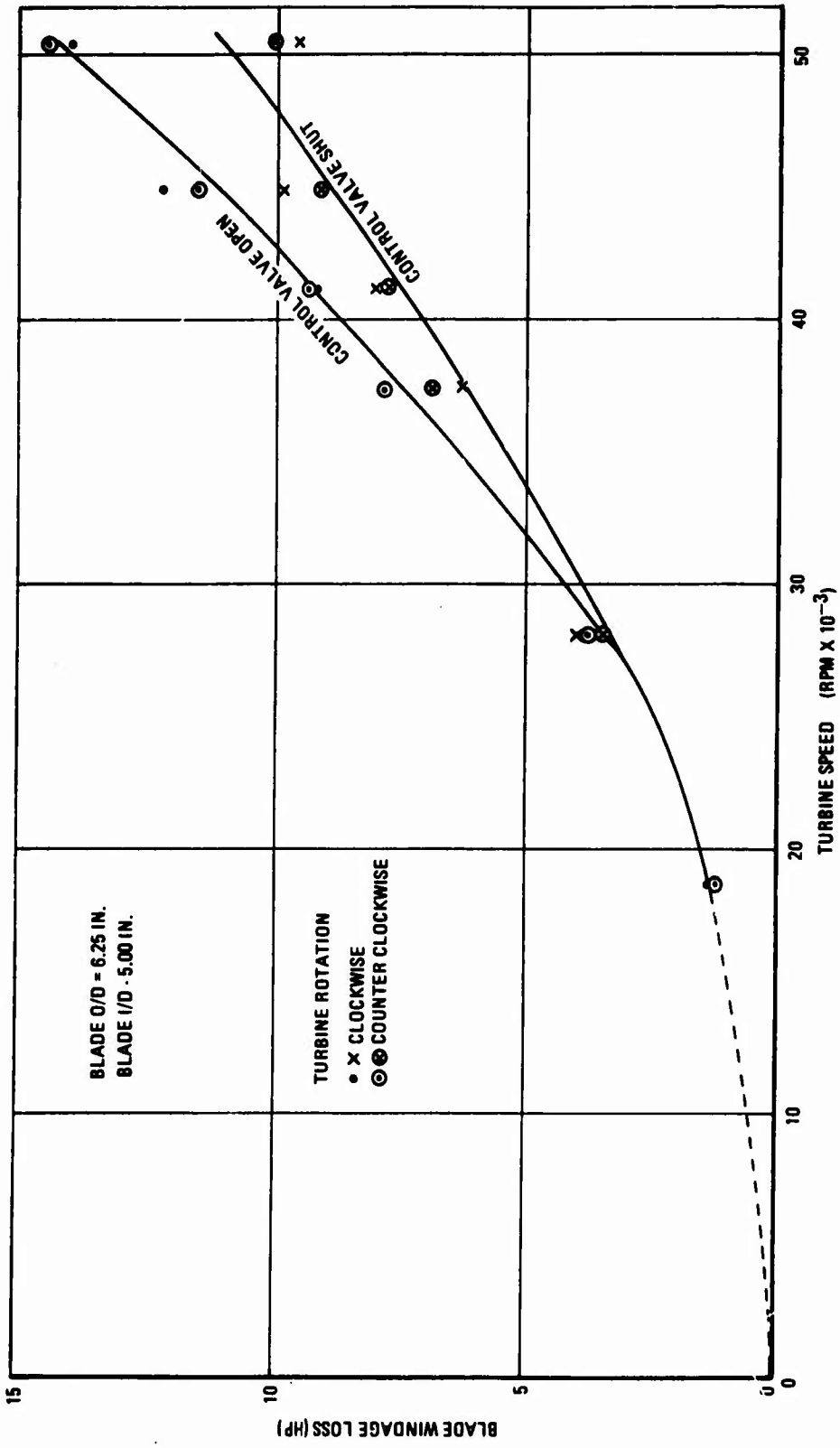

Figure 69. Blade Windage Loss.

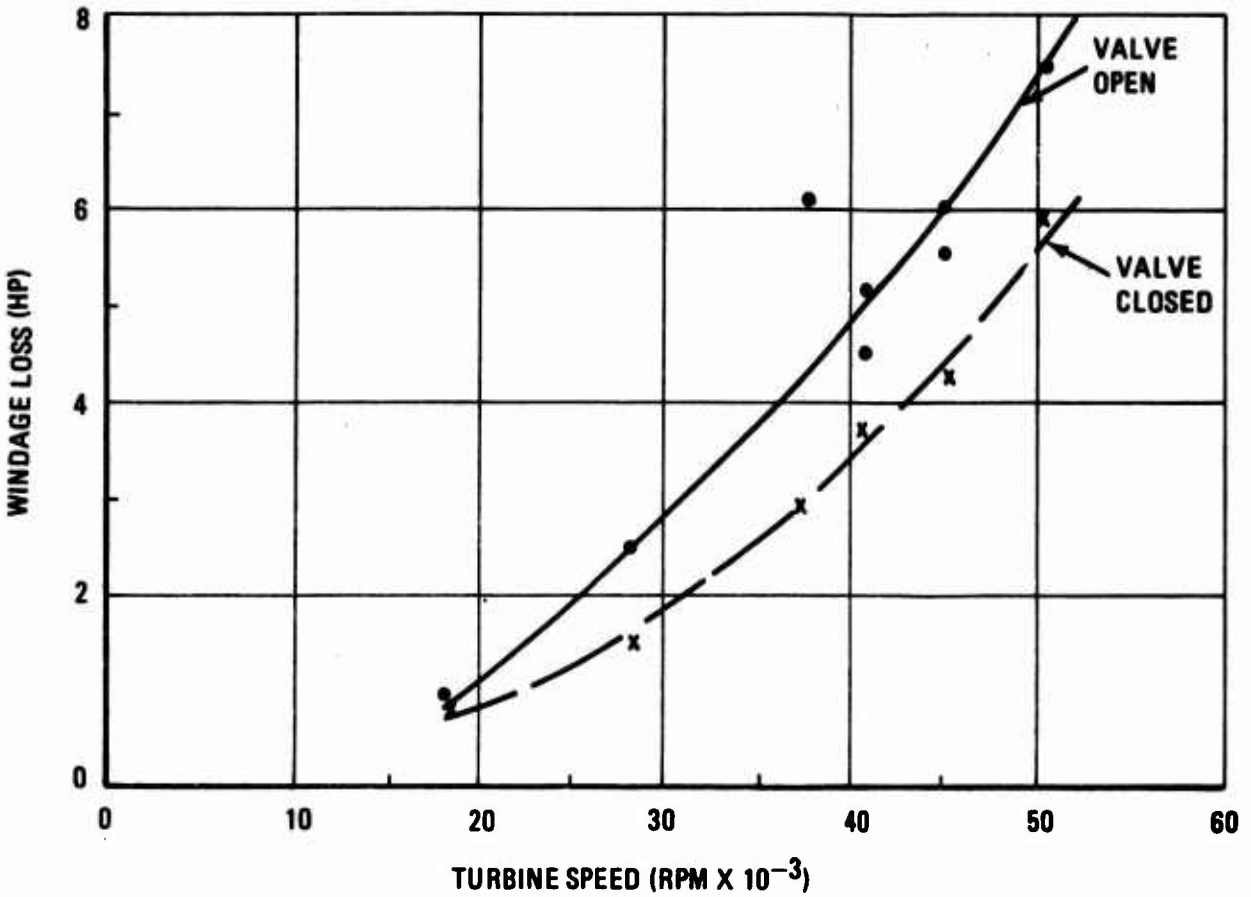

Figure 70. Disc Windage Loss.

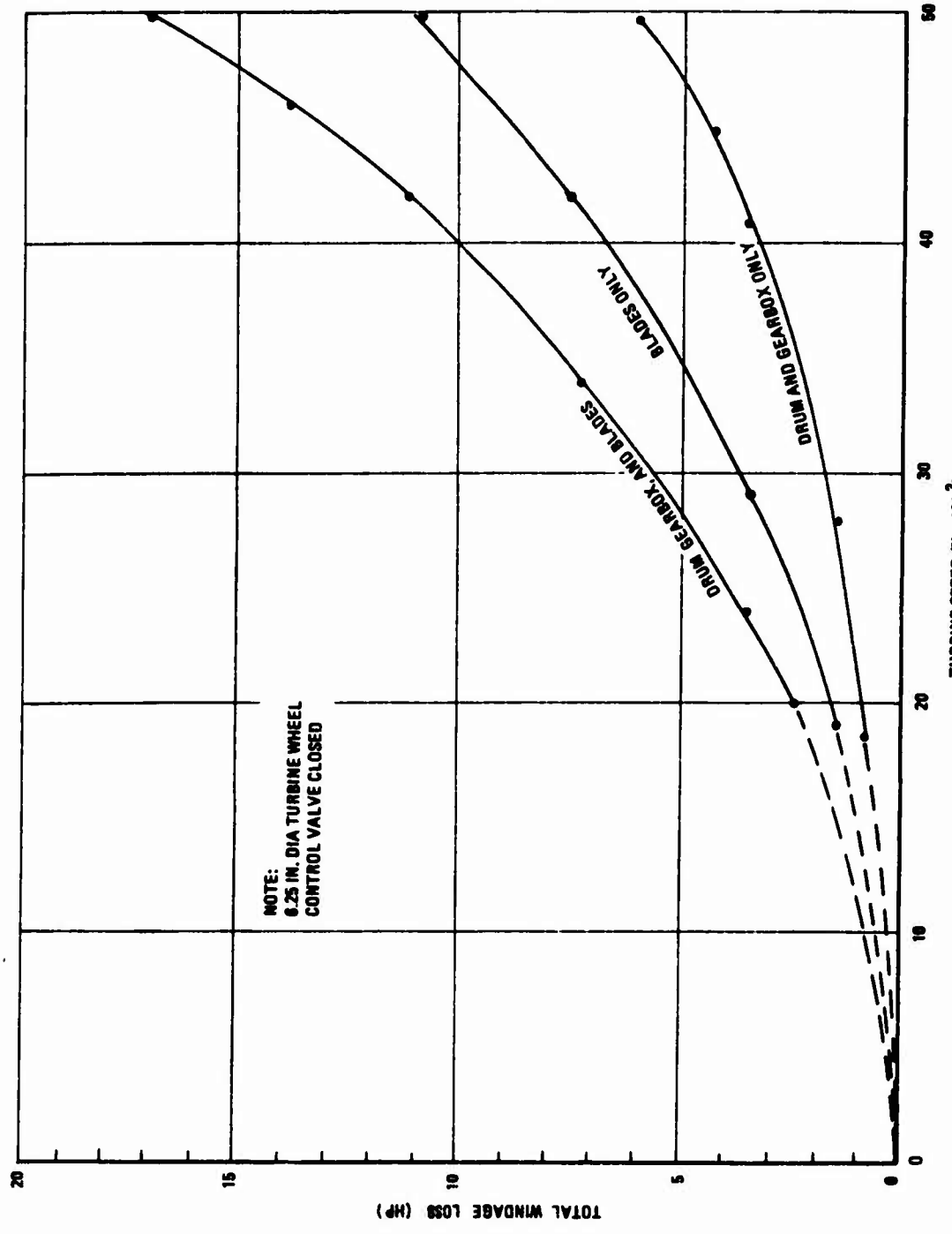

Figure 71. Total Turbine and Component Windage Loss.

TABLE XXX. WINDAGE LOSSES OF DISC WITHOUT BLADES (GEARING INCLUDED)

Control Valve Position	Dynamometer Speed (rpm)	Turbine Speed (rpm)	Windage Loss (hp)
Open			
	1000	18,750	1.071
	1500	28,200	2.53
	2000	37,600	6.171
	2200	41,300	4.53/5.15 (2 runs)
	2400	45,000	5.55/6.03 (2 runs)
	2700	50,625	7.52
Closed			
	1000	18,750	.8
	1500	28,200	1.58
	2000	37,600	2.94
	2200	41,300	3.68
	2400	45,000	4.25
	2700	50,625	5.94

and

$$\frac{P_2}{P_1} = \left(\frac{N_2}{N_1}\right)^{2.38} \quad \text{(control valve open)}$$

The tabulated values for the windage losses are not conclusive since the gearing transmission losses are not available. In any event, the windage loss of the unbladed disc portion must be considered in the analysis and design.

TEST SETUP NO. 2

A second test was conducted at another vendor facility with different turbine wheel configurations. The test objectives were:

- Verify data obtained on previous tests and discussed above.
- Demonstrate dynamic braking capability.
- Determine acceleration time from zero to maximum rpm.
- Investigate methods of reducing drag power.
- Demonstrate 200 percent of design speed reversing capability.

- Demonstrate continuity of torque/speed characteristics when changing from positive to negative rotation and vice versa.

The unit tested was a modified jet engine starter. The turbine wheel diameter (hoisting wheel) was 7 inches. To provide for reverse rotation, a 4.4-inch diameter wheel was used. The starter engine is shown in Figure 72. The test setup of this breadboard is as shown in Figure 73, where the turbine shaft passing through a gear reduction ratio of 16.4:1 was connected through a clutch to a flywheel with inertia of 18 slug-ft^2.

The drag power losses of the 7-inch wheel in reverse rotation were determined by driving a hydraulic motor with the air-turbine motor and then measuring the pressure and flow parameters of the hydraulic system at various speeds.

The test results of power drag under various conditions are shown in Figure 74. Note the very significant difference in power-drag reduction with a shrouded wheel baffle plate.

The next series of tests consisted of establishing the effectiveness of the turbine wheel as an aerodynamic brake (dynamic brake) and to get a "feel" of acceleration time from zero to maximum speed in both directions with the inertia wheel connected.

The recorder traces (Figure 75) indicate acceleration times with either wheel, braking capability with either wheel, and smooth transition from forward to reverse rotation and vice versa. These tests were conducted many times with very good repeatability.

This series of tests proved the feasibility of directly coupling a reversing wheel on the hoisting wheel with little penalty in the hoisting mode. This is based on the fact that the estimated drag power is a function of the diameter to the fifth power ($HP_{\infty}D^5$). The reversing wheel is expected to be approximately one-half of the hoisting wheel with relatively small resulting drag. At 40,000 rpm, the drag shall be about one horsepower.

The fact that the power drag of the hoisting wheel can be reduced by various configurations is helpful in that the reversing wheel can be small. For our application, the maximum tip speed will be limited to approximately 1,800 fps. Subject to nozzle area limitations, the hoisting wheel should be as small as possible.

There is not the slightest doubt about dynamic braking capability of the axial wheel design as shown in Figure 75. The

inertia wheel used in this test is approximately 1,000 times as high as the equivalent inertia that will be seen by the turbine shaft in hoisting application (turbine wheel inertia not compared here). In spite of this, rather rapid speed accelerations and decelerations were accomplished in both directions of rotation. Subsequent analysis in the control system area indicated that control response for the hoisting application is very good.

The 200-percent reversing empty cable payout should constitute not the slightest problem. In the hoisting mode the hoisting speed with an unloaded cable will be approximately 198% of the design speed.

The remaining tests to be conducted would be the "proper matching" of the hoisting and reversing wheels.

The power/speed characteristics test data, including the magnitude of drag power losses for the hoisting and reversing wheel, are summarized in Figure 76.

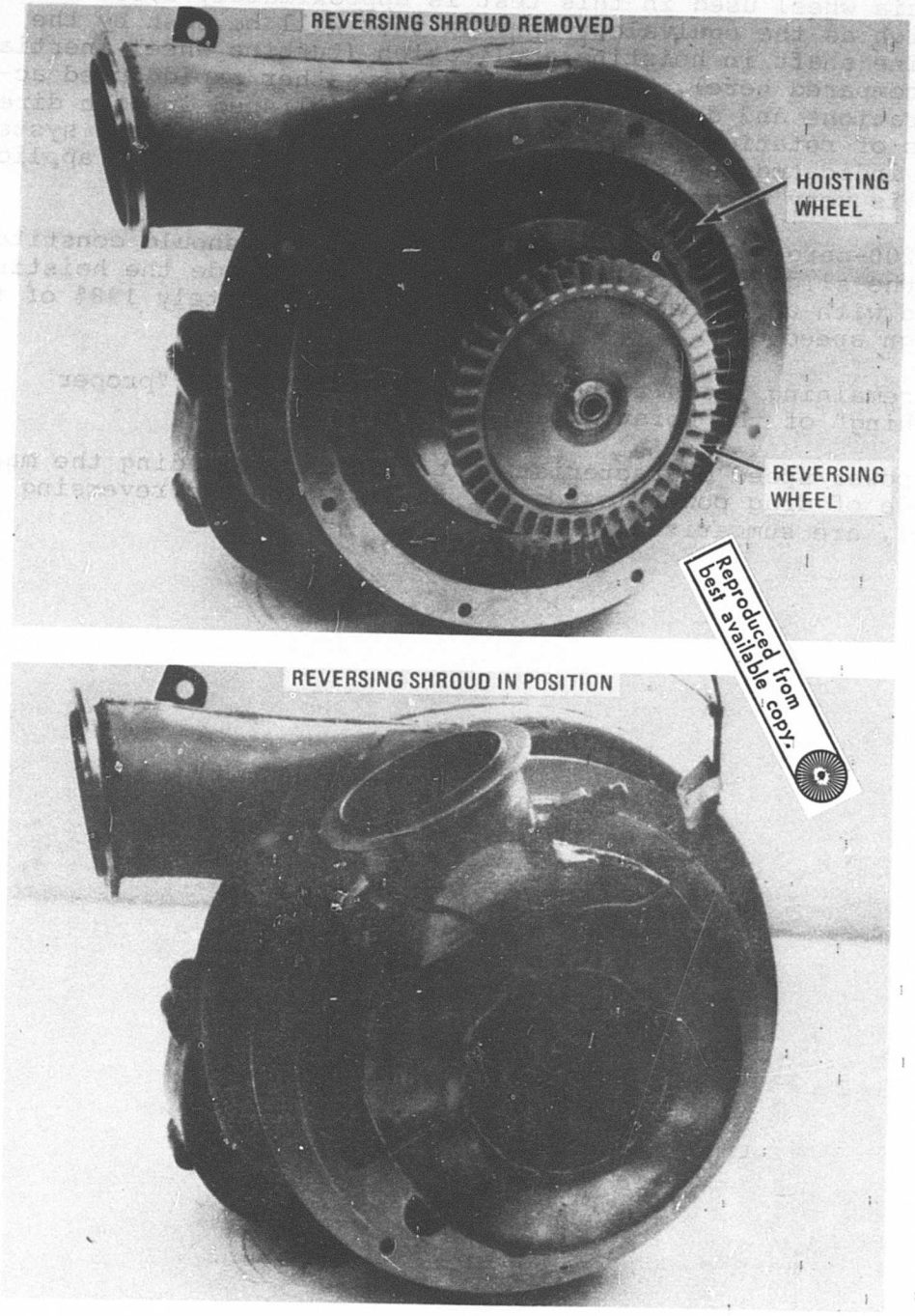

Figure 72. Air Turbine Motor Modified To Combine Hoisting and Reversing Functions (Sundstrand).

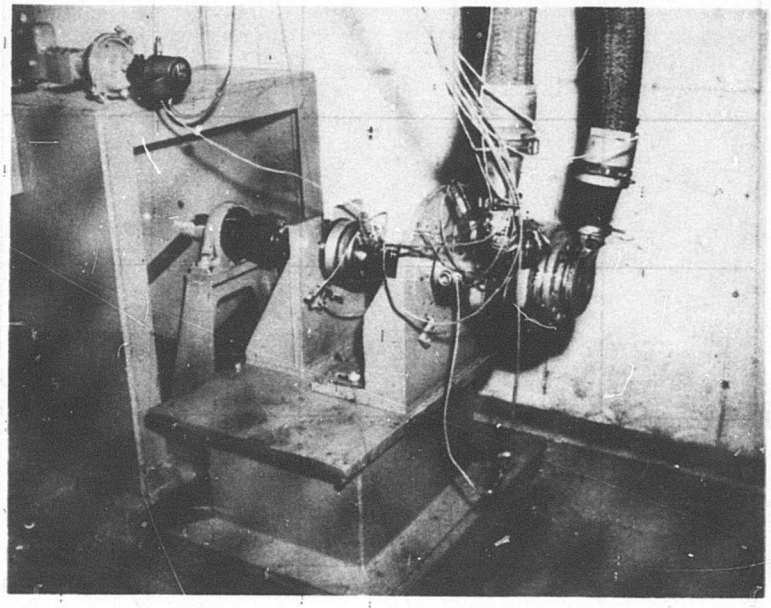

Figure 73. Breadboard Unit on Test Stand.

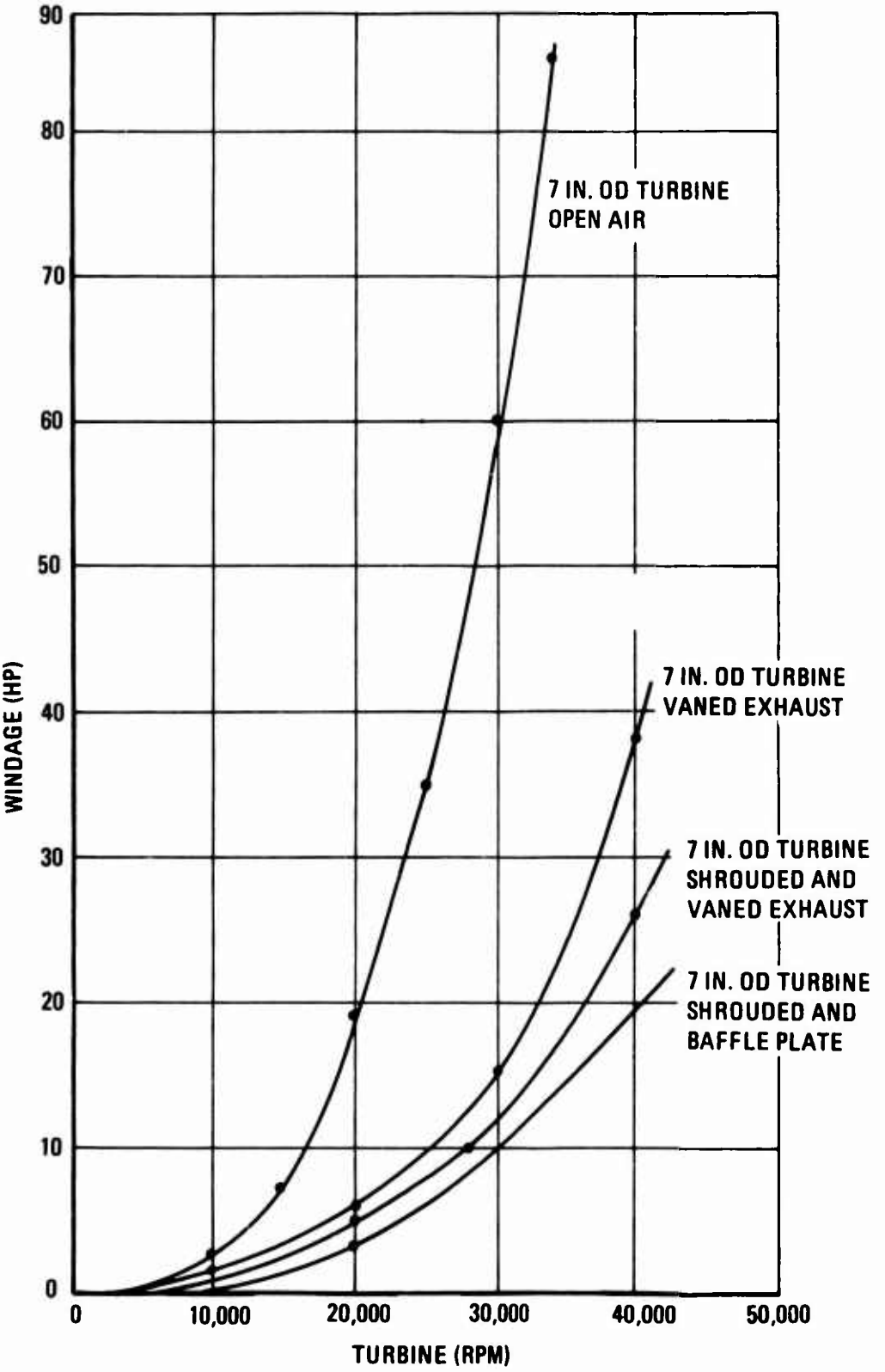

Figure 74. Effects of Windage-Control Devices (Sundstrand).

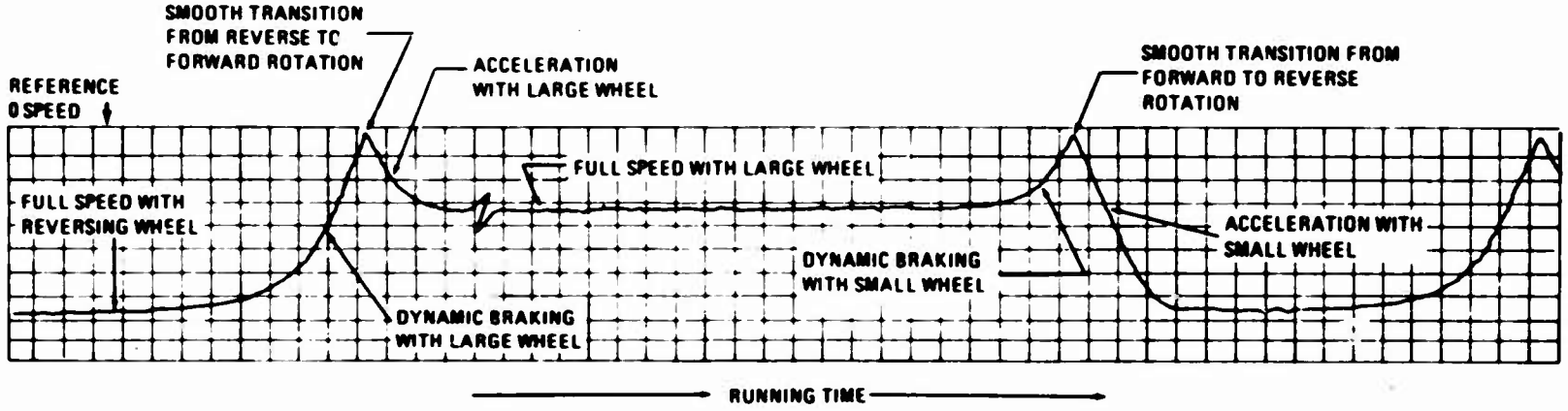

Figure 75. Composite Trace of Modified Air-Turbine-Drive Speed Characteristics.

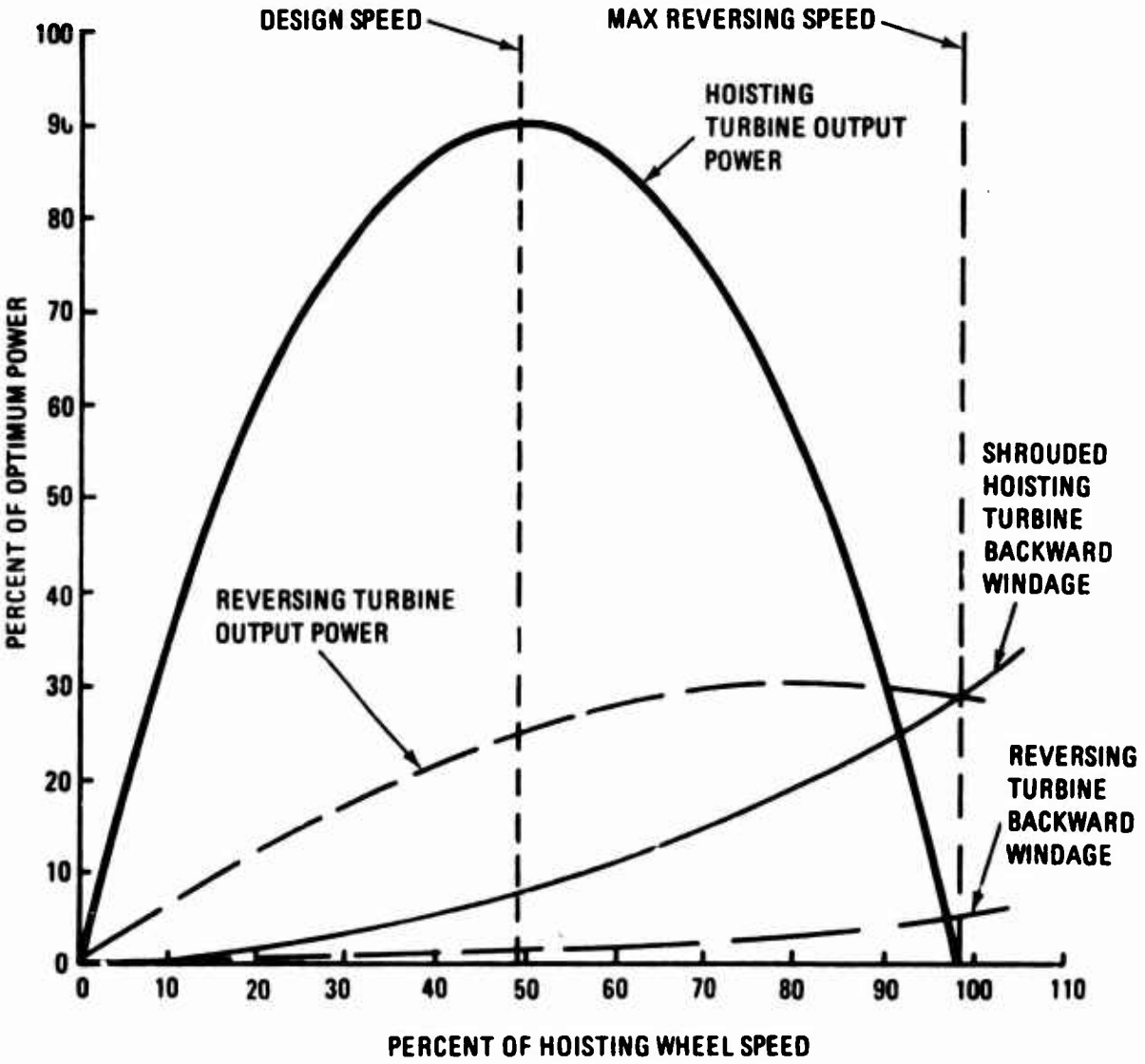

Figure 76. Summary of Hoisting and Reversing Wheel Performance.

STRESS ANALYSIS SUMMARY

Structural analysis of the cargo hoist system is based on a 20-ton system capacity. The analysis approach for the turbine blades and turbine disc include consideration of the following.

CENTRIFUGAL BLADE STRESSES

The stress levels in a rotating beam are determined numerically, assuming that the mass of the blade is concentrated at discrete points along the axis and that the section of beam between the two points is massless but possesses the elastic properties of a real beam. This method is used to determine forced-vibration amplitude ratios and may be used to determine "static" deflections and stress levels.

NATURAL FREQUENCY OF AXIAL BLADES BY "BEAM THEORY"

This analysis is based on the "Beam Theory", which assumes that cross-sectional dimensions of the blade are considered small in comparison to the spanwise length. The solution determines the flexural and torsional frequencies and mode shapes of cantilever blading. Flexural frequencies are corrected for rotation of the blade about the rotor axis.

TURBINE DISC ANALYSIS

The turbine disc contour and thickness are obtained by designing the wheel as a constant-stress disc with the rim load equal to the platform and blade load. The calculated stresses in the disc include radial stresses, tangential stresses, and effective stresses. The effective stresses or equivalent stresses are computed from the Henky-Von Mises theory of failure. All calculated stresses are those occurring at maximum operating speed, and include the centrifugal loading and the worst effect of temperature gradient, manufacturing tolerances, and balance-ring material removal. The wheel-burst speed is based on the average tangential stress in the disc and includes a burst factor. The burst factor, or material utilization factor as it is sometimes called, is multiplied times the material ultimate strength; this value is equal to the disc average tangential stress at the burst speed of the wheel.

For the hoist drive system, a high-speed air-turbine gearbox reduces the turbine speed by a 12.2:1 gear reduction ratio, which is further reduced at the hoist drum by a 30.4:1 gear reduction ratio.

A three-stage planetary drive system was selected for the cable drum drive. For the high-speed air-turbine drive, a two-step parallel shaft drive was selected. Both drives are spur-gear arrangements, which are inherently simple; the torques and speeds involved allow a compact package with minimum size and weight.

The bearings and gears have been sized conservatively--bearings having a B-10 life of 3,600 hours and gears having a life equivalent to an aircraft life of 10,000 flight hours. In all gears, a 25° pressure angle is used to provide good bending strength with reasonable sliding velocities.

HOIST-DRUM TRIPLE-PLANETARY REDUCTION GEARBOX

Strength substantiation and size selection for the hoist-drum drive-system components are summarized in Tables XXXI to XXXIV. Output power from the high-speed air turbine drive is shared equally between the dual-drum system. Design ultimate power is 94, which results from a 60-percent cargo payload distribution to the critical hoist, combined with a 2.5g payload inertia factor and a 1.15 cable angle factor.

For fatigue design, a cubic mean cable load is determined from the payload fatigue spectrum and percentage of occurrence. The cubic mean power for fatigue design is 14.5, which corresponds to the calculated cubic mean cable load of 7,990 pounds.

AIR TURBINE HIGH-SPEED GEARBOX

Tables XXXV to XXXVIII present design analysis data for the air turbine high-speed gearbox. The gears and bearings have been designed for a cubic mean power of 12 at design speed.

TABLE XXXI. GEAR DATA--HOIST-DRUM TRIPLE-PLANETARY REDUCTION GEARBOX

Gear	Diametral Pitch	Pitch Diameter (in.)	Face Width (in.)	Speed (rpm)
1st Stage Sun Gear #1	10.78	1.300	.950	4360
1st Stage Planet Gear #2	9.68	5.580	.750	524
1st Stage Drum Ring Gear	9.95	12.250	.850	58.5
2nd Stage Sun Gear #3	9.60	2.500	1.150	414
2nd Stage Planet Gear #4	10.09	4.860	1.000	124
2nd Stage Drum Ring Gear	9.95	12.250	1.150	14.3
3rd Stage Sun Gear #5	10.00	3.000	1.750	58.5
3rd Stage Idler Gear #6	9.95	4.624	1.620	38
3rd Stage Drum Ring Gear	9.95	12.250	1.800	14.3

TABLE XXXII. GEAR LOADS--HOIST-DRUM TRIPLE-PLANETARY REDUCTION GEARBOX

Gear	Ultimate Design Load (lb)	Cubic Mean Load (lb)
1st Stage Sun and Planet Gear #1 and #2	697	107
1st Stage Carrier Post	1,394	215
1st Stage Drum Ring Gear	697	107
2nd Stage Sun and Planet Gear #3 and #4	3,700	570
2nd Stage Carrier Post	7,400	1,140
2nd Stage Drum Ring Gear	3,700	570
3rd Stage Sun and Planet Gear #5 and #6	18,160	2,800
3rd Stage Carrier Post	36,330	5,590
3rd Stage Drum Ring Gear	18,160	2,800

TABLE XXXIII. SHAFT TORQUE--HOIST-DRUM TRIPLE-PLANETARY REDUCTION GEARBOX

Shaft	Ultimate Design Torque (in.-lb)	Cubic Mean Torque (in.-lb)
Input Shaft	1,360	210
1st Stage Carrier	13,880	2,130
2nd Stage Carrier	81,740	12,600
1st Stage Drum Input	12,800	1,970
2nd Stage Drum Input	68,020	10,480
3rd Stage Drum Input	333,760	51,400

TABLE XXXIV. BEARING LOADS--HOIST-DRUM TRIPLE-PLANETARY REDUCTION GEARBOX		
Bearing	Ultimate Design Load (lb)	Cubic Mean Load (lb)
1st Stage Planet Bearing	1,394	215
2nd Stage Planet Bearing	7,400	1,140
3rd Stage Planet Bearing	36,330	5,590

TABLE XXXV. GEAR DATA--AIR TURBINE HIGH-SPEED GEARBOX				
Gear	Diametral Pitch	Pitch Diameter (in.)	Face Width (in.)	Speed (rpm)
High Speed Pinion #4	36	1.000	.700	53,500
High Speed Gear #3	36	3,417	.625	17,200
Intermediate Pinion #2	20	1.100	1.150	17,200
Output Gear #1	20	3,950	1.100	4,360

TABLE XXXVI. GEAR LOADS--AIR TURBINE HIGH-SPEED GEARBOX		
Gear	Ultimate Design Load (lb)	Cubic Mean Load (lb)
High-Speed Pinion #4	444	42
High-Speed Gear #3	444	42
Intermediate Pinion #2	1,378	131
Output Gear #1	1,378	131

TABLE XXXVII. SHAFT TORQUE--AIR TURBINE HIGH-SPEED GEAR BOX		
Shaft	Ultimate Design Torque (in.-lb)	Cubic Mean Torque (in.-lb)
High Speed	222	21
Intermediate	757	72
Output	2,720	258

TABLE XXXVIII. BEARING LOADS--AIR TURBINE HIGH-SPEED GEAR BOX		
Bearing	Ultimate Design Load (lb)	Cubic Mean Load (lb)
A	134	13
B	310	29
C	722	68
D	1,100	104
E	689	65
F	689	65

HOIST-DRIVE DESIGN FOR 20-TON-CAPACITY SYSTEM

The 20-ton hoist-drive system design was based on the following:

- Analysis and preliminary design conducted in Phase I
- Design-support tests conducted for the purpose of substantiating analyses
- System operational concept demonstration testing observed by Eustis Directorate personnel
- Continuous technical dialogue with various pneumatic system and component designers and fabricators substantiating design concept and performance feasibility
- Review and "hardening up" of Phase I analytical effort

The culmination of the above resulted in a 20-ton hoist-drive system design represented in the following drawings shown in Figures 77 through 81.

The single most significant departure from the Phase I analytical and preliminary design effort was the dual-drum and paired-cable approach. Subsequent design studies revealed that this approach will have to be modified. The substantiation for this modification was based on a 28-ton hoist system presently in the design process for Advanced Technology Component Development for the HLH helicopter.

This approach applies equally to the 20-ton hoist system, and is as follows.

A design trade-off study comparing various drum arrangements and deployment schemes was conducted. The results of this study led to the definition of the hoist as a paired-cable system utilizing parallel drums with a single-point payout (SPP).

This system offers the best weight potential, eliminates lateral trim changes as a function of tension member payout, and permits the use of smaller-diameter tension members, which will facilitate handling and tension member producibility. In addition, it also affords an opportunity to incorporate a comparator type nondestructive test system for safety.

The original winch design concept was assumed to be a conventional level-wind design. Subsequently, a single-point payout winch configuration was developed which was competitive with the level-wind hoist. To limit the hoist bulk and also to provide an opportunity to consider the development of a system to compare cable condition, a number of configurations for twin-cable hoists have been evolved. These configurations were compared, together with the basic single-cable hoist, to enable the selection of a suitable concept for design development. The studies are discussed below.

SINGLE-CABLE HOISTS

Development of design concepts for single-point payout hoists and analysis of the drum stress have resulted in a design concept that appears to offer the advantages of the SPP hoist with a weight saving over the level-wind design.

A comparison of the relative merits of the two design concepts resulted in selection of a concept for further development.

Level-Wind Hoist

A cross section of the level-wind design comparable with the SPP design is shown on Figure 82. The side-load rollers are attached to traversing carriages mounted on a pair of leadscrews. The leadscrews terminate at the hoist side frames, supported in bearings and driven from the cable drum to synchronize movements. With the cable fully stowed, the hook will exit from the tunnel approximately 9 inches from the aircraft centerline on the left-hand side. With 100 feet of cable deployed, the cable will be approximately 9 inches from the aircraft centerline on the right-hand side.

Single-Point Payout Hoist

The SPP hoist concept is shown in Figure 83. The reduction gearing, primary drive, ATM, and brake will be essentially the same as for the level-wind hoist. Whereas in the level-wind concept the final drive is direct from the gearbox to the inside of the drum, in the SPP design the final drive is to a central

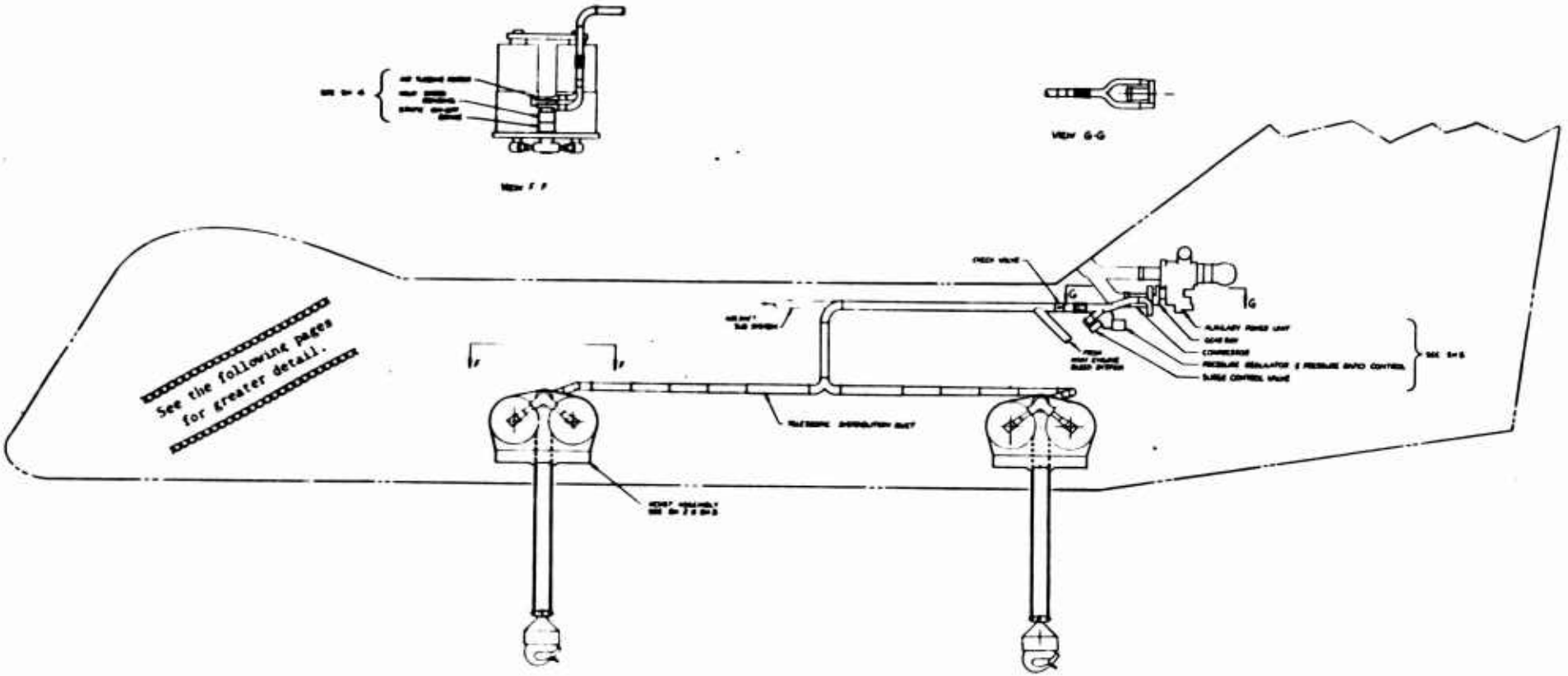

Figure 77. General Arrangement of System.

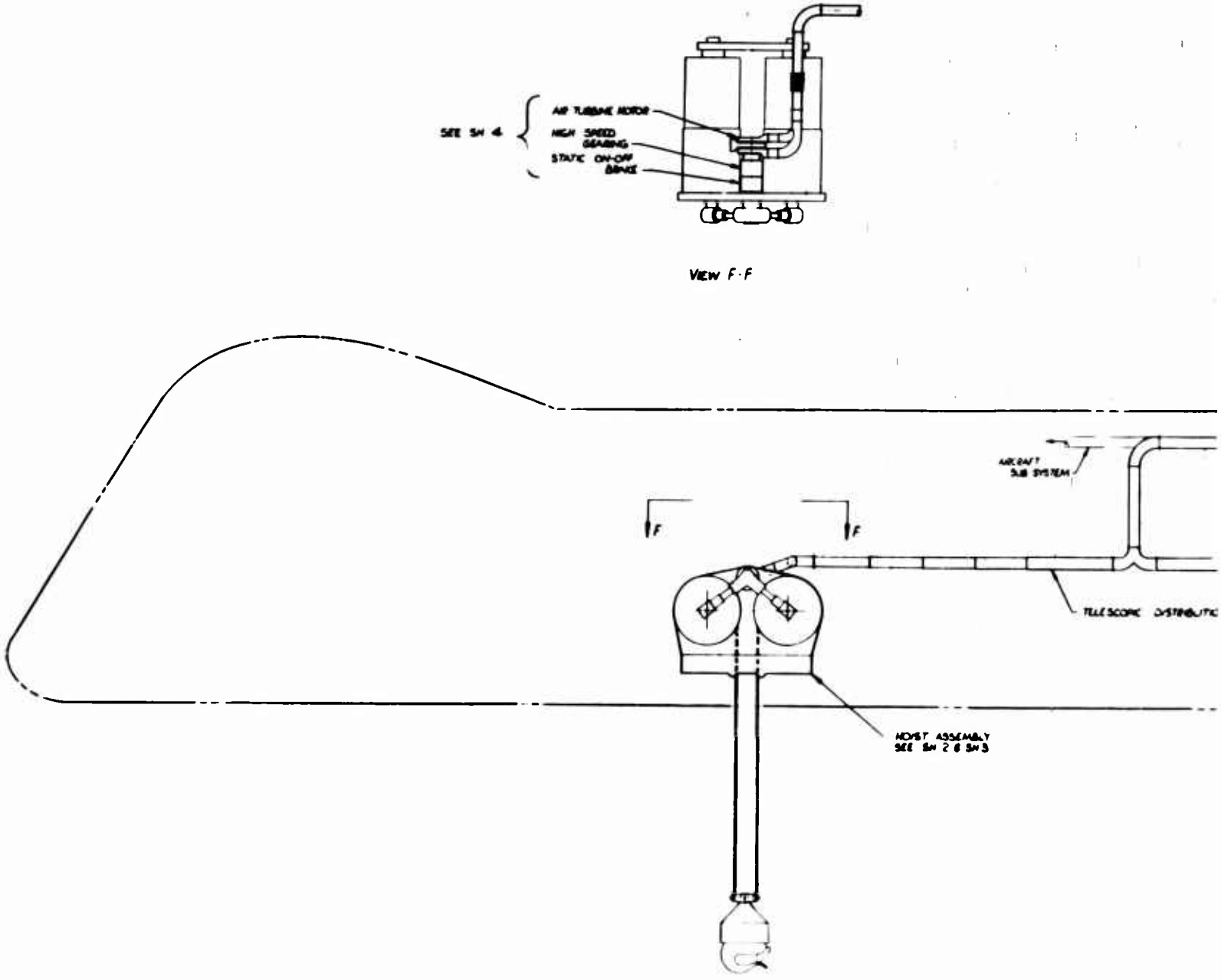

Figure 77. General Arrangement of System.

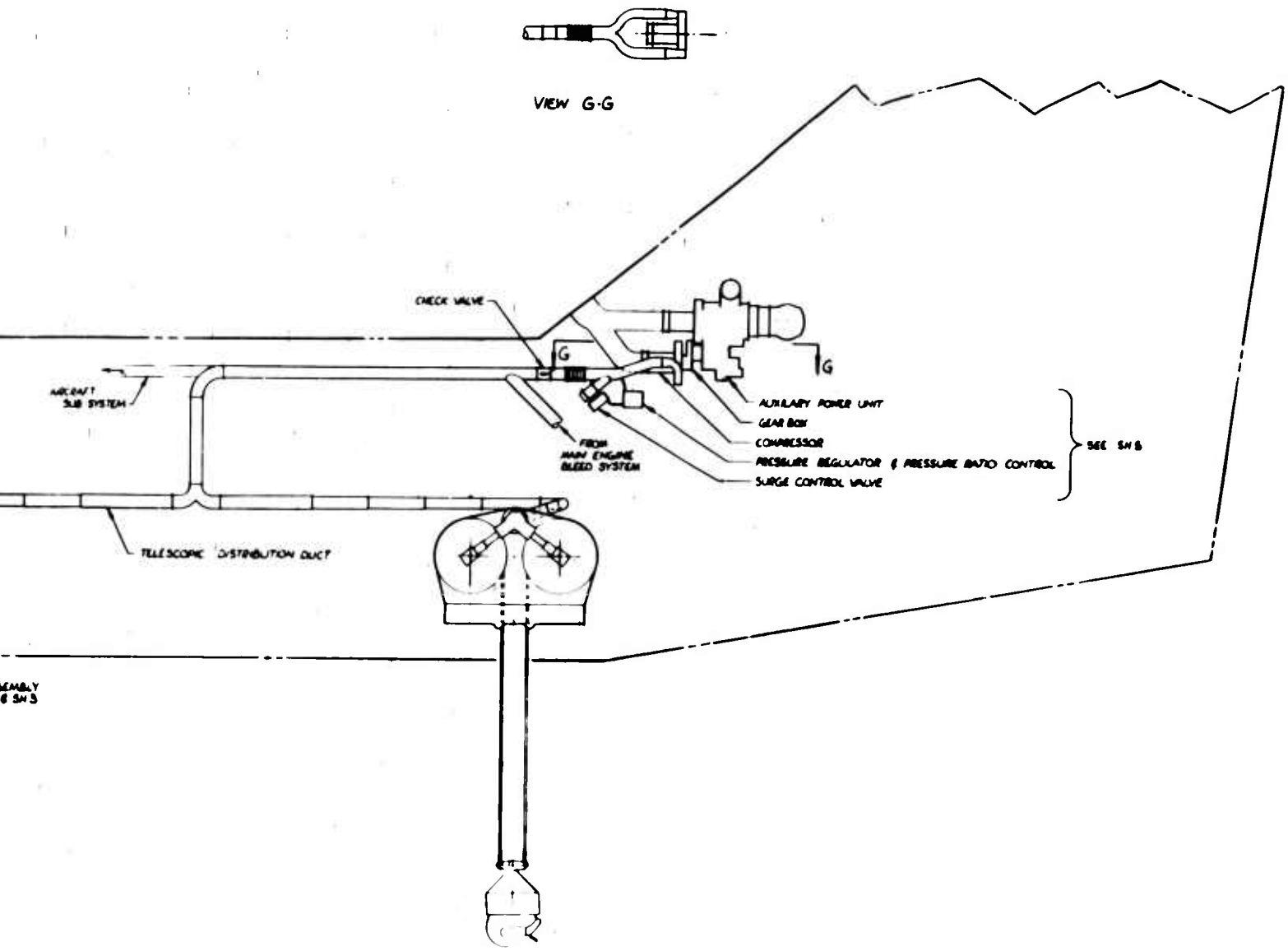
VIEW G-G
CHECK VALVE
G
G
AIRCRAFT SUB SYSTEM
FROM MAIN ENGINE BLEED SYSTEM
AUXILIARY POWER UNIT
GEAR BOX
COMPRESSOR
PRESSURE REGULATOR & PRESSURE RATIO CONTROL
SURGE CONTROL VALVE
SEE SH 8
TELESCOPIC DISTRIBUTION DUCT

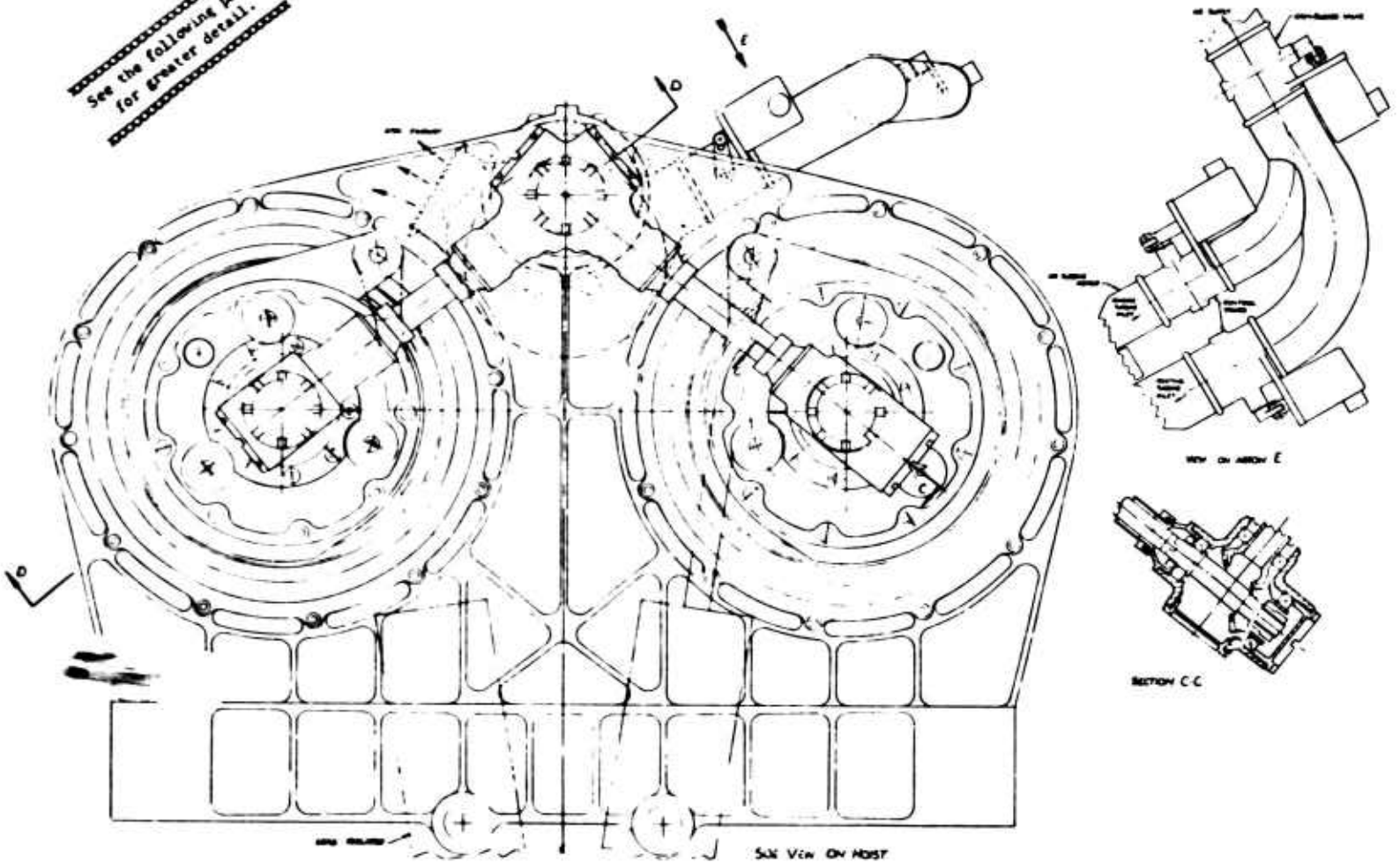

Figure 78. Section Through Hoist.

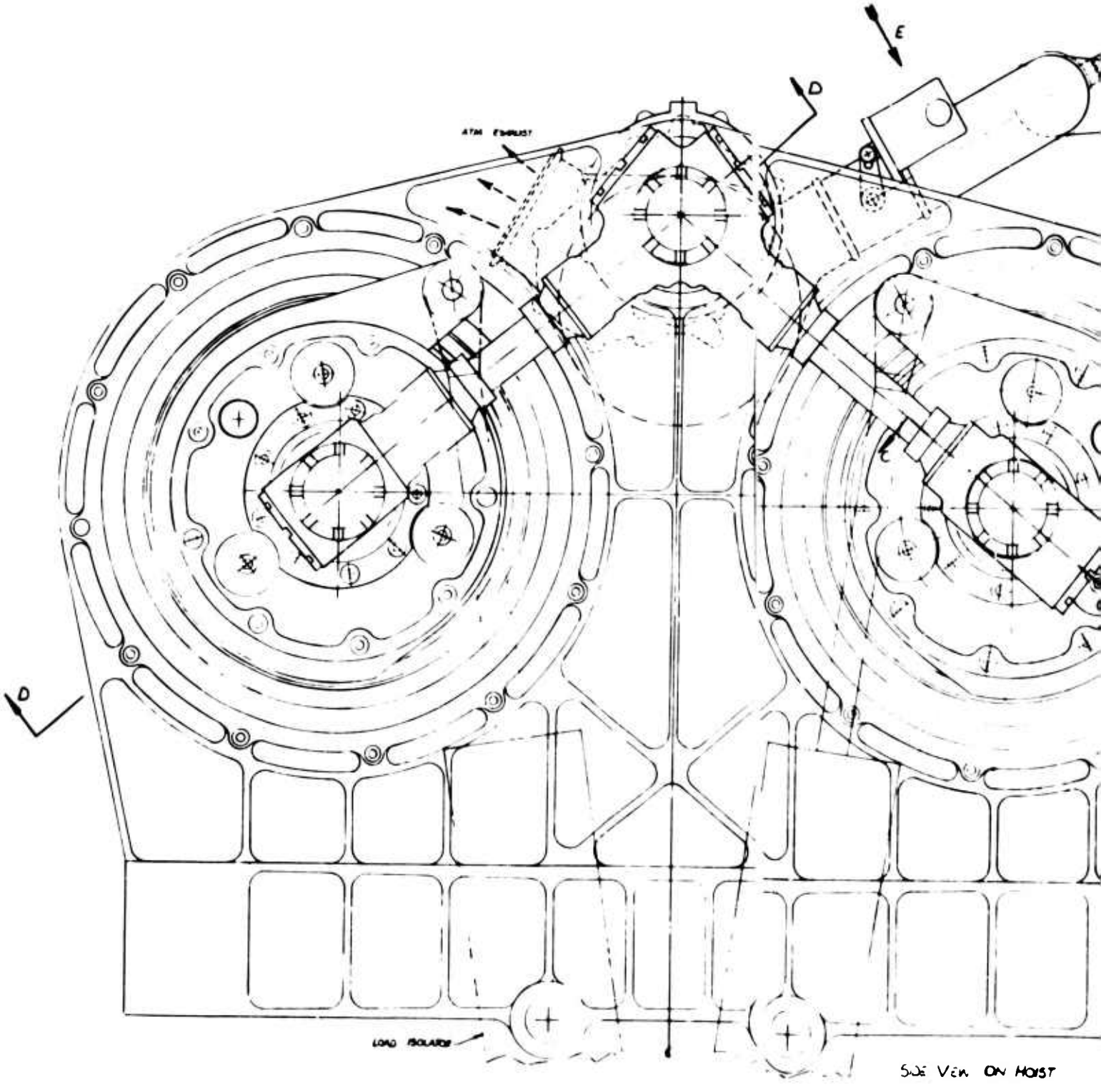

Figure 78. Section Through Hoist.

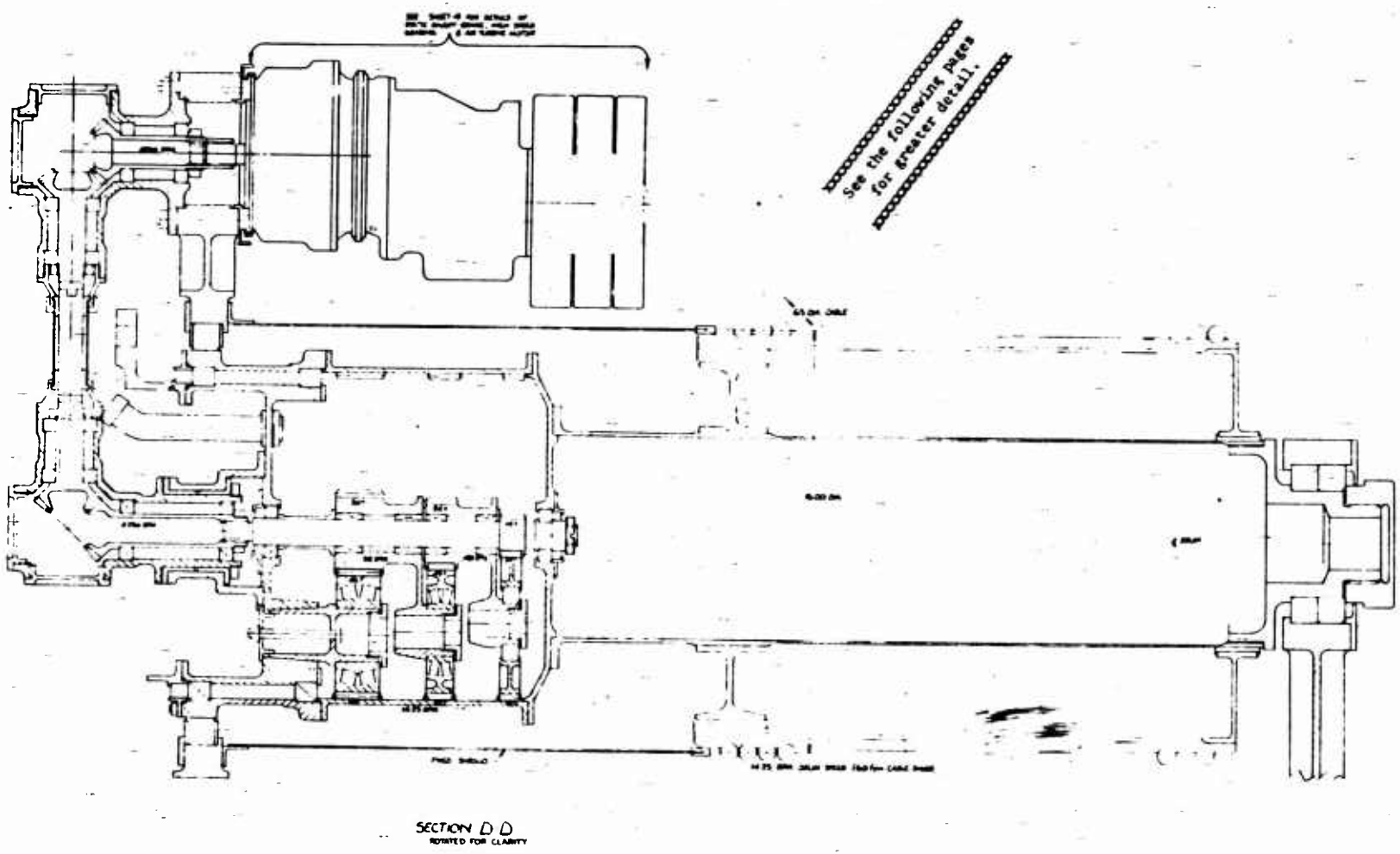

Figure 79. Side View of Hoist.

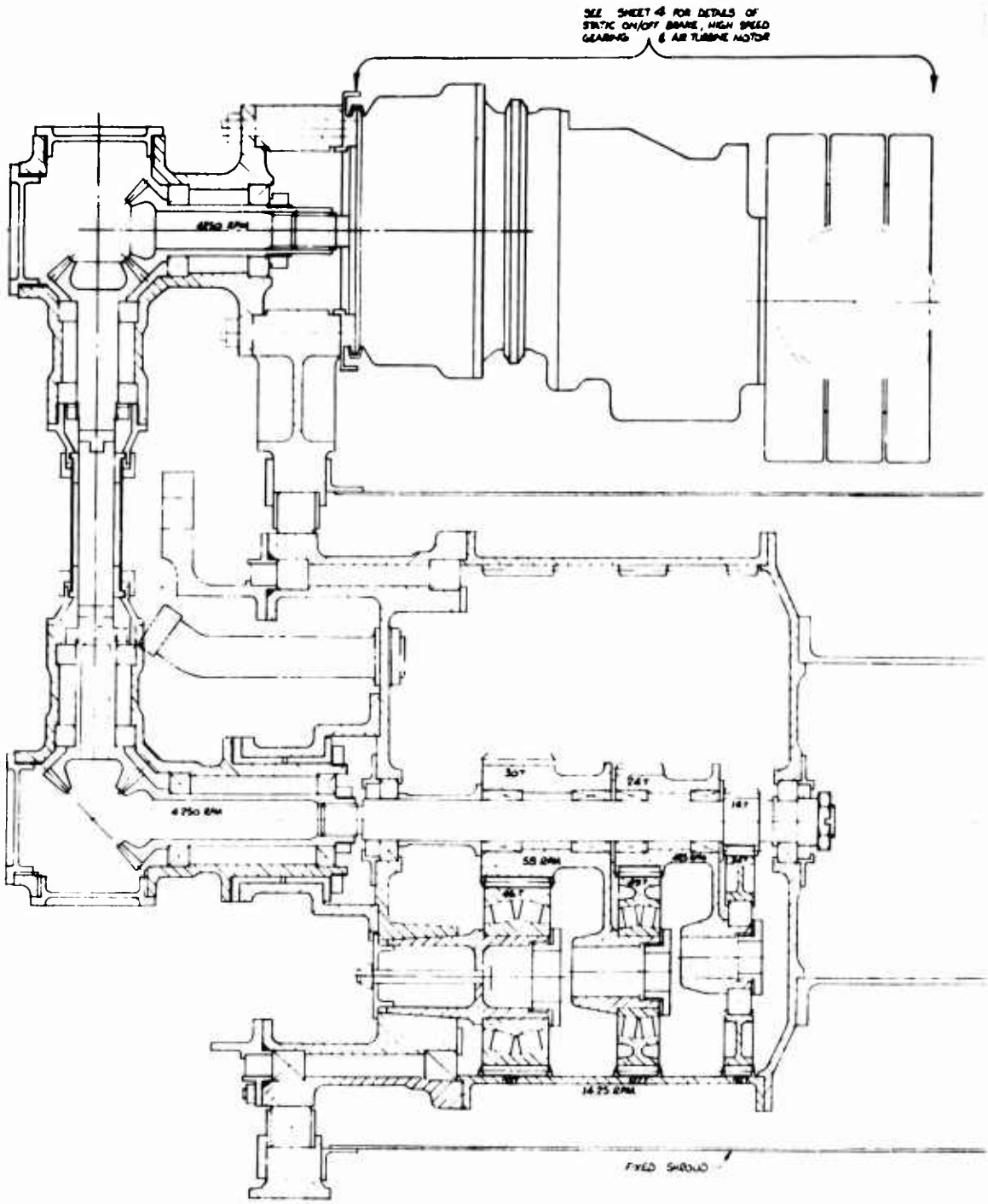

SECTION D-D
ROTATED FOR CLARITY

Figure 79. Side View of Hoist.

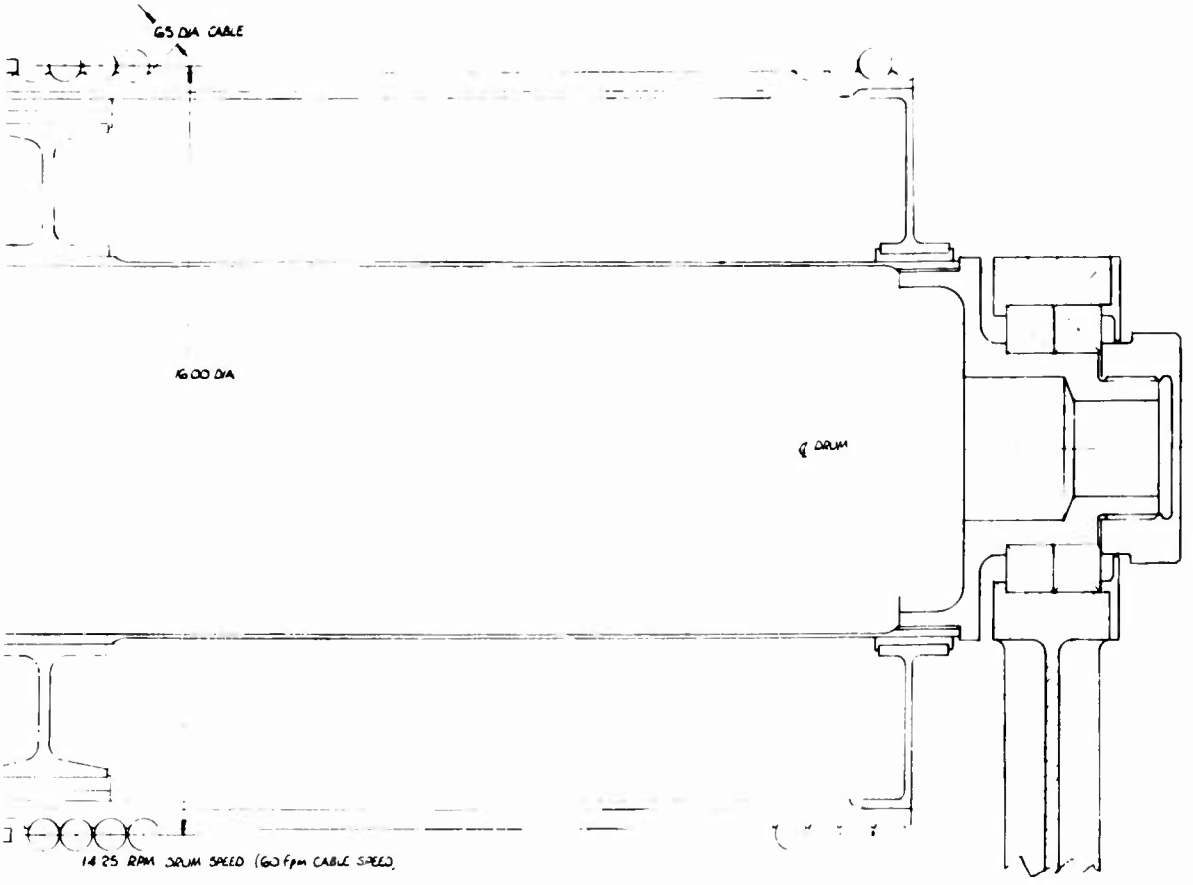
.65 DIA CABLE
16.00 DIA
℄ DRUM
14.25 RPM DRUM SPEED (60 fpm CABLE SPEED)

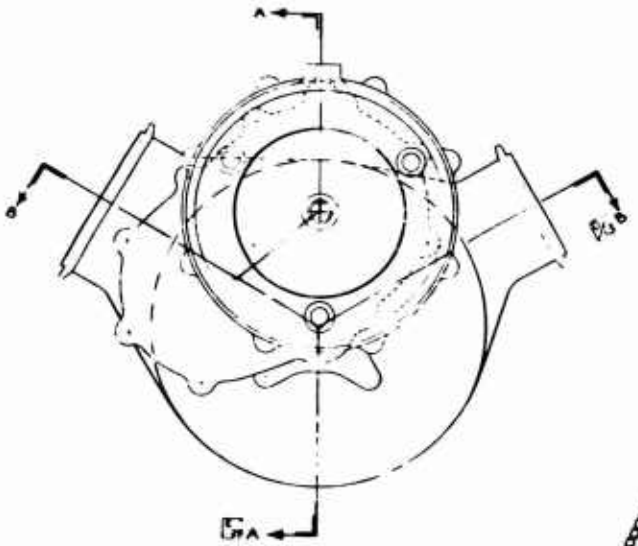

See the following pages for greater detail.

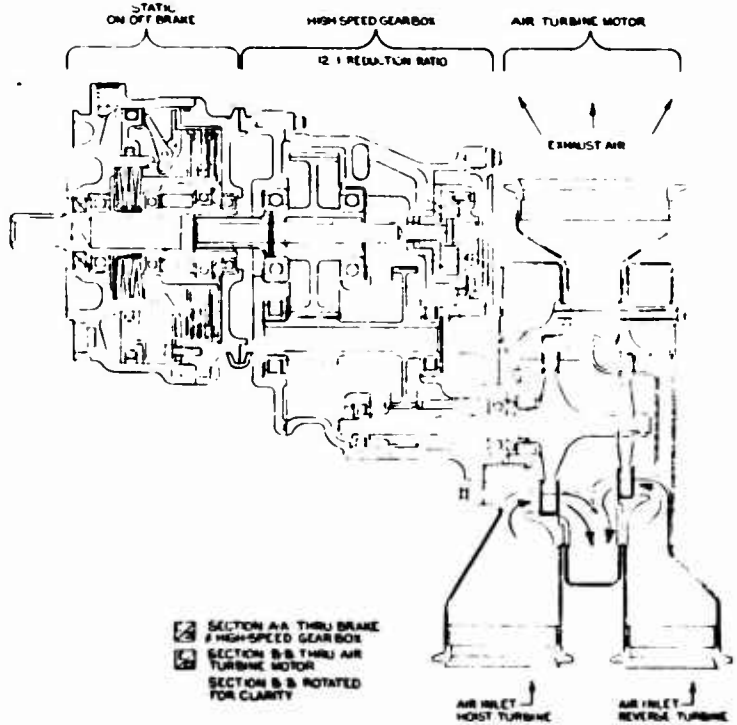

Figure 80. Arrangement of ATM, High-Speed Gearbox, and Brake.

Preceding page blank

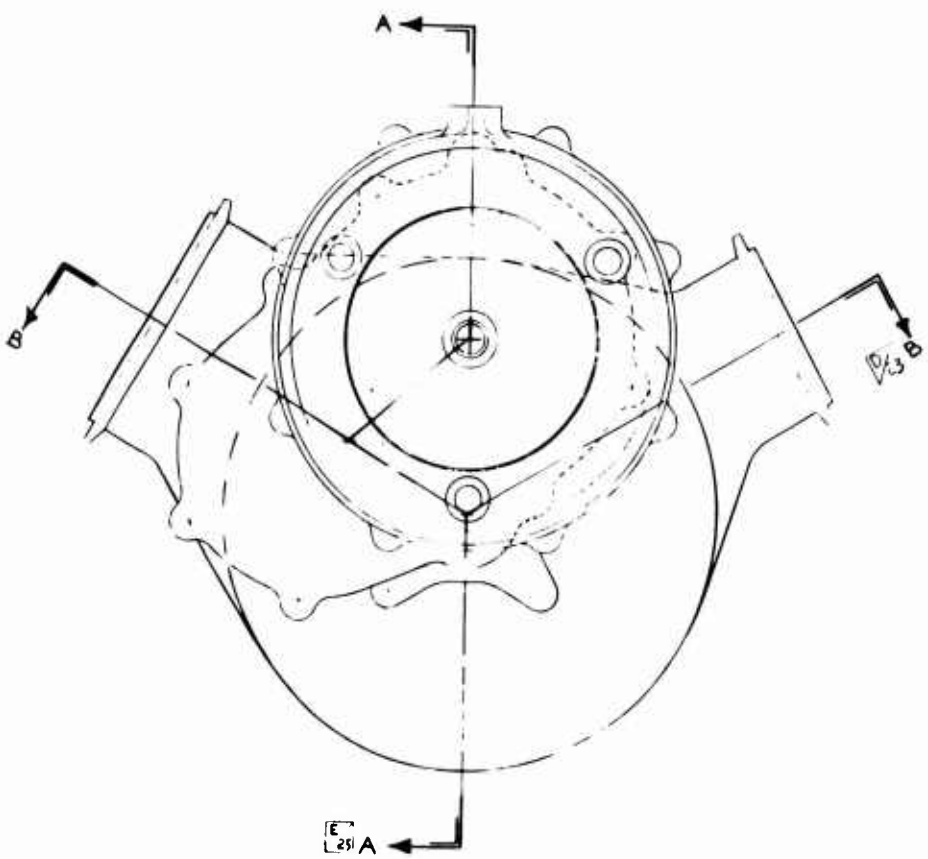

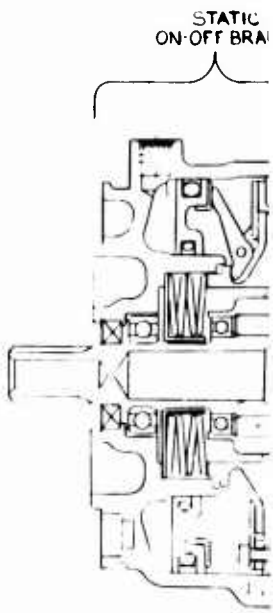

Figure 80. Arrangement of ATM, High-Speed Gearbox, and Brake.

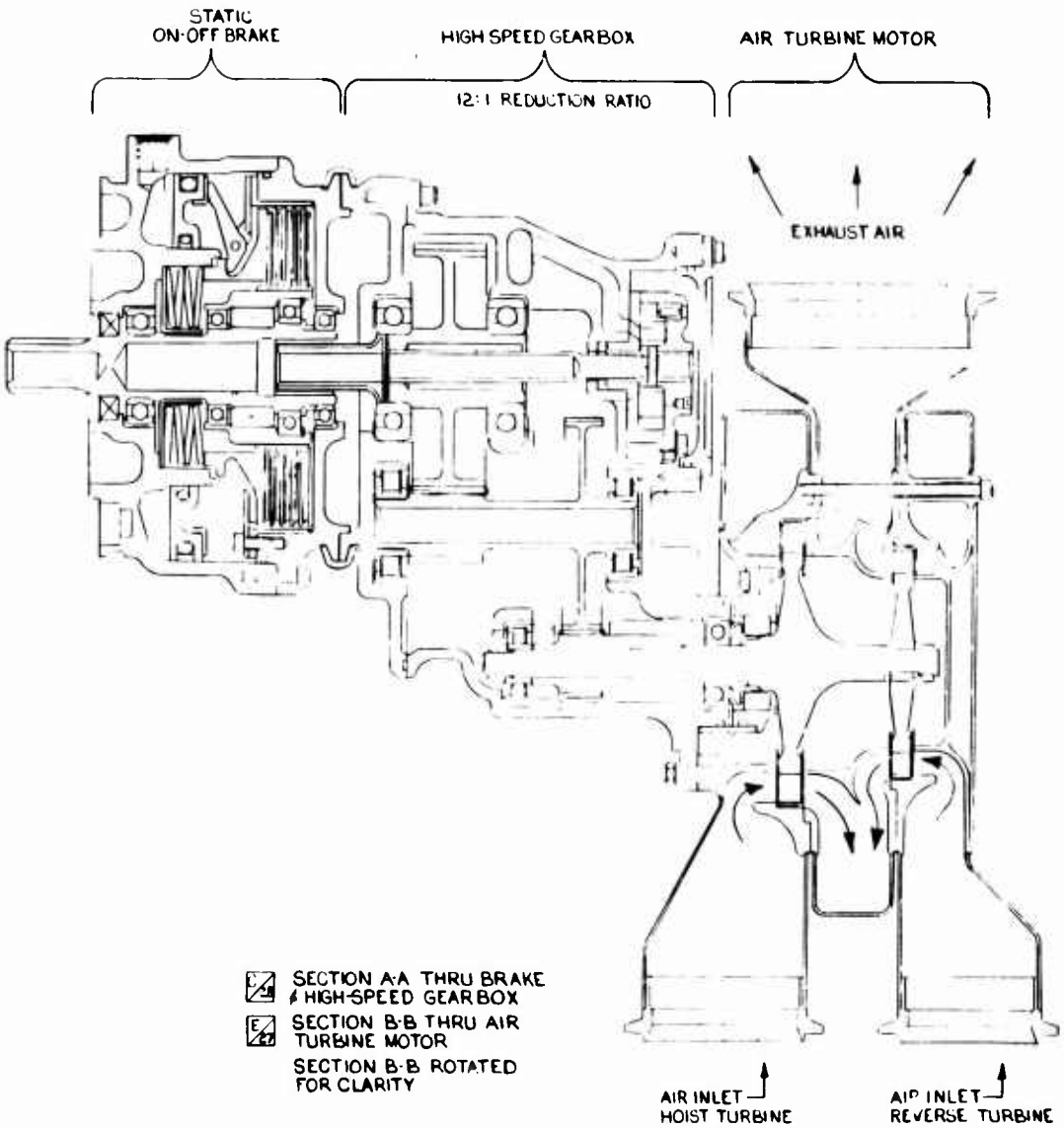
STATIC
ON-OFF BRAKE
HIGH SPEED GEARBOX
12:1 REDUCTION RATIO
AIR TURBINE MOTOR
EXHAUST AIR
SECTION A-A THRU BRAKE & HIGH-SPEED GEARBOX
SECTION B-B THRU AIR TURBINE MOTOR
SECTION B-B ROTATED FOR CLARITY
AIR INLET HOIST TURBINE
AIR INLET REVERSE TURBINE

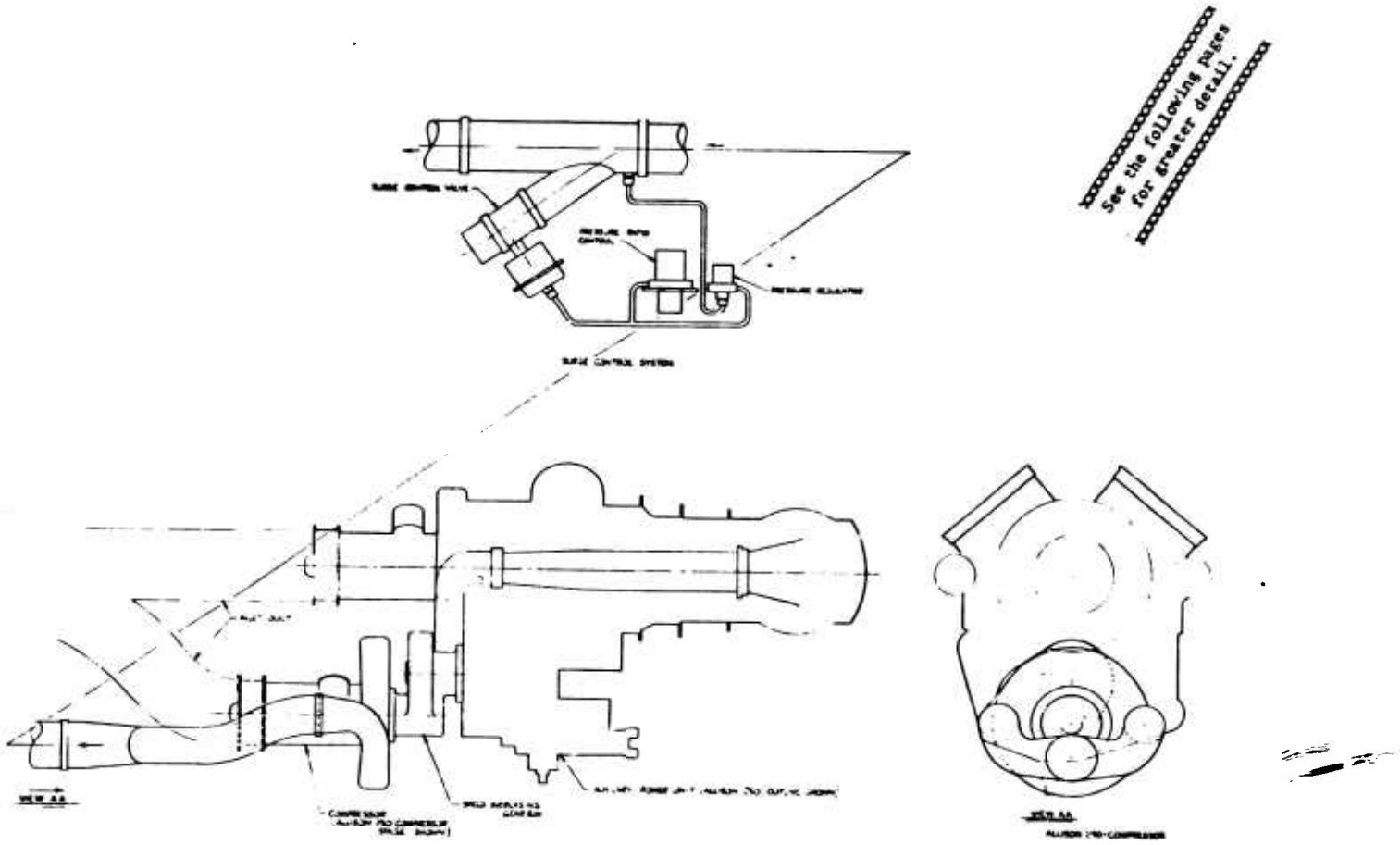

Figure 81. Arrangement of Compressor on APU.

Preceding page blank

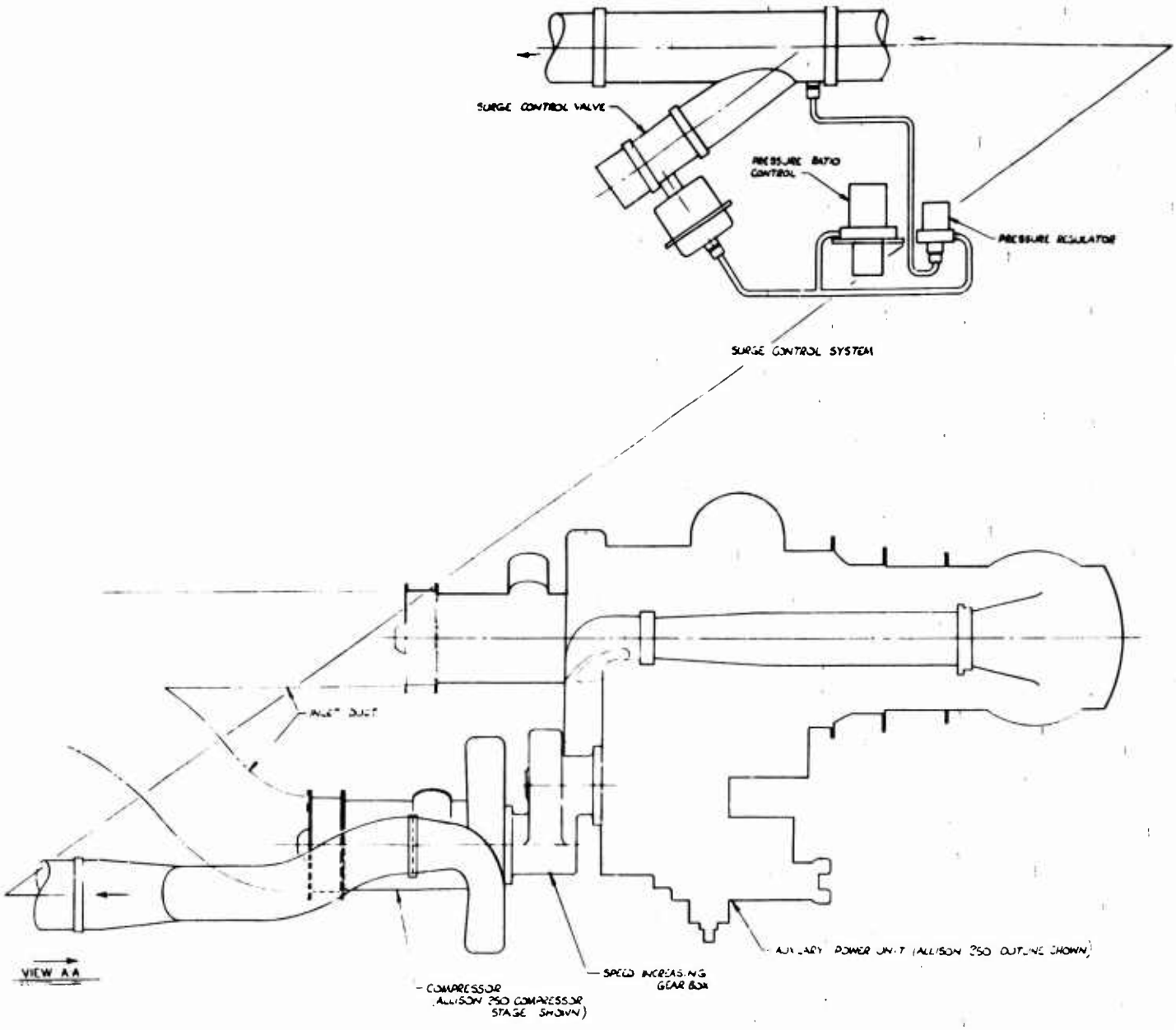

Figure 81. Arrangement of Compressor on APU.

Preceding page blank

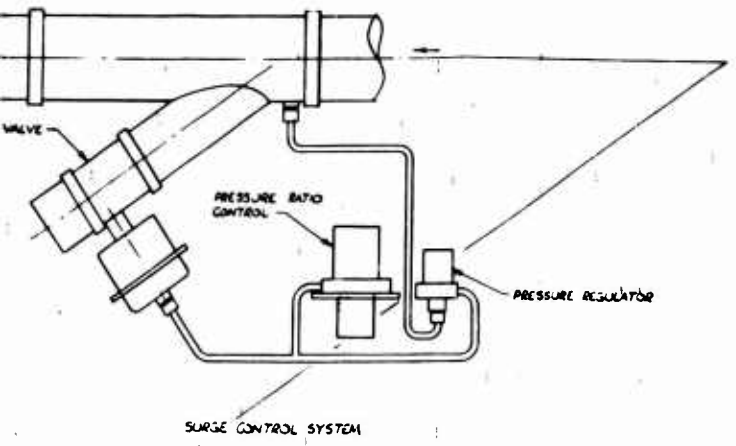

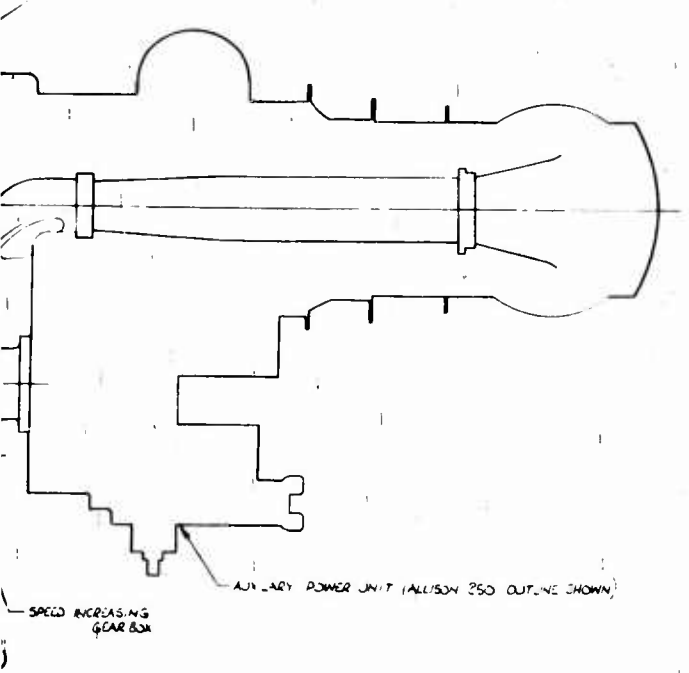

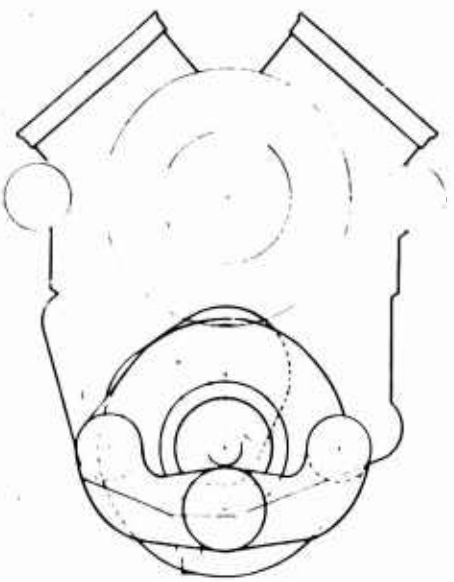

VIEW AA

ALLISON 250-COMPRESSOR

ressor on APU.

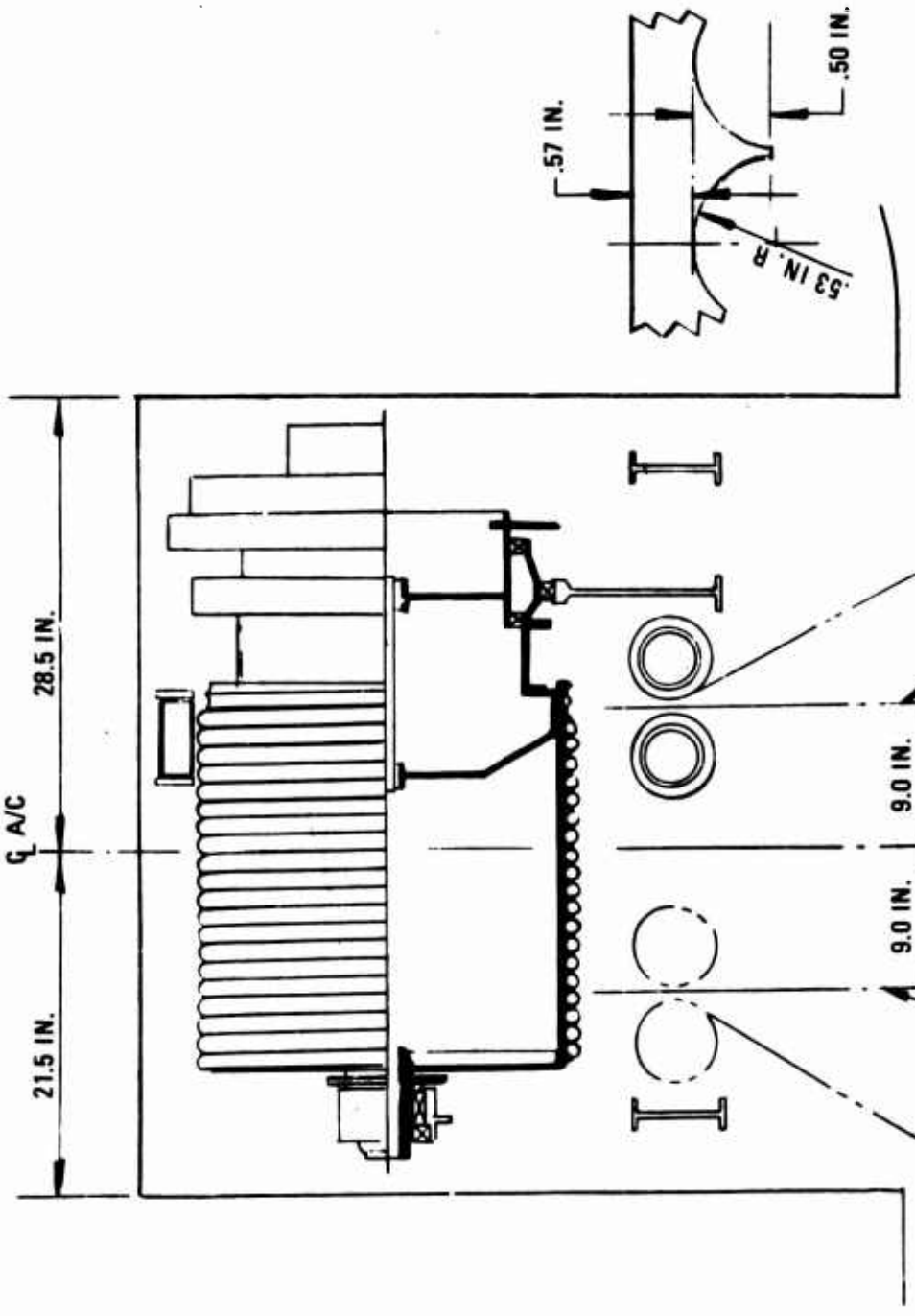

Figure 82. Level-Wind Hoist.

Preceding page blank

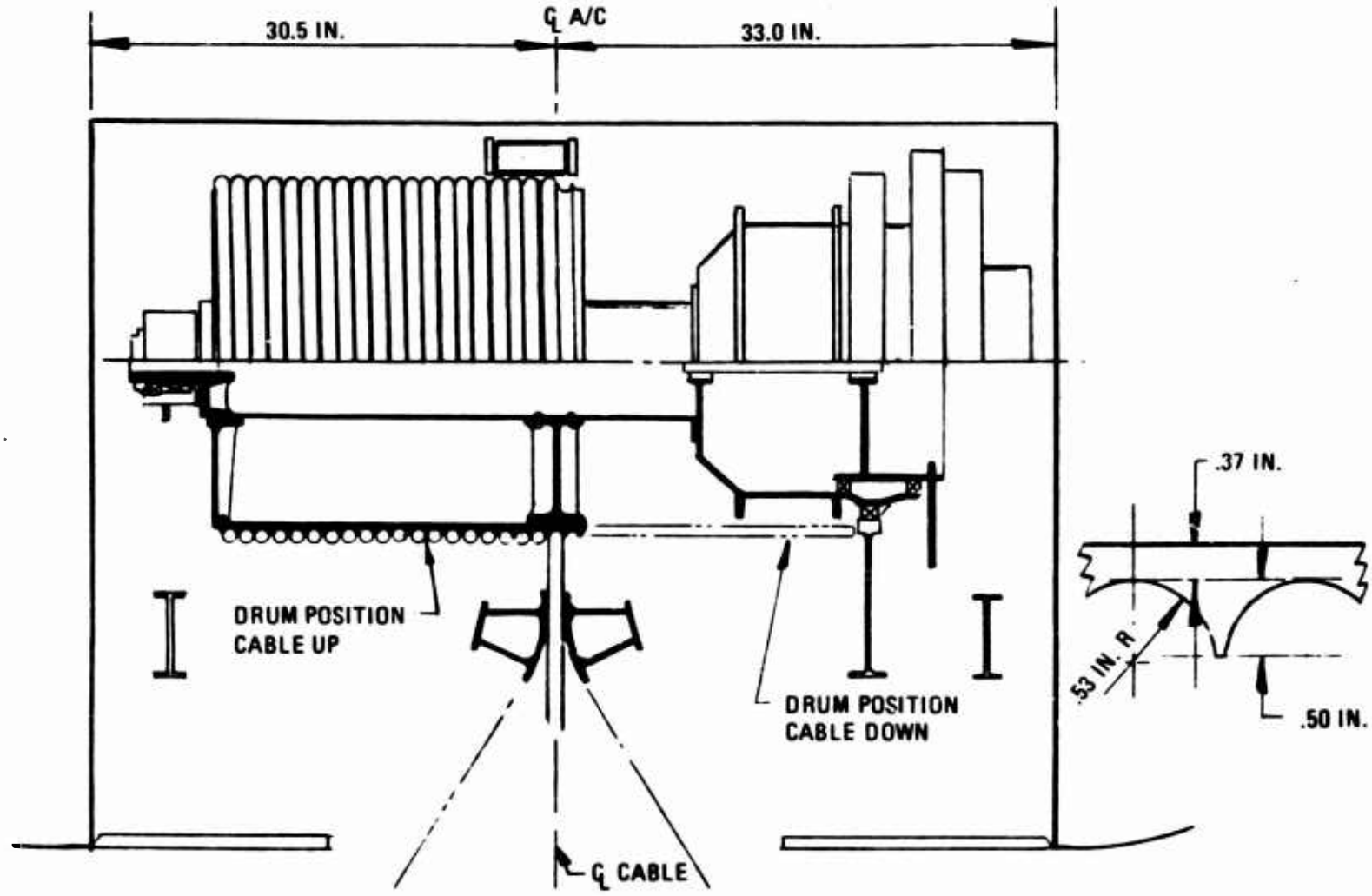

Figure 83. Single-Point Payout Hoist.

support tube extending from the gearbox housing to the far support frame. At a location coincident with the aircraft centerline, a flanged disc with integral ribs is mounted on the central support tube. The outer rim of this disc mounts a number of linear ball-race housings. Grooves on the inside surface of the cable drum match the linear ball races. The balls then support the cable drum and transmit the driving torque. The cable drum has a closure disc at its far end which locates on the central support tube. The outer drum is therefore free to move laterally while under torque. The cable exits between two side load rollers supported on the hoist lateral frame members. As the cable pays out, the drum will move across the aircraft. A locating roller supported on the hoist frame and running inside the drum cable groove ensures the alignment of cable and drum.

Advantages of SPP Configuration:

- Provision of a constant payout point
  - -- No lateral CG shift
  - -- Ease of location for external load snugged to fuselage, e.g., pod, fuel tank
  - -- Easier installation of external conductor system
- Elimination of level-wind mechanism--leadscrews, ball nuts, bearings, drives, and covers
- Weight advantage--system weight advantage of approximately 90 pounds

Disadvantage of SPP Configuration

- Increased length requires wider tunnel

Dual-Cable Hoists. Dual-cable hoists promise a number of advantages over the single-cable hoist:

- The dual-cable system may provide a possibility of developing a "condition comparator" system to give advanced warning of possible cable failure.
- Smaller cables have greater flexibility and higher strength/weight ratios than larger cables.

- Use of handed pairs of cables would permit the use of rotating-cable construction. Rotating cables generally have higher strengths than nonrotating cables.

- Smaller diameter cables would be easier to handle, store, and install.

Three basic configurations of dual-cable hoist are considered.

Twin-Drum In Line

The configuration shown in Figure 84 consists of two drums mounted on a common axis, driven by a centrally positioned low-speed gearbox. The drums would have opposite-handed helices such that with the cables fully up, the cable spacing would be approximately 16 inches; when fully down, the spacing would be approximately 42 inches. The lower end of the cables would terminate at an equalizing beam. The cables pass between side-load rollers as they leave the drums; these rollers are mounted on lead screws and synchronized to the drum rotation to ensure correct positioning of the cable. Configurations with 24-inch and 18-inch-diameter drums were considered. The 18-inch-diameter configuration was rejected due to excessive width requirement. With cables fully out, the limit for lateral angle, retaining load sharing on the cables, is approximately 16 degrees. This angle is a function of the length of the equalizing box, and to obtain the 30-degree angle capability required by the aircraft system requirements document, this beam would have to be approximately 34 inches long, increasing the tunnel width to 82 inches. A tunnel width in excess of 70 inches would involve a considerable structural weight penalty.

Single-Drum, Twin Cables

The configuration shown in Figure 85 is essentially similar to the single-cable level-wind hoist. The principal difference is that the drum has a two-start helix, permitting two identical cables to be wound side by side. The side-load roller arrangement will require a third roller. The equalizing beam will be short and there will be no side angle restrictions. The disadvantage of a level-wind hoist--the cable moving across the aircraft--is inherent in this design.

Twin Parallel Drums

The arrangement of two drums side by side, driven from a common ATM and high-speed gearbox, would permit either a level-

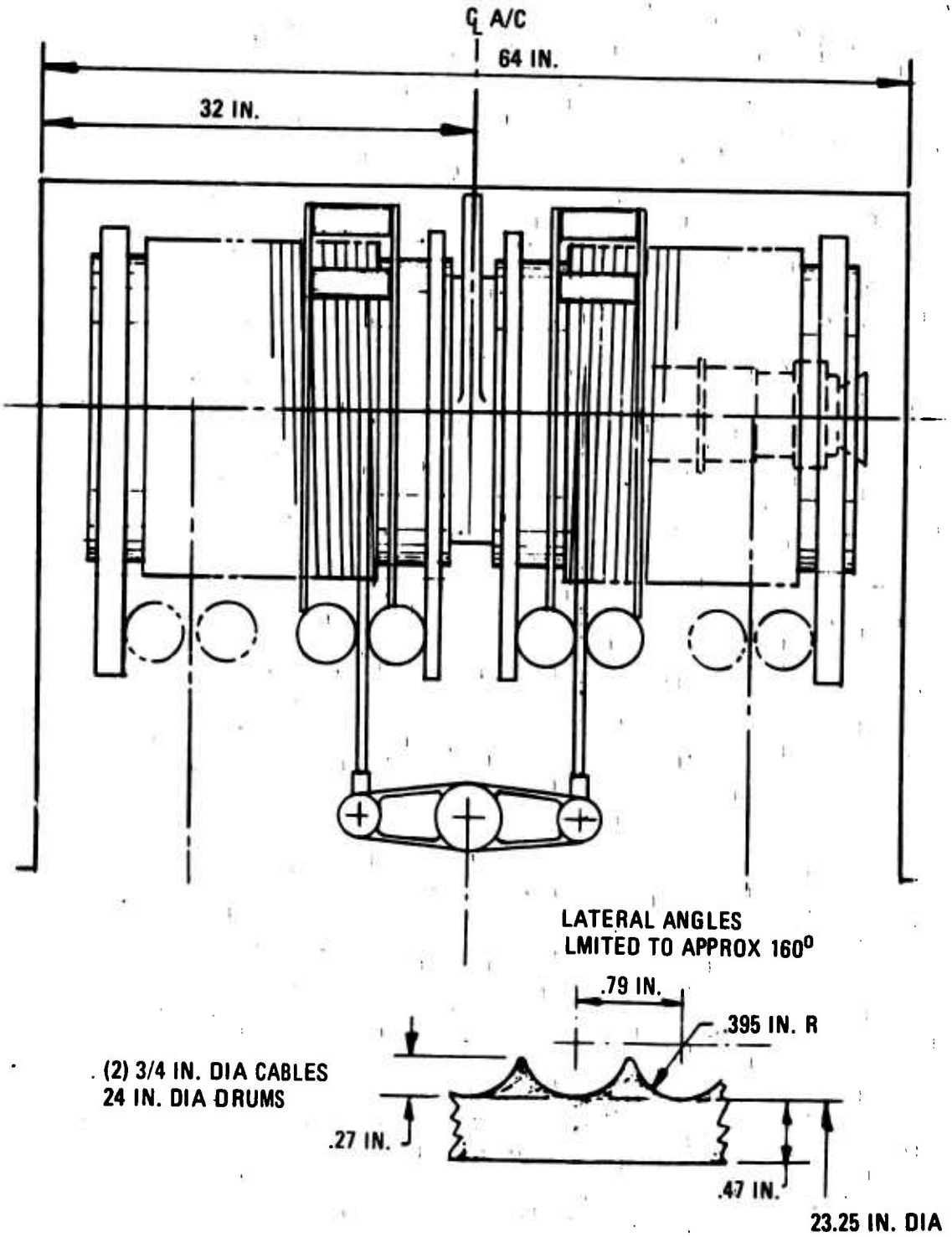

Figure 84. Twin-Drum In-Line Hoist.

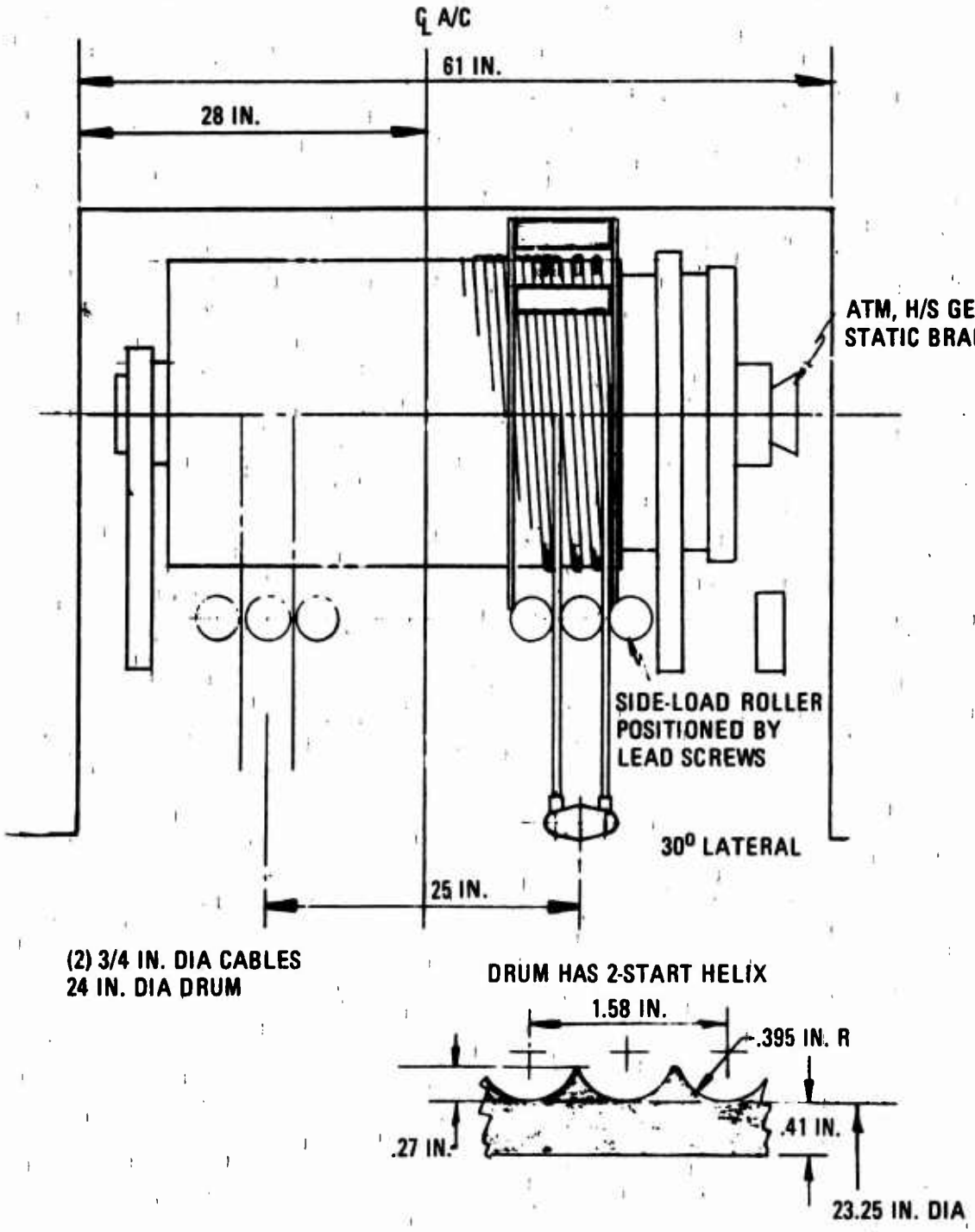

Figure 85. Single-Drum Twin-Cable Hoist.

wind or an SPP configuration. The configurations are shown in Figures 86 and 87.

This arrangement results in a relatively compact unit with no geometric restrictions to the lateral cable angles. Advantage can be taken of using smaller drums without the unit width being excessive.

Major Factors Influencing Configuration Selection:

a. Weight

The weights used in this study have been determined to provide an order of preference for the configurations. They are not based on detailed layouts and must be considered preliminary.

b. Size

Hoist size has been determined on the basis of assumed tension member size. Final tension member selection will influence hoist size. Configurations requiring a tunnel width in excess of 70 inches or a length from center of tension member to end of tunnel in excess of 30 inches have been omitted from the candidate configurations.

c. Cable Angle Limits

All configurations have been based on longitudinal cable angles of 30° forward and 40° aft. One configuration has limitations on lateral angles of approximately +16°. Analysis of data from the recently conducted flight tests of the 347 helicopter with external loads will provide some basis for establishing a realistic lateral angle requirement. The ASRD currently requires a 30° coning angle capability.

SINGLE-POINT PAYOUT VS. LEVEL WIND

Configurations maintaining a single-point payout have some advantages over the level-wind system, as discussed in the description of single cable hoist configurations.

An additional advantage of the single-point payout is the reduction in the maximum reaction at the structure interface. For example, the reaction of a corner-mount fitting for an ultimate cable tension of 145,000 pounds vertically of the hoist arrangement shown in Figure 87 would be 36,250 pounds. For the configuration shown in Figure 86, the maximum reaction of a corner fitting could be as high as 87,000 pounds. The

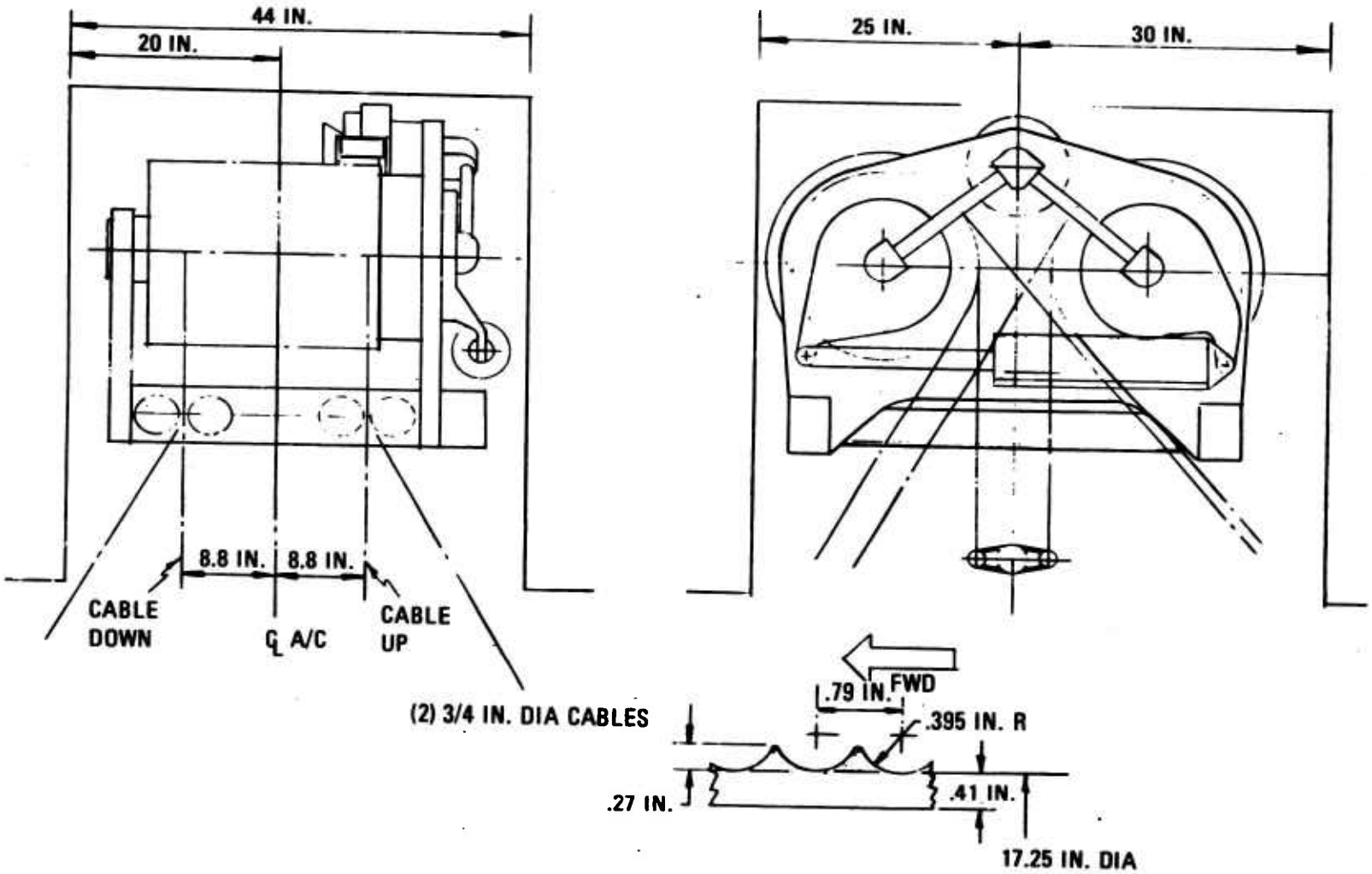

Figure 86. Level-Wind Twin-Drum Hoist.

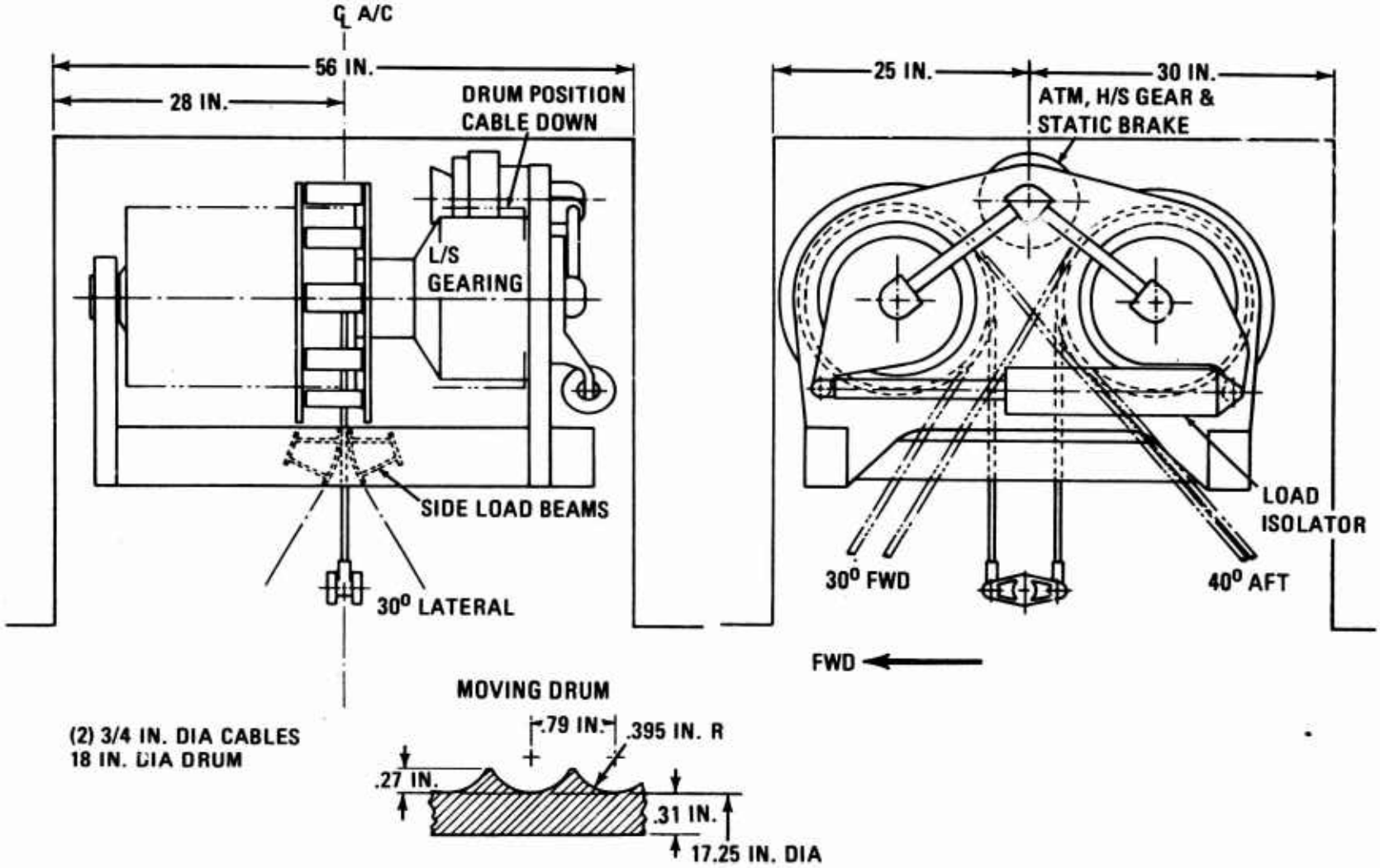

Figure 87. Single-Point Payout Twin-Drum Hoist.

configurations shown in Figures 83 and 87 utilize a sliding-drum concept, requiring the use of multiple linear ball race units as splines. Although it is a new concept for hoist design, there do not appear to be any insurmountable technical problems involved.

MAINTAINABILITY AND RELIABILITY

A product-assurance assessment of each configuration in terms of maintainability and reliability was conducted to establish a ranking. This ranking is shown in Table XXXIX.

WEIGHT DEVELOPMENT

Cable Weight

Using estimated cable strength values based on potential development, a 145,000-pound cable would be 1.18 inches in diameter. On the same basis, a 72,500-pound cable would require an area of .53 square inch. Assuming that a further 10-percent strength improvement is possible by use of rotating cable, then area = .9 X .53 = .476 square inch; diameter = .78 inch. Using MIL-C-1511 cable weight of approximately 2.83 pounds per square inch per foot, 1.18-inch-diameter cable weighs 2.59 pounds per foot and .78-inch-diameter cable weighs 1.13 pounds per foot.

Figure 88 shows the relationship of area to cable strength.

Length of cable on a 24-inch drum is 120 feet; length of cable on an 18-inch drum is 116 feet.

- 120 feet of 1.18-inch-diameter cable = 120 X 2.59 = 311 pounds
- 2 X 120 feet of .78-inch-diameter cable = 2 X 120 X 1.13 = 271 pounds
- 2 X 116 feet of .78-inch-diameter cable = 2 X 116 X 1.13 = 262 pounds

Structural Interface Weight

The cargo hoist system proposal weight breakdown included 175 pounds for track and fittings, of which 140 pounds was for the load-reacting fittings on the tunnel sidewall. Additionally, the structure weight breakdown had 300 pounds allocated to direct backup for the hoist installations. Considering this as

a total--440 pounds--and adjusting for the increased load results in 440 X 1.25 = 550 pounds of installation structure.

Assuming that this 550 pounds is a direct function of the sum of the maximum reaction, the structure weight will vary for the configurations considered as shown in Figure 89.

Hoist Comparison

Hoist parameters for each configuration are summarized in Table XXXIX. Weights shown are for a single-hoist assembly.

System Comparison

The complete system comparisons are shown in Table XL.

LOAD ISOLATION ANALYSIS

An external load isolator analysis by Boeing's Technology Dynamics Group was conducted. Suspension-mode natural frequencies and pilot response to 1000-pound 1/rev. vertical rotor forces have been computed using a proposed external load isolator stiffness which is proportional to the load carried by the isolator. Effects of cable flexibility, winch rotation, rigid body, and flexible fuselage modes were included. Isolation mode frequencies were slightly below the desired 1.50 to 2.0 Hz range at long cable lengths and pilot response was about +.05g at 1/rev, primarily due to rigid-body fuselage pitching. Essentially, no reduction of the natural frequencies of the uncoupled fuselage flexible modes occurred when the load was coupled to the fuselage with the proposed isolator characteristics in the range of static and maneuver conditions currently considered (minimum isolation load to maximum load at maximum g condition). This program is current with scheduled milestones and activities.

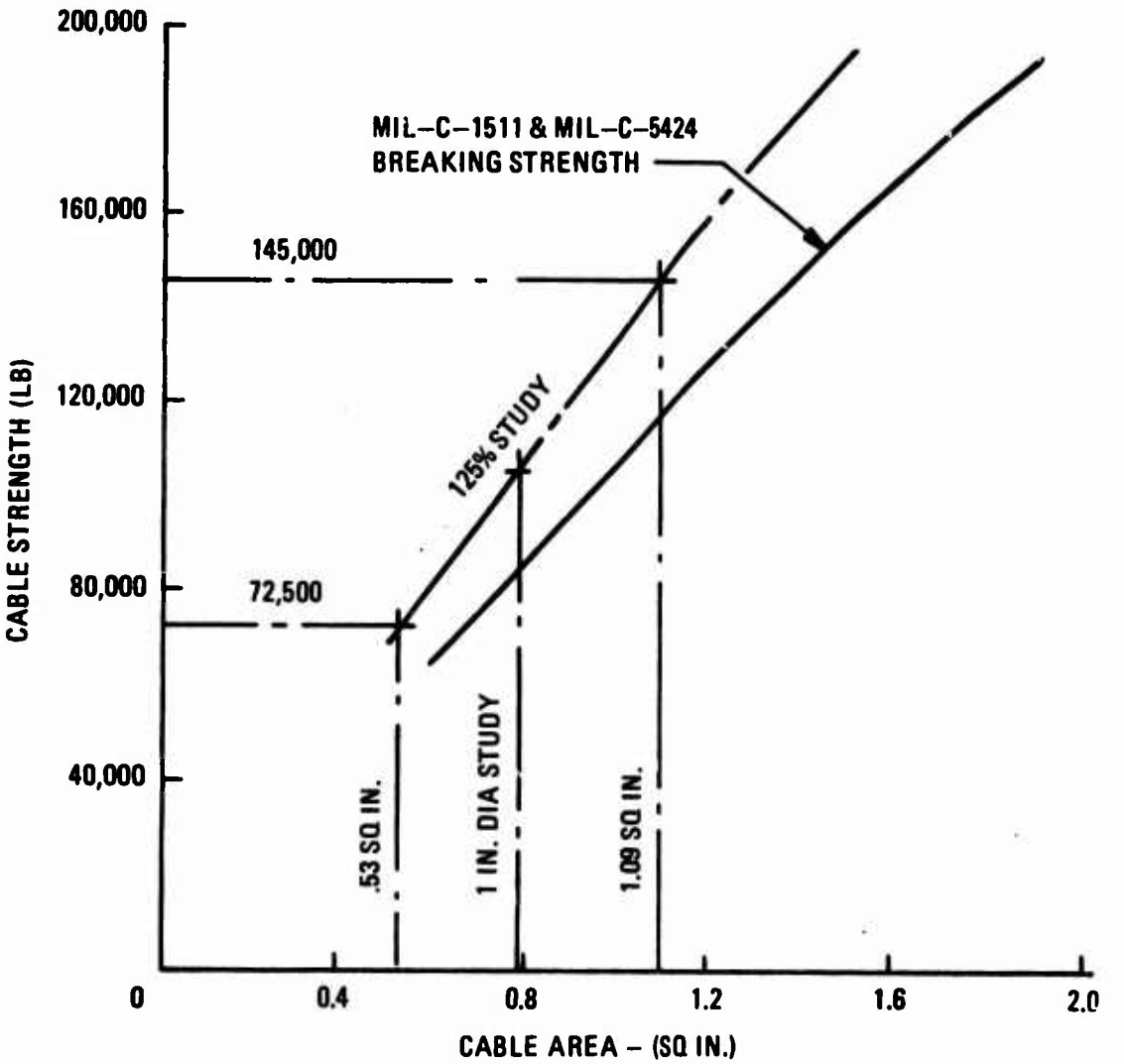

AREA OF 145,000 LB TENSION MEMBER = 1.09 SQ IN. DIA = 1.18 IN.

AREA OF 72,500 LB TENSION MEMBER = .53 SQ IN.

LESS 10% DUE TO USE OF
ROTATING CABLES = .9 X .53 = .476 SQ IN. DIA = .78 IN.

Figure 88. Cable Area Versus Cable Strength.

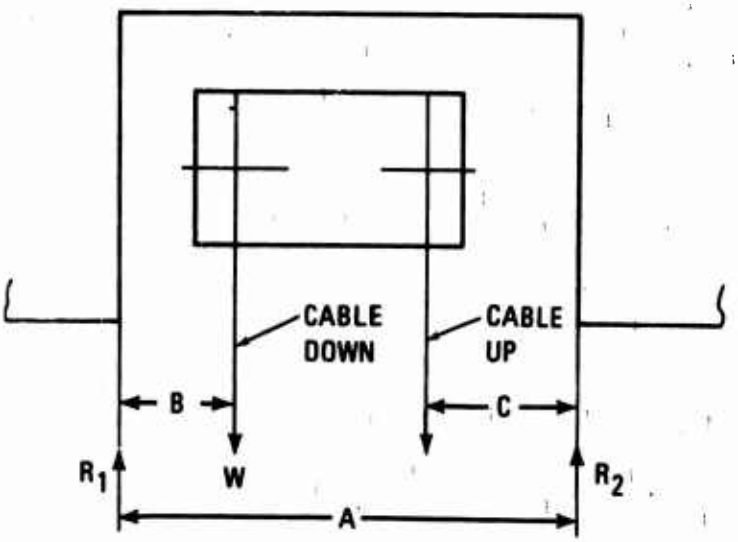

CONFIGURATION	DISTANCE (IN.) A	B	C	SIDEWALL REACTION (PERCENTAGE OF W) MAX R_1	MAX R_2	$R_1 + R_2$	STRUCTURE WEIGHT (LB)
SINGLE CABLE HOISTS							
LEVEL WIND (FIGURE 82)	50.0	12.5	19.5	.75	.61	1.36	550
SINGLE-POINT PAYOUT (FIGURE 83)	63.5	30.5	33.0	.52	.48	1.00	405
DUAL CABLE HOISTS							
TWIN-DRUM IN LINE (FIGURE 84)	64.0	32.0	32.0	.50	.50	1.00	405
SINGLE-DRUM-TWIN-CABLE (FIGURE 85)	61.0	15.5	20.5	.75	.66	1.41	570
LEVEL-WIND TWIN-DRUM (FIGURE 86)	56.0	28.0	28.0	.50	.50	1.00	405
SPP TWIN-DRUM (FIGURE 87)	44.0	11.0	15.4	.75	.65	1.40	567

Figure 89. Structural Interface Weight.

TABLE XXXIX. SUMMARY OF HOIST PARAMETERS

Configuration	Weight* (lb)	Tunnel Width (in.)	Lateral Cable Angle (deg ±)	Lateral Cable Travel (in. ±)	Rank	
					Maintainability	Reliability
Single-Cable Hoists						
Level Wind (Figure 82)	1151	50.0	30	9.0	-	-
Single-Point Payout (Figure 83)	1059	63.5	30	0.0	-	-
Dual-Cable Hoists						
Twin-Drum In Line (Figure 84)	1369	64.0	16	0.0	4	4
Single-Drum Twin-Cable (Figure 85)	1244	61.0	30	12.5	3	1
Level-Wind Twin-Drum (Figure 86)	1142	56.0	30	0.0	2	2
SPP Twin-Drum (Figure 87)	1202	44.0	30	8.8	1	3

*Includes: cable drum, drum-support frame, low-speed gearing, level-wind or equivalent mechanism, provisions for cable cutter. Drum thickness based on use of Carpenter Custom 455 steel of 280,000 PSI UTS.

TABLE XL. SYSTEM WEIGHT SUMMARY

Weight (lb)						
Two Hoist Drums & Support Assys	Two Cable Assys	Installation Structure	Constant Weight*	Subtotal	Structure** Weight	System Total
2302	622	550	975	4449	374	4075
2118	622	405	975	4120	275	3845
2738	542	405	975	4660	275	4395
2488	542	570	975	4575	387	4188
2284	524	405	975	4188	275	3913
2404	524	567	975	4470	385	4085

*Weight not considered as varying with configuration:

Track Rollers	11 lb
Misc. Attaching Hardware	15
Cable Cutter	11
Isolator	90
ATM, Brake, & High-Speed Gear	50
Trolley Drive	20
Hook and Swivel	85
Unit Total	282 lb

Unit Total X 2	564 lb
Controls	80
Single Point Tracks (175-140)	35
Misc. Attaching Hardware	25
System Total	779 lb

Increase of 25% for higher load = 1.25 X 779 = 975 lb

**Structural weight - 68% of installation weight; carried as structure weight in aircraft weight breakdown.

CONCEPT STUDY MODEL

To illustrate the preliminary design of the pneumatic concept, a "breadboard" nonpowered model was fabricated (Figure 90) using a compact mechanical arrangement with existing hardware for the following major functional components: fixed-geometry-nozzle axial turbine ATM (including manifolding), forward rotation control, and gearbox. The static on-off brake and the reversing nozzle (and manifold) were simulated. The gearbox has a 15:1 gear reduction with an output speed of approximately 2000 rpm. Turbine and nozzle arrangement and operation are observable through manifold openings as shown in Figure 90; the ATM is hand-operable.

Components of the model were originally designed for a main engine "dual" turbine starter rated at approximately 100 hp when operated with cold gas (bleed air). Gearing was designed for approximately 400 hp to withstand power transfer from a solid propellant cartridge starter. The 100 hp unit weighs approximately 42 pounds consisting of 25 pounds for the tubing, gearing, and assembly; 4-1/2 pounds for the valve; and the balance for the turbine assembly and housing.

Subsequent development (Phase II) based on modified performance requirements in order to achieve 200% design speed for cable payout dictated investigation of different wheel design configurations.

Tests to substantiate concept development are discussed under System Concept Demonstration Testing, pages 143 through 158. The test unit used is shown in Figure 72.

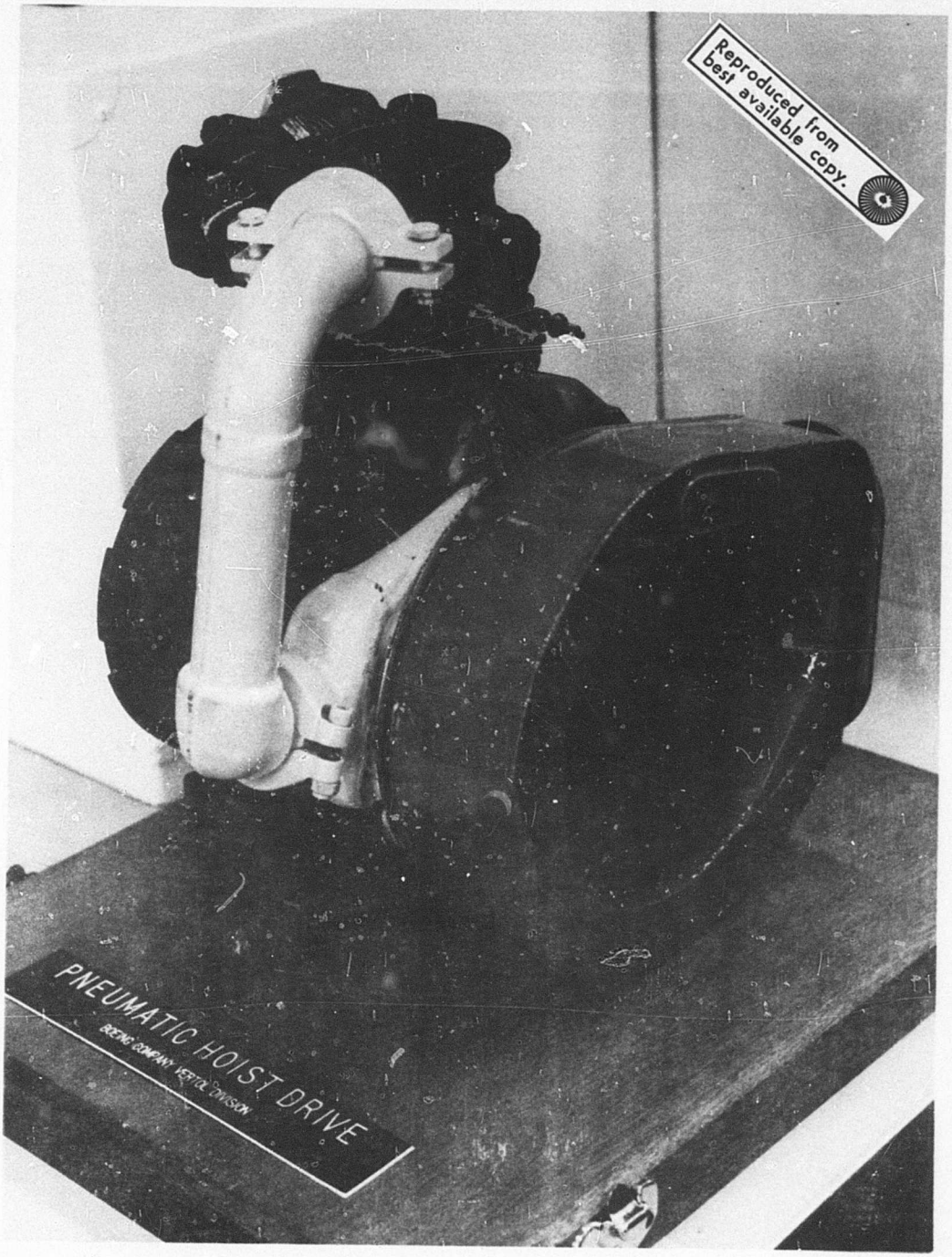

Figure 90. Pneumatic Hoist Drive Concept Study Model (Sheet 1 of 2).

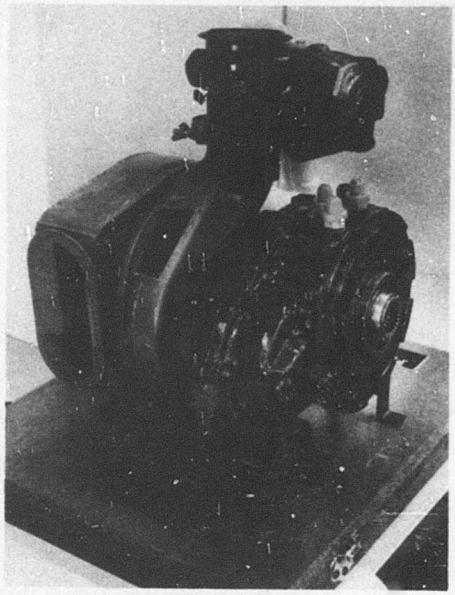

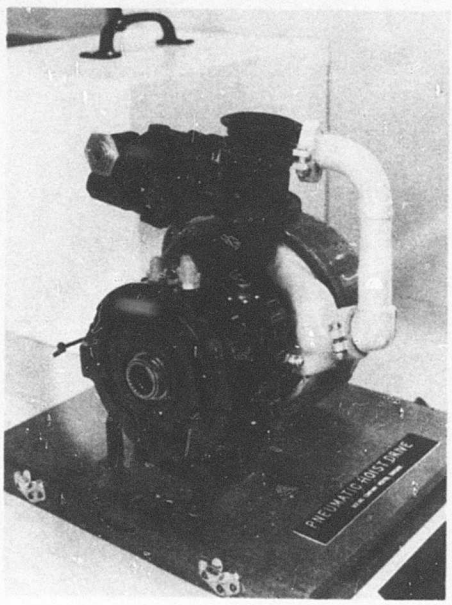

Figure 90. Continued (Sheet 2 of 2).